



HAL
open science

Partially perfluorinated derivatives as powerful components for artwork restoration

Yuqing Zhang

► **To cite this version:**

Yuqing Zhang. Partially perfluorinated derivatives as powerful components for artwork restoration. Material chemistry. CY Cergy Paris Université; Università degli Studi di Firenze, 2022. English. NNT : 2022CYUN1088 . tel-03736246

HAL Id: tel-03736246

<https://theses.hal.science/tel-03736246>

Submitted on 22 Jul 2022

HAL is a multi-disciplinary open access archive for the deposit and dissemination of scientific research documents, whether they are published or not. The documents may come from teaching and research institutions in France or abroad, or from public or private research centers.

L'archive ouverte pluridisciplinaire **HAL**, est destinée au dépôt et à la diffusion de documents scientifiques de niveau recherche, publiés ou non, émanant des établissements d'enseignement et de recherche français ou étrangers, des laboratoires publics ou privés.



UNIVERSITÀ
DEGLI STUDI
FIRENZE



PhD thesis

Partially perfluorinated derivatives as powerful components for artwork restoration

PhD student: Yuqing Zhang
21st, March, 2022

Jury

Pr. Donatella Giomi	Università degli Studi di Firenze	Examiner
Pr. Rodorico Giorgi	Università degli Studi di Firenze	Examiner
Dr. Agnès Lattuati-Derieux	C2RMF	Guest (Director of thesis)
Pr. Nadège Lubin-Germain	CY Cergy Paris Université	Guest (Director of thesis)
Pr. Anna Maria Papini	Università degli Studi di Firenze	Examiner
Pr. Yves Queneau	ICBMS-Université de Lyon	Rapporteur
Pr. Antonella Salvini	Università degli Studi di Firenze	Guest (Director of thesis)
Pr. Nathalie Steunou	Université Versailles St-Quentin-en-Yvelines	Examiner
Pr. Elisabetta Zendri	Università Ca' Foscari Venezia	Rapporteur

Acknowledgement

The joint PhD thesis has obtained a great deal of help and support from different people of different organizations, especially with the Covid pandemic background. I would like to take this opportunity to express my gratitude.

Firstly, I would like to thank all the members of the jury, for having accepted to review this thesis. Thank you for being the rapporteurs, Pr. Yves Queneau from ICBMS-Université de Lyon (also for reviewing this project since the mid-thesis report), and Pr. Elisabetta Zendri from Università Ca' Foscari Venezia, as well as for being the examiners, Pr. Donatella Giomi from Università degli Studi di Firenze, Pr. Rodorico Giorgi from Università degli Studi di Firenze, Pr. Anna Maria Papini from Università degli Studi di Firenze, and Pr. Nathalie Steunou from ILV-Université Versailles St-Quentin-en-Yvelines.

As a joint PhD thesis, the research work has been supported by laboratories in France and Italy. I would like to thank the director of the BioCIS laboratory, Dr. Mouad Alami; the director of the biological chemistry team, Pr. Thierry Brigaud; the director of Department of Chemistry 'Ugo Schiff', Pr. Barbara Valtancoli; the director of CNR-IGG, Pr. Antonello Provenzale; the previous and current directors of C2RMF, Ms. Isabelle Pallot-Frossard and Mr. Jean-Michel Loyer-Hascoët for welcoming me to carry out the research work of this thesis in their laboratories. I would like to thank the previous head of the research department of C2RMF, Dr. Michel Menu, for joining this project as the co-proposer and welcoming me in C2RMF.

I would like to thank the financial support of the thesis from Fondation des Sciences du Patrimoine (FSP). I also thank Ecoles d'été France Excellence - heritage science summer school organized by FSP and French Embassy in China, for opening the door of the interesting research field combining chemistry, physics with art. I thank the scientific coordinator of FSP, Dr. Anne-Julie Etter, for introducing me to researchers in FSP. I would like to thank the PhD school of CY Cergy Paris Université for being host of the PhD project and the PhD school of Università degli Studi di Firenze for being the co-joint party.

I would like to express my gratitude to the directors of this thesis: Pr. Nadège Lubin-Germain, Pr. Antonella Salvini and Dr. Agnès Lattuati-Derieux.

I thank Pr. Nadège Lubin-Germain for her interest to propose, develop this PhD project and offer me the PhD opportunity at the first place. I thank her for giving me so much professional and personal support, help, understanding, encouragement and trust during every step of the project, since the first email from her. I thank her for always available for me to provide the solutions with her kindness, calmness, optimism, intelligence, patience and persistence in any difficult situation during the PhD project (no matter the administration difficulties, scientific difficulties or personal difficulties). And I thank her for her every "do not worry" to me.

I thank Pr. Antonella Salvini for her interest in this project, and giving me warm and thoughtful welcome in beautiful Florence and her laboratory. I also thank her for the very logical guidance to the experiments, the very patient and careful review, and great availability to my manuscript writing. I would like to especially thank her for providing the great help both in professional and personal sides, during the Covid pandemic in 2020. I thank her for organizing my presence in laboratory by always giving me the biggest convenience (no matter the traffic, the administration files or the lunch arrangements) during the pandemic. It was a very stressful period for everyone, but she provided me the unforgettable care and help. I also thank her for the constant encouragements, firm support and valuable suggestions after I left Florence.

I thank Dr. Agnès Lattuati-Derieux for her interest to join this project, and giving me warm welcome in C2RMF and the organic chemistry team. I also thank her for communicating about my presence in C2RMF every week during the pandemic, for helping me communicate with many colleagues for my scientific or non-scientific askings and being the translator of French and English. I especially thank her for the efforts in climate chamber and UV light searching, contacting and fixing, with different laboratories and colleagues during the breakdown of the machine. I would like to thank her for the careful, efficient and patient review for my manuscript, even in very difficult situation. I also thank her for organizing the essential meetings with all my supervisors concerning my progress in the last year, encouraging me to be optimistic and giving me help during difficult time of the project, and providing me scientific suggestions for my research.

I would like to express my gratitude to the co-supervisors of this thesis: Dr. Florian Gallier, Pr. Mara Camaiti and Mme. Myriam Eveno.

I thank Dr. Florian Gallier for his interest in this project and giving me warm welcome in BioCIS. I also thank him for the great availability, rich and solid chemistry knowledge, very clear and patient explanation in the synthesis work. I thank him for providing great help with his scientific ideas for the preparation of presentations and the review of my manuscript. I also would like to thank him for the encouragements when I facing the difficulties and stress in experiments, presentations and project progress. And I especially thank him for good ideas to improve the reactions, design the route and propose the target for the synthesis, and for the tolerant understanding to my mistakes in the lab work.

I thank Pr. Mara Camaiti for her interest to join this project and the warm welcome in her laboratory. I thank her for the great availability, scientific and rich heritage-science knowledge, and inspiring explanations for my research, especially in stone protection and painting restoration work. I especially thank her for the support and help in the different characterization tests on stone materials, and for the inspirations to think outside of the box during the experiment material searching and building. I also thank her for the careful and patient review of my presentations and manuscript, and for organizing my work during the pandemic period in Florence.

I thank Mme. Myriam Eveno for her interest in this project, and providing me a great deal of help for my research in blanching painting restoration. I thank her for the clear guidance of instruments, the scientific ideas concerning the sample preparations, and intelligent consideration on developing different methodologies for evaluating the efficacy of the restoration. I especially thank her for always giving me efficient and helpful response to every difficulty in painting restoration work, for contacting with many colleagues to help solve my problems, especially for all the help with searching and fixing of the climate chamber and UV light. I also thank her for the careful and patient review of my manuscript.

I thank all my supervisors again for their good work, serious and scientific attitude to research, kindness and patience to me (and my English), eventually to provide me a nice research environment with multidisciplinary backgrounds.

I would like to thank the colleagues in BioCIS for their help to this thesis. I thank Dr. Jacques Uziel, Dr. Angélique Ferry and Dr. Simon Gonzalez, who are from the glycochemistry group, for their help with my synthesis work, and for their warm regards and encouragement to this project and me. I thank Abdelhakim Ouarti, Jonathan Martins, Julien Fievez, Pr. Leandro Soter, Dr. Nazarii Sabat, Dr. Nina Bozinovic, Rodolphe Kabou who shared the same lab with me in Cergy, for the help, support, advice, encouragement, talk, laugh and music during my stay in lab. I thank Pr. Anna Maria Papini, Aurélie Honfroy, Camille Lozada, Dr. Chiara Zanato, Clément Grisel, Dr. Clément Sanchez, David Branquet, Dr. Elisa Peroni, Dr. Evelyne Chelain, Francesco Terzani, Dr. Grégory Chaume, Guy Gouarin, Dr. Hendrick Rusche, Jocelyne Gougerot, Pr. Julien Pytkowicz, Dr. Karine Guitot, Dr. Keyvan Rahgoshay, Dr. Maciej Malinowski, Dr. Morgane de Robichon, Dr. Lizeth Boderó, Nadia Hbali, Dr. Nathalie Lensen, Dr. Olivier Monasson, Quentin Joachim, Thanh Van Tran and Vanessa Delahaye for their advice, encouragement, help and talk during my stay in BioCIS. In addition to research work, I also thank my colleagues and friends in BioCIS for organizing the game evenings, escape games, barbecue, Mölkky, theme park tour, secret Santa and so on to have a relaxing and enjoyable time. I thank those people I met in BioCIS again for forming a friendly environment and leaving me different valuable memories by their own way.

I would like to thank the colleagues in Florence for their help to this thesis. I thank Alice Cappitti and Silvia Giorgi from the lab of 'Ugo Schiff', for their help to my lab work, especially for the NMR experiments, and for helping switch off my reactions (with the precise alarm clock warning). I thank Luigi Vivaldi, Maria Grazia Balzano, Sara Baracani who also shared the same lab with me, for their help in lab. I thank Dr. Donatella Giomi, Jacopo Ceccarelli, Marika Pinto for providing help with my experiments. I also thank those colleagues and friends in 'Ugo Schiff' for the lunches, coffee, cookies, cakes, talk and laugh. I thank Dr. Alessandra Papacchini, Cristiano Romiti and Dr. Yijian Cao from the lab of CNR-IGG, for their help and advice to my lab work, especially for water repellency tests, contact angle measurements and aging process. I would like to thank Zaineb Bakari for her support, especially in the first lockdown period of 2020, and the interesting visitings in Italy. I thank all those colleagues and friends again for their warm welcoming and help, and giving me the valuable memories about Florence.

I would like to thank the colleagues in C2RMF for their help and support to this thesis. I thank Dr. Anaïs Genty-Vincent for her helpful advice and discussion on blanching painting topic. I thank Dr. Hitomi Fuji for the help in chemical reagent order, guidance for the microscope, the help in organic chemistry lab and the warm regards to this project and me. I thank Gilles Bastian for the great help with pigments and mock-up sample preparation. I thank Éric Laval for the great help with FEG-SEM training and SEM-EDS experiments. I thank Christel Doublet for the help with instruments and interpretation of SEM-EDS results. I thank Dr. Vincent Cartigny for the help for FEG-SEM. I thank Dr. Clotilde Boust, Yoko Arteaga, Dr. Thomas Calligaro, Dr. Xueshi Bai and Véronique Illes for the great help with spectro-colorimetry analysis. I thank Anne Maigret for the great help with photograph taking, especially for her patience, and great availability. I thank Alexis Komenda for the great help for photograph taking. I thank Dr. Johanna Salvant for the training in FT-IR. I thank Dr. Nathalie Balcar and Dr. Antoine Trosseau for their nice sharing of the desks. I thank Oceane Anduze and Clémence Touzeau for their help in my research. I thank Dr. Anne-Solenn Le Hô and Dr. Ina Reiche for the concerning about climate chamber. I thank Nicoletta Palladino for the help of climate chamber. I thank Dr. Mathilde Tiennot for the help with pigments. I thank Juliette Robin-Dupire, Sreyneth Mes, Fabien Yvan, Bi Ran, Rémi Petitcol, Jizhen Cai, Sybille Manyà, Dr. Lucile Brunel, Alexandra Dumazet, Florian Bourguignon, Raphael Moreau for the lunches, talks and help. I thank all those colleagues in C2RMF again for the great help to this thesis with their expertises.

I especially thank Dr. Marguerite Jossic from Musée de la Musique, Pr. Odile Fichet and Dr. Emilande Apchain from LPPI for the great help with providing the climate chambers for the sample aging.

I would like to thank Acc&ss Paris-Nord, and Cité internationale universitaire de Paris for the help with my and foreign researchers' administration and accommodation in France.

Finally, I would like to thank my parents for all the support during my PhD study, who believe in me more than myself. I would like to thank my friends for all the support during my PhD study, who allow me to share with the moments of life.

Contents

Abbreviations	1
Chapter 1.....	3
Introduction	3
1.1 Stone protection.....	6
1.1.1 Stone materials	6
1.1.2 Stone degradation: causes and mechanisms	6
1.1.3 Stone protection	11
1.2 Blanching easel painting restoration.....	16
1.2.1 Easel painting	16
1.2.2 Stratigraphy of an easel painting.....	16
1.2.3 Blanching in easel paintings	25
Chapter 2.....	36
Aim of the thesis	36
2.1 The objectives of the restoration	36
2.2 Proposed compounds for restoration	36
2.2.1 Partially perfluorinated C-glycosides.....	36
2.2.2 Partially perfluorinated hydroxylated oligoamides	37
2.3 Selection of the promising compounds for restoration	37
Chapter 3.....	39
Partially perfluorinated C-glycosides.....	39
3.1 Introduction.....	39
3.1.1 Literature: C-glycoside synthesis	39
3.1.2 Literature: reactivity on to C-glycoside methylketones.....	48
3.1.3 Partially perfluorinated carbohydrates	54
3.2 Results and discussion.....	57
3.2.1 Target compounds: Partially perfluorinated C-glycosides.....	57
3.2.2 Synthesis.....	58
3.3 Conclusion	68
3.4 Experimental Part.....	70
Chapter 4.....	79
Partially perfluorinated oligomers	79
4.1 Introduction.....	79
4.1.1 Polyamide.....	79
4.1.2 Functionalized polyamides.....	80
4.2 Results and discussion.....	84
4.2.1 Synthesis of the non-perfluorinated oligoamides.....	85
4.2.2 Synthesis of partially perfluorinated oligoamides.....	99

4.3 Conclusion	117
4.4 Experimental part	118
Chapter 5.....	124
Stone protection	124
5.1 Introduction.....	124
5.2 Experimental part.....	126
5.2.1 Materials	126
5.2.2 Ultraviolet (UV) irradiation.....	126
5.2.3 Stone sample selection	126
5.2.4 Coating procedure.....	127
5.2.5 Methods for treatment evaluation	127
5.3 Results and discussion.....	130
5.3.1 Solubility of the partially perfluorinated derivatives	130
5.3.2 Resistance to photodegradation	131
5.3.3 Stone sample selection	140
5.3.4 Coating procedure.....	142
5.3.5 Water repellency.....	145
5.3.6 Chromatic effect.....	149
5.3.7 Contact angle	151
5.3.8 Vapor permeability.....	153
5.4 Conclusion	154
Chapter 6.....	156
Blanching easel painting restoration.....	156
6.1 Introduction.....	156
6.2 Experiment	160
6.2.1 Materials	160
6.2.2 Sample preparation.....	160
6.2.3 Preparation of partially perfluorinated derivatives for restoration treatments... 162	
6.2.4 Treatments	162
6.2.5 Methods of treatment evaluation.....	164
6.2.6 Removal of the treatment (Reversibility test)	166
6.2.7 Evaluation of the reversibility.....	166
6.3 Results and discussion.....	166
6.3.1 Treatments on the pure pigments.....	166
6.3.2 Treatments on blanching paint-layer mock-up samples.....	172
6.4 Conclusion	201
Chapter 7.....	203
Conclusions	203
7.1 Synthesis of partially perfluorinated derivatives.....	203

7.1.1 Partially perfluorinated C-glycosides.....	203
7.1.2 Partially perfluorinated oligoamides.....	204
7.2 Restoration performance	204
7.2.1 Stone protection	204
7.2.2 Blanching painting restoration	205
7.3 Summary.....	206
Bibliography	207
Abstract.....	222
Résumé.....	223

Abbreviations

Ac	Acetyl
ACN	Acetonitrile
AcOEt	Ethyl acetate
Ac ₂ O	Acetic anhydride
aq.	Aqueous
Ar	Aryl
Bn	Benzyl
Boc	<i>tert</i> -Butyloxycarbonyl
Bu	Butyl
Bz	Benzene
Cyclo	Cyclohexane
CDI	1,1'-Carbonyldiimidazole
DCM	Dichloromethane
DCE	Dichloroethane
DMAP	4-Dimethylaminopyridine
DMF	Dimethylformamide
DMSO	Dimethyl sulfoxide
EDC	1-Ethyl-3-(3-dimethylaminopropyl)carbodiimide
equiv.	Equivalent
Et	Ethyl
Fmoc	Fluorenylmethyloxycarbonyl
FEG-SEM	Field emission gun scanning electron microscope
FT-IR	Fourier transform infrared spectroscopy
GC-MS	Gas chromatography-mass spectrometry
HRMS	High-resolution mass spectrometry

HOBt	Hydroxybenzotriazole
IR	Infrared spectroscopy
Me	Methyl
NMR	Nuclear Magnetic Resonance
Nu	Nucleophile
Ph	Phenyl
Piv	Pivaloyl
PPTS	Pyridinium p-toluenesulfonate
RH	Relative humidity
r.t	Room temperature
SEM-EDS	Scanning electron microscopy - Energy dispersive X-ray spectroscopy
T	Temperature
<i>t</i> Bu	<i>tert</i> -Butyl
TEA	Triethylamine
Tf	Triflate
TFE	2,2,2-Trifluoroethanol
THF	Tetrahydrofuran
TMS	Trimethylsilyl
TMSCN	Trimethylsilyl cyanide
TMSOTf	Trimethylsilyl trifluoromethanesulfonate
UV	Ultraviolet

Chapter 1

Introduction

Stone as porous and naturally polar material has been widely used in artworks like sculptures, monuments, statues and architectures both in ancient and contemporary time. The natural elegance, sturdy nature, and versatility have made stone as a popular material for sculptors for many centuries. The history of stone sculpture takes us as far back as to the Paleolithic era, and it is considered as the oldest mobiliary art in the history of civilization [1]. For example, *The Venus of Willendorf* is an 11.1 cm tall Venus figurine, carved from an oolitic limestone, which is estimated to have been made around 25,000 years ago [2] (figure 1-1 a). Lecce stone is characterized by warm, golden color and ease to be finely carved. It was widely used in the Baroque architectures, which flourished in the 17th and 18th century [3] (figure 1-1 b). Nowadays, artists are continuing to use different stone materials to express their creation, for example, the Carrara marble sculptures made by Pablo Atchugarry [4] (figure 1-1 c).



a



b



c

Figure 1-1: a) *Venus from Willendorf*, oolitic limestone; b) *Palazzo Persone* (seventeenth century), Baroque architecture, Lecce stone; c) *Carrara marble sculptures*, Pablo Atchugarry, 1990s-2000s

On the other hand, easel painting is another important art form accompanied the human history. They are executed on a portable support such as panels or canvas, instead of on a wall. It is likely that easel paintings are known to the ancient Egyptians. The 1st-century-AD Roman scholar Pliny the Elder already refers to a large panel placed on an easel. Only in the 13th century, easel paintings became relatively common, finally superseding in popularity mural, or wall paintings [5]. Easel paintings are expressing artists' minds, and observation of human-being's society with different styles of techniques. This can be shown both in paintings of High Renaissance by Leonardo Da Vinci (figure 1-2 a) or in modern paintings by Piet Mondrian (figure 1-2 b).

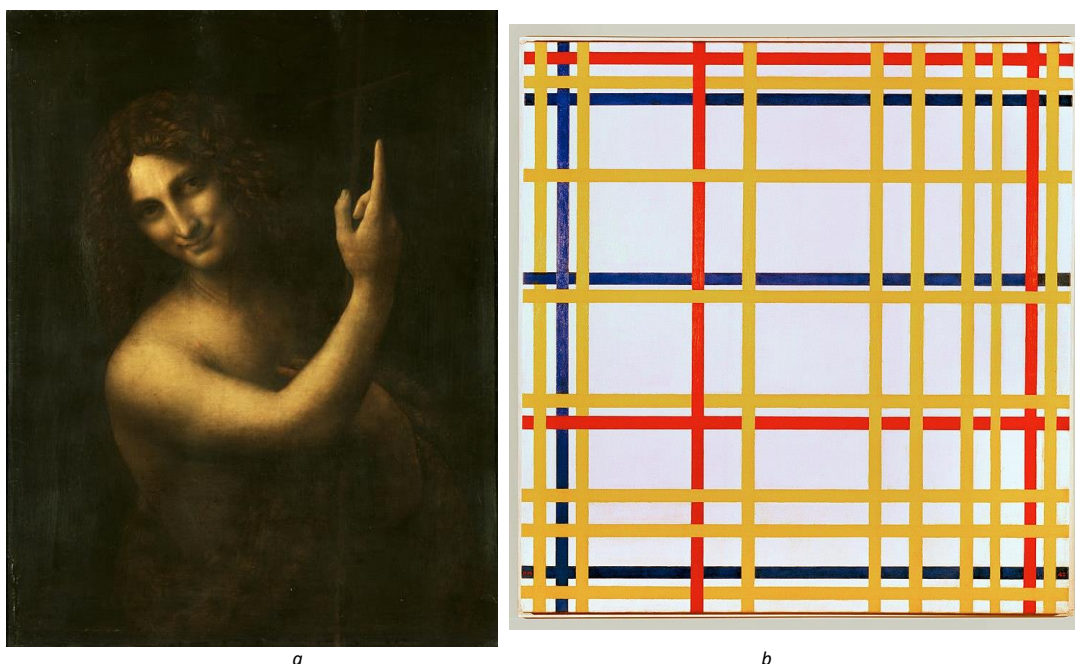


Figure 1-2: a) *Saint John the Baptist* c. 1507–1516, Leonardo Da Vinci, ©C2RMF, Louvre; b) *New York City I*, 1942, Piet Mondrian, Musée National d'Art Moderne – Centre Georges Pompidou

However, like other artworks and cultural heritage, the survival of stone artworks and easel paintings is a challenge because of diverse degradations due to environmental conditions, anthropogenic and biological influences. In particular, water is commonly considered to be one of the main factors causing deterioration of stone artworks because it can start and promote harmful physical, chemical and biological processes. For example, the devastating flood happened in 1966 in Florence (Italy) severely and sometimes irreversibly damaged stone sculptures and monuments [6].

Chemistry was recognized to play an important role to recover damaged artworks after that flood. Different problems of degradation and aging caused by the action of water have been investigated after this event. In particular, different polymeric products, especially amide derivatives of perfluoropolyethers were synthesized and investigated as water-repellents on different stone materials at the University of Florence and in specialized research units of the Consiglio Nazionale delle Ricerche (CNR) [7]. However, products, which can give good water-repellency, effective adhesion on stone as well as environmentally friendly practices during restoration, are still unmet need.

More recently, the Girodet de Montargis Museum (France) was severely damaged by the flood of June 2016. The museum provisional reserves were submerged. 5900 works have remained under water for 72 hours and almost all of the paintings now show significant blanching phenomena [8] (figure 1-3).

Blanching is an alteration, explained by common moisture-induced clouding alteration affecting varnish and paint layers of easel oil paintings. Blanching can appear after water damage, storage in a humid environment or moisture-based restoration. Depending on the degree of deterioration, the pictorial composition can be partially opacified or even completely concealed by veil whitish.

The lack of effective and durable treatments to overcome blanching of paint layers is frequently mentioned by restorers. Common restoration treatments for blanching paintings are usually recognized as “folklore”, like rubbing with egg or oil, treatment with solvents, *etc.* Those restoration treatments are not sufficiently efficient and blanching reappears on the paintings. Recently, perfluoropolyether diamide was reported to be a promising restoration product for blanching paintings. It leads to an innovative idea of restoration treatments for blanching paintings by using compounds containing perfluorinated chains [8][9].



Figure 1-3: Portrait d'Alexandre Dumeis, François-Hippolyte Debon, Musée Girodet, Montargis © C2RMF/P. Salinson;

The objective of this PhD thesis is to study and identify innovative products for an adequate restoration of the stone artworks and blanching easel paintings. In particular, partially perfluorinated derivatives including C-glycosides and oligoamides were proposed. The general introduction of this thesis is divided into two topics: stone protection and blanching painting restoration. Before giving solutions to preventing or remedying conservation or restoration problems of artworks, it is of paramount importance to define and understand the potential causes responsible for those problems. Therefore, the potential causes responsible for decayed stones and blanching easel paintings will be firstly introduced in each topic. Then the methodologies and treatments for stone protection and blanching painting restoration will be also introduced.

1.1 Stone protection

1.1.1 Stone materials

Stones or rocks, are naturally occurring solid aggregates, constituted of one or more types of minerals or, in some cases, non-mineral solid materials such as obsidian, pumice and coal [10]. Formed during the process of genesis, rocks are classified into three broad categories: igneous rocks, sedimentary rocks and metamorphic rocks [11]. Lecce stone, Pietra Serena sandstone and Carrara marble are the lithotypes used in this PhD research project. Among those rocks, Lecce stone and Pietra Serena are sedimentary rocks, and Carrara marble is a metamorphic rock.

- Lecce stone has been used for a long time as construction material for historical buildings in south of Italy, especially during the Baroque period, but it is widely used even nowadays. It is a bioclastic limestone with 93–97 % calcite (CaCO_3) [12].
- Pietra Serena was frequently used during the Renaissance period for ornamental purposes. It is mainly constituted by sandy fraction, clay matrix (alumina, Al_2O_3 and silica, SiO_2 and a small amount of calcite) [13].
- Carrara marble is popular for its use in sculptures and building decors. It is predominantly constituted of calcite [14].

1.1.2 Stone degradation: causes and mechanisms

1.1.2.1 Terminology clarification

In order to avoid the confusions and inaccuracy in studies on stone degradation, the ICOMOS International Scientific Committee for Stone (ISCS) has proposed a scientific, systematic and simplified glossary for the benefits of scientists, conservators and practitioners. General terms, such as alteration, degradation, decay and deterioration are well-defined and distinguished [15].

- **Alteration** is modification of the material that does not necessary imply a worsening of its characteristics from the point of view of conservation. For instance, a reversible coating applied on a stone could be considered as an alteration.
- Chemical or physical modifications of the intrinsic stone properties leading to a loss of value, like historical, artistic and scientific values, or to the impairment of use; declining in condition, quality, or functional capacity can be assigned to **decay** or **degradation**. For example, blurring of a tombstone is a typical **decay** phenomenon.
- Furthermore, process of making or becoming worse or lower in quality, value, character, *etc.* is **deterioration** or **depreciation**, *e.g.* fungi colonization on outdoor stone architecture.

1.1.2.2 Causes and mechanisms

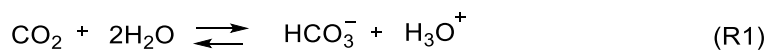
Before taking an action to prevent or to remedy the decay of stone, the causes that were responsible for the degradation should be understood. Intrinsic properties of stone and extrinsic conditions are two main categories of causes related to stone degradation. Intrinsic properties of stone refer to mineralogical composition, textures, porosity, pore shapes, pore size distribution, and grain size, etc. [16]. Extrinsic conditions include climate (temperature, humidity, rainfall), position within an area (urban or rural areas), previous conservation treatments, other anthropogenic activities. The intrinsic properties and the extrinsic conditions are necessary causes for developing stone degradation. Among those causes, liquid water has been regarded as one of the most fundamental agents accounting for stone degradation. That is because liquid water can induce or promote degradation phenomena through chemical, physical and biological processes. Those processes include deposition of atmospheric contaminants, salt crystallization, freeze/thaw cycles, and biodeterioration [17]. How liquid water is involved in those processes is introduced in the next paragraph.

- **Deposition of atmospheric contaminants**

Limestone (mainly calcite: CaCO_3), and sandstone (mainly calcium silicate) are hardly soluble in neutral water at environment temperature, but become more soluble in carbon dioxide/ sulfurous oxide/nitrogen oxide water solution [18].

- Carbon dioxide (CO_2) chemical process

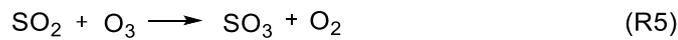
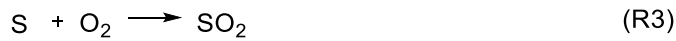
Gaseous CO_2 is dissolved in liquid water, for example in raindrops, and then transported on stone surface. It can erode the materials by chemical reactions.



As indicated by the equilibrium, calcium carbonate is transformed into calcium bicarbonate *via* this reversible reaction, which will occur when the environment conditions *e.g.* rainfall and temperature, are favorable. The damage is observed when the resultant soluble part of the material is washed away by rainfall, which is strong enough to cause the so called - leaching effect. Furthermore, when water evaporates, precipitation of calcite forming white crusts, can occur.

- Sulfurous oxides (SO_x) chemical process

Sulfurous oxides are from anthropogenic and natural sources, like combustion of fossil fuel and volcano eruption. Primary sulfurous compounds in the atmosphere can react with other atmospheric components (OH radicals, O_3), giving new species, for instance some secondary pollutants [19].



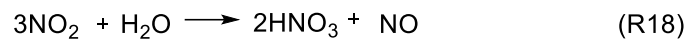
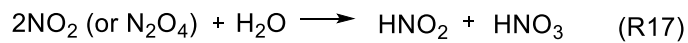
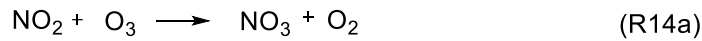
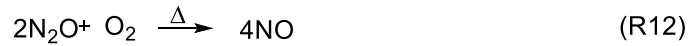
Those secondary pollutants reacting with water produce damaging effects on stones.



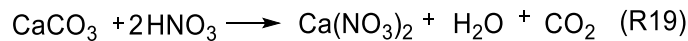
H_2SO_3 can be oxidized to H_2SO_4 by other atmospheric pollutants, *e.g.*, elemental atoms (Pb, Ni, C) from gasoline, diesel, coal combustion, aerosols of pollutants. Calcium carbonate is transformed to calcium sulfate (R9) and normally, calcium sulfate grows on the surface of calcite crystals. Sulfates are soluble in neutral water, so they can be washed away by raindrops if the stone is in an unsheltered position, causing material loss. Sulfates can also crystallize to form gypsum crystals with two molecules of water (R10). Gypsum crystals have different crystallographic properties from carbonate and silicate crystals, *e.g.*, morphology, dimension, contraction expansion coefficient, deliquescent point that will develop internal stress within substrates. When soot derived from all processes of fuel combustion is deposited on gypsum, undesired black crust is formed, partially due to the peculiar morphology of gypsum crystals [20].

- Nitrogen oxides (NO_x) chemical process

Nitrogen oxides, *i.e.*, NO, NO₂, N₂O have both anthropogenic and natural origin, *e.g.*, fuel combustion, biomass burning, lightning *etc.* They can react with other atmospheric components, for instance, oxygen (O₂), hydroxyl radicals (OH), ozone (O₃) [21].



Nitrous acid and nitric acid are both strong acids and calcium carbonate will be dissolved and washed away gradually (R19) [22].



- **Salts crystallization**

Salt crystallization in rocks (and in other construction materials) results from the combined action of salt transport through the porous network and the in-pore crystallization under different environmental conditions. The crystallization pressure exerted by the crystals on the pore surface is the main agent responsible for damage.

When water evaporates from a salt-bearing stone, the concentration of salt increases until it precipitates. Change in temperature, generally a decrease, may also lead to supersaturation of the solution, resulting in crystallization of salts. When supersaturation exceeds the threshold for a certain salt, nucleation initiates and leads to the growth of crystals. Crystallization pressure depends on the existence of a thin layer of aqueous solution that remains between the crystal and pore wall, which permits diffusion of the ions to the growing crystal surface. If this thin layer of solution did not exist, the crystal would come into contact with the pore wall, the growth would stop, and no crystallization pressure would be exerted, protecting the material from damage. The reason for the formation of a liquid film between salt crystal growing and the pore surface is the action of repulsive forces (*i.e.*, disjoining pressure). The repulsion may result from electrostatic interaction and structural forces, hydration forces being the most relevant structural forces in electrolyte solutions; the *van der Waals* forces are attractive at salt-mineral interfaces. In the real scenarios, decay severity and rate vary. If water evaporation occurs on the surface of the stone, then the crystals form a structurally harmless but aesthetically impairing deposit on the surface called

“efflorescence”. However, if water evaporates fast before arriving the stone surfaces, salts precipitate inside the porous structures (a phenomenon called “subflorescence” or “cryptoflorescence”) and severe damage can result. [23]

- ***Freeze – thaw cycle***

Freeze–thaw cycle is an important physical decay process occurring on stones. Natural stones are porous materials that have a total porosity ranging from 2 % (*e.g.* dolomitic marble, serpentinite) to 50 % or greater (*e.g.* tuff, Lecce stone), with a typical average pore-size between 20 nm to 50 µm. As a consequence, water is imbibed and accumulated inside the porous structure *via* various ways such as capillary absorption and raindrops penetration. When the environmental temperature reaches the ice-point, water crystallizes with a 9 % volume expansion. Tensile stress is exerted directly on the pore structure, damaging stones with the same mechanism as salt crystallization [24].

Furthermore, water flow originated when the frozen rock is thawed may act as precursor for successive decay phenomena or facilitate some specific damages. The fractured pores favour water uptake and its flow through the stone, introducing extra problems. Wetted clay minerals and wetted soluble salts are important causes for stone degradation when they interact with temperature and humidity fluctuations. In fact, potential decay patterns may be swelling of clay minerals and salt crystallization [25].

- ***Biodeterioration***

Biodeterioration on stone was firstly defined as “any undesirable change in the properties of a given material caused by the activity of organisms” [26]. The change could be disintegration and irreversible transformation of the substrate. However, the presence of unwanted organisms is not always considered as the cause of material damage but only the cause of an aesthetic damage. An important property of stone material that relates to biodeterioration is bioreceptivity. The concept of bioreceptivity was defined by Guillitte as the aptitude of a material to be colonized by one or several groups of living organisms [27]. Biological species commonly found on or inside stones are lichens, fungi, bacteria (autotrophic, heterotrophic), algae, mosses (or non-vascular plants) and vascular plants. The consequence of biological activity of those organisms on stone surfaces is the formation of biofilms, coloured patinas, encrustations and the presence of vegetative and reproductive bodies. Moreover, the stony structure can be interested to dwindling, erosion, pitting, ion transfer, and leaching processes.

Biodeterioration can lead the stone decay through physical or chemical processes involving water. One example is the degradation by lithophilous Algae and Cyanobacteria. These photoautotrophic organisms can develop well on exposed stone whenever a suitable combination of dampness, warmth and light occurs. Growth is more prominent in spring and autumn. These micro organisms are very sensitive to moisture content as they develop and reproduce in a water film on the stone surface. Bright green coloration develops on all areas that are sufficiently moist and not subjected to direct sunlight. Their presence always indicates a high moisture content of the substrate. Depending on the kind of organism and

on the cycle phase, dark green, brown, grey and pink colored patinas may also occur. In urban atmospheres pollution may prevent the development of algae and other organisms.

Therefore, liquid water has been considered to have the highest responsibility for stone degradation, since it promotes the chemical, physical and biological processes of degradation of stones. Surface water inhibition treatment is an indispensable action to protect stones from those degradations.

1.1.3 Stone protection

By definition, stone protection is an active treatment that is operated directly on stone objects, providing hydrophobic properties or resistance to deterioration agents (*e.g.*, pollution, microorganisms) without reducing the original vapor permeability. That means a protective product for stones is usually applied as a surface coating capable to prevent the contact between the substrate and the deterioration agents [28]. In particular, treating the stone by water-repelling products is a useful method to give the hydrophobic properties, and protect stone materials from liquid water.

Our research focused on the design and study of water-repelling products for stone protection. According to the standard recommendations, the essential requirements for a substance to be considered as a protective agent for stone artifacts include (1) hydrophobicity; (2) good adhesion to stone substrates; (3) good permeability to water vapor; (4) good chemical and physical compatibility with stone substrates; (5) good chemical, physical, thermal, and photo-oxidative stability; (6) good solubility in environmentally benign and safe solvents; (7) no perceivable color change of substrates; (8) reversibility, *etc* [29]. The common water-repellent products used for stone protection will be introduced in the following paragraph.

1.1.3.1 Traditional materials for stone protection

The history of surface treatment of stone objects dates back to ancient Greek and Roman periods, when natural materials such as oils and waxes were used for protection and polishing purposes. Oil (walnut oil; linseed oil *etc.*), wax (beeswax; ceresin wax *etc.*), natural resins (rosin; dammar; mastic *etc.*) and their mixtures were prevailing as water repellents until the advent of 19th century when the petroleum industry revolution broke out. Beeswax, paraffin wax and its modern equivalent micro-crystalline wax were widely applied as water repellents for sculptures in 19th century and early 20th century. In the meanwhile, other traditional methods based on sacrificial layers such as plasters, stucco or paint were used for surface maintenance [30].

1.1.3.2 Synthetic polymeric materials for stone protection

Since the second half of 20th century, large varieties of synthetic polymeric materials, originally manufactured for industrial applications, have almost totally replaced natural resins in stone protection. The main reasons for their popularity are their diversity in type

and range of applications and the possibility of individualised or performance-oriented adjustment during production [31]. Among those synthetic polymers, acrylic and silicon-based products, perfluoropolyethers (PFPEs) are the most representative compounds [32].

- **Acrylic polymers**

Polymers based on various acrylics, which are known as Paraloids, are widely used in the protection of stone. Polyacrylics are synthesized by the addition polymerization of the corresponding monomers. Derived from acrylic [CH₂=CH-COOR] and methacrylic esters [CH₂=C(CH₃)-COOR] obtained from different alcohols, acrylic polymers used in stone conservation contain acrylates and methacrylates in the form of homopolymers and copolymers. Acrylic-based protective materials have moderate hydrophobicity and well adhering properties. Among all the acrylic resins commercially available, Paraloid B72 (figure 1-4) as a representative product, is the most widely used product in stone protection till now. It is soluble in most organic solvents, *e.g.*, ketones, esters, aromatic and chlorinated hydrocarbons [33].

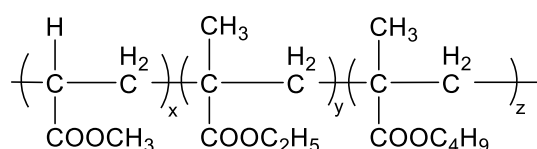
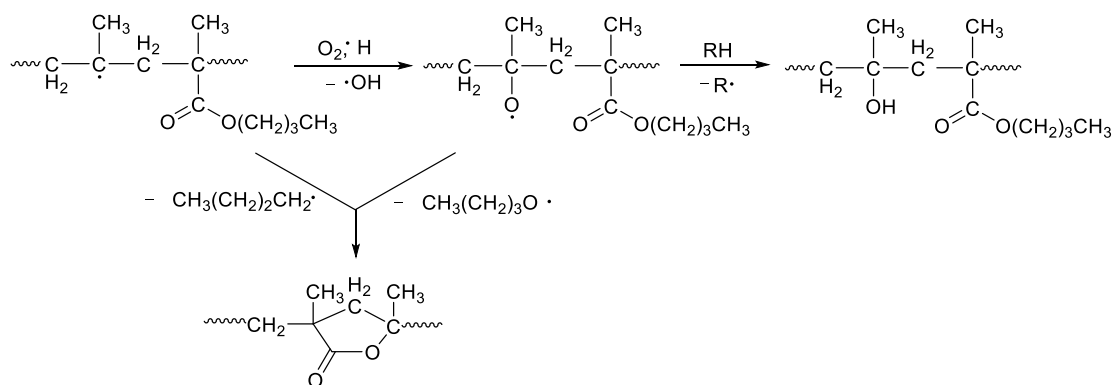


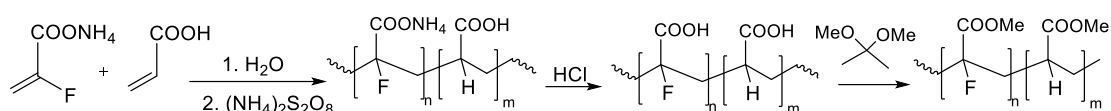
Figure 1-4: Paraloid B72

However, polyacrylics have been proved to have low photo-oxidative stability. Upon exposure to UV radiation, the side ester groups and the hydrogen in the α position to the ester group break away from the polymers and may cause formation of small fragments and extensive crosslinking. Oxidation is favored by the presence of hydrogen atoms located on the tertiary carbon of the acrylic units, or eventually by the ester groups of the side chain, which may be easily removed by radicals formed in the system through Norrish I and Norrish II type reactions as side chain reactions. This chemical decay of the acrylic-based polymers can lead to the formation of oxidized species such as γ -lactones (scheme 1-1), which finally causes yellowing polymeric coating appearance on the stone surfaces [32a].



Scheme1-1: Chemical decay of the acrylic-based polymers

Two procedures used to improve the properties of acrylic resins include copolymerization and blending. An example of blending is the dissolution of B72 in an alkoxy silane (*e.g.* methyltrimethoxysilane), which induces high adhesive properties for consolidation applications. On the other hand, the comonomers used in copolymerization are frequently fluorinated monomers [33b]. Mazzola *et al.* reported the synthesis of polyacrylic esters containing variable amounts of fluorine in the α -position of the main chain to improve resistance towards photo-degradation by the higher stability of the C–F bonds. These products were obtained from copolymerisation of ammonium 2-fluoroacrylate and acrylic acid. The polyacrylic acids were esterified using different procedures with BF_3 or TMSCl as catalysts [34] (scheme 1-2).



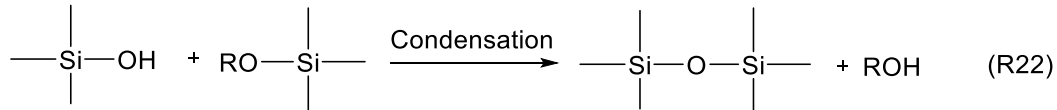
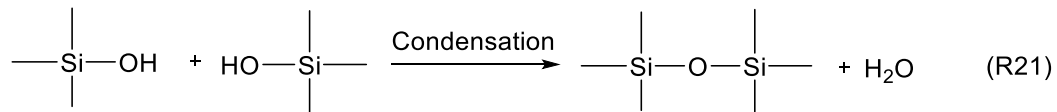
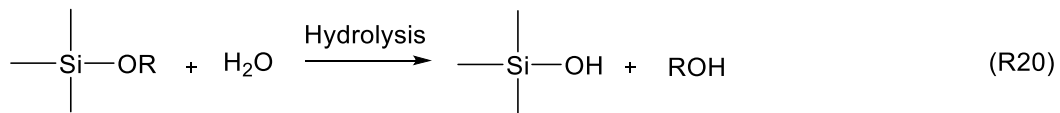
Scheme 1-2: Synthesis of polyacrylic esters containing variable amounts of fluorine

- **Silicon-based compounds**

Since 1960s, silicon-based resins have been introduced and widely used as protective products for stone. Silicon-based resins derive from step-growth polymerization, during which water or alcohol molecules are usually eliminated, causing volume changes. Various commercial products have different polymerization degree, *e.g.* monomers (alkyl alkoxy silanes), oligomers (poly alkyl alkoxy silanes) and polymers (polysiloxanes). They have stronger resistance to atmospheric deteriorating agents (*e.g.* solar radiation, heat, humidity) in comparison with acrylic resins, ascribing to the stronger Si–O bond (110 kcal/mol) than C–O bond (80 kcal/mol) [35].

During protection treatments of stone, silicon-based resins are either applied as pure resins or in solution, relying on the polymerization degree: monomers, oligomers and polymers. Among them, oligomers are frequently employed as protective agents. They generally form transparent polymers with good adhesive properties, excellent water repellence and good chemical, thermal and photo-oxidative stability [36].

The alkoxy silanes (or silanes) such as methyltrimethoxysilane (MTMOS) and tetraethoxysilane (TEOS) have widely been used as protective and/or consolidation materials since 1980s [35]. After the application of the protective coating on the stone surface, the alkyl alkoxy silanes are hydrolyzed by water to produce alkyl alkoxy silanols [R20]. Then, alkyl alkoxy silanols condense to form a polysiloxane (or silicone) with elimination of water or alcohol (R21 and R22) [33b]. The alkyl-modified alkoxy silane-based coatings are mostly known as organic–inorganic hybrid systems because of their alkyl groups as organic component and silicon backbone as inorganic one [37].



One significant feature of silicon-based compounds as water repellent is their adhesion property. These products form hydrogen bonding with substrates and expose their alkyl group to solid/air interface in order to give the desired hydrophobicity. However, the alkoxy silanols can also react with hydroxyl groups of some specific stones, *e.g.* sandstone [31]. Figure 1-5 shows the proposed interaction between the silicon-based compounds and the stone substrate. The reaction with stone and the *in-situ* polymerization may cause great problems for removal and reapplication. The poor reversibility is shown by the significant reduction of their solubility after complete polymerization. Therefore, the treatment does not satisfy the basic requirement, which is reversibility, for stone protection.

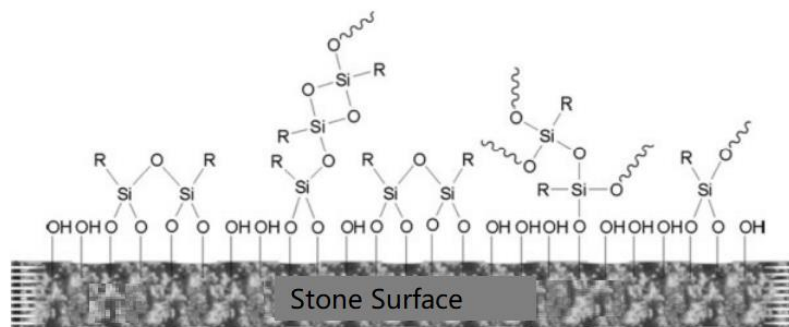


Figure 1-5: Proposed interaction between silicon-based compounds and stone substrate. [33b]

- **Fluorinated Polymers**

Fluorocarbon polymer makes excellent hydrophobic surface coatings as stone protection product. The hydrophobic properties of a material can be evaluated by measuring the contact angle of a drop of water deposited on the surface. If a surface has a contact angle with water that is more than 90°, then the surface is classed as hydrophobic, if the contact angle is less than 90°, the surface is hydrophilic. The higher the contact angle, the more hydrophobic, or water-repellent, a surface is. The maximum contact angle is 180° for a completely spherical droplet. If the contact angle is reduced to less than 90°, then the surface is more hydrophilic; and it approaches to 0° if the water sheets over the whole surface (*i.e.*, super-hydrophilic coating) [38]. One basic approach to increase the contact angle and surface hydrophobicity is to change the surface chemistry by lowering the surface energy. Among various polymers that are known as protective materials with critical surface

tension less than water (72×10^{-3} N/m) and hence poorly wetted by water, fluoropolymers are well known because of their unique properties such as photostability, oil and water repellency, antifouling property, and minimized critical surface tension. Because of their small size, fluorine atoms can shield a fluorinated carbon atom without any steric stress. Fluorine is difficult to polarize. This results in low intermolecular force and hence low surface tension of fluoropolymers. [38][39]

Perfluoropolyethers (PFPEs) are oils with relatively low molecular weights (5000-7000 g/mol). The ether linkage (C-O-C) endows high flexibility to polymer chains, and PFPEs have low $T_g < -90$ °C. Owing to high bond energy of C-F bond and to highly electronegative fluorine atoms, PFPEs possess high hydrophobicity, high chemical, thermal and photo-oxidative stability. Therefore, PFPEs have been suggested and applied as water repellents for stone conservation since 1980s. Fomblin YR® (figure 1-6), the non-functionalized oil, derived from photo-oxidation of hexafluoropropene, was the first PFPE compound used for stone protection [40]. However, it showed a weak interaction with the stone material, shortening the duration of the protective action. The adhesion between the stone substrate and the basic PFPE coating is *via van der Waals* force and, thus, is very weak when such compound is directly attached to substrates [7].

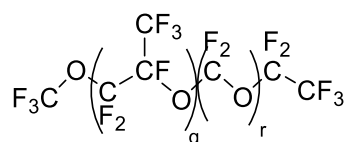


Figure 1-6: Fomblin YR®

In order to increase the interaction between PFPEs and stone substrates, polar groups (typically amide functions) were introduced to the basic PFPE. PFPE bound to polar groups showed better hydrophobic properties and improved the durability of the water repellency. This behavior was explained by the interaction with the stone through dipolar interactions between the -CO-NH- groups and the polar surface [41]. Unfortunately, due to the limited solubility of these compounds, their use as protective agents for historical stone artifacts has been abandoned since 1995. Eligible protective materials for stone artworks are required to have good solubility in non-toxic, environmentally friendly solvents. Recently, a new low average molecular weight hydrophobic agent containing short perfluoropolyether fragments linked to an oligo(ethylenesuccinamide) chain (SC2-PFPE), soluble in environmentally friendly solvents, was synthesized [42].

The synthesis of a series of partially perfluorinated oligoamides using perfluoropolyether segments grafted to the two ends of the oligoamidipamide [43] and oligosuberamide [44] were reported. Detailed information about the synthesis will be given in the section 4.1.2.2. Those partially perfluorinated oligoamides showed good solubility in alcoholic and hydro-alcoholic solvents. Application can be done by simply brushing or depositing their solutions on stone surface. Also, good hydrophobic effect and durable adhesion to the polar substrate were achieved on stone substrates with different porosity (like Lecce stone and marble). Considering their good performance on stone protection, our work has been inspired by those partially perfluorinated oligoamides. To promote solubility in alcoholic solvents and

modify the interactions with the substrate, hydroxyl functions using dimethyl tartrate and C-glycoside are proposed to be introduced in partially perfluorinated derivatives.

1.2 Blanching easel painting restoration

1.2.1 Easel painting

Painting is the application of color on a surface. This is the simplest general definition that can be made. Easel painting is a term in art history for the type of midsize painting that would have been painted on an easel, as opposed to a fresco wall painting, a large altarpiece or other pieces that would have been painted resting on the floor, a small cabinet painting, or a miniature created sitting at a desk, perhaps also on an angled support. It does not refer to the way the painting is displayed; most easel paintings are intended for framed and wall hanging displays [45]. Humans have expressed themselves in an artistic form since the beginning of mankind. One of the most important form of this expression is the easel painting, which presence has been witnessed throughout the history. The significance of these artworks derives from the fact that they are reflecting knowledge as historical documents representing political and social standings and to evoke emotions. They express the artist's ideas through a two dimensional form and depending on the choice of materials or techniques that can be used the painter creates a distinctive visual image [46].

Moreover, paintings have a complex, and heterogeneous layered structure containing various inorganic and organic materials: support (wood, canvas), pigments, binders and varnishes. During time, paintings may suffer different degradations due to the action of environmental factors (light, temperature and humidity), inadequate storage conditions and human interventions [47]. In the following, the details about layered structure of easel painting will be introduced.

1.2.2 Stratigraphy of an easel painting

The term easel painting describes an object consisting of a support, like canvas, wood or paper on which a colored layer has been applied. Generally speaking, all paintings follow the same structure with some variations depending on the substrate and the artist's choice of materials and techniques.

The structure of an easel painting is usually made of a support, size layer, preparatory layer, paint layer and sometimes a varnish (figure1-7) [48].

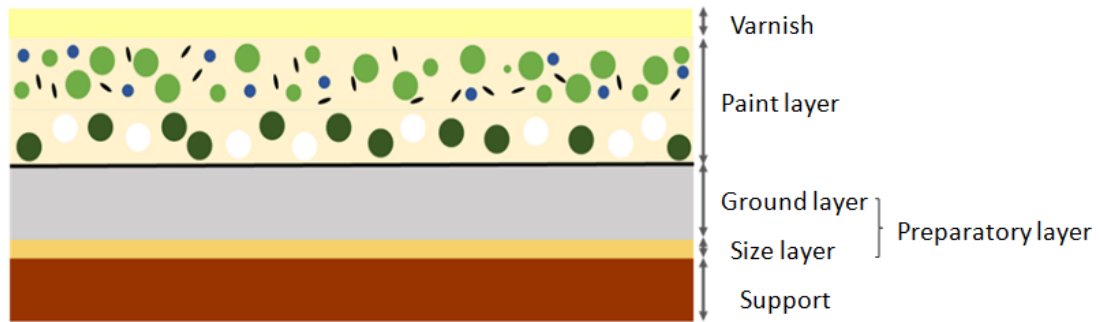


Figure 1-7: The structure of an easel painting

Support: Supports can be categorized based on the level of rigidity. The most used materials are wooden panels and the canvas.

The preparatory layer: It is applied between the support and the paint layer in order to smoothen the surface and reduce the binder absorption from the paint layer by the support.

Paint layer: It is the painted layer composed of a binder and pigments and it is the most essential part of the painting.

Varnish: It is a transparent coating, which covers the paint layer providing an aesthetic function altering the optical properties and protecting the paint layer from mechanical scratches and dirt [49].

1.2.2.1 Support

Portable supports for paintings were firstly formally mentioned in Elder Pliny's book "Natural History chapters on the history of art" in which he wrote: "Protogenes was not at home, but a solitary old woman was keeping watch over a large panel placed on the easel". [50]. The main supports used in easel paintings over the centuries in Europe are the wooden panels (oak, walnut, poplar, conifers, etc.) and the canvas stretched on a frame. Copper, leather, glass, stone or even paper supports are more rare, but they were also used as supports in easel paintings [48].

Wood has been used as a support since the encaustic paintings of the ancient Roman Egypt period. From 12th to 14th century in Italy, painting on panels started to be works of great importance, mainly altarpieces or other religious works. Textile as a support is traced in the ancient Egypt where natural fibers were used, and the most common choice of canvas is linen. After 13th century, textile is used as a structural component in panel paintings. When decline of panel painting started in the Renaissance period, the use of canvas started to become popular. The rise of oil painting led to the evolution of the support media. The canvas support has many advantages, which can explain its rapid adoption by painters [51]. It was less expensive compared to wood, it could create larger paintings with less weight, it can be easily rolled up and therefore it was easier to transport [52]. Wood panels are also heavy and can tend to split. A support with flexibility has to be used to avoid mechanical stress. Fabric stretched over a frame resolved the two major problems of weight and elasticity [53]. The main types of canvases are:

- Linen canvas: The linen textile originates from flax, which is the most common ancient plant fiber used in ancient times. Chemically, the fibers are 70 to 80 % cellulose and contain the same amount of oil found in plant seeds. Fiber cells are presented under microscope as long transparent, cylindrical tubes, which may be smooth or striated lengthwise. Flax is a particularly inextensible fiber. It stretches only slightly as tension increases, so linen is more difficult to stretch than cotton canvas but on the other hand it is a very durable substrate [54].
- Cotton: cotton is another material for canvas. Cotton has shorter fibers than linen and is composed of almost pure cellulose meaning that it is easily affected by acids and bleach. Consequently, it can only be used after sized before the application of oil paint in order to be protected against acidity [55].
- Commercially prepared Canvas: An alternative choice for artists who do not wish to prepare a painting support themselves is to use commercial canvas. The preparation of a canvas is a complicated process, which requires long time. For that reason, artists frequently choose this simpler option. The main disadvantage is that it is not possible to know the exact consistency of the materials and the solution that was used for the preparation of the canvases [56].

1.2.2.2 Preparatory layer

The preparatory layer contains a number of layers, which are present between the support and the paint layer [46]. The purpose of this layer is to create a solid, compact and smooth surface to decrease the irregularities of the support and stabilize it. Preparatory layer is sealing the support and reduces penetration of the binder, which can cause damage in the support. Additionally, it affects in a positive manner the aesthetic effect of the paint layer since the optical properties of the preparatory layer act on the visual behavior of the upcoming layers [57].

- ***Size layer***

The support is first prepared with an application of size after being stretched. The Merriam Webster online Dictionary (accessed January 2013) notes that the word size is used to describe a layer applied to stiffen or fill pores in different surfaces. Size is a diluted glue, most typically made from animal skins. The use of starch and flour paste have also been described. As a general rule, size layers do not seem to contain pigments or fillers; however small additions of pigments that render the layer distinguishable from the support are mentioned in some sources [46]. The size prevents the binder in the subsequent layers of the painting from being absorbed into the support, thereby weakening the painting. In addition, the size prevents the penetration into the support of binders and vehicles that may have a deleterious effect on the support material. In the case of canvas, the size also shrinks the fabric to a taut and smooth membrane (held, of course, by the stretcher) [45].

- **Ground**

Ground layer covers the sized support to further protect it from the adverse effects of binders and to block the absorption of the binder into the support. It consists of a filler or a pigment mixed with an organic binder that gives the appropriate elasticity and impermeability. The distinction between pigments or fillers lies in the function of the particles. Fillers mainly provide bulk, although they may also influence rheological behavior, whereas pigments consist of particles that have a distinct effect on the layer colour.

It is essential to apply this layer to isolate the support from the paint layer as the binder from the paint layer can deteriorate the fibers of the canvas. Moreover, it reduces the irregularities of the support creating a flat surface for the application of the paint layer and provides the desired optical effect that the painter wants to achieve since it creates a colorant surface as substrate [58]. Each type of ground is suitable for a particular support. The composition of the ground also depends on the pictorial technique used like oil or tempera. Generally, for rigid supports (wood panels) it is preferred to use water-based grounds, while for flexible supports (textile) it is better to use oil-based grounds that have better flexibility. The most commonly used grounds can be classified in two categories according to their composition:

-Gesso ground: They were water-based calcium carbonate or gypsum grounds mixed with animal glue. Calcium carbonate (CaCO_3) was the most used filler by the northern Europe artists and the Flemish school. On the other hand, calcium sulphate, or gypsum (calcium sulphate dihydrate, $\text{CaSO}_4 \cdot 2\text{H}_2\text{O}$) was most commonly found in southern Europe and especially in Italy and Greece [59]. Gesso grounds were developed for panel paintings and were also used in canvases during the transitional period from wooden supports to canvases. The most common ground preparation used today is a gesso containing a binder of acrylic polymer, which replaces the animal skin glue used in traditional gesso. Traditional gesso grounds produce a white, opaque surface. In addition to its protective function, the ground also acts as a reflective surface beneath the paint film [60].

-Oil grounds: They were oil-based grounds that use a drying oil the most common being linseed and walnut oils as binders. The oil binders were usually mixed with white or colored pigments. In the case of a colored ground the most used pigments were natural earths while for white color ground lead white was used, due to its siccativ properties. In 17th century sources written in English, oil-based ground layers applied to canvas are often described with the term primer [61]. The act of applying a preparatory layer is referred to in historical recipes as priming [62].

The illustration of a painting shown in figure 1-8 is known as a cross-section, which depicts the layers of a painting as seen from its edge, perpendicular to the normal surface view [46].

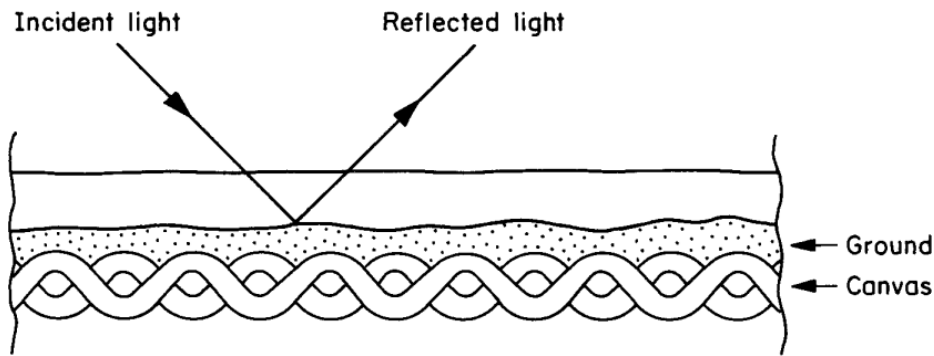


Figure 1-8: Light passing through a layer of paint and reflected by the ground layer. Not all paint films allow light to pass to the ground, and the amount of light reflected is dependent upon the characteristics of the pigment and binder components of the paint.

This view allows us to understand, in this case, how light interacts with the painting. As we will see in discussing the optical properties of paint films, light passes into the film and may penetrate up to the ground. If the light is reflected back by the dense white surface, we will perceive luminosity in the painting, a quality cherished by many painters. However, some grounds are not white. The painter can decide to add certain colors to the ground mixture to act as a base for overlaying colors. A cool tone (blue-gray or green) sometimes underlies the warm colors of flesh. A brilliant white ground may well confer desirable characteristics to the paint film, but to many painters, it is a disturbing surface to face when starting a painting. A thin layer of color called an imprimatura may be applied over the ground to act in a way similar to a toned ground, and may also serve to seal a somewhat absorbent gesso. Painters sometimes find these colors useful as the painting develops. Areas of either toned ground or imprimatura may be visible in a finished painting [45].

1.2.2.3 Paint Layer

The term paint layer characterizes a dye substance, forming a thin layer that is placed on the top of the preparatory layer. The thickness of the layer depends on the aesthetic effect that the artist wishes to achieve as well as the type of materials that he uses. It consists of a binding medium that is transparent and homogeneously distributing the particles of the powdered coloring material. These materials are defined as pigments, providing the paint layer with the color and exhibiting hiding properties. The pictorial layers of oil paintings consist of pigments ground in a binder (oil) and possibly additives (fillers, diluents, resins) [45] (figure 1-9). The proportions of the various elements depend on the nature of the pigments (oil uptake) and the desired properties in terms of rheology (viscosity, consistency, adhesion) and appearance (color, roughness, shine, opacity, transparency, etc.).

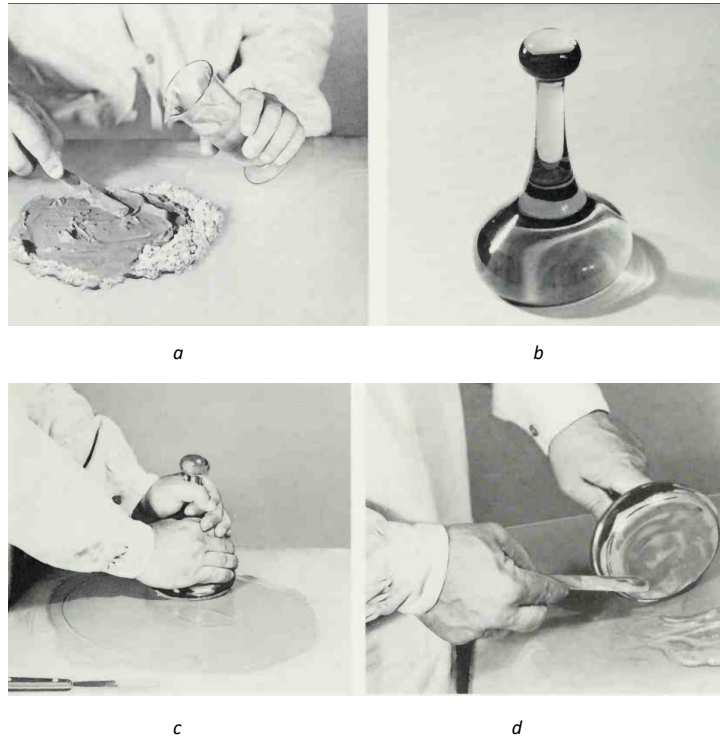


Figure 1-9: a) Mixing dry pigment and oil to a stiff paste consistency; b) A glass muller for grinding colors; c) Grinding the oil and pigment paste to a smooth dispersion; d) Gathering the batch during grinding

The choice of the binder and the pigments depend on the type of support that the artist will choose to use as well as the optical characteristics the painter intends to highlight. Though the centuries, artists have experimented various materials and application methods to achieve their vision.

- **Binders**

Binders are substances that have the ability to form a thin layer where the pigment particles hold together. When the binders are in liquid form, they act as a dispersing agent (vehicle) for the pigments to form a homogeneous paste. After application of this paste on the substrate, through a physical or chemical procedure, the particles of the pigments stay on the surface where they were applied [63].

The binding media can be classified according to their chemical properties (table 1-1) [46]. In this work, drying oil is chosen as binder.

Classes of organic molecules	Natural products
Proteins	Animal glue Egg white Egg yolk (also contains lipids) Casein (also contains sugars and lipids)
Lipids	Drying oils Waxes
Carbohydrates	Plant gums (polysaccharides) Honey (simple sugars)

Table 1-1: Classification of natural binders by composition

Each binding medium is characterized by specific physical, chemical, and optical properties that provide a different aesthetic result in the painting. The binding media must have film-forming properties. This means that the binder must have cohesion, internal strength to hold together the paste and adhesion for binding the paste to the substrate [64]. Moreover, the binder film has a porosity, which is either intrinsic of the material or due to collection of holes, fissures, breaks, and cracks existing in the film. These properties are influenced by the way in which the film is formed and the processes that take place during aging [65].

A material must have specific optical properties in order to be used as a binder. The most important optical properties are transparency and colorless, since the color of the pigment has to be highlighted. Its binder has a specific refractive index, which can influence the aesthetic quality of the paint layer by changing its opacity [66].

Drying oil will be mainly introduced in the following content, considering it was used in the research project of this PhD thesis.

The most common drying oils used in oil paints are linseed, walnut, and carnation (poppy) oils due to their drying properties, meaning their properties to dry and make a solid film. An oil is considered to be drying if, exposed to air, it is able to form a solid film. From a purely chemical point of view, oils are essentially made up of triglycerides (glycerol triesters) formed from saturated fatty acids (5-15 % by mass) and unsaturated (85-95 %), a small amount of free fatty acids and impurities (mucilaginous substances, sterols, etc.) that the purification of the oil aims to eliminate. The most represented fatty acids in the triglycerides of drying oils are palmitic acid (C16:0), stearic acid (C18:0), oleic acid (C18:1), linoleic acid (C18:2), and linolenic acid (C18:3). The average fatty acid composition for linseed, walnut, and poppy oils is reported in table 1-2 [67].

Fatty acids	Palmitic acid	Stearic acid	Oleic acid	Linoleic acid	Linolenic acid
Number of C	16	18	18	18	18
Number of C=C	0	0	1	2	3
Notation	C16:0	C18:0	C18:1	C18:2	C18:3
% linseed oil	4-10	2-8	10-24	12-29	48-60
% walnut oil	9-11	1-2	11-18	69-77	3-5
% poppy oil	3-8	0,5-3	9-30	57-76	2-16

Table 1-2: Average fatty acid composition of drying oils used in easel painting

The dryness of oil mainly depends on the number of double bonds (unconjugated in the case of linseed, walnut, and poppy oils). Indeed, the oxidation mechanism that allows the "drying properties" of oils relies on crosslinking of double bonds present in acids. Thus, the more double bonds an oil contains, the faster the film formation will be. An oil must contain at least 65% of polyunsaturated carboxylic acids to act as a drying oil [68]. The good drying properties of linseed oils can be explained by its high percentage of linolenic acid containing 3 double bonds (48-60 %). In addition, heavy metals such as lead are initiators of oxidation, the addition of litharge (PbO) therefore increases the drying properties of the oil [69].

- **Pigment**

In easel painting, there are two types of coloring matters: pigments and dyes. According to Abraham Pincas, around 600 pigments and more than 3000 dyes are surveyed [70]. Pigments can be defined as "fine powders white or colored, insoluble or poorly soluble in the dispersion medium". The number of pigments available to painters has increased considerably over the years, mainly since 19th century with the development of chemistry and the arrival on the market of synthetic pigments.

By comparison, the options available to artists of 14th till 18th century, were very limited. The pigments commonly used during this period in Western painting were about 15. The most common were three blues, azurite (copper carbonate), ultramarine blue (lazurite), and smalt (cobalt glass), and possibly 4 reds, red lead (lead tetroxide), vermilion (mercury sulfide), iron oxide red, and carmine (made from the dried bodies of the cochineal, a South American insect) [46]. As the blanching of easel paintings often occurred in 16th till 18th century, those most common pigments were considered in the research project of the present PhD thesis [71].

The pigments used in our work are reported in the following table 1-3.

Pigment	Chemical composition
White lead	$2\text{PbCO}_3 \cdot \text{Pb(OH)}_2$
Calcium Carbonate	CaCO_3
Ivory Black, genuine	$\text{Ca}_3(\text{PO}_4)_2, \text{C}$
Raw Umber, greenish dark	$\text{Fe}_2\text{O}_3, \text{MnO}_2$
Green earth	$(\text{K,Na})(\text{Fe}^{3+}, \text{Al, Mg})_2(\text{Si, Al})_4\text{O}_{10}(\text{OH})_2$
Ultramarine blue	$\text{Na}_{8-10}\text{Al}_6\text{Si}_6\text{O}_{24}\text{S}_{2-4}$
Copper(II) acetate monohydrate	$\text{Cu(OAc)}_2 \cdot \text{H}_2\text{O}$
Blue Verditer, synthetic azurite	$2\text{CuCO}_3 \cdot \text{Cu(OH)}_2$
Azurite natural, standard	$2\text{CuCO}_3 \cdot \text{Cu(OH)}_2$
Lapis Lazuli, natural ultramarine	$(\text{Na, Ca})_8[(\text{SO}_4, \text{S, Cl})_2(\text{AlSiO}_4)_6]$
Ultramarine Ash	$(\text{Na, Ca})_8[(\text{SO}_4, \text{S, Cl})_2(\text{AlSiO}_4)_6]$
Red ochre	$\text{Fe}_2\text{O}_3, \text{FeTiO}_3$
Vermilion	HgS

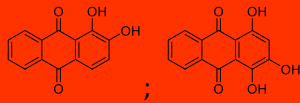
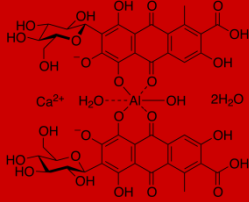
Natural Cinnabar	HgS(mineral)
Madder Lake, genuine	Alizarin ;Purpurin 
Red Lead, Minium	Pb ₃ O ₄
Carmine	
Lead Tin Yellow II	Pb(Sn,Si)O ₃
Lead oxide yellow	PbO

Table 1-3: Organic and inorganic pigments

- **Additives**

Numerous additives can also be used to modify the rheological properties, among which we can cite fillers and vehicle (or diluents). The most common filler used in easel painting is chalk (calcium carbonate). Its addition is justified by the need to have more consistency in the pictorial material, without changing its colour [72]. The refractive index of carbonate calcium (1.51-1.65) is similar to that of oil (1.48 for fresh oil and about 1.55-1.56 for an oil dating 17th century) [73]. Therefore, crushed in oil, the calcium carbonate will appear transparent and allow light to penetrate deeper into the pictorial layers, giving the impression of a layer slightly translucent. This property was often used by 17th and 18th century painters [74]. The addition of calcium carbonate might be motivated by technical (increase in consistency and transparency of the layer and decrease in the drying properties) or economical reasons (lower price than pigments).

The vehicle is compatible with the binder: water with egg, gums, and acrylic polymers; turpentine or petroleum distillate with oils. When mixed with the pigment and the binder, the vehicle allows the paint to be spread more easily and becoming a bit more transparent. It might also assist in drying the film. In all cases, the vehicle evaporates as the film dries.

1.2.2.4 Varnish

The painting can be coated after completion with a thin layer of varnish. The varnish is a transparent liquid material that performs two primary functions: it protects the paint film from abrasion, pollutants in the atmosphere, moisture, and dirt. Moreover, it can alter the reflective characteristics of the paint. The painter can find that certain colors have dried matte while others have dried glossy. If the desired effect is a glossy surface, the application of a gloss varnish will make all colors uniformly glossy [63]:

Over the centuries, varnishes have been prepared from a wide variety of resins: rosin,

sandarac, copal, mastic or dammar typical of 19th century. From middle of 20th century, the use of synthetic varnishes intensified in the field of restoration of easel paintings, for example: Paraloid B72 (high molecular weight acrylic resin) MS2A (ketone resin), Laropal A81 (urea-aldehyde resin) or Regalrez 1094 (low molecular weight hydrocarbon resin). The varnishes can be categorized according to their composition and drying process [75]:

- Oil resin varnishes:

They were first introduced in 14th century. They were a mixture of drying oils with resins, prepared by dissolving powdered resin into hot oil. This type of varnish dries by oxidative polymerization of the oil to produce a glossy and insoluble film.

- Spirit varnishes:

In 16th century spirit varnish gradually replaced the oil varnishes. This type of varnish was prepared by solubilizing resins, as well as some other resinous materials like shellac, dammar, and sandarac in a solvent, which evaporates during the drying process. The most common solvents used were alcohol and essential oils like turpentine. These varnishes are easily removable that is a very good characteristic for conservation process.

1.2.3 Blanching in easel paintings

1.2.3.1 Terminology clarification

The term “blanching”, literally, “to make white by withdrawing color”, is used to describe the whitish appearance on easel paintings. [76] This definition is essentially based on a visual appreciation. Therefore, that is confusing in the literature descriptions when the different mechanisms behind the phenomenon are considered. Summarizing data reported in the literature, we can say that there are mainly three points related to the term “blanching” to note and clarify.

- In the literature, blanching has been used mostly as a generic term to describe any whitening caused by a physical defect in the paint layer or the surface of paintings. [76][77]
- However, some authors use the term as a synonym to “whitening” but do not necessarily intend to imply a physical degradation of the paint film. [78]
- The term “bleaching”/“fading” and “blanching” should be well distinguished. “Bleaching”/“fading” is also used to describe a whitish appearance on paintings. But “bleaching”/“fading” specifically refers to discoloration/color loss of the pigments in particular of organic pigments such as the Red and Yellow Lake that are light-sensitive and are susceptible to photochemical degradation. [79]

In this thesis, the term “blanching” refers to the whitish appearance on easel paintings induced by a physical defect.

1.2.3.2 Causes

Blanching is a frequent alteration appearing on easel paintings, which can affect the varnish layer and also the paint layer, strongly altering the visual aspect of the paintings (figure 1-10). It is an optical phenomenon that is induced by a physical degradation. Genty *et al.* reported that blanching is recorded in 875 paintings among the total 22438 paintings reported in EROS (European Research Open System) database available for consultation at the C2RMF. [71] It is commonly encountered by conservators in the old master easel paintings between 16th and 18th century. Depending on the degree of degradation, the paint composition can be hidden partially or totally by a whitish haze. Blanching does not appear homogeneous. Altered, less altered, and unaltered areas can coexist within a same color range. [8] Moreover, blanching is a recurring phenomenon with the limited performance of traditional restoration treatments. Understanding the causes that promote the formation of blanching is extremely important. In that way, paintings that are susceptible to this phenomenon can be recognized and measures can be taken to prevent the formation or aggravation of blanching. However, studies performed in the 80s and 90s, did not report full understanding of the causes of blanching as a complex alteration on easel paintings. [76][78] A big advance on the causes responsible for blanching came in 2010, by Genty *et al.* [71]. The proposed causes behind blanching are summarized according to those literatures. Those causes could be roughly divided into two categories according to previous researches and will be discussed herein further.



Figure 1-10: a) Blanching on varnish layer. Louis Crignier, *Jeanne d'Arcen prison*, 1824, Musée de Picardie. © C2RMF/Anne Maigret; b) Blanching on paint layer. Jean-Baptiste Siméon Chardin, *Les attributs des arts*, 1765, Musée du Louvre. © C2RMF/Pierre-Yves Duval. [71]

- **External cause of blanching: Humidity**

One proposed cause of blanching is relative humidity. Humidity coming from the storage environment could contribute to the blanching phenomenon. For example, blanching was reported to appear on the paintings kept in an excessively humid environment, such as churches and storerooms, by Rioux and Mills. [80] The high humidity could be also due to water damage like flood or rain. Dandolo *et al.* reported about the painting “*Le Jeune Trioson*” that was severely damaged because of the exceptionally severe flood of the Loing river in 2016, when several areas of the museum were submerged, including a storage area where the painting was located. [81] Severe blanching of the varnish layer followed prolonged

contact with water, strongly affecting the legibility of the painting. Lank reported about an 18th century Venetian oil painting on canvas that had been accidentally left in a leaking case during several days of heavy rain. The paint below the varnish was completely blanched. [82] Moreover, humidity leading to blanching could be related to aqueous conservation treatments. Groen reported when restorers in England were asked about their experience with blanching. It seemed clear for them that water was the main reason whether used in cleaning, blister laying or relining. [76] In particular, the combination of heat and moisture, which are required in glue-paste lining processes is often suggested as a cause of blanching in 17th century paintings. [83] Wyld *et al.* also reported that the relining of "*Landscape with the Marriage of Isaac and Rebekah*" (painted by Claude Lorraineca 1600-1682) in 17th century, using an aqueous adhesive helped the blanching appearing in the painting [80b]. In one of Groen's research, nearly all of the blanching paintings by Claude and Gaspard Dughet (1615-1675) had been relined with a water-based starch paste. [76] Although the paste has not been fully investigated, starch in the paste indicated that the mixture was based on water. However, it is important to add that the majority of works relined does not present any blanching. That implies that humidity (and heat) as an external factor is necessary but not sufficient to make a painting blanching. Therefore, humidity from the storage environment, water damage, or the conservation treatments, is a main external cause for blanching. But the internal factor of easel paintings themselves must be also considered.

- ***Internal causes of blanching: pigment, binder, drier, and varnish***

- **Pigment**

An interesting feature of blanching in easel painting noticed by researchers is that blanching is confined to certain color areas in the easel paintings. For example, Groen reported that in the paintings by Claude and Dughet, blanching was generally restricted to dark areas, especially green and brown ones. [76] In the paintings by Salvator Rosa and Honthorst the blanching appeared on the blues as well; Keith *et al.* reported that the blanching of "*The Large Dort*" (Aelbert Cuyp 1620-1691) particularly appeared in certain areas of the green foreground landscape. [83]

A more extensive investigation of the color area affected by blanching, was led by Genty *et al.* using the data collected from EROS. They investigated 371 blanching paintings and 80 deeply blanching paintings in the database. The result shows that blanching mainly appeared on green, blue, brown, dark and more rarely on other colors such as red, orange and yellow (figure 1-11). 73 % of blanching is located on green, brown, and blue areas in deeply blanching paintings. [71]

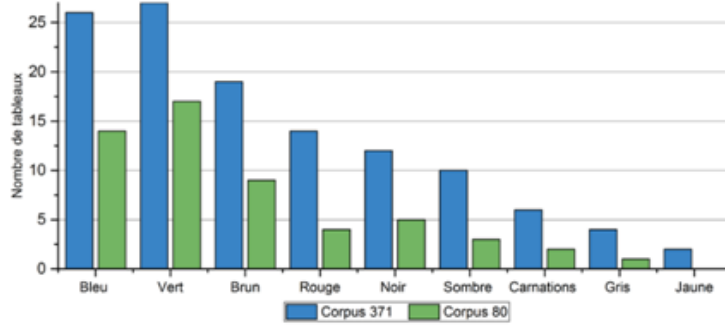


Figure 1-11: Occurrence of the blanching in different pigments [71]

All these observations demonstrate that the pigment composition of the paint in those color areas may in some way be involved in blanching formation. After deeper investigations of the blanching areas, Groen reported that paint sections, which contain significant amounts of chalk and hygroscopic pigments rich in silicates, namely green earth, brown, ochre, ultramarine, and smalt, are more easily affected by blanching. [76] Moreover, the mock-ups study by Genty *et al.* revealed a dependence on the pigment nature for blanching formation. Blanching could be reproduced on mock-ups made up of the pigments raw umber and green earth but not on samples made of azurite and ivory black keeping other conditions unaltered during sample preparation and aging process. [84]

Therefore, all the researches above described, indicate that the nature of the pigment, as an internal cause, has affected blanching in easel paintings.

- **Binder and extender**

Binder and extender are two other causes behind blanching according to previous results.

Concerning the nature of the binder, paintings made only with egg as a binder do not show blanching. Tanhuanpää studied a painting by the Finnish artist Unto Pusa, which was obtained with a mixed technique by using oil and tempera. The study results show that only the parts with oil displayed blanching, but the part prepared with egg did not. [85]

Moreover, Genty *et al.* investigated the evolution of the binder preparation processes driven from the 127 recipes in 19 old painting treatises in France [71]. The research was focused on the oils and driers used. The investigation revealed oils as binders hardly changed (linseed oil and walnut oil) between 16th and 19th century. The development of oil painting took place between 15th century and 19th century. Before 15th century, painters used tempera. And the use of oil was done very sparingly. At the beginning of 20th century, the oil was gradually replaced by acrylic. So blanching of paintings is more typical at the time that oil was commonly used as a binder.

Another important result obtained from their investigation is the use of the drier litharge that was often added in a large portion during the binder preparation process. Additionally, a surprising discovery by Groen was the demonstration of large quantity of chalk mixed with hygroscopic pigments in the blanching parts of Dughet and Claude paintings. [76] Moreover, the mock-up study by Genty *et al.* reports that proper quantities of litharge and the presence of chalk contribute to the blanching alteration. [84]

Considering all the information above described, it is reasonable that the nature of the

binder and extender are also the internal parameters affecting the blanching. The proper drier and presence of chalk facilitate the blanching.

- **Varnish**

As mentioned above, blanching is also observed on varnish layer of easel paintings. The research of Genty *et al.* shows that the property of varnish material is another factor that might have an influence on blanching. [84] Genty *et al.* successfully reproduced blanching on natural varnish (mastic and dammar) mock-up samples after aging, through immersion of the samples into distilled water for 31 days at room temperature. During tracking of this aging process, although both of the two natural varnish materials show blanching phenomenon, the alteration kinetics are different between mastic and dammar. The dammar varnish blanching appears more rapidly. Nevertheless, after 31 days, blanching is more visible for the mastic than for the dammar varnish. Moreover, synthetic varnish materials (Paraloid B72, Laropal A81, Regalrez 1094, MS2A) were also aged upon the same conditions. But no blanching could be observed in the synthetic varnish mock-ups. Therefore, the varnish material can also be considered an internal factor responsible for blanching.

In conclusion, the external cause is humidity and the internal causes are pigment, binder, extender, and varnish treatments that can affect blanching occurrence in easel paintings. Although Genty *et al.* developed a deep investigation on the causes of blanching, as a complicated alteration on easel paintings, blanching has been studied little by scientists worldwide. The causes responsible for blanching still need to be more clearly and fully understood from a scientific point of view.

1.2.3.3 Nature of blanching

Visualization of submicronic to micronic pores is a major advance toward the understanding of blanching of paint and varnish layers. This visualization of structural modification was detected thanks to Scanning Electron Microscopy (SEM) and an innovative approach requiring no sample preparation helps to maintain the original structures of blanching layers during SEM experiments.

- ***Porous structure in blanching paintings***

Groen reported blanching areas in Dughet's classical landscape ("Stourhead") were examined by SEM. It was observed that part of the surface was covered by tiny holes, 0.5 μm in diameter, many others smaller. The presence of these holes was not restricted to the surface layer; in the micrograph they are also sitting underneath. [76]

Recently, Genty *et al.* demonstrated the presence of a similar structural modification with pores, in blanching paintings. Concerning blanching of varnish, Field Emission Gun Scanning Electron Microscopy (FEG-SEM) was used to characterize the samples from two paintings with blanching varnish layers: "*Jeanne d'Arc en prison*" by Louis Crignier (1790–1824), and "*Vue de la fontaine de l'Encelade avec Jupiter foudroyant*" by Jean Cotellet (1642–1708). The results demonstrate a high correlation between the localization of the porosity in the

stratigraphy of varnish layers and the blanching. The pores are present in layer 3 that has become white and opaque but not in layers 4 and 5 (figure1-12). [84]

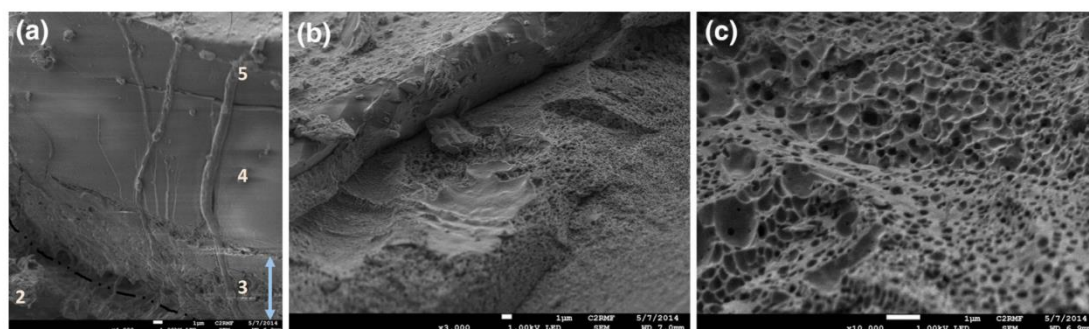


Figure 1-12: Varnish sample from Louis Crignier, *Jeanne d'Arc en prison*. FEG-SEM images at 1 kV; scale bar 1 μm . a) Edge of the sample, the presence of porosity in the blanched layer 3; b) Surface of the altered layer 3; c) Detail of the surface of layer 3. © C2RMF / A.

Genty-Vincent. [84]

The pore size ranging from 100 nm to 1 μm was measured. Moreover, no porosity was observed in the unaltered samples. On the other hand, a set of 40 paint layer microsamples from 12 French, Flemish, and Italian blanched oil paintings, ranging from the 16th to 18th century, were investigated using FEG-SEM. The results show that paint layers affected by that alteration have a highly porous structure compared to the ones that are not affected by blanching. Due to the presence of pigments, the internal structure of a paint layer differs from the one of a varnish layer. Pigment particles impose some constraints to the formation of pores, which are less spherical. In all samples, the range of porosity from about 100 nm to 2 μm was noticed. Moreover, complementary analysis by phase contrast X-ray nanotomography has shown that for the blanching of pictorial layers, the pores are localized in the binder. (figure 1-13) [8]

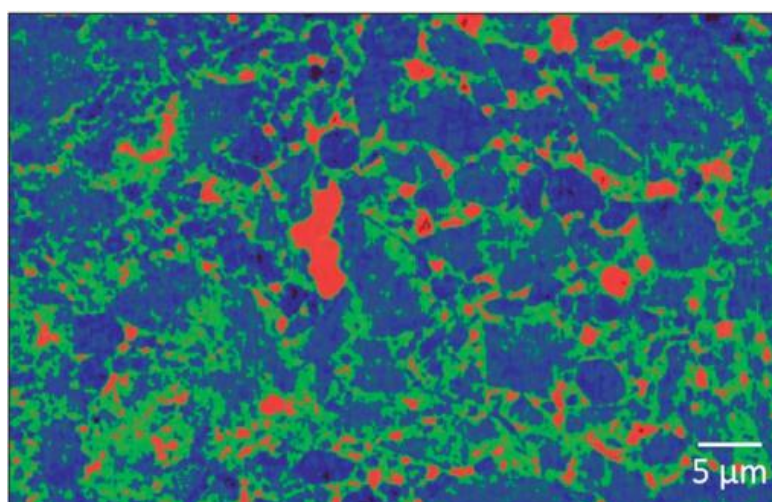


Figure 1-13: Complementary analyze by phase contrast X-ray nanotomography. The pigments are shown in blue, the binder in green and the pores in red. Johannes van der Bent, *Landscape, Figures and Animals*, 1650-1690, oil on canvas (inv. 794.1.1), Musée des Beaux-Arts

in Rennes. © C2RMF / A. Genty-Vincent.[8]

Meanwhile, the same phenomenon reported by Genty *et al.*, was also reproduced on

mock-up samples that were prepared according to historical recipes, by exposing the samples to heat (40-60 °C), high humidity (40-80% RH), and UV light (300–400 nm range). [84]

The visualization of pores both in varnish and paint layers made a major improvement to understand the nature of blanching. Summarizing the results of the researches above described, highly porous structures are observed on the blanching areas of easel paintings with SEM, but no pores are observed in unaltered areas. Therefore, the structure modification is considered highly related to blanching formation.

- **Blanching: an optical phenomenon**

The presence of porosity in the blanching areas of ancient paintings and mock-ups could lead to light scattering and as a consequence leading to opacification of the paint surface. For example, the difference in refractive index between the varnish ($n = 1.53-1.55$) and the pores probably filled with air ($n = 1$) contributes to a strong light scattering in the layers. The porosities can be assimilated to spherical particles, and the scattering Rayleigh and Mie theories can therefore explain the visual appearance of the altered varnishes. The mock-up varnish samples showed the pore size distribution corresponding to the exposure time in distilled water. A pore size of 20 to 300 nm with a maximum in the range 40 to 50 nm has been noticed near the surface after 1.5 days immersion in water. The sample has a pore size ranging from 25 nm to 1 μm after 5.5 days immersion. Finally, the opaque white sample totally altered, is composed of a combination of small and interconnected large pores of 25 nm–2 μm after 31 days water immersion.

The Rayleigh theory is used for particle sizes much smaller than the wavelength of light (radius of maximum 25 nm). When the particle size is greater than 50 nm, the Mie theory should be used. When the pore size increases, the porosity concentration becomes relatively high, and it induces an interconnection between the pores. Consequently, the percentage of solid matter will be too low to ensure the layer cohesion, leading to a possible disconnection between the varnish and the paint layers. This case has already been observed on the painting of Louis Crignier in the much-altered areas. (figure 1-14)

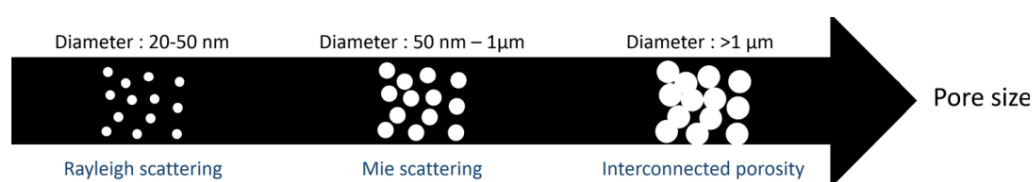


Figure 1-14: Correspondence between the visual appearance of the layer, the pore size, and the involved optical phenomenon [84]

As for the blanching paint layer, the pores are located in a binder surrounded by pigments, and the impact on the visual appearance is similar. As the pores have a size of more than 50 nm, the blanching can be explained by the Mie scattering of light.

Moreover, analyses have been performed on varnish and paint samples by FT-IR spectroscopy and GC-MS to determine if blanching is linked to a chemical modification of molecules in varnish and paint samples. The results have shown there is no significant

difference between altered and unaltered samples.

Therefore, blanching is an optical phenomenon that can be explained by light scattering theory. The light scattering by the pores explains the visual appearance of blanching. Although the mechanism of pore formation is still under investigation, recent results demonstrated that as molecular modifications could not be detected by GC-MS and FT-IR, blanching is mostly a physical phenomenon. [84][85]

Those conclusions can have a major impact for the development of appropriate conservation treatments to overcome the blanching of easel oil paintings.

- **Possible mechanism for pore formation**

The possible explanations for blanching in paint-layer and varnish layer are presented in the following paragraphs.

- **Varnish layer**

Genty *et al.* proposed a possible explanation for the blanching of varnish layer of easel paintings. [71] The natural varnish material (mastic and dammar) contains non-polar polymer (like polycadinene, cis-1,4-poly- β -myrcene) and a resin component. The resin of the natural varnish material contains tetracyclic compounds, which can carry polar and ionizable carboxylate groups. Metal cations were revealed to be present in natural varnish to form complexes with carboxylic acid moieties. Cations most present in the varnishes studied up to now are calcium, followed by sodium and also potassium cations.

By the strong force of interaction between anions and cations, carboxylic acids and metal carboxylates present in varnishes form dimers, then multiplets and finally ionic clusters. Those polar clusters will consequently be hydrated spontaneously in the presence of water molecules. The volume variation and micro-segregation could be induced by hydration of the clusters. And the variation in volume and micro-segregation induce the formation of pores. During varnishes drying, despite water in the pores was evaporated the cavities remained formed but empty. The light is then diffused by the pores, inducing a blanching effect in the macroscopic scale.

However, in the case of the synthetic varnish material (Laropal A81, Regalrez 1094, MS2A), the constituent molecules do not contain ionizable groups and they are highly hydrophobic. Therefore, they would not be hydrated and no micro-segregation would occur. Finally, there is no pore and as a result and no blanching with those synthetic varnish material occurs.

That can also explain the mock-up varnish samples by the synthetic material that did not reproduce blanching. [84]

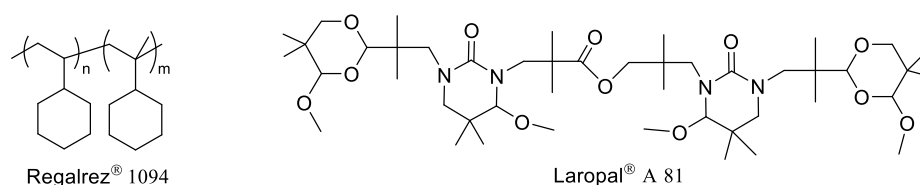


Figure 1-15: Regalrez 1094, Laropal A81[87][88]

- Paint layer

Genty *et al.* proposed ionic clusters could be formed during the preparation process of binder. [71] Drying oils (linseed oil and walnut oil) in binder are mainly made up of triglycerides and free fatty acids (0.5 to 2 % of the total weight). Indeed, ancient treatises frequently recommend heating the oil with water and litharge. The heating could promote the hydrolysis of triglycerides and forming free fatty acids. The driers, litharge, and chalk could form metal carboxylates with the free fatty acids. Free fatty acids and metal carboxylates could be able to form clusters. Similar with the natural varnish material, the hydration of the ionic clusters will cause volume variation and micro-segregation, and consequently pore formation. This hypothesis could correspond to the phenomenon observed in blanching mock-up samples produced by Genty *et al.* [71][83] The ancient treatise reports the use of heating oil up to 100 °C with water and with 4.8 % (w/w) litharge. FT-IR analysis proved the presence of lead carboxylates. The mock-ups were prepared mixing the binder with a large quantity of chalk (30% w/w) and pigments. After aging the mock-ups in a humid environment, the blanching was successfully reproduced in green earth and raw umber as pigments. Therefore, reproduction of blanching in paint-layer mock-ups was in agreement with the proposed explanation.

In addition, Epley *et al.* [89], proposed a possible explanation for blanching of paints containing hygroscopic dryer (litharge and chalk) and pigments (green earth, brown ochre, ultramarine and smalt). Because of their hygroscopic nature, these driers and pigments can absorb water on their surface. The swelling and shrinking of the paint upon changes in moisture, could cause disconnection between the pigment and the medium. The lack of close contact between pigments and media through the formation of pores could then increase scattering of the light with an impact into the the painting appearance.

We can conclude, that although the mechanism of pore formation requires further investigations, this could mostly be ascribed to physical effects more than to molecular modifications that up to now have never been detected according to some recent research results.

1.2.3.4 Restoration

Up to now, the investigation of the nature of blanching shows that blanching on varnish and paint layers on easel paintings are optical phenomena, and the visual appearance of blanching is caused by light scattering by the pores into the layers. Therefore, the treatments for restoration will be effective and long lasting, only if the material absorbs or sustainably fills the pores, in order to limit the diffusion of light.

Traditional and innovative restoration treatments used to decrease and hopefully completely remove blanching from easel paintings are reported in the following paragraphs.

- ***Traditional restoration treatment for blanching paintings***

Wyld *et al.* specify a number of traditional methods of treatment, such as rubbing with egg or oil, treatment with solvents, scraping off the top layer of the paint,

“Pettenkof(t)erring”, and the use of heat. [79b] Koller *et al.* reported the use of wax against blanching. [9] Lank reported the use of high boiling point dimethylformamide vapour to restore blanching oil paintings. [81] In some cases, solvents, such as diacetone alcohol, glycol, cellosolve solvent, cellosolve acetate, morpholine, triethanolamine, dimethylethanolamine, and dimethylformamide were reported to be used for restoring blanching oil paintings. [8] However, these methods were not recognized as scientific methods but more related to “folklore”. Moreover pores are not permanently filled and the blanching reappears.

- **Innovative restoration treatment for blanching paintings**

Recently, Genty *et al.* reported the use of perfluoropolyether diamide (DC6G900) with a molecular weight of 1840 g/mol on restoration of blanching paintings (figure 1-16). [8] DC6G900 is chemically inert and thermally stable. It has a viscosity of 1850 cP at 25 °C and a surface tension of 0.02 N/m. [71]

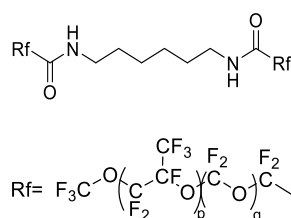


Figure1-16: DC6G900

The restoration performance of DC6G900 and other products were evaluated on old blanching paintings (table 1-4). For the area treated with diacetone alcohol and dammar, blanching reappeared once the solvent was evaporated. However, blanching was effectively decreased by DC6G900 being still effective after 30 days. Moreover, DC6G900 can be easily removed with perfluorooctane, which keeps the restoration treatment reversible. Therefore, DC6G900 as a perfluoropolyether diamide is a promising product and it offers new perspectives for restoration of blanching easel paintings, according to the results by Genty *et al.* [71] This compound was also used as stone protective agent.

Moreover in the present PhD project we modified DC6G900 introducing hydroxyl, amide and amine functions, in order to create a stronger interaction between the porous paint materials. The perfluorinated residue was also modified to reduce environmental impact problems.

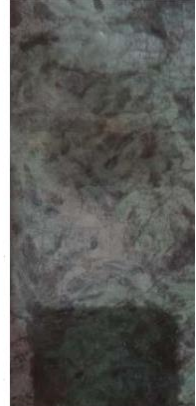
	Blanching	T= 1 min	T= 5 mins
Diacetone alcohol			
Dammar			
DC6G900			
	T= 3 days	T = 9 days	T= 1 month
Diacetone alcohol			
Dammar			
DC6G900			

Table 1-4: Restoration performance of different products on blanching painting by Jean Cotelle the Younger, View of the entrance to the labyrinth with the cabinet of birds, nymphs and loves, 1688, inv. MV730, National Museum of the Palace of Versailles and the Trianon. ©

C2RMF / A. Genty-Vincent. [71]

Chapter 2

Aim of the thesis

2.1 The objectives of the restoration

As two essential parts of artworks and cultural heritage, stone artworks and easel paintings are attacked by diverse degradations due to environmental conditions, anthropogenic, and biological effects. In particular, the present PhD thesis was focused on two restoration issues mainly induced by liquid water or moisture, which are stone degradation and blanching of easel paintings.

According to previous researches, partially perfluorinated compounds (especially partially perfluorinated oligoamides) have provided promising restoration performance on those restoration issues, for example, good water repellency as stone protection products and decreasing blanching in easel paintings by filling the pores. Inspired by those promising results, two families of partially perfluorinated derivatives with hydroxyl groups are proposed and designed as restoration products for stone protection and blanching painting restoration in this thesis.

2.2 Proposed compounds for restoration

2.2.1 Partially perfluorinated C-glycosides

The first series of compounds proposed is partially perfluorinated C-glycosides.

C-glycosides are carbon-linked analogues of naturally occurring sugars have high hydrophilic properties due to the polar hydroxyl groups. Those hydroxyl groups could be expected to give good adhesion on polar stone substrates by hydrogen bonding. Also, hydroxyl groups can be compatible to the porous structures appearing in blanching easel paintings and help the molecules entering into the pores. Meanwhile, hydrophobicity of the compound can be realized by introducing perfluorinated chain into C-glycoside. Thus, C-glycosides with perfluorinated tails could give good water repellency to protect the stone materials from water by pushing the fluorinated segments on the outer surface and to achieve a good coating on the stone materials. In addition to the hydrophilicity and water repellency, C-glycosides themselves possess an improved stability towards acid, base and enzymatic hydrolysis due to their C-C bond between aglycone and sugar. That can contribute to the good stability of the partially perfluorinated C-glycosides as restoration products, together with the high stability of C-F bonds in the perfluorinated chain. Eventually, the proposed C-glycoside with a perfluorinated tail, could demonstrate good hydrophobicity and good adhesion for stone protection, and filling the pores in blanching paintings.

Based on all the advantages mentioned above, partially perfluorinated C-glycosides are proposed and were synthesized as the target compounds. It is necessary to mention that protected partially perfluorinated C-glycosides were also synthesized as controls, in order to investigate if hydroxyl functions in C-glycosides can improve the restoration efficacy as expected. Moreover, the structure modification could give the compounds different physical properties, like the different physical states, solubility *etc.*, which could also influence the restoration performance.

2.2.2 Partially perfluorinated hydroxylated oligoamides

Moreover we proposed partially perfluorinated hydroxylated oligoamides.

Oligoamides with mono-carboxylic functionalized PFPE blocks have demonstrated good water repellency on stone materials in previous results, such as partially perfluorinated oligo(ethylenesuccinamide), partially perfluorinated oligoadipamide, and partially perfluorinated oligosuberamide [42, 43, 44]. In order to further improve the interaction between partially perfluorinated oligomers and polar substrates, partially perfluorinated hydroxylated oligoamides are proposed as different target compounds in this thesis. Dimethyl L-tartrate was also considered as initial comonomer to provide the hydroxyl groups for the oligoamides. Furthermore, a different perfluorinated residue was selected to reduce the impact on the environment.

As a result, hydroxyl groups together with amide groups can contribute with a good hydrophilicity to the target molecules. Those polar groups could be expected to give good adhesion on polar stone substrates by hydrogen bonding or dipolar interactions. They are also expected to be compatible to the porous structures appearing in blanching easel paintings and helping the molecules to enter into the pores. Eventually, those amphiphiles containing also perfluorinated chains are supposed to show good water repellency, and good adhesion (long-term durability) on stones. They are also supposed to decrease the blanching by filling the pores in blanching easel paintings.

Similar to the protected C-glycosides, partially perfluorinated oligoamides without hydroxyl groups were also synthesized, in order to observe the role of OH groups as anchoring functions to polar substrates. Moreover, diamines and triamines were respectively used as different amine sources in the synthesis. Those modifications of the molecule structures were designed to have different average molecular weights, different solubility, polarity *etc.* Consequently, their restoration performance were hypothesized to be different.

2.3 Selection of the promising compounds for restoration

All those proposed partially perfluorinated derivatives with molecular structures and different properties like molecular weight, polarity, solubility *etc.* were tested on different stone materials and blanching painting samples. Water repellency, wetting properties, vapour permeability, chromatic effect, ability to fill pores and reversibility of the treatments and *etc.*, after the synthetic products applied on the stone materials and paint materials, were examined as parameters of their restoration performance. At the end, the promising

compounds were selected according to the results of their performance for specific restoration purposes. In addition, interesting modifications of the molecular structure designed were proposed to improve the restoration efficacy.

Chapter 3

Partially perfluorinated C-glycosides

3.1 Introduction

3.1.1 Literature: C-glycoside synthesis

The continuing depletion of fossil resources and increasing environmental consciousness stimulate our society to search for alternative renewable feedstocks for chemical synthesis. [90] Carbohydrates have stimulated much interest in synthetic chemistry, as they are abundant, inexpensive, renewable and easily available. Also, the complex structure of carbohydrates makes their synthetic chemistry diverse. [91] Carbohydrate synthesis mainly involves protecting-group transformations, glycosylation reactions, oxidations/reductions and C-N/C-C bond formation. [92]

In the overwhelming majority of carbohydrates found in nature, the carbohydrates do not occur in a free form, but the monosaccharides are linked to each other or to other types of compounds (aglycones) by glycosidic bonds. In carbohydrate chemistry, when an organic molecule in which sugar is bound to a non-carbohydrate moiety, the molecule is named as glycoside. Generally, glycosides can be linked by an *O*-, *N*- (as native carbohydrate structures), *S*- and *C*-glycosidic bonds (figure 3-1). [93, 94] Among those glycosides, *C*-glycosides are resistant to both acidic and enzymatic hydrolysis, because the natural anomeric centre has been transformed from a hydrolytically labile *O*, *N* or *S* acetal link to an ether. [95] As a result, *C*-glycosides have gained considerable importance over the last few decades. [96]

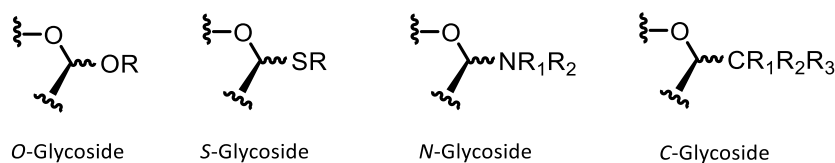


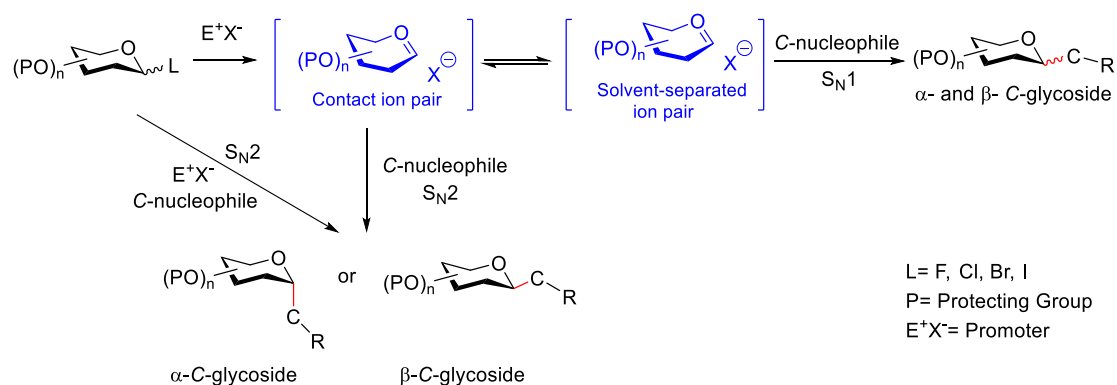
Figure 3-1: *O*-, *N*-, *S*- and *C*-glycoside

Different synthetic approaches are currently available for the synthesis of *C*-glycosides. Among the various available synthetic protocols, synthesis using β -*C*-glycosidic ketone is considered as highly versatile that led to a diverse array of interesting carbohydrate derivatives. This ketone has been identified as an easily accessible starting material that could bring large libraries of potential molecules with different applications, including self-assembled supramolecular gels and surfactants. [93] Therefore, the stable and versatile keto *C*-glycoside is considered as a suitable starting material for the synthesis of fluorinated *C*-glycosides in our project. The next step needed to be considered is choosing the suitable methodology for ketone-incorporated *C*-glycoside synthesis.

There are several methods commonly used to synthesize *C*-glycoside

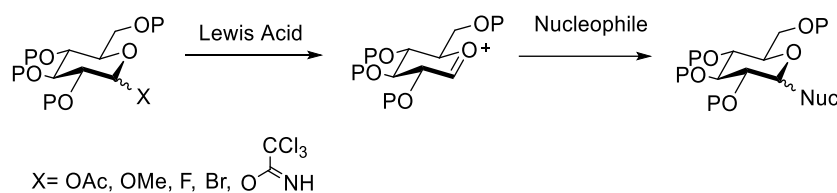
- Synthesis of C- glycosides *via* electrophilic/cationic species

One of the most widely used methods for the formation of C-glycosides involves electrophilic/cationic species derived from the sugar component. For instance, an S_N2 -like substitution of a glycosyl bromide/iodide, or a contact ion pair by C-nucleophiles, or through a solvent-separated ion pair analogous to those involved in the S_N1 -type O-glycosylation. [97] (scheme 3-1)



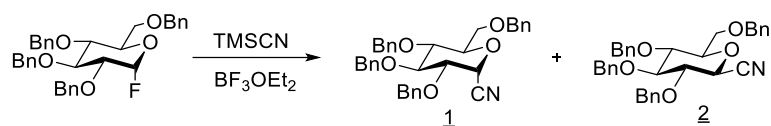
Scheme 3-1: Glycosylation via electrophilic/cationic species

In S_N1 -type approach, the saccharide serves as an electrophile which reacts with a carbon-based nucleophile to create a new carbon-carbon linkage. The substrate can be rendered electrophilic in several ways, the most common of which is activation of the anomeric substituent under Lewis acidic conditions to generate an oxocarbenium ion (scheme 3-2). The nucleophile then attacks the C1 position to form the C-glycoside, and the resulting stereochemistry is primarily substrate controlled. [98][99]



Scheme 3-2: The nucleophile attacks the C1 position through oxocarbenium ion method

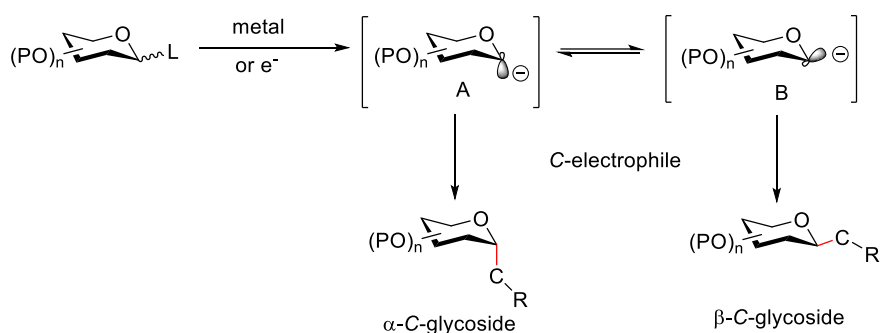
In these reactions, each component must be carefully selected in order to obtain high yields and selectivities. Acetates, ethers, halides, and trichloroacetimidates are examples of viable leaving groups, and typical Lewis acids include BF_3OEt_2 , TiCl_4 , TMSOTf, and SnCl_4 . This methodology has been successfully demonstrated with a range of nucleophiles, the simplest of which is cyanide. For example, reacting tetrabenzyl glucosyl fluoride in the presence of BF_3OEt_2 results in a mixture of anomers that is dependent on the Lewis acid concentration. [100] (scheme 3-3)



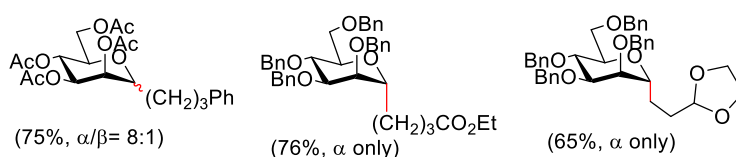
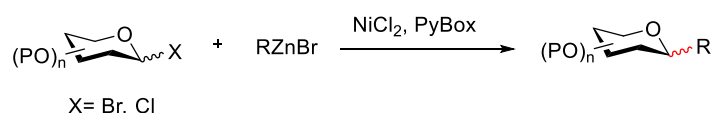
Eq of BF ₃ OEt ₂	% α(1)	% β(2)
0.05	30	70
1.0	100	0

Scheme 3-3: Tetrabenzyl glucosyl fluoride reacted with cyanide

The transition-metal-mediated cross-coupling reactions, constitutes an alternative to the synthesis of C-glycosides. [101] (scheme3-4) Substrates and catalysts serve as the two major parameters for transition-metal-mediated stereoselective C-glycosylations. As an example, Negishi cross-coupling of mannosyl bromides or chlorides with primary alkyl zinc reagents using NiCl₂ as the catalyst and pyridine-linked bis(oxazoline) (PyBox) as the ligand gave C-mannosides in good yields with high α-selectivities (α/β = 8:1 to α only). (scheme3-5) [102]

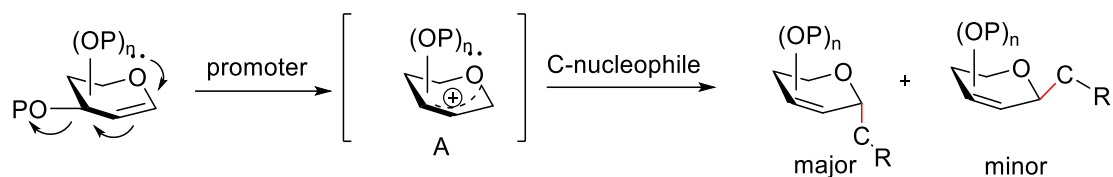


Scheme 3-4: Use of the transition-metal-mediated cross-coupling reactions



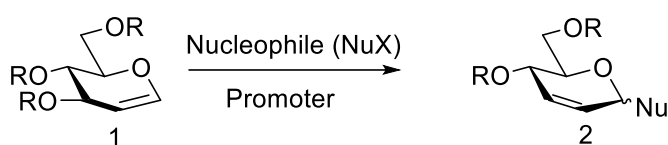
Scheme 3-5: C-alkylation with glycosyl halides through Negishi cross-coupling

Glycals are one of the most widely used electrophilic cationic sugar species for constructing the anomeric C-C bonds of C-glycosides. Usually, electrophilic C-glycosylation of glycals with C-nucleophiles takes place through Ferrier rearrangement through the oxonium ion (A) to provide 2, 3-unsaturated C-glycosides, favoring the formation of α-anomer. (scheme3-6) [103][104]



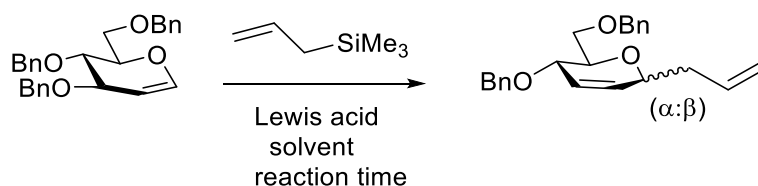
Scheme 3-6: C-glycosylation with glycols

The transformation of glycols (1,5-anhydrohex-1-enitols, *e.g.*, 1, scheme 3-7) into 2,3-unsaturated glycosyl derivatives (*e.g.*, 2, Nu = OR) was first reported by Ferrier. This reaction is now currently known as Ferrier Rearrangement (FR), or the Ferrier (I) reaction. [105][106]



Scheme 3-7: Ferrier Rearrangement

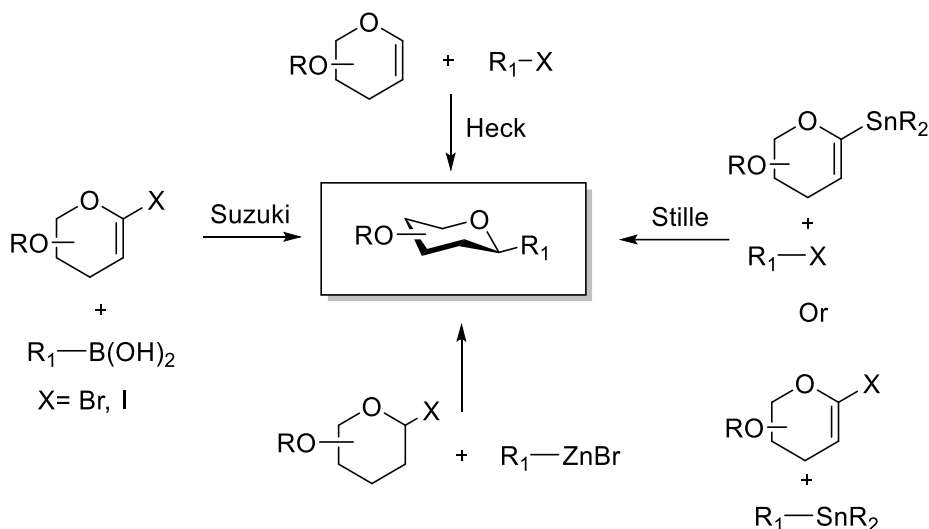
Different types of carbon nucleophiles – including allylsilanes, allyl-, alkyl-, aryl-, and alkynylmetal reagents, TMS-CN, isonitriles, enol derivatives, and aromatics – are able to react with Ferrier cations to give unsaturated C-glycosides. Allyltrimethylsilane has traditionally been a nucleophile of choice for testing the usefulness of promoters in FR leading to unsaturated C-glycosides. (scheme3-8) [107][108][109][110]



Entry	Reaction conditions	Yield, %	α/β ratio
1	InBr ₃ , CH ₂ Cl ₂ , 3h	90%	9:1
2	Bi(OTf) ₃ , CH ₃ CN, 10min	88%	10:1
3	ZrCl ₄ , CH ₃ CN/CH ₂ Cl ₂ , 1h	64%	4:1
4	HClO ₄ ·SiO ₂ , CH ₂ Cl ₂ , 0.5h	75%	11:1

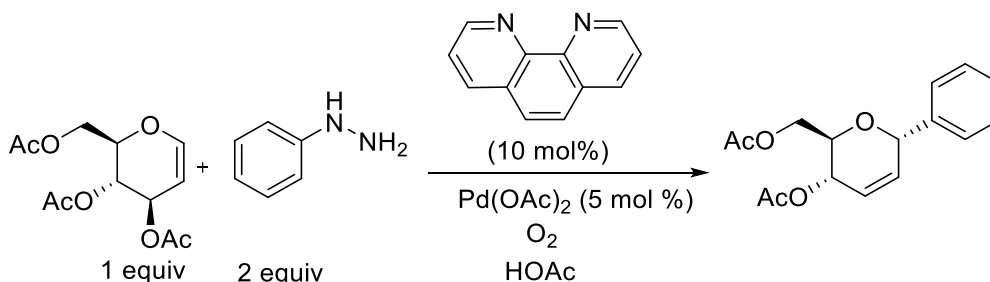
Scheme 3-8: Ferrier Rearrangement of tri-O-benzyl-D-glucal in the presence of allyltrimethylsilane and different acid catalysts.

In addition, a number of approaches including Heck, Suzuki, Stille and Negishi-type reactions have been developed for the synthesis of C-glycosides employing glycols as key starting materials (scheme 3-9) [93]



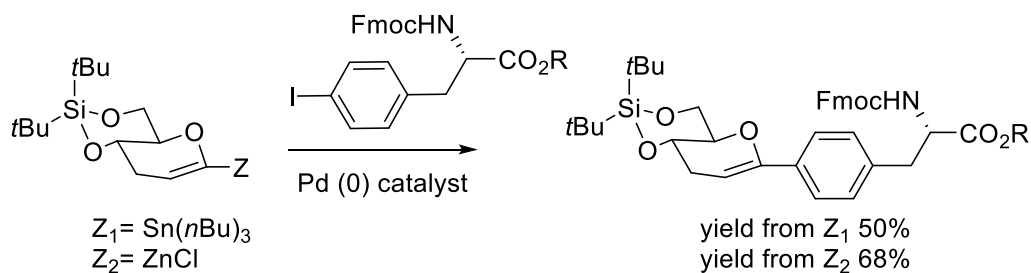
Scheme 3-9: Cross coupling reactions on glycols

An efficient Heck-type C-glycosylation method with glycols, catalyzed by palladium, has been developed by Liu *et al.* Pure α -C-glycosides were obtained when (3*R*)-glycols were employed at 65°C, with 90% yield. (scheme3-10) [111]



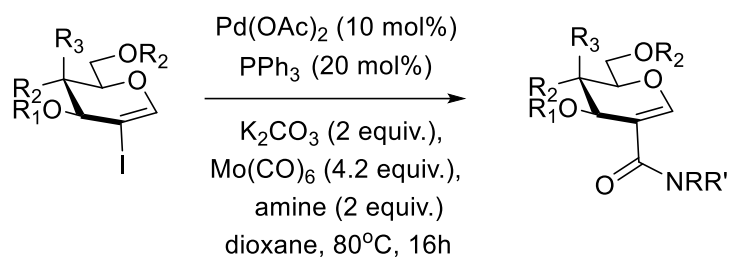
Scheme 3-10: Heck-type C-glycosylation method with glycols

Palladium-catalyzed cross-coupling reactions were used to create the carbon-carbon bond in C-glycosyl analogues of phenylalanine (scheme3-11). The cross-coupling of a metalated glycol with an iodoaryl derivative afforded the desired C-glycosyl compound. Both Stille ($Z_1 = \text{Sn}(n\text{Bu})_3$) and Negishi ($Z_2 = \text{ZnCl}$) conditions were tried, and the latter proved more efficient. [112][113]



Scheme 3-11: The cross-coupling of a metalated glycol with an iodoaryl derivative

A convenient and straightforward synthesis of 2-amidoglycals through a palladium-catalyzed aminocarbonylation reaction between 2-iodoglycal partners and diverse amines in the presence of a “CO” source has been developed by Ferry A. *et al.* (scheme 3-12). [114]

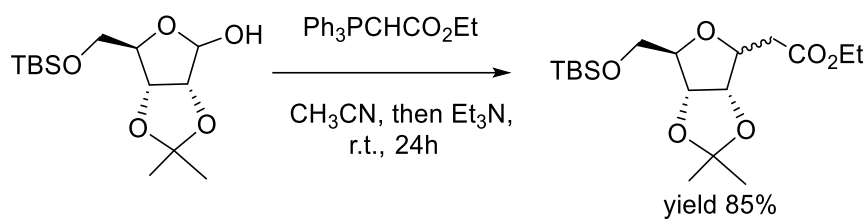


Entry	Starting material	Amine	Product/ Yield ^a
1			70%
			62%
2			75%
			71%
3			65%
			45%

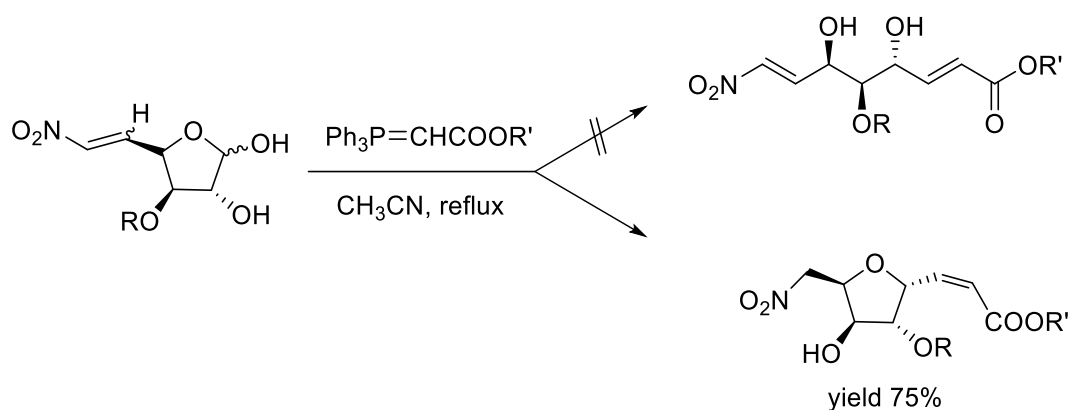
^a Yields were determined on the isolated products

Scheme 3-12: A convenient and straightforward synthesis of 2- amidoglycals

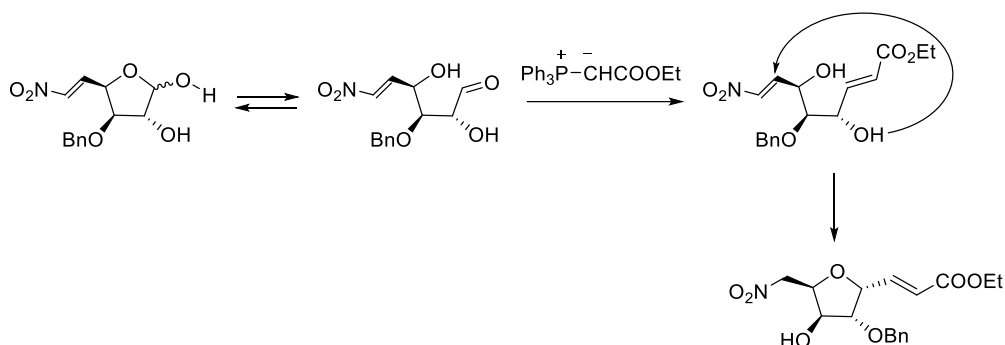
Sugar lactols can react through the Mitsunobu reaction, the Wittig reaction or Horner–Wadsworth–Emmons (HWE) olefination/Michael addition, or acid-mediated C-glycosylation with C-nucleophiles to provide C-glycosides. Coupling of pyranosyllactols with C-nucleophiles was usually found to give 1,2-trans C-glycosides, whereas C-glycosylation with furanosyllactols often led to a mixture of anomers. Treatment of lactol with Wittig reagent $\text{PPh}_3\text{CHCO}_2\text{Et}$ gave a mixture of C-glycoside in 85 % yield [115], whereas exposure of 5,6-dideoxy-5,6-dehydro-6-nitro-D-glucofuranose to $\text{PPh}_3\text{CHCO}_2\text{Et}$ resulted in the formation of α -C-vinyl glycoside in 75 % yield through Wittig olefination and subsequent oxy-Michael addition. (scheme3-13, 3-14, 3-15) [116]



Scheme 3-13: Treatment of lactol with Wittig reagent $\text{PPh}_3\text{CHCO}_2\text{Et}$ gave a mixture of C-glycoside

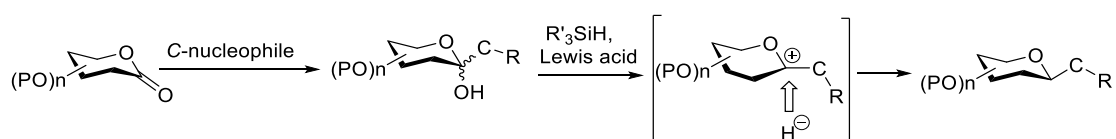


Scheme 3-14: α -C-vinyl glycoside



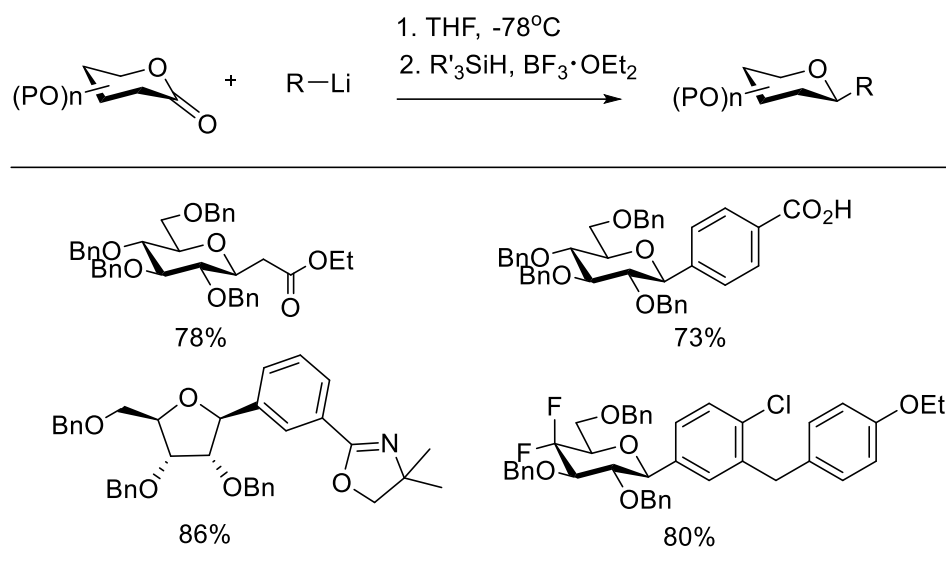
Scheme 3-15: Tentative mechanism for the formation of α -C-vinyl glycoside

Sugar lactones have found wide applications for C-glycosylation since the 1900s. Sugar lactones can react with C-nucleophiles to give hemiketals, which are usually reduced by silane and Lewis acid through hydride attack on the α -face of the oxocarbenium ion intermediate (A) because of the kinetic anomeric effect, affording β -C-glycopyranosides as the major products without acetoxy group participation. (scheme3-16) [117][118]



Scheme 3-16: Plausible mechanistic scheme for C-glycosylation with sugar lactones

Nucleophilic addition of lithium enolate or aryl lithium to sugar lactones followed by reduction using silane and $\text{BF}_3 \cdot \text{OEt}_2$ afforded the corresponding C-glycosides in good yields with complete β -selectivity. (scheme3-17) [119][120][121][122][123]



Scheme 3-17: C-glycosylation of Lithium enolate or aryl Lithium with sugar lactones

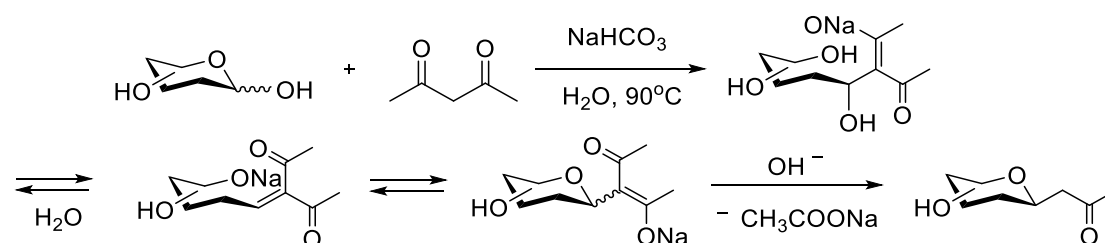
Although those different methods have been developed to access to the C-glycoside, the glycochemists toolbox is applicable almost only to the protected glycosides. Those C-C linking reactions are mostly burdened by the need for protecting-group installation, expensive substrates, specific reaction conditions, and unsatisfactory low overall product yields. As a result, those many steps, leading to long, complex syntheses leave a heavy impact on the environment. Additionally, the reactions are performed in organic solvents and, in many cases, use many hazardous moisture and air sensitive reagents and/or catalysts. As renewable raw materials, direct utilization of natural-like unprotected sugars opens the possibility to suppress the protection/deprotection steps shortening the chemical synthesis. Benefits of that are diverse: economic and environmental. However, the direct C-glycosidation reactions of unprotected carbohydrates are often difficult, and the C–C bond formation reaction of unprotected carbohydrates has been considered as a task of enzymes.

One of difficulties in reactions of unprotected carbohydrates may be the presence of polyhydroxy groups in carbohydrates. In many reactions of carbohydrates, hydroxy groups must be protected first to avoid the acidic protons of the hydroxy groups react with reagents and/or that the hydroxy groups interrupt hydrogen bonding necessary for the catalysis and stereocontrol. Another difficulty with direct C-glycosidation reactions of unprotected carbohydrates lies in the cyclic hemiacetal form of the aldoses. Although the aldehyde carbonyl group of the aldoses may be a good site to react with nucleophiles, the closing of the ring could lead to a mixture of α,β -furanosides and α,β -pyranosides and that could cause a complicated separation process as well as a drop in yield. [124] Therefore, many nonenzymatic, chemical C-glycosidation reactions of carbohydrates have been performed on preactivated forms of carbohydrates with protected hydroxy groups or on specific precursors bearing functional groups for the bond formation at the anomeric carbons. [125]

Considering atom- and step-economy, direct reactions on unprotected carbohydrates are more preferable than reactions requiring protection and deprotection steps and/or strategies requiring the synthesis of preactivated forms for the reactions at the anomeric carbons. [126][127]

Direct use of unprotected sugar lactols for coupling with C-nucleophiles represents an attractive approach and route to C-glycoside

In 1986, Gonzalez *et al.* reported the first one-step procedure to synthesize C-glycoside directly by reacting unprotected carbohydrates with barbituric acid derivatives in water. [128] Later, Lubineau *et al.* investigated this green reaction by reacting 1,3-diketone with unprotected carbohydrates dissolved in alkaline aqueous media (scheme 3-18) [95]. It proceeds *via* a Knoevenagel's reaction between activated methylene and a naked aldose followed by a Michael-type intramolecular addition and a retro-Claisen aldol condensation. At room temperature, a mixture of the four possible α,β -furanosides and α,β -pyranosides stereoisomers, could be obtained. The exclusive formation of the β -pyranoside stereoisomer came from thermodynamic control (around 90°C) under basic conditions.



Scheme 3-18: Lubineau reaction

It is interesting to note that, in the presence of CeCl_3 instead of NaHCO_3 , polyhydroxyalkyl- or C-glycosyl furans are formed. [129] Such dichotomy was also observed with the use of indium chloride as the catalyst. [130] Thermodynamic Knoevenagel condensation (Lubineau reaction) was applied to different carbohydrates, such as 2-acetamido sugars, fucose, lactose and various pentoses including, xylose, arabinose and 3-deoxy arabinose.

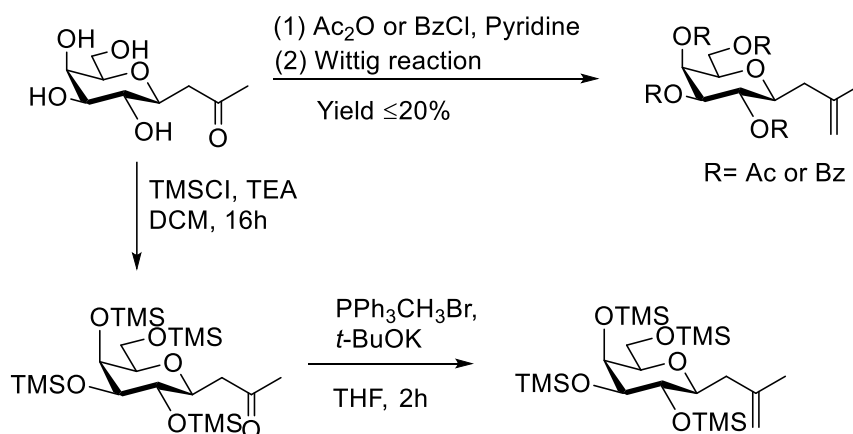
Lubineau reaction is a very convenient method for the preparation of pure β -C-glycosidic ketones in one step directly from the unprotected sugar. The greenness of these synthons, at least for two of them, was not noticed by Lubineau when he has developed their synthesis, since green chemistry was not yet an outstanding concept defined as “the utilisation of a set of principles that reduces and eliminates the use of generation of hazardous substances in the design, manufacture and application of chemical products”. Today, modern chemical synthesis should be based upon the twelve green chemistry principles. [131][132] The use of renewable materials such as carbohydrates, which constitute 75 % of the vegetal biomass is one of the twelve principles. The atom economy is another salient feature since this concept highlights the importance of the incorporation of all the atoms; for a total synthesis it means that protection and deprotection of carbohydrates should be avoided; if not, the global atom economy dramatically decreases. This situation is worse when considering the global reaction mass efficiency and the global material economy. [133][134] These metrics are proportional to the atom economy; the coefficient of proportionality depends on the yields,

the excesses of reactants, the use of auxiliaries, such as solvents which participate greatly to the waste. As a matter of fact, the prevention of waste is the principle number 1 of green chemistry. The importance of such prevention was emphasized as soon as 1992 by Sheldon through the promotion of the E-factor defined as the ratio between the mass of the total waste and the mass of the final product. Indeed, the global material economy (GME), named by analogy with the global atom economy, and defined as the ratio between the mass of the final product and the mass of the inputs is correlated to the E factor by the following relationship: $GME = 1/(E+1)$. As a green chemistry methodology, this C-glycosylation reaction has been developed on an industrial scale by the research group of L’Oreal, a leading company in cosmetics. With D-xylose, a major constituent of hemicelluloses, as a renewable feedstock, and soda as the base, Lubineau reaction gives β -C-D-xylopyranosylpropan-2-one which, after reduction of the carbonyl group, leads to alcohol as an equimolar mixture of diastereoisomers. This mixture, marketed in cosmetic skincare products under the name of ProXylane™ by L’Oréal is a very effective activator of glycosaminoglycans biosynthesis which play a major role in the organization of the extra-cellular dermal matrix and in skin hydration. Industrial synthesis was optimized for a minimal E factor and consequently a maximal global material economy. [94][135] Based on all those considerations, Lubineau reaction is used for synthesis of the keto C-glycosides which is starting from the renewable carbohydrates in this thesis.

3.1.2 Literature: reactivity on to C-glycoside methylketones

3.1.2.1 Wittig reaction

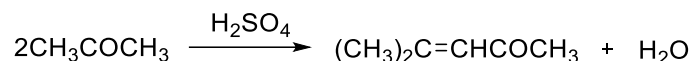
The Wittig reaction of trimethylsilyl protecting C-glycosidic ketone proceeded well and resulted in the formation of C-glycosidic alkene in high yield. Acetate and benzyl protecting C-glycosidic alkene can also be synthesised by direct protection of sugar hydroxyl group using acetyl chloride or benzylchloride followed by Wittig reaction. However, the yield isolated by using this synthetic strategy was 20 % or less. (scheme 3-19) [93]



Scheme 3-19: Wittig reaction on C-glycosides methylketones

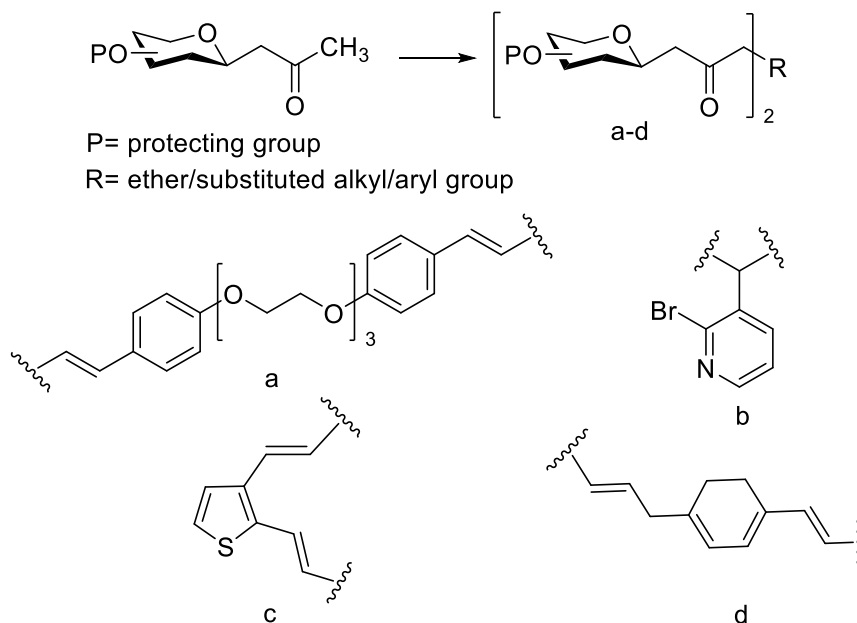
3.1.2.2 Aldol condensation of C-glycoside ketones

The Aldol condensation takes its name from aldol (3-hydroxybutanal), a name introduced by Wurtz who first prepared this β -hydroxy aldehyde from acetaldehyde in 1872. [136] The Aldol condensation includes reactions producing β -hydroxy aldehyde (β -aldols) or β -hydroxy ketones (β -ketols) by self-condensation or mixed condensations of aldehydes and ketones, as well as reactions leading to α, β -unsaturated aldehydes or α, β -unsaturated ketones, formed by dehydration of intermediate β -aldols or β -ketols [137]. (scheme3-20)



Scheme 3-20: Aldol condensation

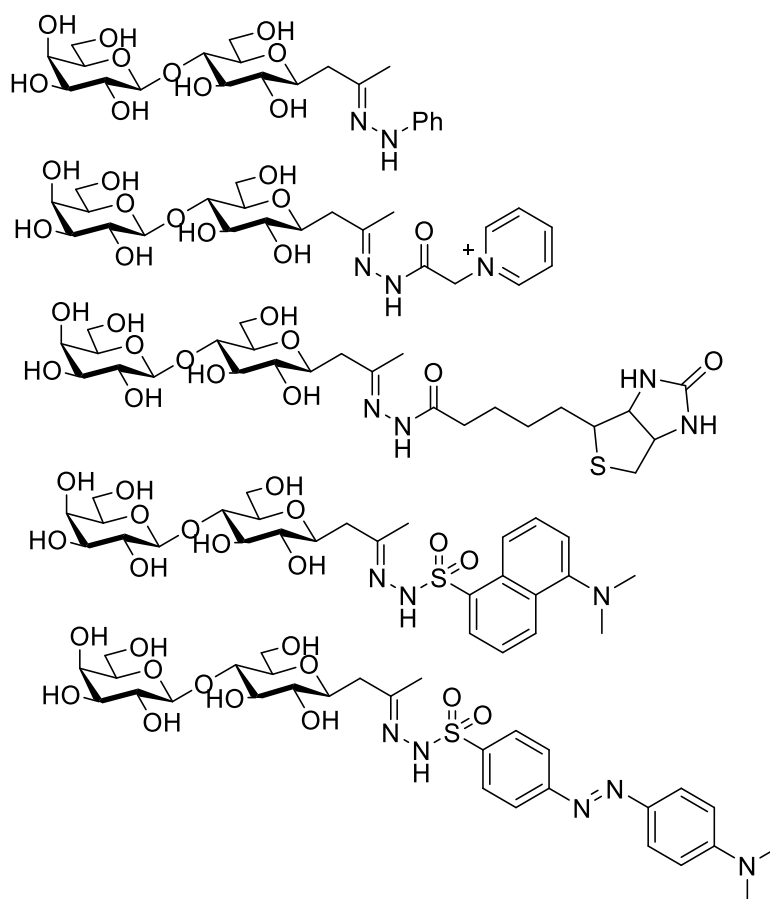
A class of C-disaccharides bearing different linking units such as triethylene glycol (TEG), substituted alkyl and aryl moiety was synthesised involving aldol condensation of β -C-glycosidic ketones with TEG-dialdehydes, aromatic dialdehyde (isophthalaldehyde) and heterocyclic dialdehyde (thiophene-2,3-dicarbaldehyde). The resulted α, β -unsaturated- β -C-glycosidic ketones could undergo Michael addition with another molecule of β -C-glycosidic ketone to give the substituted alkyl ketone linked C-disaccharide derivatives (a-d). In this reaction, the solvent ratio and equivalents of β -C-glycosidic ketones determined the nature of the product formation (scheme 3-21) [138].



Scheme 3-21: Synthesis of ether-, substituted alkyl- and aryl- linked C-disaccharides.

3.1.2.3 Functionalized C-glycoside ketohydrazones

Many of the biological processes were mediated by glycosylation through the interaction of carbohydrates with corresponding proteins and the different linkages present in the glycosides determine its function. [93] In reducing sugars, the structural integrity is lost due to the ring opening under various circumstances and the resultant structure was significantly varied from the parent molecule. In order to defeat such limitations, a new class of sugar-based hydrazines and hydroxylamines were developed by the condensation reaction of C-glycoside ketone with phenylhydrazine, (carboxymethyl)pyridiniumhydrazide or (carboxymethyl)-trimethylaminohydrazide (Girard's reagents P and T), dansylhydrazine (a fluorescent reagent (scheme 3-22) [139]. Similarly biotinylated carbohydrates were synthesized and found application in biotin-avidin chemistry [140][141].

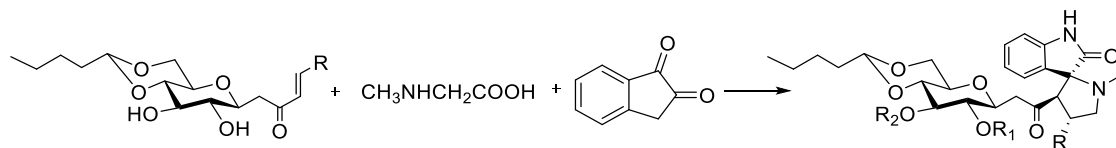


Scheme 3-22: Molecular structures of C-glycoside ketohydrazones

3.1.2.4 Synthesis of spirooxindoles

Intermolecular cycloaddition reactions of azomethine ylides with dipolarophiles derived from α,β -unsaturated ketones and acetylenic moiety lead to a number of interesting heterocyclic compounds. These complex molecules are useful for the construction of diverse chemical libraries of drug-like molecules. One-pot reaction of various α,β -unsaturated

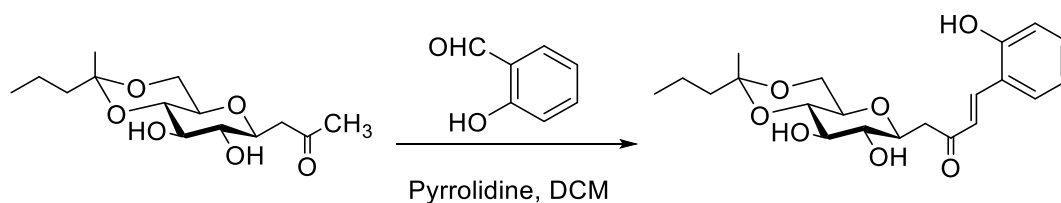
β -C-glycosidic ketones (a) derived from β -C-glycosidic ketone with the azomethine-ylide derived from isatin (1H-indole-2,3-dione) and sarcosine (*N*-methylglycine), afforded sugar substituted monospirooxindole-pyrrolidines. (scheme3-23) [142]



Scheme 3-23: Synthesis of spirooxindoles

3.1.2.5 Self-assembled supramolecular gels based on C-glycosidic ketones

Typically, gels are soft nanomaterials whose mechanical properties lie between viscous liquids and elastic solids. In a particular solvent system, gently balanced order resting between precipitation and solubilization of the molecules can be called a gel-state. In the gelation process, the molecules self-assemble to form a three-dimensional fibrous network which entraps the solvent through capillary forces and resist the flow of the medium. Considering the reversibility of weak interactions such as *H*-bonding, π - π stacking, *van der Waals* forces, *etc.*, supramolecular gels are different from macromolecular gels as they can be cycled between free-flowing liquids and non-flowing materials in a reversible manner. Amphiphiles of *C*-glycosides were derived by a straightforward aldol condensation reaction of β -*C*-glycosidic ketone with various aromatic and heteroaromatic aldehydes at ambient temperature in the presence of a catalytic amount of pyrrolidine in DCM. (scheme3-24) [143]



Scheme 3-24: Synthesis of α,β -unsaturated- β -*C*-glycosidic ketone as gel

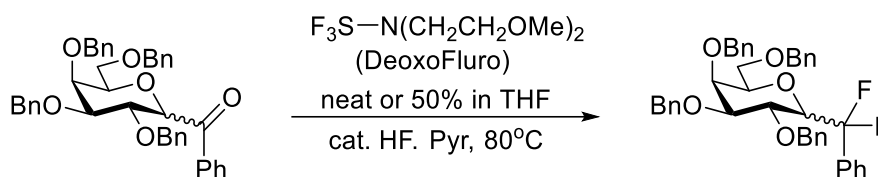
3.1.2.6 Halogenation

Halogenation can be realized on keto *C*-glycoside. Bromoketones were obtained by L-proline-catalyzed bromination at the α -positions with respect to the ketone functionalities in EtOH with the yield 61 %. Later, a greener methodology was explored on the same reaction. Bromine, a reagent with acute toxicity was replaced by polymer-bound pyridinium tribromide, whose toxicity is lower. The same bromoketone was obtained with a slightly lower yield at 54 %. (scheme3-25) [144]



Scheme 3-25: Synthesis of Bromoketone

Sollogoub *et al.* reported the difluorination of glycosylaryl ketones, with the presence of an active reagent at 80 °C in THF and longer reaction times. α -Aryl-CF₂-galactoside was obtained in good yield (77 %) whereas its β homologue in only 23 % yield (scheme 3-26) [145].

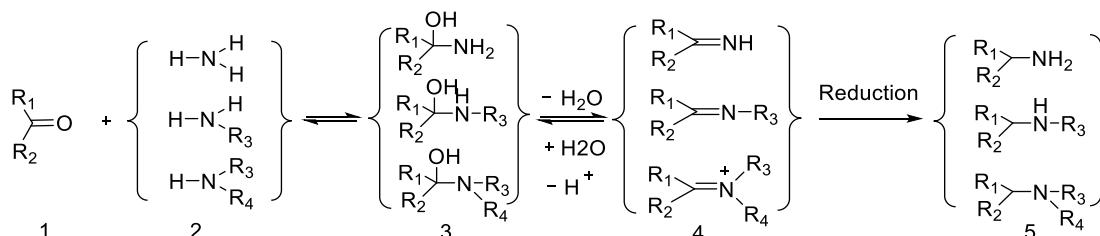


Scheme 3-26: α -Aryl-CF₂-galactoside

3.1.2.7 Reductive amination

Most glycan analysis tools are highly dependent upon various linkage chemistries that involve the reducing-terminus of carbohydrates. Reductive amination of the carbohydrate is based on imine formation between an amine reagent and the anomeric carbonyl group of a reducing carbohydrate, followed by reduction to an open chain glycamine derivative. The imines themselves are generally unstable, with the equilibrium favoring free carbonyl, except when stabilized by alpha-nitrogens such as in hydrazones and oximes. [146]

The reductive amination of carbonyl compounds is a highly useful, robust, and broadly employed transformation for the synthesis of further functionalized amines and has become a workhorse of synthetic chemistry. Generally, the reaction proceeds *via* the initial formation of an intermediate carbinolamine 3 (scheme 3-27), which dehydrates to form an imine (Schiff base) or iminium ion 4. Reduction of 4 produces the amine product 5. Some reports provided evidence suggesting a direct reduction of the carbinolamine 3 as a possible pathway leading to 5. [147][148][149]



Scheme 3-27: Reductive amination

There are two distinct approaches generally adopted for reductive amination reactions: the indirect or stepwise approach in which an imine is pre-formed between an amine and a suitable carbonyl substrate, which is then exposed to a suitable hydride source (*e.g.*, NaBH₄, metal catalyst/H₂). We describe the reductive amination reaction as direct when the carbonyl compound and the amine are mixed with the proper reducing agent without prior formation of the intermediate imine or iminium salt. The direct reductive amination is most convenient, and it is usually the method of choice. [150]

In terms of the reductants employed for direct reductive amination, borane-based reagents feature heavily in this area and a number of reagents and reagent systems have been developed. These include sodium cyanoborohydride (NaBH₃CN), sodium triacetoxyborohydride (NaBH(OAc)₃), pyridine–borane complex (pyr–BH₃), picoline–borane complex (pic–BH₃), NaBH₄/Mg(ClO₄)₂, NaBH₄/Ti(Oi-Pr)₄, borohydride exchange resin, Zn/AcOH, Zn(BH₄)₂/ZnCl₂, Zn(BH₄)₂/SiO₂, Bu₃SnH/SiO₂, and PhSiH₃/Bu₂SnCl₂. Of these, NaBH₃CN and NaBH(OAc)₃ are perhaps the most widely employed. [151]

The choice of reducing agent is very critical to the success of the reaction. The reducing agent must reduce imines (or iminium ions) selectively over aldehydes and ketones under the same reaction conditions. Indirect or stepwise reductive amination reactions involve the preformation of intermediate imines (from ammonia or a primary amine and an aldehyde or a ketone) or sometimes enamine or iminium species (from secondary amines and aldehydes or ketones) followed by reduction in a separate step. The choice of reducing agent is not as critical as in the direct reactions since there will be no competition or interference from a carbonyl compound. [150]

The two most commonly used direct reductive amination methods differ in the nature of the reducing agent. The first and older method is catalytic hydrogenation. [147][152][153] The success of this procedure requires the reduction of the carbonyl compound to be relatively slow. Catalytic hydrogenation is economical, convenient, and a very effective reductive amination method, particularly in large-scale reactions. On the other hand, in many cases, the reaction may give a mixture of products and low yields depending on the molar ratios and the structure of the reactants. [164] It has seen limited use with compounds containing carbon-carbon (and other) multiple bonds and in the presence of reducible functional groups such as nitro and cyano groups. Another limitation is associated with compounds containing divalent sulfur that may inhibit and deactivate the catalyst. [155][156].

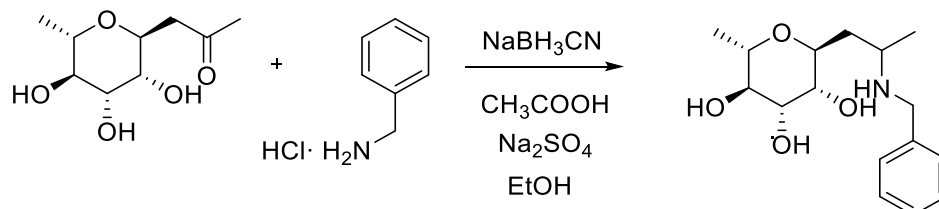
The second method utilizes hydride reducing agents. The use of hydride reagents in reduction of Schiff bases appeared in scattered reports in the 1950s [157]. The first study of a direct reductive amination procedure using a hydride reagent was reported by Schellenberg in 1963, in which he used sodium borohydride (NaBH₄) as the reducing agent. [158] In 1971, Borch reported the first practical hydride procedure for direct reductive amination in which he used the more selective sodium cyanoborohydride (NaBH₃CN) as the reducing agent. The successful use of NaBH₃CN is due to its different selectivities at different pH values and its stability in relatively strong acid solutions (~pH 3) as well as its good solubility in hydroxylic solvents such as methanol. [159] Some reported limitations are the requirement of a large excess of the amine, the sluggish reactions with aromatic ketones and with weakly basic amines, and the possibility of contamination of the product with cyanide.

[160] The reagent is also highly toxic and produces toxic byproducts such as HCN and NaCN upon workup. [161]

The next major advancement came in 1989 when Abdel-Magid *et al.* introduced a new procedure for reductive amination of aldehydes and ketones using sodium triacetoxyborohydride as reducing agent that has become one of the most used in carrying out reductive amination reactions with a large number of applications and literature reports. [162]

Comparative studies on the use of sodium triacetoxyborohydride versus other literature methods clearly showed it to be the reagent of choice in most cases. [163] The reactions are convenient, easy to conduct, and easy to work up, and the isolated yields are usually good to excellent. Most products were isolated by simple extraction and salt formation without the need for chromatographic purification. Since the introduction of this procedure, it has been applied to the synthesis of a large number of amine substrates and continues to be an outstanding reagent for reductive amination reactions. In general, addition of 1 equiv of a weak acid or using amine salts of weak acids increases the rate of reductive amination. Acetic acid is commonly used as the weak acid additive. Addition of strong acids or using their amine salts may completely stop the reaction. Most ketone reactions require the addition of 1 equiv of acetic acid to speed up the reaction. [150]

In the L'Oréal patent of DalkaoCsiba Marie *et al.*, the reductive amination was realized on keto L-Rhamnose with benzylamine hydrochloride, using NaBH₃CN as reductive reagent in ethanol at room temperature. 1 equiv of acetate acid was added to increase the rate of reductive reactions. [164] (scheme 3-28)



Scheme 3-28: Reductive amination of Keto L-Rhamnose

In terms of the solvent media conventionally used for these processes, while a variety of solvents have been used, chlorinated solvents feature heavily with CH₂Cl₂ and 1,2-dichloroethane (DCE) among the most common with DMF also widely used: a SciFinder survey revealed that 25 % of reductive amination reactions employed chlorinated solvents (CH₂Cl₂ and DCE). However, other solvents such as THF, and acetonitrile were also used with successful results. In general, many polar aprotic solvents were suitable solvents for this reaction. [165]

3.1.3 Partially perfluorinated carbohydrates

Perfluorochemicals are organic compounds in which all or nearly all of the hydrogen atoms are replaced by fluorine atoms. They are water insoluble, chemically and biochemically inert. Their inertness results from the strong C-F bonds (about 116 kcal/mol, *i.e.* 20 kcal/mol more

than a standard C-H bond) and a dense coating of electron-rich, repellent fluorine atoms which protect the carbon backbone. Moreover, the introduction of a perfluoroalkylated chain into a molecule enhances both hydrophobic and lipophobic interactions and can profoundly alter the molecule's structure and properties, thus generating new behavior and potential for additional applications. [166]

Amphiphiles with perfluoroalkyl chains are effective surfactants and tend to form ordered supramolecular assemblies more easily than their hydrocarbon counterparts. Some representatives of this group of surfactants were tested as emulsifiers for artificial oxygen carriers (fluorocarbon emulsions), as components in drug delivery systems or contrast agents based on fluorocarbons. [167]

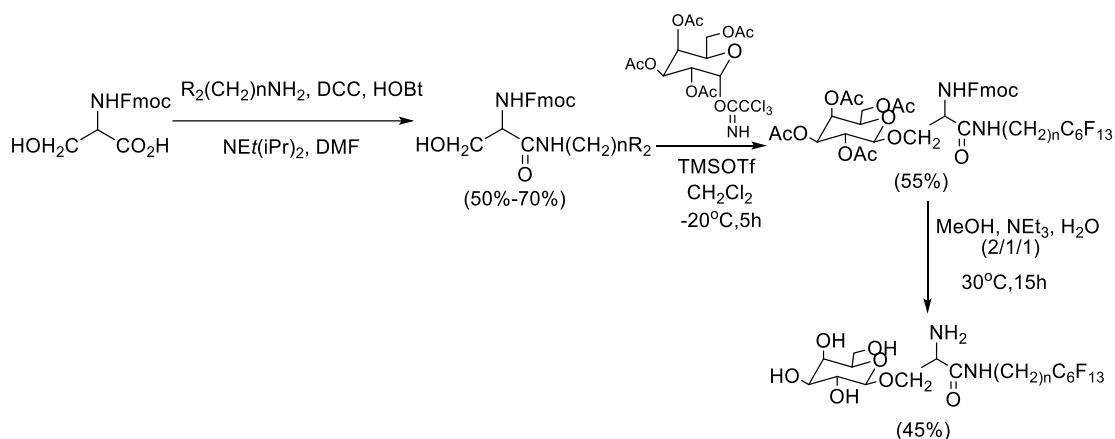
Polar heads of the amphiphiles derive from polyols, sugars, amino acids, phosphatides, polyoxyethylene moieties, trishydroxymethyl moieties, and combinations.

Perfluoroalkylated monosaccharides which contain the strongly hydrophobic perfluoroalkyl chain and a biocompatible polar head group have potential pharmaceutical (biocompatible formulations) and biochemical (extraction of membrane proteins) applications.

F-alkyl tails differ from hydrogenated ones with respect to their volume, their rigidity and, most importantly, by the stronger hydrophobic interactions they develop [166]. The strongly enhanced hydrophobic effect developed by F-alkyl chains as compared with their hydrocarbon analogs, combined with a definite lipophobic effect, results in a wily tendency for fluorinated amphiphiles to self-assemble when dispersed in water with other solvents [168].

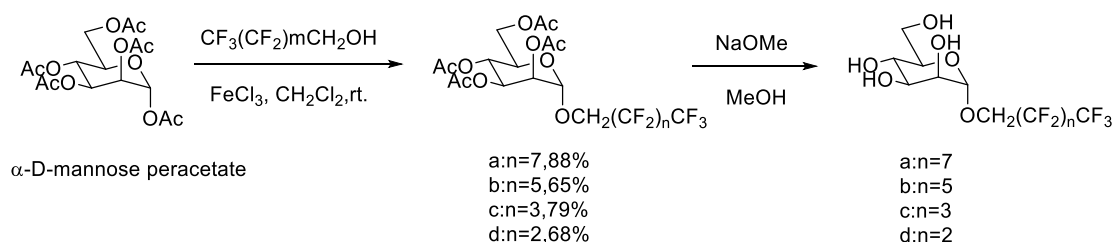
In the synthesis of perfluorinated carbohydrates, the perfluorinated chain is more often introduced into *O*-glycosides. Riess *et al.*, Filler *et al.*, Clary *et al.*, and El Ghoul *et al.* [166] synthesized various carbohydrates containing perfluoroalkyl chains attached to the carbohydrate skeleton *via* ester, ether, amide, or phosphate functions.

Clary *et al.* reported the synthesis of the single-chain amphiphiles was performed in three steps starting from Fmoc-DL-serine. Glycosylation of these compounds with 2,3,4,6-tetra-O-acetyl- α -D-galactopyranosyl trichloroacetimidate catalyzed by trimethylsilyl trifluoromethanesulfonate, TMSOTf (Schmidt method), gave the β -galactosides 55 % yields. After Fmoc and acetyl deprotection in a MeOH/NEt₃/H₂O (2/1/1) mixture, the galactosides were obtained in 45 % yields [169] (scheme 3-290).



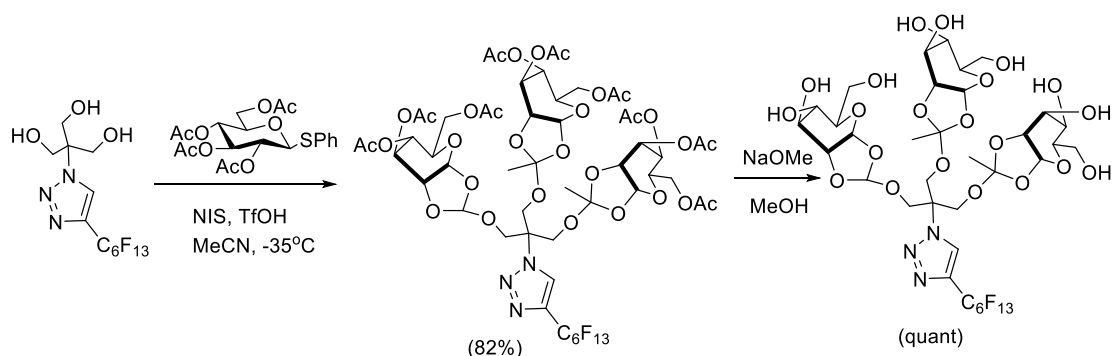
Scheme 3-29: Synthetic route to the fluorocarbon single chain serine-galactosyl amphiphile.

Razgulin *et al.* reported synthesis of perfluoroalkyl mannosides from commercially available peracetyl derivatives [170] (scheme 3-30).



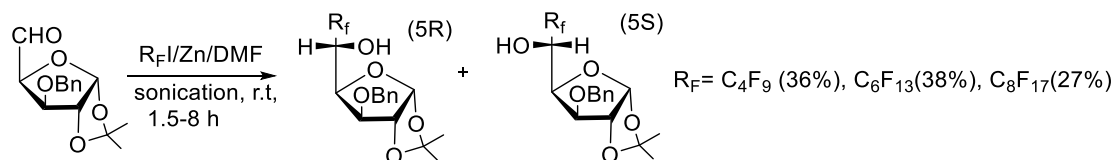
Scheme 3-30: Synthesis of perfluoroalkyl mannosides from commercially available peracetyl derivatives

Surfactants with three monosaccharide-based heads and a perfluoroalkyl tail have been synthesized by the same research team, using β -thiophenyl-peracetylglucoside as sugar donors to react with perfluoroalkyl triazole. In this case, the use of an excess of both the thioglycoside and NIS yielded the tri-orthoglycosylated product in an 82 % yield. This semifluorinated amphiphile shows interesting self-assembly and pharmaceutical emulsion stabilizing properties [170] (scheme 3-31).



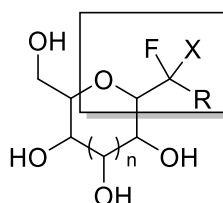
Scheme 3-31: Glycosylation and deprotection of fluoroalkyl triol

Miethchen and co-workers reported the nucleophilic F-alkylation of the aldehyde in furanose using a sonochemically assisted Barbier-type reaction with perfluorobutyl, perfluorohexyl or perfluorooctyl iodide in the presence of zinc (solvent: DMF), under sonication [171] (scheme 3-32).



Scheme 3-32: Perfluoroalkylation using different perfluoroalkyl chains

However, introducing the perfluorinated chain to C-glycosides is rarely reported. In fact, concerning the C-glycoside, there are more literatures describing to introduce fluoroalkyl group (CF_3 or CF_2H) instead of perfluoroalkyl chain into C-glycosides [172]. (scheme 3-33). Hence it is necessary to explore methodologies to synthesize C-glycosides with perfluoroalkyl chain.



Scheme 3-33: Fluoroalkyl group was introduced into C-glycosides

3.2 Results and discussion

3.2.1 Target compounds: Partially perfluorinated C-glycosides

In this part of synthesis, the target compounds are non-commercial partially perfluorinated C-glycosides. The target amphiphile C-glycosides were proposed as potential restoration agents for stone materials and blanching easel paintings.

The C-glycoside compounds which are carbon-linked analogues of naturally occurring sugars has high hydrophilic properties due to the polar hydroxyl groups, that could be expected as the hydrophilic end to keep good adhesion to stone substrates. Also, the hydrophilic ends can be affined to the porous structures appearing in blanching easel paintings.

On the other hand, there is rising interest on applying perfluoro-compounds on restoration as water repellents, due to the unique properties of fluorine atom and the C–F bond. The fluorine atom has a low *van der Waals* radius of 1.47 Å (intermediate between the hydrogen and oxygen atoms) and is strongly electronegative (4.0 on the Pauling scale). The C–F bond is consequently short (1.35 Å) and has high dissociation energy of 116 kcal mol⁻¹ (the strongest single bond of organic chemistry). Moreover, among various organic materials, fluorinated and perfluorinated compounds have been proved to have the lowest surface

energy (16–18 mN/m), which give them excellent hydrophobicity [173].

As a result, introducing perfluorotails into C-glycosides could make the molecule as amphiphiles. The hydrophilic head is OH groups of carbohydrates, and the hydrophilicity of partially perfluoro-C-glycosides can give an effective interaction and adhesion with the polar and porous stone and blanching paintings. The hydrophobic end is the perfluorotail, and it is expected to protect the artworks from water.

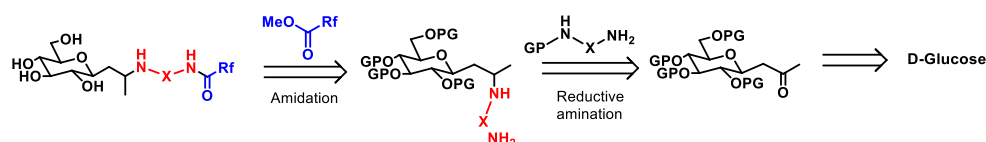
Considering that Mecozzi *et al.* reported the self-assembly properties of fluorinated carbohydrate-based surfactants, and the well-known phenomenon of surface segregation, the partially perfluorinated C-glycosides are expected to be able to push the fluorinated segments on the outer surface and to achieve a good coating on the materials [169].

Therefore, synthesis of C-glycosides with perfluorochain is proposed for this thesis based on all the unique properties above.

3.2.2 Synthesis

3.2.2.1 Synthesis route

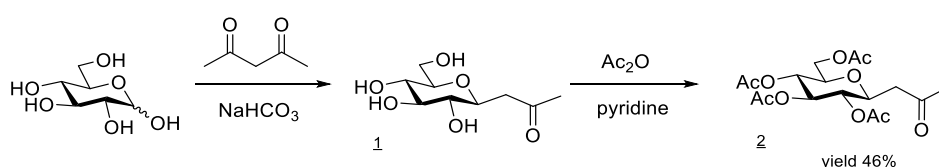
In the synthesis design, amine or amide are proposed as functional groups to connect the C-glycosides and perfluorochain. Perfluorochain can be introduced through the amidation using perfluoroester and the free amine end of C-glycosides. The C-glycosides with free amine can be obtained by reductive amination of keto C-glycoside. Moreover, the perfluorochain can be directly introduced through reductive amination between perfluoroamine and C-glycosidic ketone. And the crucial keto C-glycoside can be obtained from the natural, renewable and cheap C-glycoside by the Lubineau reaction. The synthesis route is presented as the following retro synthetic scheme 3-34.



Scheme 3-34: Retro synthetic route

3.2.2.2 Synthesis of partially perfluoro-C-glycosides

Starting from unprotected carbohydrates, C-glycosidic ketone was prepared in alkaline aqueous media *via* the Lubineau reaction as described in literature [95]. Compound **1** was acetylated to give the protected C-glycosidic ketone **2**. [174] (scheme 3-35)



Scheme 3-35: Synthesis of acetylated C-glycosidic ketone

Starting from the water solution of D-glucose (10 g), sodium bicarbonate and pentane-2,4-dione were added. The reaction mixture was stirred at 90 °C for 48 h, according to the procedure of Lubineau reaction. After heating, the reaction mixture was washed with CH₂Cl₂ and treated with Dowex resin. Followed by concentrating the aq. mixture, brown oil was obtained. That brown oil was reheated in water with NaHCO₃ for two days to afford β-C-glycosyl anomer. The configuration at the anomeric centre as a β-configuration was confirmed through the large coupling constant ³J_{1,2} of 9.4 Hz in ¹H spectra (δ = 3.64 ppm).

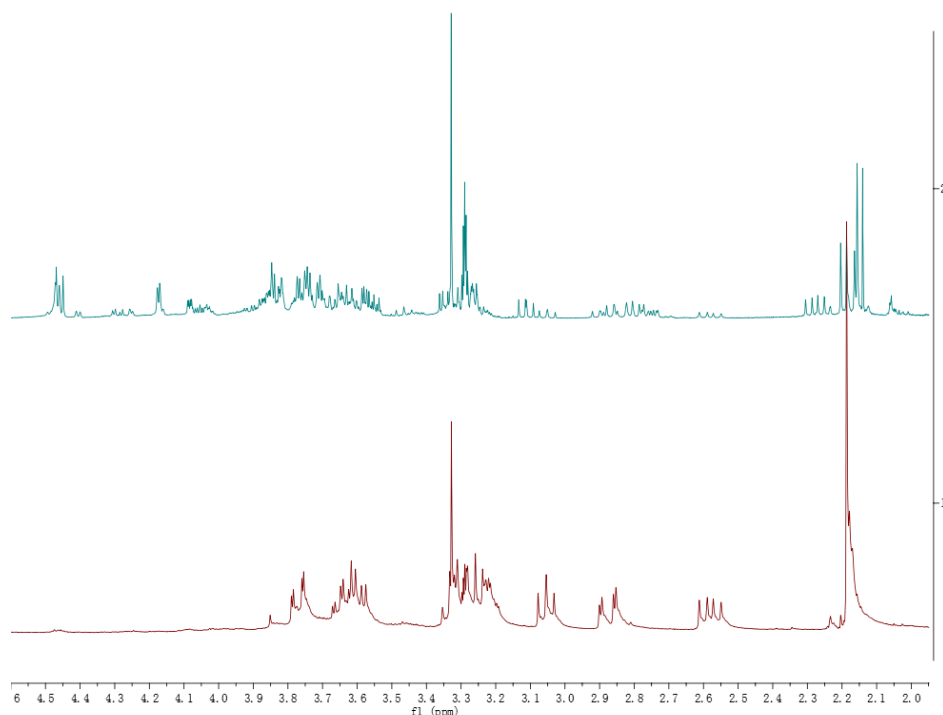
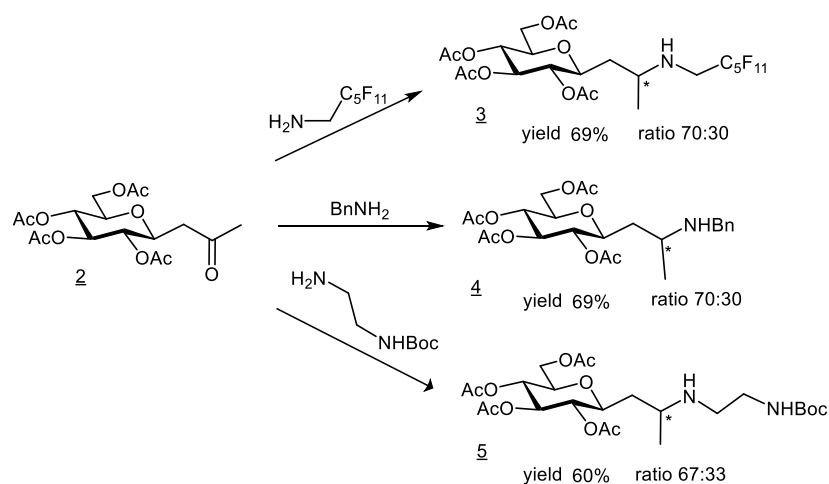


Figure 3-2: Green line: ¹H NMR spectra of the mixture of α,β-furanosides and α,β-pyranosides stereoisomers; Red line: ¹H NMR spectra of the final β-pyranoside stereoisomer after reheating.

In summary, β-C-glycosidic ketone was successfully obtained through the convenient, one-step, and green chemistry synthesis methodology.

1H,1H-Perfluorohexylamine (1.5 eq) as the source of perfluorochain was introduced to C-glycoside in compound **3** via one-pot reductive amination in dichloromethane, with sodium triacetoxyborohydride (2.2 eq) as the reductive agent. MgSO₄ (2.0 eq) was used for scavenging H₂O which was produced during the reaction. AcOH (20 % mmol) was used to speed up the reductive amination. Finally, compound **3** is obtained in 69 % yield (scheme 37). Moreover, compound **3** is one of the final target compounds for restoration of stone and painting.

Next, Benzylamine and N-Boc-ethylenediamine were chosen as other amine source to react with compound **2** using the same methodology to give the reductive amination products **4** and **5** in medium yield (scheme 3-36). The characterizations of the product were carried out by NMR and HRMS.



Scheme 3-36: Synthesis of acetylated C-glycosidic amines; Conditions: amine (1.5eq)

The ^1H NMR spectrum was shown in figure 3. With the help of COSY, H3' of compound **3** is confirmed by the doublet signal at 1.04 ppm. H4' next to CF_2 is confirmed by the signal at 3.05-3.39 ppm.

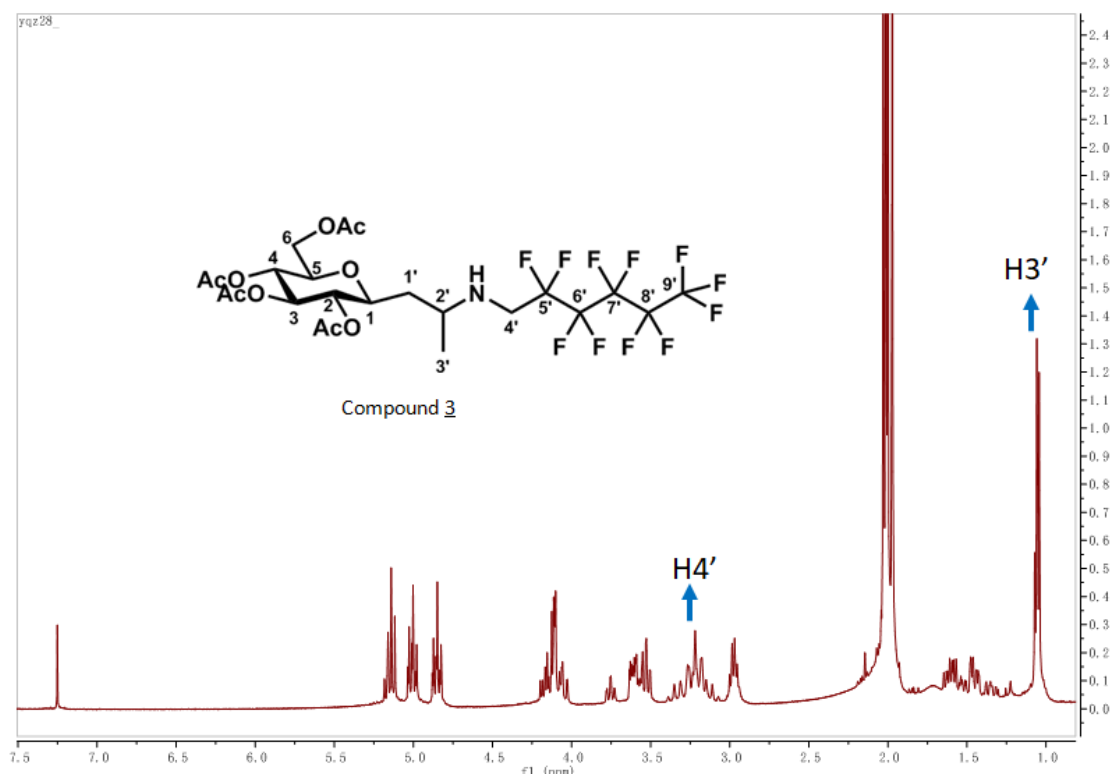


Figure 3-3: ^1H NMR spectrum of compound **3**

The ^{19}F NMR spectrum of compound **3** is shown as following figure 3-4.

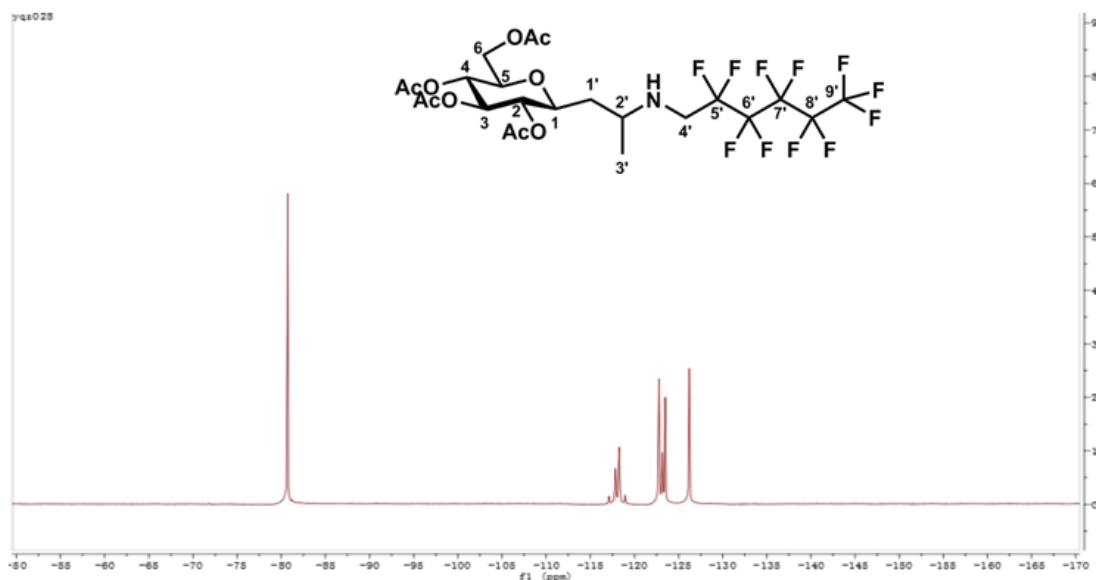
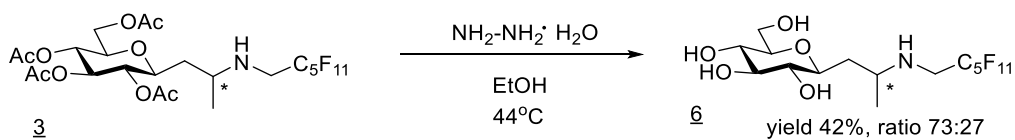


Figure 3-4: ^{19}F NMR spectrum of compound 3

Deacetylation was performed on compound 3 with hydrazine monohydrate in ethanol to give the deprotected product 6. (scheme3-37) The unprotected partially perfluorinated C-glycoside is one of the target compounds. OH groups are the hydrophilic head and perfluoro chain works as the hydrophobic tail in compound 6. Meanwhile, in the protected partially perfluorinated C-glycoside 3, the hydrophilic heads are protected by acetyl groups and the molecule can be helpful for understanding the function of OH groups.



Scheme 3-37: Synthesis of deacetylated fluorinated C-glycoside

^1H NMR spectrum of compound 6 is shown as following figure 3-5.

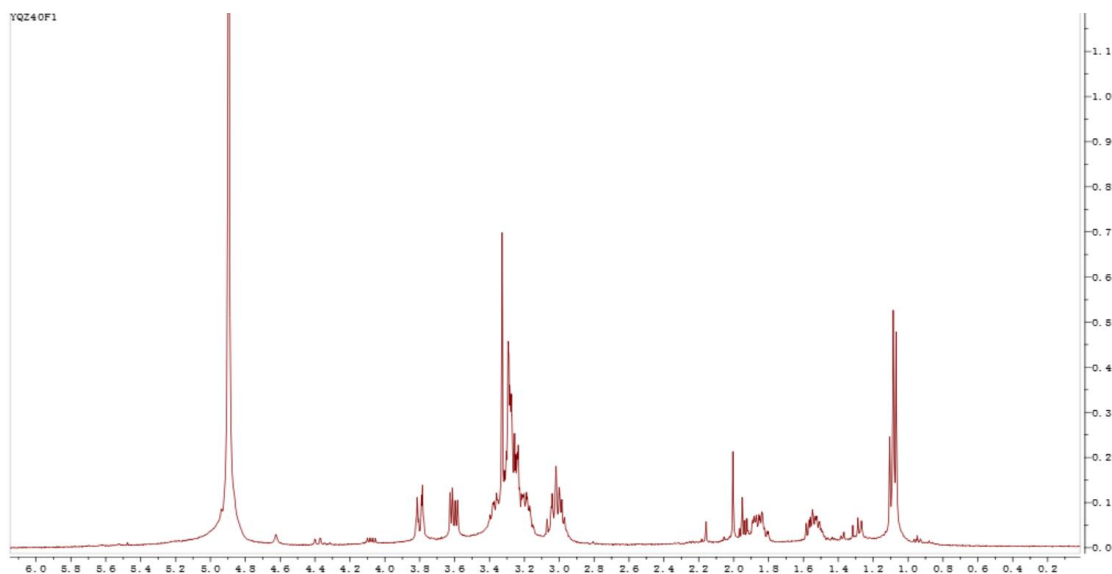
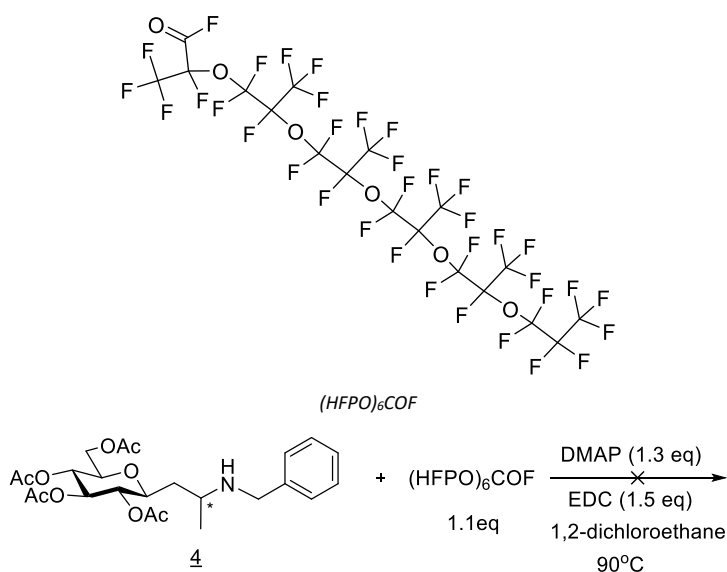


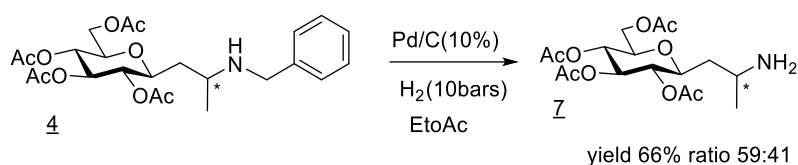
Figure 3-5: ^1H NMR spectrum of compound 6

In the next synthesis, the secondary amine of compound 4 was used as nucleophile to react with perfluoroacyl fluoride $(\text{HFPO})_6\text{COF}$. In this amidation reaction, DMAP was used as nucleophilic activator, and EDC can eventually be introduced to further activate the perfluoro acyl fluoride and 1,2-dichloroethane as the solvent. However, the reaction did not work. (scheme3-38)



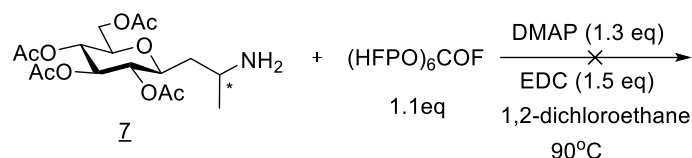
Scheme 3-38: Amidation reaction

Because of the low reactivity of compound 4 as a secondary amine, the benzyl group in compound 4 was removed by Pd/C in the presence of hydrogen to give compound 7 with a free amine function. (scheme 3-39)



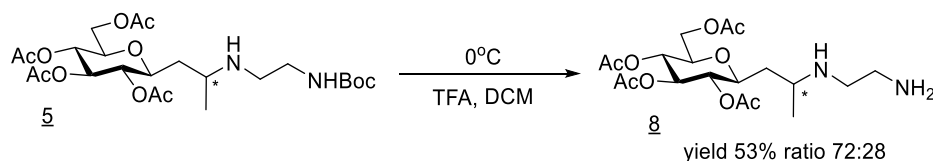
Scheme 3-39: Synthesis of C-glycosidic amine Z

Compound Z was used to react with (HFPO)₆COF with DMAP and EDC in 1,2-dichloroethane at 90 °C. (scheme3-40) However, no target C-glycoside with perfluorochain was obtained. The possible reason behind the non-working reaction could be that the amine groups in compound Z are hindered by the secondary carbon in the compound and consequently leading to the low activity of amine.



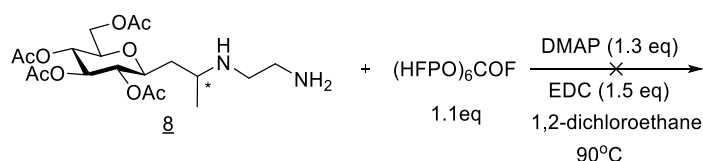
Scheme 3-40: Introducing the perfluorinated chain by (HFPO)₆COF to C-glycosidic amine Z

Therefore, Boc group in compound 5 was removed by TFA in DCM to give compound 8 with an increased activity of amine than compound Z. (scheme3-41)



Scheme 3-41: Synthesis of C-glycosidic amine 8

No target compound was obtained from compound 8 with the same methodology (scheme 3-42).

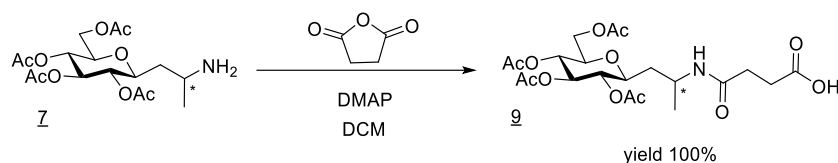


Scheme 3-42: Introducing the perfluorinated chain by (HFPO)₆COF to C-glycosidic amine 8

Using more active amine did not succeed to obtain the target compound with perfluorochain, which could indicate that the possible reason for failing could be the low solubility of (HFPO)₆COF in the reaction system, and also the relatively low reactivity of acyl fluoride. Considering the perfluorohexylamine was successfully introduced into C-glycoside in compound 3 and 6, it was used in the next synthesis as the perfluorochain source.

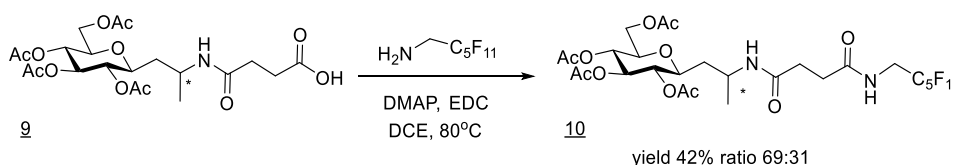
To create amide bond in the C-glycoside containing free amine and also keep an active end to act with perfluoroamine, succinic anhydride was reacted with compound Z via amidation

using DMAP as the nucleophilic catalyst in DCM to give C-glycosidic acid 9. (scheme3-43)



Scheme 3-43: Synthesis of C-glycosidic acid

1H,1H-Perfluorohexylamine was introduced into C-glycosidic acid 9 using DMAP as the nucleophilic catalyst and EDC as carboxyl activating agent for the coupling of primary amines to yield amide bond and get compound 10 (scheme 3-44).



Scheme 3-44: Synthesis of compound 10

As partially perfluorinated C-glycosides, Compound 3 and compound 6 were tested as protective agents for stone on Lecce stone samples. In the water capillary absorption test, both of the compounds show low protective efficacy. The previous research on stone protective agents shows -CONH- functional groups in the molecule can interact with stone material with dipolar reaction, which can give the molecule a good adhesion onto the stone material [41, 42, 43]. Also, polyfluorourethanes, containing the urethane function groups (-OCON-), appear to present in protective and consolidating products for stone materials [175][176]. Inspired by those research results, the new synthesis target were proposed, incorporating the urethane function group -OCONH- to C-glycosides as the the protecting groups. Two new target compounds were: (figure 3-6)

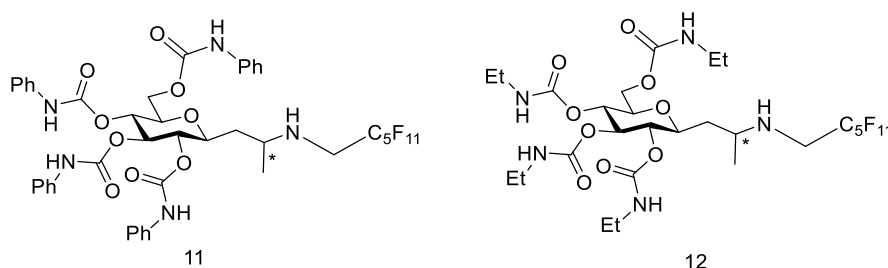
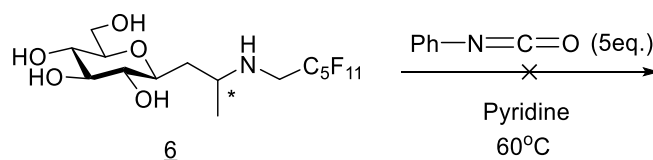


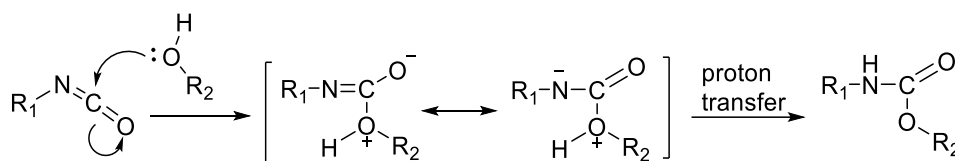
Figure 3-6: New target compounds with -CONH-

In those two molecules, the perfluorotails are supposed to keep the good hydrophobicity and the -CONH- could show dipolar interactions with the polar stone or painting materials. There are two routes leading to target 11. The first route is starting from compound 6 with Phenyl isocyanate (PhNCO). (scheme 3-45)



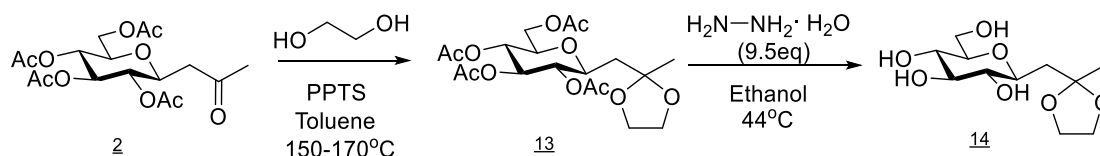
Scheme 3-45: Synthesis of target compound 11

However, from the TLC and ^1H NMR, no obvious signs of new target compound were observed. The possible reason could be the nucleophilicity of OH in compound 6 is influenced by the perfluoro chain, and decrease the reactivity of the nucleophilic addition of the OH groups. The general mechanism of isocyanate/ alcohol reaction is shown as following in the scheme.[177] (scheme 3-46)



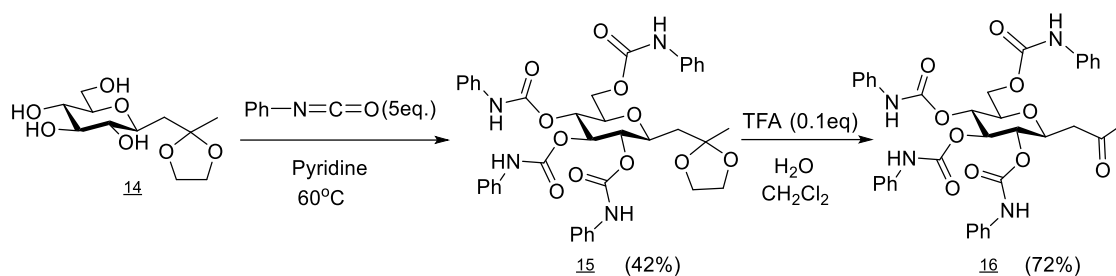
Scheme 3-46: General mechanism of isocyanate / alcohol reaction.

The other synthesis route to target 11 is starting from compound 2 and PhNCO. At the end, the perfluorohexylamine is introduced through reductive amination. The first step was using ethylene glycol to react with compound 2 to get the acetal 13. PPTS (Pyridinium *p*-toluenesulfonate) was used as a weakly acidic catalyst. Deprotection of 13 was performed with hydrazine hydrate in ethanol at 44 °C. The compound 14 was obtained after column chromatography.



Scheme 3-47: Synthesis of compound 14

Next step is introducing the CONH into compound 14 by reacting with PhNCO in pyridine at 60 °C. Compound 15 was obtained with 42 % yield. The moderate yield probably is due to the low solubility of compound 15 in common solvent. Deprotected ketone 16 was obtained using TFA and H₂O in dichloromethane, with 72 % yield.



Scheme 3-48: Synthesis of compound 16

^1H NMR spectrums of compound 15 and 16 are shown as following figure 3-7. An obvious change of chemical shifts of CH_3 can be observed from 1.32 to 2.14 ppm, due to the deprotection of carbonyl.

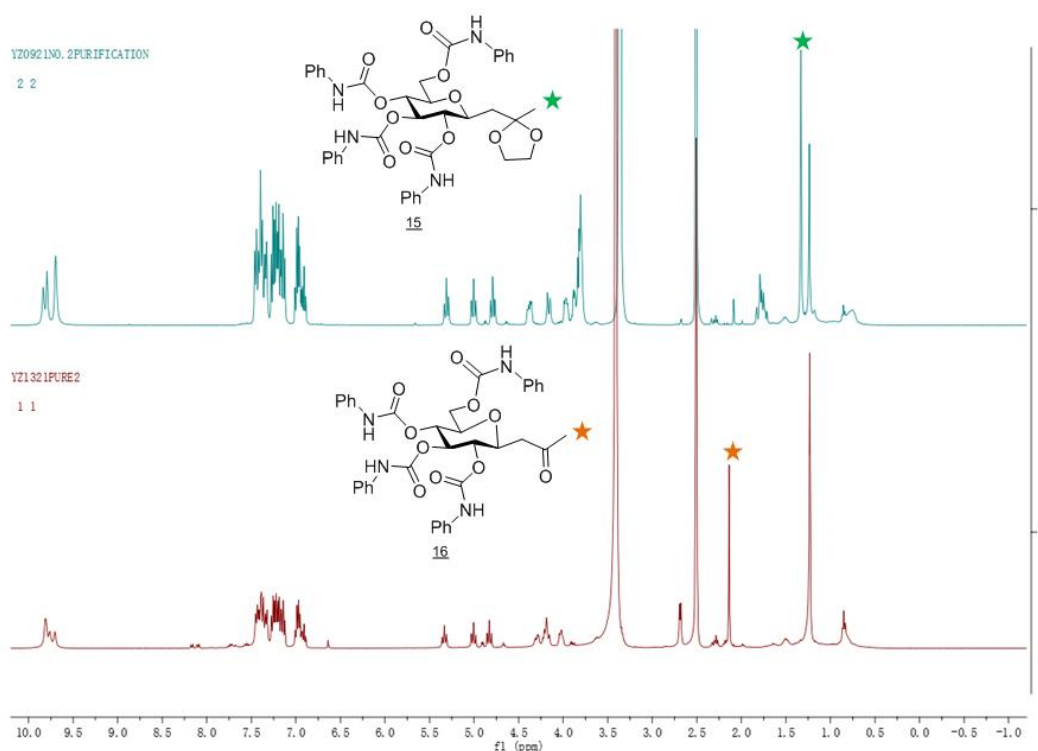
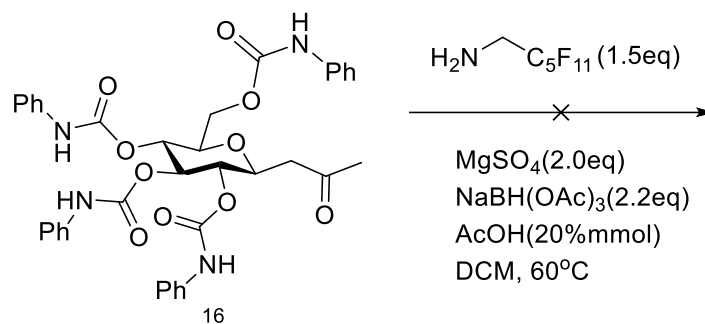


Figure 3-7: ^1H NMR spectrums of compounds 15 and 16

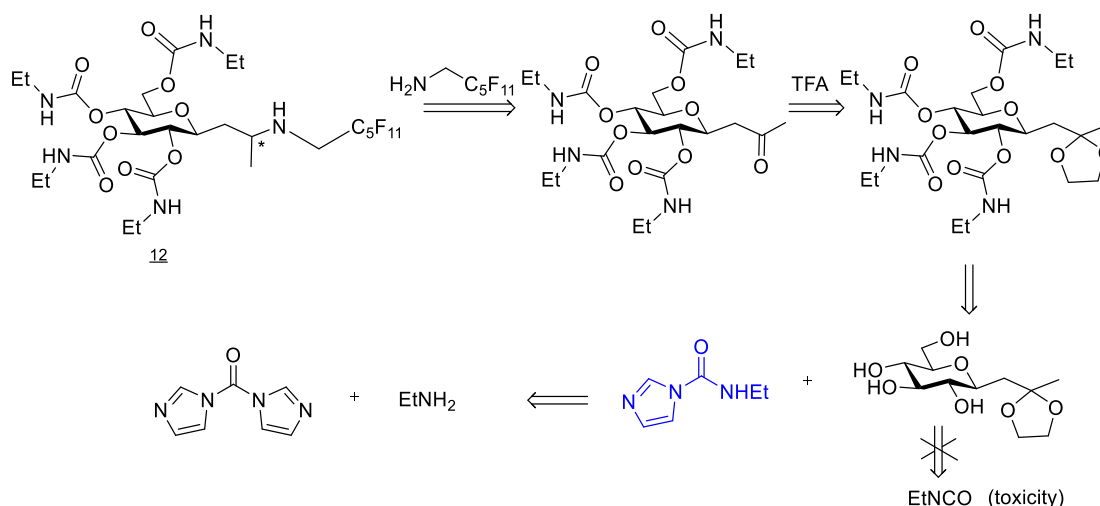
The last step to obtain the target compound is the reductive amination of 16 with perfluorohexylamine. Similar conditions were used like producing reductive amination product 3 (scheme 3-49). Considering the steric hindrance of Phenyl groups, the reaction was heated at 60 °C.

However, from the result of HRMS, no target reductive amination product was obtained. The possible reason could be the steric hindrance from the protecting groups in glycoside and the lower the reactivity of the electrophilic ketone.



Scheme 3-49: Synthesis of target compound **11**

Concerning the target compound **12**, ethyl isocyanate is undesirably used to introduce -CONH- in C-glycoside due to its toxicity and handling difficulties. Therefore, in the synthesis of compound **12**, 1,1-carbonyldiimidazole (CDI) and ethylamine were proposed to be the substitution of ethyl isocyanate. The retro synthetic scheme 3-50 of compound **12** is shown as following.



Scheme 3-50: Retro synthetic route of compound **12**

Secondary amines have long been known to react with CDI to give stable carbamoylimidazoles in high yields. Conversely the reaction of CDI with primary alkyl amines is prone to symmetrical urea formation, likely resulting from the dissociation of the adduct to imidazole and the corresponding isocyanate. [178]

Firstly, 1.2 eq CDI was reacted with 1 eq EtNH₂ in 10 ml ACN at room temperature. However, from the ¹H NMR spectra, the signal of symmetrical urea was observed. (figure 3-8, in green). The signals at 1.05 and 3.13 ppm are assigned to C₂H₅NHCONHC₂H₅.

During the purification by column chromatography, no pure carbamoylimidazole can be obtained. In order to avoid the formation of symmetrical urea, 3 eq CDI was used comparing with EtNH₂, and the reaction system was diluted 30 times comparing with the previous methodology. (scheme 3-51) Moreover, ethylamine was added to the reaction system drop by drop. As a result, compound **17** (65% yield) was obtained with less amount of C₂H₅NHCONHC₂H₅ as a side product than the previous methodology. The ¹H NMR spectrum

Besides, the protected partially perfluorinated C-glycoside (**C-Glc-OAc**, figure 3-10) was also successfully obtained by the similar synthesis route. **C-Glc-OAc** was synthesized as a control, in order to investigate if hydroxyl groups in C-glycosides can improve the restoration efficacy as expected. Different physical properties like physical states, solubility and color could have an influence on the restoration performance.

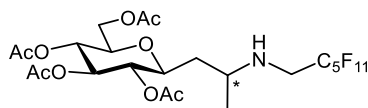
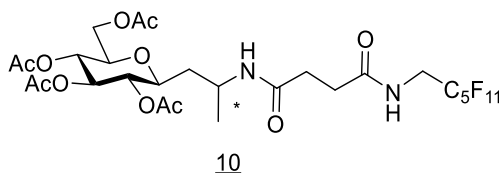


Figure 3-10: **C-Glc-OAc**

In the target molecule (**C-Glc-OH**), hydroxyls are expected to affine with polar substrates, stones and porous blanching paintings through hydrogen bonding. The compound is supposed to give good adhesion and long-term durability on stones. It could enter also into the pores and decrease the blanching in easel paintings. Meanwhile, the perfluorinated tail introduced into the molecule is supposed to form a coating on stones with efficient water repellency.

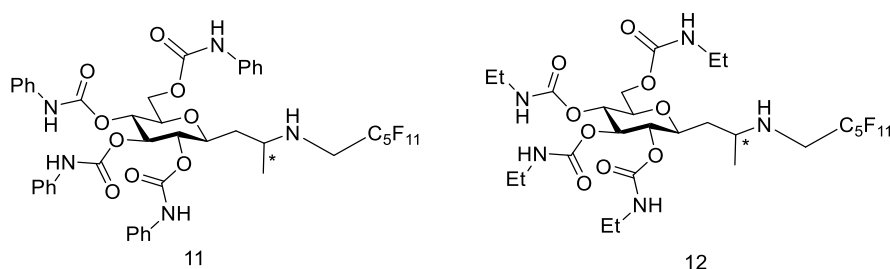
Besides, compound 10 as a peracetate C-glycoside with perfluorochain and amide functions was obtained. In order to obtain the free OH groups and increase the polarity of the molecule, a deprotected C-glycoside with perfluorochain and amide groups could be synthesized from compound 10 and used for the restoration application in the future.



10

Figure 3-11: Compound 10

Also, other two target C-glycosides 11 and 12 which contains -CONH- protected groups and perfluorochain was designed. The -CONH- could increase the interaction between the molecules and substrates, while the perfluorochain could contribute to good hydrophobicity. Their synthesis work could be developed in the future.



11

12

Figure 3-12: Target compounds 11 and 12

3.4 Experimental Part

Reactions were monitored by TLC (silica 60 F254 provided by Merck), revealed under a 254 nm UV lamp and using a 10 % sulfuric acid in ethanol, a ninhydrine solution with acetic acid in ethanol (1.5 g/500 mL plus 5 mL AcOH), a KMnO_4 solution in water (3 g plus 20 g potassium carbonate plus 5 mL 5 % NaOH in 300 mL), or a phosphomolybdic acid solution in ethanol (6 g in 100 mL). Purifications on silica gel were performed using a Macherey-Nagel 70-230 mesh silica.

NMR spectra were acquired with a BRUCKER AVANCE II 400 spectrometer. Chemical shift (δ) are reported in parts per million (ppm) relative to the residual solvent signal. Coupling constant values (J) are given in Hertz (Hz) and refer to apparent multiplicities, indicated as follows: br s (broad singlet), s (singlet), d (doublet), dd (doublet of doublet), ddd (doublet of doublet of doublet), ddt (doublet of doublet of triplet), td (triplet of doublet), t (triplet), q (quartet), qd (quartet of doublet), m (multiplet).

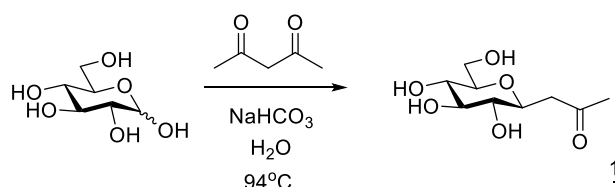
Mass spectra (MS in electronic impact (EI+) ionization mode) were measured on a Thermo Scientific ITQ 700 GC-MS spectrometer fitted with Varian column ($l = 25$ m, $\varnothing = 0.25$ mm, $df = 0.25$ μm).

HRMS analyses were performed by the Small Molecule Mass Spectrometry platform of IMAGIF (Centre de Recherche de Gif - www.imagif.cnrs.fr).

Infrared spectra (FT-IR) were recorded in ATR mode on a PerkinElmer Spectrum Two spectrometer and treated *via* Spectrum 10 software.

Melting points were recorded on a Büchi M-560 apparatus and given uncorrected.

C-(β -D-glucopyranosyl)]propanone (1)

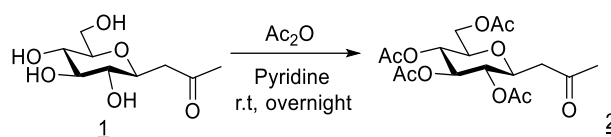


To a solution of D-glucose (10 g) in water (150 ml) were added sodium bicarbonate (7 g) and pentane-2,4-dione (7 ml). After stirring at 94 °C for 48 h, the reaction mixture was washed with CH_2Cl_2 (5 ml) and treated with Dowex resin (50X8-200, H^+ form). After concentrating the aq. mixture, the oil was resolved in water (100 ml) and followed by adding sodium bicarbonate (6 g). And the mixture was heating at 90 °C for two days. By repeating the work-up steps mentioned before, (8 g) brown oil was obtained. (Yield 65 %) The ^1H and ^{13}C were described in literature. [95]

$^1\text{H-NMR}$ (400MHz, CD_3OD):

δ 2.18(3H, CH_3); 2.58(dd, 1H); 2.86(dd, 1H); 3.04(t, 1H); 3.18-3.29(m, 2H); 3.33(t, 1H); 3.59 (dd, 1H, H_6); 3.64(td, 1H, H_1); 3.75(dd, 1H, H_6) ppm

C-(2,3,4,6-tetra-O-acetyl-β-D-glucopyranosyl)propanone (**2**)

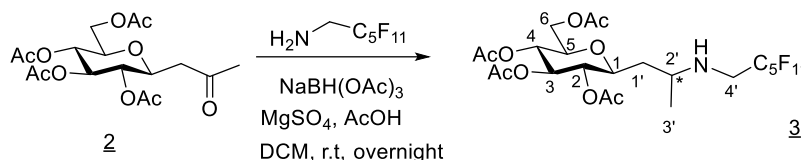


To a solution of compound **1** (12 g; 54 mmol) in pyridine (120 mL), acetic anhydride (40 mL; 424 mmol) was added under stirring. The reaction mixture is kept at room temperature over night. After reaction, the mixture was washed by HCl diluted solution and dichloromethane. The organic phase was collected and concentrated. White solid was obtained. (Yield 46 %). ¹H and ¹³C spectrums are described in literature [179].

¹H-NMR(400MHz, CDCl₃):

δ1.94(s, 3H, OAc); 1.97(s, 3H, OAc); 2.01(s, 3H, OAc); 2.03(s, 3H, OAc); 2.12(s, 3H, CH₃); 2.44 (dd, 1H); 2.69(dd, 1H); 3.64(ddd, 1H, H₁); 3.94(m, 1H, H₅); 4.01(dd, 1H, H₆); 4.19(dd, 1H, H₆); 4.84(dd, 1H, H₂); 4.99(dd, 1H, H₄); 5.15(dd, 1H, H₃) ppm

N-(2,2,3,3,4,4,5,5,6,6,6-undecafluorohexyl)-1-[C-(2',3',4',6'-tetra-O-acetyl-β-D-glucopyranosyl)]propan-2-amine (**3**)



To a solution of compound **2** (0.388 g; 1 mmol) in dichloromethane (20 mL), MgSO₄ (0.24 g; 2 mmol), acetic acid (0.0114 mL; 0.2 mmol), sodium triacetoxyborohydride NaBH(OAc)₃ (0.46 g; 2.2 mmol), and 1*H*,1*H*-Perfluorohexylamine (0.27 mL; 1.5 mmol) were added and the mixture was stirring at room temperature over night. The reaction was monitored by TLC. The reaction mixture was quenched by water (12 mL), and the organic layer was separated. The aqueous layer was extracted by ethyl acetate (3X15 mL). The combined organic layers were dried by MgSO₄ and concentrated. The white solid was purified by flash column chromatography using Cyclohexane/AcOEt 8:2 as eluent. (Yield 69 %; Ratio 70:30).

¹H-NMR(400MHz, CDCl₃):

δ1.04(d, ³J_{H3'-H2'} = 6.2 Hz, 3H, H_{3'}); 1.44(ddd, ²J = 14.5 Hz, ³J_{H1'-H2'} = 5.9 Hz, ³J_{H1'-H1} = 2.0 Hz, 1H, H_{1'}); 1.59(ddd, ²J = 14.5 Hz, ³J_{H1'-H1} = 9.7 Hz, ³J_{H1'-H2'} = 6.5 Hz, 1H, H_{1'}); 1.95(s, 3H, OAc); 1.98(s, 3H, OAc); 1.99(s, 3H, OAc); 2.01(s, 3H, OAc); 2.91-3.01(m, 1H, H_{2'}); 3.05-3.39(m, 2H, H_{4'}); 3.51(ddd, ³J_{H1-H2} = 9.5 Hz, ³J_{H1-H1'} = 9.7 Hz, ³J_{H1-H1'} = 2.0 Hz, 1H, H₁); 3.6(ddd, ³J_{H5-H4} = 9.7 Hz, ³J_{H5-H6} = 5.0 Hz, ³J_{H5-H6} = 2.5 Hz, 1H, H₅); 4.00-4.20(m, 2H, H₆); 4.83(dd, ³J_{H2-H1} = 9.5 Hz, ³J_{H2-H3} = 9.5 Hz, 1H, H₂); 4.99(dd, ³J_{H4-H5} = 9.7 Hz, ³J_{H4-H3} = 9.5 Hz, 1H, H₄); 5.12(dd, ³J_{H3-H2} = 9.5 Hz, ³J_{H3-H4} = 9.5 Hz, 1H, H₃) ppm

¹³C-NMR(101 MHz, CDCl₃):

δ20.47(C_{3'}); 20.74(COCH₃); 20.82(COCH₃); 20.84(COCH₃); 20.89(COCH₃); 38.28(C_{1'}); 46.04 (t, ²J_{C-F} = 22.3 Hz, C_{4'}); 51.07 (C_{2'}); 62.48(C₆); 68.66(C₄); 72.17(C₂); 74.35(C₃); 75.95(C₅); 76.97 (C₁), 107-121(m, C₅-C₉), 169.68(COCH₃); 169.85(COCH₃); 170.56(COCH₃); 170.84(COCH₃) ppm

¹⁹F-NMR(376.2 MHz, CDCl₃):

δ-80.7 (m, 3F, F_{9'}); -118.1 (m, 2F); -123.2 (m, 4F); -126.2 (m, 2F) ppm

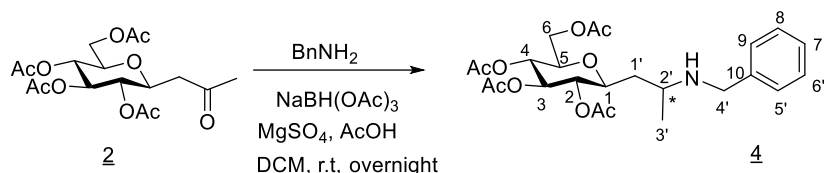
HRMS

ES+ C₂₃H₂₉NO₉F₁₁ [M+H]⁺calc = 672.1667; found 672.1661

Rf = 0.47 (Cyclohexane/AcOEt 7:3; 10% H₂SO₄ in EtOH).

IR (ATR): 1222.29, 1366.48, 1382.79, 1742.93, 2866.59, 2942.85, 3362.86 cm⁻¹.

M.P: 79.6-81.5°C

N-benzyl-1-[C-(2',3',4',6'-tetra-O-acetyl-β-D-glucopyranosyl)]propan-2-amine (4)

To a solution of compound **2** (0.388 g; 1 mmol) in dichloromethane (20 mL), MgSO₄ (0.24 g; 2 mmol), acetic acid (0.0114 mL; 0.2 mmol), sodium triacetoxyborohydride NaBH(OAc)₃ (0.46 g; 2.2 mmol), and (0.163 mL; 1.5 mmol) benzylamine were added and the mixture was stirring at room temperature over night. The reaction was monitored by TLC. The reaction mixture was quenched by water (12 mL), and the organic layer was separated. The aqueous layer was extracted by ethyl acetate (3X15 mL). The combined organic layers were dried by MgSO₄ and concentrated. The lightly yellow solid was purified by flash column chromatography using Cyclohexane/EtOAc/MeOH 4:2:1 as eluent. (Yield 67 %; Ratio 71:29).

¹H-NMR(400MHz, CDCl₃):

δ1.09(d, ³J_{H3'-H2'} = 7.2 Hz, 3H, H_{3'}); 1.42-1.52 (ddd, ²J = 19.3 Hz, ³J_{H1'-H2'} = 12.4 Hz, ³J_{H1'-H1} = 6.2 Hz, 1H, H_{1'}); 1.76(ddd, ²J = 15.4, ³J_{H1'-H2'} = 10.2 Hz, ³J_{H1'-H1} = 6.1 Hz, 1H, H_{1'}); 1.91(s, 3H, OAc); 1.93 (s, 3H, OAc); 1.96(s, 6H, OAc); 2.94-3.01(m, 1H, H_{2'}); 3.72-3.83 (m, 2H, H_{4'}); 3.48 (ddd, ³J_{H1-H2} = 19.1 Hz, ³J_{H1-H1'} = 8.0Hz, ³J_{H1-H1'} = 3.6 Hz, 1H, H₁); 3.54(ddd, ³J_{H5-H4} = 10.0 Hz, ³J_{H5-H6} = 5.4 Hz, ³J_{H5-H6} = 2.5 Hz, 1H, H₅); 3.99-4.13(m, 2H, H₆); 4.81(dd, ³J_{H2-H1} = 9.2 Hz, ³J_{H2-H3} = 9.2 Hz, 1H, H₂); 4.96(dd, ³J_{H4-H3} = 9.6 Hz, ³J_{H4-H5} = 9.6 Hz, 1H, H₄); 5.09(dd, ³J_{H3-H2} = 9.2 Hz, ³J_{H3-H4} = 9.2 Hz, 1H, H₃); 7.25(5H, H_{5'}-H₉) ppm

¹³C-NMR(101 MHz, CDCl₃):

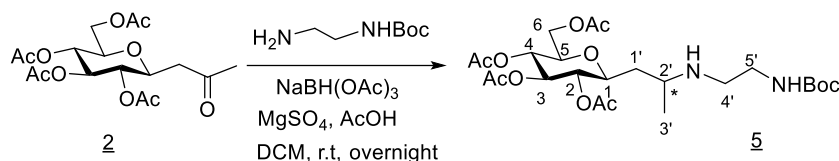
δ19.65(C_{3'}); 20.63(COCH₃); 20.65(COCH₃); 20.67(COCH₃); 20.72(COCH₃); 36.96(C_{1'}); 49.92(C_{4'}); 50.06(C_{2'}); 62.38(C₆); 68.58(C₄); 71.98(C₂); 74.14(C₃); 75.67(C₅); 76.61(C₁); 127.44; 128.42-128.61(C₅-C₁₀); 169.54(COCH₃); 169.71(COCH₃); 170.42(COCH₃); 170.71(COCH₃) ppm

HRMS

ES+C₂₄H₃₄NO₉ [M+H]⁺calc = 480.2234; found 480.2234

Rf=0.25 (Cyclohexane/EtOAc/MeOH 4:2:1; 10 % H₂SO₄ in EtOH)

N-(2-(*N*-*tert*-Butoxycarbonylamino)-1-[C-(2',3',4',6'-tetra-O-acetyl-β-D-glucopyranosyl)]propan-2-amine (**5**)



To a solution of compound **2** (0.414 g; 1.067 mmol) in dichloromethane (21 mL), MgSO₄ (0.257 g; 2.134 mmol), acetic acid (0.0122 mL; 0.2134 mmol), sodium triacetoxyborohydride NaBH(OAc)₃ (0.5 g; 2.23474 mmol), and Boc group protected amine (0.257 g; 1.6 mmol) and the mixture was stirring at room temperature over night. The reaction was monitored by TLC. The reaction mixture was quenched by water (15 mL), and the organic layer was separated. The aqueous layer was extracted by ethyl acetate (3×15 mL). The combined organic layers were dried by MgSO₄ and concentrated. The lightly yellow solid was purified by flash column chromatography using EtOAc/MeOH 8:2 as eluent. (Yield 60 %; Ratio 72:28).

¹H-NMR(400MHz, CDCl₃):

δ1.09(m, 3H, H_{3'}); 1.18(m,2H,H_{4'}); 1.37(s,9H,*tert*-butyl); 1.43-1.68 (m,2H,H_{1'}); 1.93(s, 3H, OAc); 1.96(s, 3H, OAc); 1.98(s,3H,OAc); 2.02(s,3H,OAc); 2.98(m,1H,H_{2'}); 3.57-3.62(ddd, ³J_{H5-H4} = 9.9 Hz, ³J_{H5-H6} = 4.7 Hz, ³J_{H5-H6} = 2.3Hz,1H,H₅); 3.69(m,1H,H₁); 4.06(m,2H,H_{5'}); 4.15(m,2H,H₆); 4.80(dd,³J_{H2-H1} = 9.6 Hz, ³J_{H2-H3} = 9.6 Hz, 1H, H₂1H,H₂); 4.97(dd,³J_{H4-H5} = 9.7 Hz, ³J_{H4-H3} = 9.5 Hz, 1H, H₄); 5.15(dd, ³J_{H3-H2} = 9.2 Hz, ³J_{H3-H4} = 9.2 Hz, 1H, H₃) ppm

¹³C-NMR(101 MHz, CDCl₃):

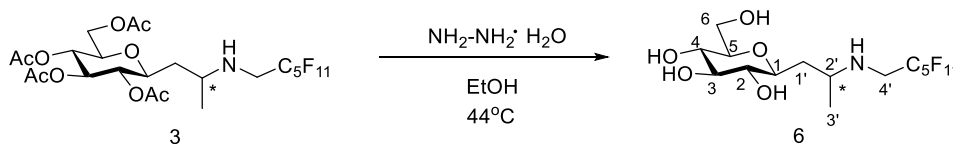
δ19.11(C_{3'}); 29.74(C_{4'}); 28.41(C_{9'}); 36.81(C_{1'}); 20.65(COCH₃); 20.66(COCH₃); 20.73(COCH₃); 20.80(COCH₃); 50.86(C_{2'}); 62.07(C_{5'}); 62.22(C₆); 68.40(C₄); 71.93(C₂); 74.14(C₃); 74.73(C₁); 74.85(C₅); 169.52(COCH₃); 169.73(COCH₃); 170.39(COCH₃); 170.78(COCH₃) ppm.

HRMS

ES+ C₂₄H₄₁N₂O₁₁ [M+H]⁺calc = 533.2710 ; found 533.2713

Rf= 0.33 (EtOAc/MeOH 8:2, 10 % H₂SO₄ in EtOH)

N-(2,2,3,3,4,4,5,5,6,6,6-undecafluorohexyl)-[1-[C-(2',3',4',6'-tetra-O-Acetyl-β-D-glucopyranosyl)]propan-2-amine (**6**)



To a solution of compound **3** (1 g; 1.49 mmol) in ethanol (20 mL), hydrazine monohydrate (708 mg; 14.16 mmol) was added. The reaction mixture was stirred at 44 °C overnight and monitored by TLC. The mixture was concentrated under reduced pressure. Lightly yellow oil was obtained after purification by silica gel with ACN/H₂O/NH₃·H₂O 20:1:1. (Yield 42 %; Ratio 73:27).

¹H-NMR (400 MHz, CD₃OD):

δ1.00(d, ³J_{H3'-H2'} = 6.4 Hz, 3H, H_{3'}); 1.41-1.50(ddd,²J = 14.3 Hz, ³J_{H1'-H2'} = 9.8Hz, ³J_{H1'-H1} = 6.3 Hz,

1H, H_{1'}); 1.71-1.77(m,1H, H_{1'}); 2.91-3.01(m, 1H, H_{2'}); 2.94-2.99(m,1H,H_{4'}); 3.17(m, 1H, H_{1'}); 3.08-3.13(dd, ³J_{H₂-H₁} = 9.6 Hz, ³J_{H₂-H₃} = 9.6 Hz, 1H, H₄); 3.19-3.21(m,1H,H_{4'}); 3.20-3.24(m,2H,H₆); 3.28(ddd,³J_{H₅-H₄} = 12 Hz, ³J_{H₅-H₆} = 8.8 Hz, ³J_{H₅-H₆} = 2.4 Hz 1H, H₅); 3.53(dd, ³J_{H₃-H₂} = 12Hz, ³J_{H₃-H₄} = 12Hz, 1H, H₃); 3.71(dd, ³J_{H₄-H₅} = 11.6 Hz, ³J_{H₄-H₃} = 11.6 Hz, 1H, H₂) ppm

¹³C-NMR(101 MHz,CD₃OD)

δ19.54(C_{3'}); 38.31(C_{1'}); 50.27(C_{2'}); 51.56(C_{4'}); 61.53(C₃; C₂); 70.37(C₆); 76.92(C₅); 78.66(C₁); 80.18(C₄) ppm

¹⁹F-NMR(376.2 MHz, CD₃OD)

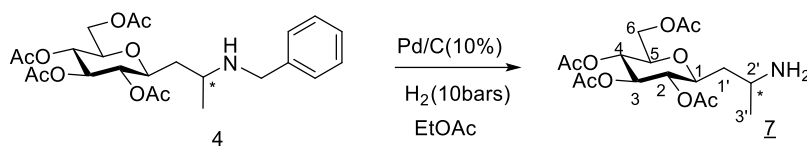
δ-80.7 (m, 3F, F_{9'}); -118.88 (m, 2F); -123.78 (m, 2F); -124.58(m,2F); -127.41 (m, 2F) ppm
Rf=0.31 (ACN/H₂O/ NH₃·H₂O 15:1:1,10 % H₂SO₄ in EtOH)

HRMS:

ES+C₁₅H₂₀F₁₁NO₅[M+H]⁺calc = 504.1167; found 504.1240

IR (ATR): 1534.6, 1623.05, 1652.22, 3044.70, 3270.64, 3469.73 cm⁻¹.

1-[C-(2',3',4',6'-tetra-O-Acetyl-β-D-glucopyranosyl)]propan-2-amine (7)



To a solution of compound **4** (0.2 g; 0.42 mmol) in EtOAc (4 mL), Pd/C 10 % (44,4 mg) was added. The mixture was stirred under hydrogen atmosphere (10 bars) for two days. After reaction, the extra Pd/C was filtrated by Celite and washed by EtOAc. After the solvent was evaporated, the crude was purified by silica gel using AcOEt/methanol 40:1 as eluent. (Yield 66 %; Ratio 59:41)

¹H-NMR (400 MHz, CDCl₃)

δ1.02(d, ³J_{H_{3'}-H_{2'}} = 6.4 Hz, 3H, H_{3'}); 1.43(ddd, ²J = 15.4 Hz, ³J_{H_{1'}-H_{2'}} = 5.9 Hz, ³J_{H_{1'}-H₁} = 2.7 Hz, 1H, H_{1'}); 1.60(ddd, ²J = 14.8 Hz, ³J_{H_{1'}-H₁} = 8.2 Hz, ³J_{H_{1'}-H_{2'}} = 3.3 Hz, 1H, H_{1'}); 1.93(s, 3H, OAc); 1.96(s, 3H, OAc); 1.98(s, 3H, OAc); 2.01(s, 3H, OAc); 3.33(m, 1H, H_{2'}); 3.46(ddd, ³J_{H₁-H₂} = 17.4 Hz, ³J_{H₁-H_{1'}} = 8.2 Hz, ³J_{H₁-H_{1'}} = 2.7 Hz, 1H, H₁); 3.57(m, 1H, H₅); 3.99-4.19(m, 2H, H₆); 4.80(dd, ³J_{H₂-H₁} = 9.6 Hz, ³J_{H₂-H₃} = 9.6 Hz, 1H, H₂); 4.96(dd, ³J_{H₄-H₅} = 9.6Hz, ³J_{H₄-H₃} = 9.6 Hz, 1H, H₄); 5.10(dd, ³J_{H₃-H₂} = 9.6 Hz, ³J_{H₃-H₄} = 9.6 Hz, 1H, H₃) ppm

¹³C-NMR (101 MHz, CDCl₃)

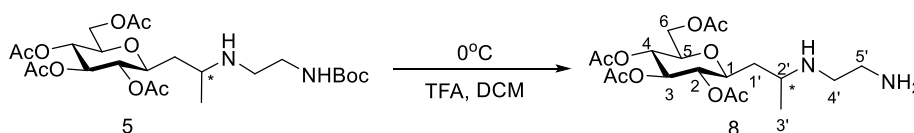
δ20.34(C_{3'}); 20.64(COCH₃); 20.70(COCH₃); 20.83(COCH₃); 20.92(COCH₃); 41.00(C_{1'}); 61.91(C_{2'}); 62.41(C₆); 68.64(C₄); 72.13(C₂); 74.17(C₃); 75.29(C₁); 75.66(C₅); 169.54(COCH₃); 169.70(COCH₃); 169.79(COCH₃); 170.16(COCH₃) ppm

HRMS

ES+ C₂₃H₂₉NO₉F₁₁ [M+H]⁺calc = 672.1667; found 672.1661

Rf= 0.4 (EtOAc/MeOH 20:1, 10 % H₂SO₄ in EtOH)

N-(Aminoethyl)-1-[C-(2',3',4',6'-tetra-O-acetyl-β-D-glucopyranosyl)]propan-2-amine (8)



To a solution of compound 5 (0.2 g; 0.375 mmol) in dichloromethane (2 ml), trifluoroacetic acid (0.2 ml; 2.61 mmol) was added at 0 °C under stirring. The reaction mixture was stirred at room temperature over night. After the solvent was evaporated, the product was obtained by purification using silica gel with ACN/methanol/ammonia 15:1:1 as eluent. (Yield 53 %; Ratio 72:28)

¹H-NMR (400 MHz, CD₃OD)

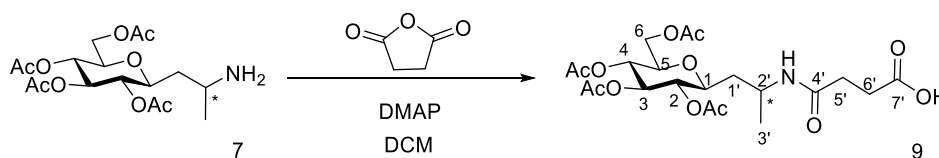
δ1.18(d, ³J_{H₃'-H₂'} = 6.8 Hz, 3H, H₃'); 1.57(ddd, ²J = 13.8 Hz, ³J_{H₁'-H₂'} = 6.9 Hz, ³J_{H₁'-H₁} = 3.4 Hz, 1H, H₁'); 1.73(ddd, ²J = 14.9 Hz, ³J_{H₁'-H₂'} = 9.2 Hz, ³J_{H₁'-H₁} = 5.2 Hz, 1H, H₁'); 1.95(s, 3H, OAc); 2.00(s, 3H, OAc); 2.01(s, 3H, OAc); 2.03(s, 3H, OAc); 3.03(m, 4H, H₄', H₅'); 3.47-3.57(m, 1H, H₂'); 3.72(ddd, ³J_{H₁-H₂} = 10.9 Hz, ³J_{H₁-H₁'} = 8.0 Hz, ³J_{H₁-H₁'} = 2.3 Hz, 1H, H₁); 3.78(ddd, ³J_{H₅-H₄} = 10.2 Hz, ³J_{H₅-H₆} = 4.1 Hz, ³J_{H₅-H₆} = 2.3 Hz, 1H, H₅); 4.14-4.27(m, 2H, H₆); 4.81(dd, ³J_{H₂-H₁} = 9.6 Hz, ³J_{H₂-H₃} = 9.6 Hz, 1H, H₂); 5.00(dd, ³J_{H₄-H₅} = 9.7 Hz, ³J_{H₄-H₃} = 9.5 Hz, 1H, H₄); 5.20(dd, ³J_{H₃-H₂} = 9.6 Hz, ³J_{H₃-H₄} = 9.6 Hz, 1H, H₃) ppm

¹³C-NMR (101 MHz, CD₃OD)

δ15.18(C₃'); 18.39(COCH₃); 19.19(COCH₃); 19.35(COCH₃); 19.44(COCH₃); 34.76(C₁'); 36.09(C₄'); 41.92(C₅'); 53.13(C₂'); 61.23(C₆); 68.04(C₄); 71.77(C₂); 73.96(C₃); 74.75(C₅); 75.58(C₁); 169.95(COCH₃); 170.15(COCH₃); 170.42(COCH₃); 171.60(COCH₃) ppm

Rf=0.38 (ACN/H₂O/ NH₃·H₂O 10 :1 :1, 10 % H₂SO₄ in EtOH)

4-(1-(2,3,4,6-tetra-O-Acetyl-β-D-glucopyranosyl)-N-propan-2-yl-amino)-4-oxobutanoic acid (9)

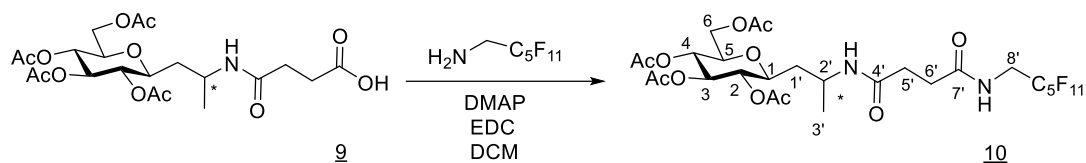


To a solution of 7 (0.18 g; 0.462 mmol) in dichloromethane (2 mL), succinic anhydride (0.069 g; 0.693 mmol), 4-dimethylaminopyridine (DMAP) (0.085 g; 0.693 mmol) was added. The reaction mixture was stirred at room temperature under Argon atmosphere overnight. After the reaction mixture was washed by NH₄Cl solution until the pH=4, NaCl solution was added to wash the organic phase. The organic parts were evaporated and white solid were obtained. (Yield 100%)

¹H-NMR (400 MHz, CDCl₃)

δ1.09(m, 3H, H₃); 1.53(m, 1H, H₁); 1.64(m, 1H, H₁); 1.94(s, 3H, OAc); 1.97(s, 3H, OAc); 1.99(s, 3H, OAc); 2.03(s, 3H, OAc); 2.46-2.72(m, 4H, H₅', H₆'); 3.49(m, 1H, H₁); 3.58(m, 1H, H₅); 4.02(m, 1H, H₂); 4.20(m, 2H, C₆); 4.79(dd, ³J_{H₂-H₁} = 9.6 Hz, ³J_{H₂-H₃} = 9.6 Hz, 1H, H₂); 4.99(dd, ³J_{H₄-H₅} = 9.6 Hz, ³J_{H₄-H₃} = 9.6 Hz, 1H, H₄); 5.10(dd, ³J_{H₃-H₂} = 9.6 Hz, ³J_{H₃-H₄} = 9.6 Hz, 1H, H₃) ppm

N-(2,2,3,3,4,4,5,5,5-undecafluorohexyl)-4-(1-(2,3,4,6-tetra-*O*-Acetyl- β -D-glucopyranosyl)-*N*-propan-2-yl-amino)-4-oxobutanoic acid (**10**)



To a solution of compound **9** (0.036 g; 0.0735 mmol) in dichloromethane (1 mL), 1H,1H-perfluorohexylamine (0.0268 mL; 0.147 mmol), 4-dimethylaminopyridine (DMAP) (0.012 g; 0.098 mmol) and 1-Ethyl-3-(3-dimethylaminopropyl)carbodiimide (EDC) (0.021 g; 0.11 mmol) were added. The reaction mixture was kept stirring at 40 °C in a closed Sovirel® tube for 24 h. After cooling to room temperature, the reaction mixture was washed by water. The aqueous phase was extracted by EtOAc. The organic phase was washed by NH₄Cl solution and NaCl solution. After the solvent was evaporated, the crude was purified by silica gel using cyclohexane/ethyl acetate 3:7 as eluent and yellow oil was obtained. (Yield 42 %; Ratio 69:31).

¹H-NMR (400 MHz, CDCl₃)

δ 1.07(d, ³J_{H_{3'}-H_{2'}} = 7.2 Hz, 3H, H_{3'}); 1.46-1.60(m, 1H, H_{1'}); 1.88(s, 3H, OAc); 1.93(s, 3H, OAc); 1.96(s, 3H, OAc); 2.02(s, 3H, OAc); 2.58(m, 2H, H_{5'}); 2.48(m, 2H, H_{6'}); 4.07(m, 1H, H_{2'}); 3.43(ddd, ³J_{H₁-H₂} = 17.4 Hz, ³J_{H₁-H_{1'}} = 10.4 Hz, ³J_{H₁-H_{1'}} = 2.6 Hz, 1H, H₁); 3.57(ddd, ³J_{H₅-H₄} = 10.1 Hz, ³J_{H₅-H₆} = 5.0 Hz, ³J_{H₅-H₆} = 2.1 Hz, 1H, H₅); 3.89(m, 2H, H₈); 4.15(m, 2H, H₆); 4.79(dd, ³J_{H₂-H₁} = 9.6 Hz, ³J_{H₂-H₃} = 9.6 Hz, 1H, H₂); 4.96(dd, ³J_{H₄-H₅} = 9.6 Hz, ³J_{H₄-H₃} = 9.6 Hz, 1H, H₄); 5.1(dd, ³J_{H₃-H₂} = 9.6 Hz, ³J_{H₃-H₄} = 9.6 Hz, 1H, H₃) ppm

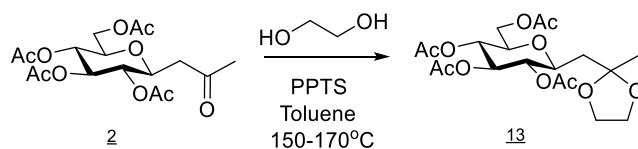
¹³C-NMR (400 MHz, CDCl₃)

δ 20.64(C_{3'}); 22.71(COCH₃); 23.35(COCH₃); 23.44(COCH₃); 23.51(COCH₃); 29.12(C_{5'}); 30.49(C_{6'}); 37.99(C_{1'}); 39.02(t, C_{8'}); 42.87(C_{2'}); 62.12(C₆); 68.46(C₄); 72.28(C₂); 73.98(C₃); 75.75(C₁); 76.11(C₅); 169.63(COCH₃); 169.80(COCH₃); 170.52(COCH₃); 170.82(COCH₃); 171.64(C_{4'}); 171.88(C_{7'}) ppm

¹⁹F-NMR (376.2 MHz, CDCl₃)

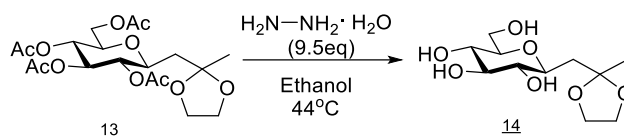
δ -80.7(m, 3F, F_{13'}); -118.1(m, 2F); -123.6(m, 4F); -126.3(m, 2F) ppm
Rf=0.35 (Cyclohexane/ EtOAc 2:8; 10 % H₂SO₄ in EtOH)

1-[2,3,4,6-tetra-*O*-Acetyl- β -D-glucopyranosyl](2-methyl-1,3-dioxolan-2-yl)methane (**13**)



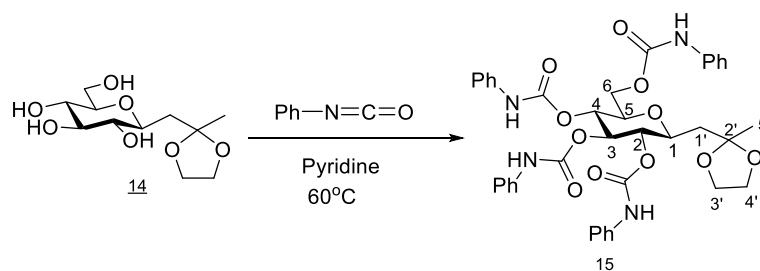
Keto C-glycoside **2** (10.32 g, 26.57 mmol, 1 eq), ethylene glycol (3.6 g, 57.9 mmol, 2.2 eq) and PPTS (Pyridinium p-toluenesulfonate) (1.078 g, 4.29 mmol, 0.16 eq) were dissolved in toluene (189 ml). The mixture was heating at 150 °C-170 °C for 3 h using the Dean–Stark apparatus. After evaporation of the reaction mixture, flash chromatography gives compound **13** with quantitative yield. The ¹H and ¹³C are described in literature [180].

1- β -D-Glucopyranosyl-(2-methyl-1,3-dioxolan-2-yl)methane (**14**)



Compound **13** (12.82 g, 26.55 mmol, 1 eq) was added into ethanol (150 ml), followed by hydrazine monohydrate (12.29 ml, 252.2 mmol, 9.5 eq). The mixture was heating at 44 °C overnight. After cooling the reaction mixture, evaporated the reaction residue and did the purification by column chromatography. Compound **14** was obtained as a lightly white solid with 100 % yield. The ^1H and ^{13}C are described in literature [180].

1-[2,3,4,6-tetra-O-(N-Phenyl)carbamoyl- β -D-glucopyranosyl](2-methyl-1,3-dioxolan-2-yl)methane (**15**)



1 equivalent of compound **14** (208.1 mg, 0.757 mmol) was dissolved in 2.7 ml pyridine and 5 equivalents of phenyl isocyanate (450 mg, 3.78 mmol) were used. The reaction mixture was heating at 60 °C. Evaporated the reaction mixture and did the purification by column chromatography. The compound **15** was obtained with 42 % yield as a white solid.

$^1\text{H-NMR}$ (400 MHz, DMSO-d_6)

δ 1.33(s, 3H, H_5); 1.77 (ddd, $^2J = 14.5$ Hz, $^3J_{\text{H}1'-\text{H}2'} = 5.9$ Hz, $^3J_{\text{H}1'-\text{H}1} = 2.0$ Hz, 2H, H_1); 3.81(m, 4H, H_3', H_4'); 3.88 (m, 1H, H_1); 3.97(ddd, $^3J_{\text{H}5-\text{H}4} = 9.7$ Hz, $^3J_{\text{H}5-\text{H}6} = 5.0$ Hz, $^3J_{\text{H}5-\text{H}6} = 2.5$ Hz, 1H, H_5); 4.18(d, $^2J=12$ Hz, 1H, H_6); 4.37(dd, $^2J=12$ Hz, $^3J_{\text{H}6-\text{H}5} = 4$ Hz, 1H, H_6); 4.79(dd, $^3J_{\text{H}2-\text{H}1} = 9.6$ Hz, $^3J_{\text{H}2-\text{H}3} = 9.6$ Hz, 1H, H_2); 5.00(dd, $^3J_{\text{H}4-\text{H}5} = 9.6$ Hz, $^3J_{\text{H}4-\text{H}3} = 9.4$ Hz, 1H, H_4); 5.31(dd, $^3J_{\text{H}3-\text{H}2} = 9.6$ Hz, $^3J_{\text{H}3-\text{H}4} = 9.6$ Hz, 1H, H_3); 6.89-7.46(m, 20H, Ph); 9.7-9.84(m, 4H, CONH) ppm

$^{13}\text{C-NMR}$ (101 MHz, DMSO-d_6)

δ 25.51($\text{C}5'$); 40.35($\text{C}1'$); 63.11($\text{C}6$); 64.31, 64.39($\text{C}3', \text{C}4'$); 69.74($\text{C}4$); 72.63($\text{C}2$); 74.73($\text{C}3$); 75.1($\text{C}1$); 76.18($\text{C}5$); 118.93, 122.90, 129.04(Ph); 153.66, 153.21, 153.09, 152.7, (HNCOO) ppm

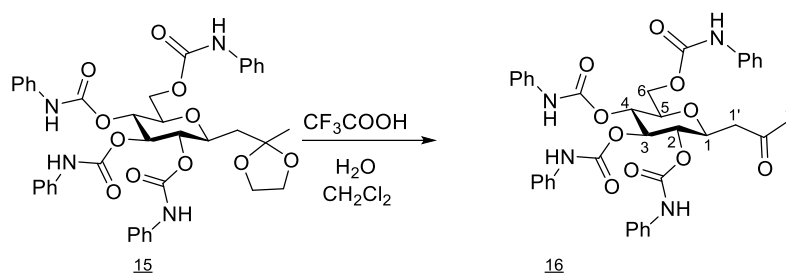
Rf=0.4 (Cyclohexane/ EtOAc 6:4; 10 % H_2SO_4 in EtOH)

HRMS

ES+ $\text{C}_{39}\text{H}_{40}\text{N}_4\text{O}_{11}$ [M+H] $^+$ calc =741.2767, found 741.2695

IR (ATR): 1300.10, 1315.63, 1379.60, 1600.25, 1705.71, 1737.23, 2874.69, 2927.07, 3340.66 cm^{-1} .

1-[2,3,4,6-tetra-O-(N-Phenyl)carbamoyl-β-D-glucopyranosyl]propan-2-one (**16**)



Compound **15** (115 mg, 0.156 mmol, 1 eq), TFA (423 mg, 3.7 mmol, 24 eq), and H₂O (28 mg, 1.57 mmol, 10 eq) were added in 2.84 ml dichloromethane. The reaction mixture was stirred at room temperature for 2 hours. Flash chromatography was used for purification. Compound **16** was obtained with 72 % yield as a white solid.

¹H-NMR (400 MHz, DMSO-*d*⁶)

δ2.14(s, 3H, H₂); 2.68(m, 2H, H_{1'}); 4.03(m, 1H, H₅); 4.16(m, 1H, H₁); 4.19(m, 1H, H₆); 4.29(m, 1H, H₆); 4.83(dd, ³J_{H2-H1} = 9.8 Hz, ³J_{H2-H3} = 9.7 Hz, 1H, H₂); 5.00(dd, ³J_{H4-H5} = 9.8 Hz, ³J_{H4-H3} = 9.8 Hz, 1H, H₄); 5.33(dd, ³J_{H3-H2} = 9.6 Hz, ³J_{H3-H4} = 9.6 Hz, 1H, H₃); 6.97-7.45(m, 20H, Ph); 9.7-9.80(m, 4H, CONH) ppm

¹³C-NMR (101 MHz, DMSO-*d*⁶)

δ30.43(C_{2'}); 45.43(C_{1'}); 76.14(C₅); 62.89(C₆); 69.47(C₄); 72.69(C₂); 74.64(C₃); 74.01(C₁); 119.67, 123.37, 129.23 (Ph); 152.68, 152.84, 153.12, 153.61 (HNCOO) ppm

Rf=0.5 (Cyclohexane/ EtOAc 4:6; 10 % H₂SO₄ in EtOH)

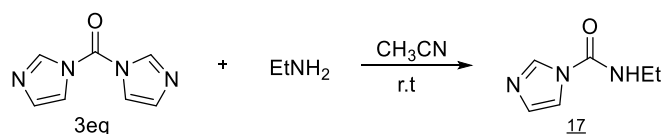
HRMS

ES+ C₃₇H₃₆N₄O₁₀, [M+Na]⁺calc =719.2432, found 719.2324.

IR (ATR): 1230.22, 1315.68, 1377.70, 1445.78, 1534.65, 1632.73, 1709.13, 2852.5, 2921.52, 2956.40, 3330.75 cm⁻¹.

MP. 240.9-243.1°C.

N-ethyl-1H-imidazole-1-carboxamide (**17**)



Carbonyldiimidazole (1.6 g, 9.87 mmol, 3 eq) was added in 30 ml acetonitrile, and ethylamine (148.2 mg, 3.289 mmol, 1 eq) was added to the reaction system drop by drop. The reaction mixture was stirred overnight at room temperature. Evaporated the reaction mixture and did the purification by column chromatography (ethyl acetate: methanol= 9:1). Compound **17** was obtained with 65 % yield.

¹H-NMR (400 MHz, CDCl₃)

δ1.27(t, ³J=7.3 Hz, 3H); 3.43-3.52(m, 2H); 7.07(m, 1H); 7.56(d, ³J=14.0 Hz, 1H); 8.30(s, 1H) ppm

Rf=0.4 (EtOAc/ MeOH 9:1; 10 % H₂SO₄ in EtOH)

Chapter 4

Partially perfluorinated oligomers

4.1 Introduction

4.1.1 Polyamide

The word “polymer” is derived from the Greek poly and meros, meaning many and parts, respectively. Polymers are macromolecules made up of multiple repeating units where the backbone is connected by covalent bonds—primary bonds. The precursors of structural units—monomers, have two or more active sites able to react with each other, forming chemical bonds and linkages *via* a process known as polymerization. Depending upon the molecular weight or polymerization degree, one could be termed “oligomer” if it has only 2–10 repeat units. The word oligomer is derived from the Greek oligos, meaning “a few.” [181]

In general, chemical properties of polymers, *e.g.*, polarity, reactivity, acidity or basicity, solubility (also influenced by the secondary forces), chemical, thermal, photo-oxidative stability, hydrophobicity are mainly determined by the chemical composition (or functional groups) and primary forces. Physical characteristics depend on micro morphology (linear, branched, network or cross-linked), macro morphology (amorphous; crystalline), melting point, glass transition temperature, viscosity, flexibility (also affected by the existing flexibilizing groups *e.g.*, methylene and ethylene oxides; stiffening groups *e.g.*, carboxyl, sulfonic groups) [182] and rigidity. Most physical properties are influenced by the polymer chains length, spatial shape and arrangements (conformation; configuration), essentially by the type and intensity of secondary forces.

There are currently a wide variety of synthetic polymers on the market that are utilized within the field of the conservation and restoration of artworks [183]. In restoration work, they are used as coatings, adhesives, fixatives, varnishes and consolidants. Polyolefins, polyesters, polyamides, polyacrylics and polyvinyls are among the most popular of the thermoplastic polymers used in this field, while among the thermosetting polymers epoxy polymers are also of interest. [184]

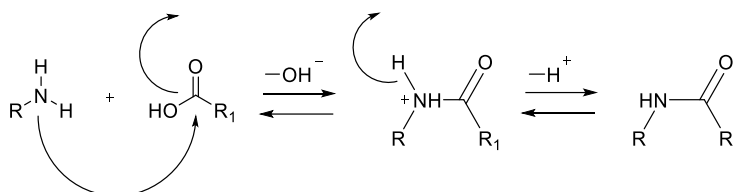
Polyamides are a widely studied polymeric class showing excellent mechanical and physical characteristics and good versatility, that allows their use in various application fields [185]. Commercial polyamides containing aliphatic amines are indicated with the term Nylon while those containing aromatic amines, such as Kevlar® and Nomex®, are called polyaramids. [186] Calaton, soluble nylon (N-methoxymethyl nylon), is widely used in conservation work. [187]

Polyamides are obtained by polycondensation reaction of monomers containing acid and/or amino groups; using differently functionalized monomers and different reaction conditions it is possible to obtain a large variety of products with different molecular weight

and with different chemical-physical characteristics. Generally, temperature should be kept above 200 °C to obtain polycondensation with the elimination of water as low molecular weight product.

The first synthesis of a polyamide dated back to 1935 and was carried out by Wallace Carothers (DuPont) that, starting from adipic acid and hexamethylenediamine synthesized the polyhexamethylene adipamide (nylon 6,6); this product was patented in 1937 [188] and marketed in 1938, having good characteristics for use as a textile fiber. In 1938 polycaprolactam (nylon 6) was synthesized, and subsequently patented in 1941 [189].

Proposed mechanisms for polycondensations are essentially the same as those proposed in the organic chemistry of smaller molecules. The synthesis of polyamides (nylons) is envisioned as a simple S_N2 type Lewis acid–base reaction, with the Lewis base nucleophilic amine attacking the electronpoor, electrophilic carbonyl site followed by loss of a proton. [181] (scheme 4-1)



Scheme 4-1: Proposed mechanism for poly condensations

At the industrial level polyamides are synthesized directly from an amino acid, or a dicarboxylic acid and a diamine or lactams.

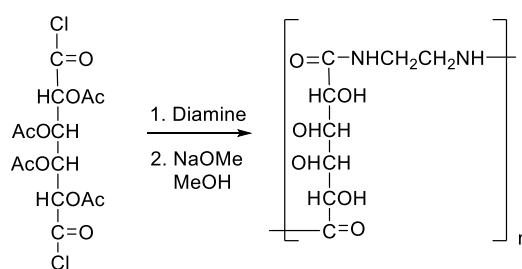
4.1.2 Functionalized polyamides

Structurally modified polyamides can provide properties which are suitable for different applications, such as aerospace and armament industry, optical switching and digital optical storage applications, chameleon materials and smart windows *etc.* [190] [191] In particular, hydroxylated oligoamides and perfluoro oligoamides are interesting for our research.

4.1.2.1 Hydroxylated oligoamide

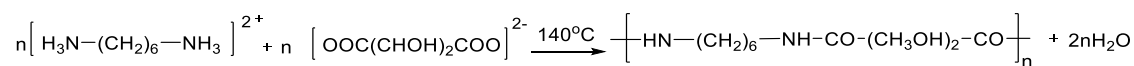
Hydroxylated polyamides are important functionalized polyamides which are used in different areas: for example, in the biomedical field the use of polyamides based on naturally occurring products is very promising due to their non-toxic and biodegradable character [192] [193]. Moreover, several other hydroxylated polyamides have been synthesized to be applied as fibers, plastics, coatings and adhesives [194] or hydrated inhibitors for oil and gas industry applications [195]. Due to their solubility in water, similar products have been also used as additives in water-based formulations and for example as curing agents for epoxy resins [196]. Moreover, hydroxylated polyamides also have a high affinity for polar materials as wood, paper, and natural fibers, which can allow them to be applied in the conservation of heritage cultural field [197].

Since 1960s, the synthesis of different hydroxylated nylons have been reported in the literature. The syntheses were carried out by the melt polycondensation method at elevated temperature (above the melting points of resulting polymers) or by interfacial polycondensation using acid chlorides. For example, Wolfrom *et al.* reported the synthesis of hydroxylated polyamide from tetra-*O*-acetylgalactaroyl dichloride and ethylenediamine by poly condensation in benzene and deacetylation [198] (scheme 4-2). However, a crosslinking reaction easily occurs to form an insoluble polymer because of the thermal degradations of resulting polyamides or of participation of hydroxyl groups in the interfacial polycondensation. [199]



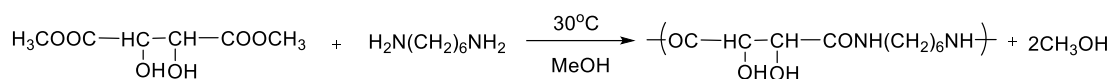
Scheme 4-2: Synthesis of hydroxylated polyamide

Minoura *et al.* were the first to report the polycondensation of D-tartaric acid with diamines. The polyamides were synthesized at high temperatures (140 °C-145 °C) by the condensation of the salt prepared from D-tartaric acid with hexamethylenediamine (scheme 4-3). [200]



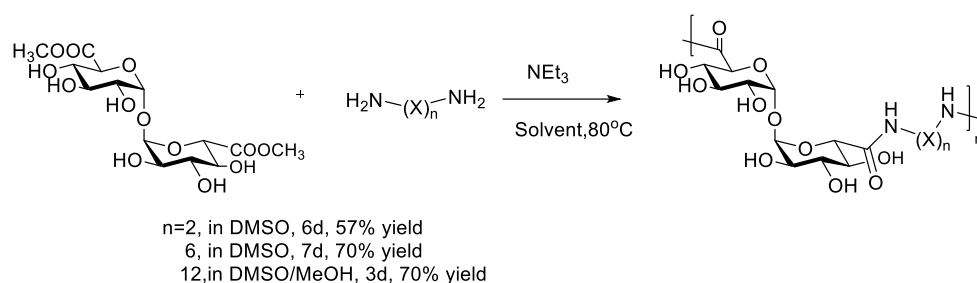
Scheme 4-3: Polycondensation of D-tartaric acid with diamines

Another method of obtaining hydroxylated polyamides is through the reactions of diesters with diamines. However, those polycondensations are usually carried out at elevated temperatures so as to shift equilibrium toward polymer formation by elimination of alcohol in the polycondensation reaction. An exception is the case of active diesters such as phenyl or thiophenyl esters, which can react with diamines under such mild conditions that the polycondensation reaction can take place at room temperature in solutions. The major advancement was in 1970s when Ogata *et al.* studied the influence of the ester derivatives of hydroxylated carboxylic acids, demonstrating that the hydroxyl groups, in α or β position with respect to the ester group, have greater reactivity than the corresponding non-hydroxylated monomers in polycondensation reactions in the presence of polar solvents. This effect has been attributed to the formation, in an intermediate stage of the reaction, of the hydrogen bonds between the hydroxyl groups of the diester and those of the $-\text{NH}_2$ of the diamine. Ogata *et al.* synthesized the poly-L-tartaramides using L-dimethyl tartarate reacted with hexamethylenediamine in methanol at 30 °C. (scheme 4-4) [199]



Scheme 4-4: Synthesis of poly-L-tartaramides

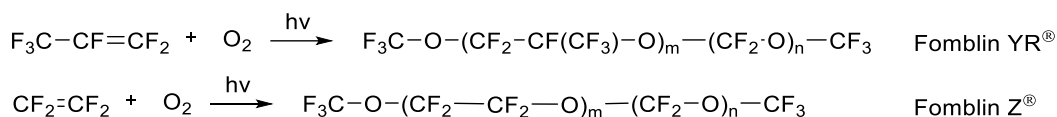
Cipriani *et al.* reported the synthesis of new oligo- or polyethyleneamides containing several hydroxyl groups starting from dimethyl ester of L-tartaric acid, D(β)-glucaric acid and α,α -trehaluronic acid, which are dicarboxylic acids derived from renewable resources [201]. Recently, Oliva *et al.* reported the synthesis of new oligoamides obtained by polycondensation of the α,α -trehaluronic acid dimethyl ester, with different diamines. All the polycondensation reactions were performed at temperatures below 100 °C. The choice of different diamines allows the modulation of the molecular weight of the products and of their physical characteristics such as T_g , hydrophilic or hydrophobic properties, and solubility. [202] (scheme 4-5)



Scheme 4-5: Polycondensation of the α,α -trehaluronic acid dimethyl ester with different diamines.

4.1.2.2 Perfluorinated oligoamide

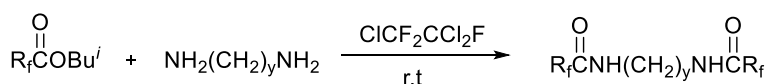
The common point of fluorinated polymers is the partial or total replacement of the hydrogen atoms in the molecule with fluorine, an element that confers hydrophobicity and greater thermal, chemical and photo-oxidative stability owing to the C-F bond. C-F bond is one of the strongest bonds with the dissociation energy equaling to 116 kcal/mol, while very low free surface energy. It has been reported that the hexagonal closed alignment of $-\text{CF}_3$ groups of *n*-perfluoroicosane shows the lowest surface free energy of any solid—6.7 mJ/m² (water: 72.8 mJ/m²) [203]. All those features make fluoropolymers good candidates for the heritage conservation area. Fluoroelastomers and perfluoropolyethers are two main fluorinated compounds used in the heritage conservation. Fluoroelastomers are primarily used as binder and filler for fractures, joints. The perfluoropolyether oils are colorless and transparent, with a relatively high viscosity depending on the molecular weight, the type of monomer and the presence or absence of polar functional groups [204]. These products are highly water repellent, particularly stable to UV radiation and reversible. Depending on the manufacturers, there will be different methods of synthesis. For example, Montefluos (Montedison) began to produce these oils in the early 1960s by photo-oxidation of fluorinated monomers such as perfluoroethylene $\text{CF}_2=\text{CF}_2$ and perfluoropropene $\text{CF}_3-\text{CF}=\text{CF}_2$. With the photo-oxidation, double bonds break and oxygen atom is inserted resulting in the formation of the ether. [205] (scheme 4-6)



Scheme 4-6: Synthesis of perfluoropolyether Fomblin YR[®] and Fomblin Z[®]

These products are called Fomblin YR[®] and Fomblin Z[®], and have been used for the protection of stone material for a few decades, especially the Fomblin YR[®]. However, those products show poor adhesion to a supporting material.

In order to increase the adhesion between the protective agents and stone materials, Piacenti *et al.* reported the synthesis of perfluoropolymers bearing polar groups, -CONH-, capable of "fixing" them to the stone. The synthesis of partially perfluorinated polyetheric amides was performed using esters of perfluoropolyetheric mono- and di-carboxylic acids, and ethylenediamine, hexamethylenediamine and piperazine in 1,1,2-trichlorotrifluoroethane at room temperature under nitrogen. (scheme 4-7) [41]



$\text{R}_f = \text{CF}_3\text{O}-(\text{CF}_2-\text{CF}(\text{CF}_3)-\text{O})_m-(\text{CF}_2-\text{O})_n-\text{CF}_2-$;
 Average molecular weight of 425 (G440), 880 (G900) and 2380 (G2200).
 $y = 2, 4, 6$

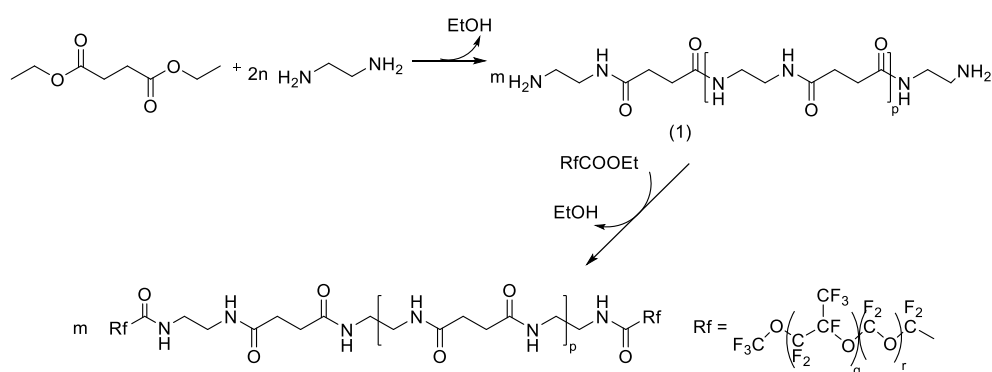
Scheme 4-7: Synthesis of partially perfluorinated polyetheric amides

Those partially perfluorinated polyetheric amides show a good adhesion on the bioclastic limestone, especially the hexamethylenediamine derivatives. Moreover, the partially perfluorinated polyetheric amide from hexamethylenediamine and G900 was reported to show promising performance on blanching painting restoration by Genty *et al.* [71]

Unfortunately, the limited solubility of mono- or di-amide is not suitable for the application in stone protection. Normally they require the use of a solvent to reduce the viscosity and allow them to be sprayed. Chlorofluorocarbons (CFCs), *i.e.* 1,2,2-trichloro-1,1,2-trifluoroethane (A113), have proven to be inexpensive and effective solvents, but due to their disbenefit in inducing ozone depletion they first retarded the wide application of perfluoropolyethers, and then stopped it when CFCs were banned.

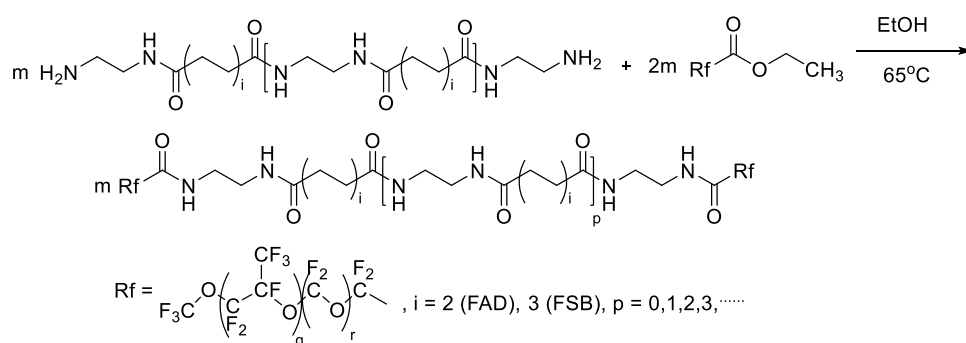
Camaiti M *et al.* reported the two-step synthesis of fluorinated oligo(ethylenesuccinamide) (FSC), which is bearing both polar groups within the chain and hydrophobic end groups. The first step of the synthesis is from diethyl succinate and ethylenediamine with the molar ratio 1:2, and the oligoamide with free amine ends (1) can be obtained after 7 hours of heating at 90 °C in THF. The second step is using ethyl ester of monocarboxylic perfluoropolyether acid to react with the oligoamide (1) in EtOH at 80 °C for 25 hours. The molar ratio between oligoamide (1) and PFPE-ester was 1:1.9. The final fluorinated oligoamide is soluble in hot alcohols or hydro-alcoholic solvents, which makes possible its application on many surfaces without any environmental negative impact due to the solvent. After being tested on a porous calcarenite and investigated by Magnetic Resonance Imaging, the result shows that the final fluorinated oligo(ethylenesuccinamide) modifies the wettability of porous

substrates like Lecce stone in a drastic and durable way. [42] (scheme 4-8)



Scheme 4-8: Two-step synthesis of FSC

Recently, Yijian *et al.* reported the synthesis of partially fluorinated oligoamides using perfluoropolyetheric segments grafted to the two ends of oligoadipamide (FAD) and oligosuberamide (FSB), using the similar methodology with FSC (scheme 4-9). FSB shows good solubility, and FAD shows intermediate solubility in alcoholic and hydro-alcoholic solvents at room temperature. FAD is generally more effective for the protection of low porous stone, like marble. FSB demonstrates high water inhibition efficacy on both low and highly porous stones. [43][44]



Scheme 4-9: Synthesis of partially perfluorinated oligoamide FAD and FSB

4.2 Results and discussion

Target compounds of synthesis are partially perfluorinated hydroxylated oligoamides. Hydroxylated oligoamides with perfluorinated tails were proposed as the target compounds, which would be used in stone material protection and blanching painting restoration to compare their behaviour with that of similar compounds without hydroxyl groups in order to observe the role of these functional groups as anchoring to polar substrates. In fact, the presence of polar groups such as hydroxyls can change interactions with supports and physical characteristics. Depending on the number of hydroxyl and amide groups in the molecules, as well as on the length and number of perfluorinated chains, the new compounds may have different specific properties (*e.g.* solubility, T_g) which may be of interest as protective or consolidating agents for preserving the cultural heritage. Firstly, the

designed molecules are supposed to show good hydrophobicity. In fact, the stone degradation is mainly caused by water, while the humidity can equally favor various degradation processes which also induce the formation of porous structure in easel painting leading to blanching phenomenon. The perfluorinated groups are introduced to give the molecules necessary hydrophobicity due to the low surface energy, and work as the water repellents. Secondly, concerning the polarity properties, these are important for the interaction with the stone and for the penetration into the porosity of the paintings. The polar groups can have an effective interaction and adhesion with the naturally polar stone material by dipolar interaction or hydrogen bonding, and the molecules can be “fixed” on the stone materials. For the restoration of blanching paintings, the polar groups can help the molecule enter the porous structures interacting with the more polar components of the pictorial film and change the diffusion of light, and eventually the blanching can be decreased or eliminated. Therefore, the designed molecules have two opposite functionalities, which provide water repellence while maintaining polarity for interacting with substrates. Last but not least, a good solubility of the proposed oligomers in non-toxic, environmentally benign solvents is required. Therefore, the partially perfluorinated hydroxylated oligoamides which can facilitate secondary interactions with matrices having structural polar features, through durable and reversible non-covalent bonds, were proposed as the target compounds.

The synthesis of these compounds involves in a first step the synthesis of the non perfluorinated product which is subsequently functionalized with the perfluorinated chains.

4.2.1 Synthesis of the non-perfluorinated oligoamides

4.2.1.1 Methodology: the choices of monomers

- **L-(+)-Tartaric acid dimethyl ester** is the derivatives from L-(+)-Tartaric acid which is a renewable resource. Tartaric acid (2,3-dihydroxybutanedioic acid) is a naturally occurring dicarboxylic acid containing two stereocenters. It exists as a pair of enantiomers and an achiral meso compound. The dextrorotatory enantiomer of (R,R)-L-(+)-tartaric acid is widely distributed in nature. L-(+)-Tartaric acid is a white crystalline diprotic acid. This aldaric acid occurs naturally in many plants, particularly grapes, bananas and tamarinds (as well as in other fruits) and it is commonly combined with baking soda to function as a leavening agent in recipes. Its monopotassium salt is found as a deposit during the fermentation of grape juice. It is one of the main acids found in wine. The “traditional” production method is the extraction from by-products of the wine industry. However new methodologies, such as the production for oxidation of some carbohydrates, or the treatment with nitric acid of glucose, lactose or starch, are under development. A very interesting alternative method is the oxidation of glucose in presence of oxidase and peroxidase (45% conversion) or the electrolysis of saccharic acid in an acid solution or with H₂O₂. Another method is the oxidation with bromine or chlorine from fumaric or maleic acid. [206]

In our study, dimethyl L-tartrate (figure 4-1) was chosen as one of the monomers for the

production of polyamides because it has two hydroxyl groups in the molecule, which can make the final product affine to polar stone material and painting layer. Also, it has a structural feature similar, at least partially, to a sugar due to its two hydroxyl groups. That gives the oligomers a closer structure to the other series of target compounds in our research, which is partially perfluorinated C-glycosides.

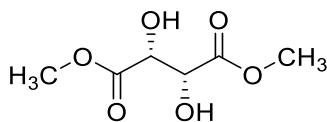


Figure 4-1: Dimethyl L-tartrate

- **Diethyl succinate** (figure 4-2) is derived from succinic acid. Succinic acid is a naturally occurring four-carbon dicarboxylic acid with the molecular formula $C_4H_6O_4$. Succinic acid is naturally formed by most living cells as an outcome of anaerobic digestion and it is a co-product of particular interest in biorefineries production. It is a common organic acid, which can be used in many food, chemical, and pharmaceutical industries as a precursor to generate many chemicals such as solvents, perfumes, lacquers, plasticizer, dyes, and photographic chemicals. Succinic acid is also used as an antibiotic and curative agent. It also finds application as a surfactant, ion chelator, and as an additive in various industries. [207]

Diethyl succinate was selected as monomer to improve the solubility in alcohol and the hydrophobicity of the final perfluorinated derivatives.

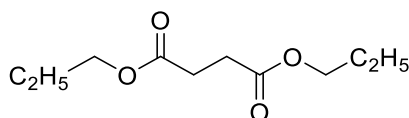


Figure 4-2: Diethyl succinate

- **Diethylenetriamine** and **ethylenediamine** (figure 4-3) were selected as the amine blocks for the synthesis to analyse the role of two different amines in the performance of the final products.

The selected amines can react with esters of dicarboxylic acid to form the $-CONH-$ functional group, which can interact with polar materials through dipolar interaction or hydrogen bonding. Those amide groups make the final product affine to polar materials. Moreover, the amide group is more stable than other polar groups such as the ester ones.

By combining different amine blocks with esters units of different diacids, it is possible to modulate the molecular weights and the physical characteristics of the products, such as hydrophilic or hydrophobic properties, and solubility.

Contrary to ethylenediamine, in the diethylenetriamine, the $-NH-$ group not involved in the amidation reaction can interact with polar material with an additional hydrogen bonding, providing different physical characteristics and properties.

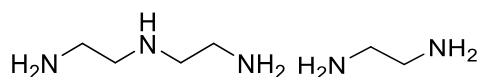


Figure 4-3: Diethylenetriamine and ethylenediamine

In summary, the choice of monomers was made in order to balance the presence of polar groups to favour interactions with polar substrates and hydrophobic parts.

4.2.1.2 Synthesis

The synthesis of non-fluorinated oligoamides were based on the condensation between an ester and an amine group in the step growth polymerization. The procedures used for the synthesis of oligoamides were specific in order to obtain products with the structural characteristics required for their use as stone protective agents or blanching painting restoration agents. In fact, polymers with too high molecular weights or unwanted degradation products could be obtained from hydroxylated monomers by heating their salts at high temperature as reported for the industrial synthesis of common nylons. Therefore, instead of using acid, esters of dicarboxylic acids were used with diamine for amide formation in mild reaction conditions avoiding salt formation between diacid and diamine which requires higher temperature for the condensation reaction. Using this procedure, the low temperature (80 °C) avoids alteration of the hydroxylated portions. Aiming at obtaining oligoamides with terminal amine groups for successive reactions, the molar amount of amine was kept in slight excess with respect to the selected stoichiometric ratio diamine/diester (1:1 or 2:1). The synthesis of oligoamides were carried out in polar solvent, suitable for solubilizing all reagents, which was methanol.

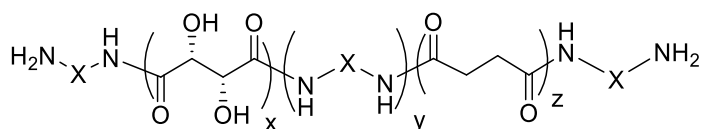
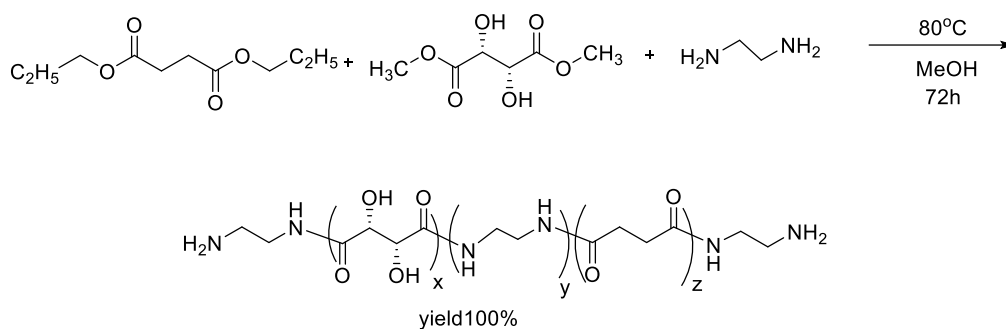


Figure 4-4: Target non-perfluorinated oligoamides

- Synthesis of oligoamide 1 (EST).

The first synthesis of non-fluorinated oligoamide was realized *via* polycondensation reactions by using ethylenediamine, dimethyl L-tartrate, and diethyl succinate as initial monomers. The reaction was performed using methanol as solvent, at 80 °C in methanol for 3 days (scheme 4-10). The molar ratio of diethyl succinate/dimethyl L-tartrate /ethylenediamine was 1:1:2, however, a very small excess of the diamine was generally used in order to obtain oligoamides with two terminal amine groups.



Scheme 4-10: Synthesis of ethyleneoligoamide 1 EST

The work-up was carried out filtering by büchner funnel and washing the solid by methanol and ethyl ether; the residual solid was dried under reduced pressure at room temperature and was isolated giving a 100 % yield. The product is light yellow crystalline solid.

The synthesis of the desired oligoamide was confirmed by NMR spectroscopy. In $^1\text{H-NMR}$ spectrum (figure 4-5):

- i. The presence of signals between 3.2 and 3.5 ppm attributable to the CH_2 group in α position to the amide group confirms the formation of an amide bond: CH_2NHCO (2 methylene groups in the middle of chain from tartrate units and succinate units $\text{CO-NH-CH}_2\text{-CH}_2\text{-NH-CO}$, and the CH_2 in the terminal amino groups $\text{CO-NH-CH}_2\text{-CH}_2\text{-NH}_2$)
- ii. Signal at 4.56 ppm is attributable to protons of tartrate units CO-CHOH-CHOH-CO ;
- iii. The presence of a signal that can be attributed to the CH_2 in α position to the terminal amino group $\text{NH-CH}_2\text{-CH}_2\text{-NH}_2$ at 2.97 ppm;
- iv. Signals at 2.52 and 2.54 ppm are attributable to protons of 2 methylene groups in α position of 2 carbonyl groups $\text{NH-CO-CH}_2\text{-CH}_2\text{-CO-NH}$.

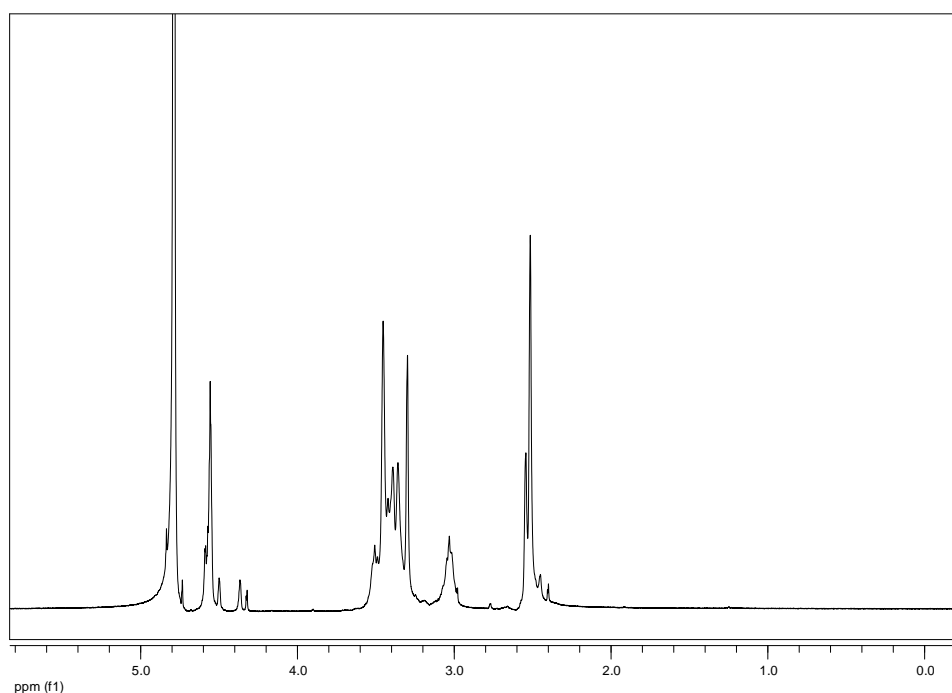


Figure 4-5: $^1\text{H-NMR}$ spectrum in D_2O of oligoamide 1 EST

During the step-growth polymerization, the monomers initially form oligomers which grow gradually but as in the chain-growth polymerization, molecules of different lengths are formed and the final product will be composed by macromolecules with a different degree of polymerization. Necessarily, the molecular weight of the polymers must therefore be indicated using average values in order to take into account these differences. The use of $^1\text{H-NMR}$ spectral integration method was previously applied by other authors to estimate number average molecular weights (M_n) [208]. In our work, specific equations were applied for each oligoamide in agreement with its structure. First of all, using $^1\text{H-NMR}$ spectroscopy was possible to determine the presence of amino groups at the end of the polymeric chain. As the $\text{CH}_2\text{-NH}_2$ signal falls in a quite clean region, the corresponding integral was used as the reference value and set as 2 when one amino group was present at the end of chain or 4 when both end groups were amino groups. Then the integrals of the other signals were evaluated with respect to this value and, in particular, the areas of the signals related to the CH-OH , CH_2CONH and to the $\text{-CH}_2\text{NH-CO}$ groups were determined. Since the integral of signal area is proportional to the number of protons, it is possible to calculate the number "x", "y", "z" of the repeating units of the oligoamide according to the following data:

$$\int \text{-CH}_2\text{NH}_2 = 8.37 \text{ ascribing to } 4\text{H}$$

$$\int \text{-CHOH} = 10.97 = 2x \text{ ascribing to } 2\text{H for } x \text{ tartaric units}$$

$$\int \text{-CH}_2\text{NHCO} = 52.66 = 4y+4 \text{ ascribing to } 4\text{H for } y \text{ internal diamidounits} + 4\text{H for two amido in terminal diamine units}$$

$$\int \text{-CH}_2\text{CONH} = 21.94 = 4z \text{ ascribing to } 4\text{H for } z \text{ succinic units}$$

The elaboration of the integrals obtained in $^1\text{H NMR}$ spectrum, permits to evaluate that the product is composed by repeating units having an average of 2.62 L-tartrate units and 2.62 of succinate units, 6.24 ethylenediamine, with two amino terminations: consequently, the average molecular weight is 887.92 g/mol.

In $^{13}\text{C-NMR}$ spectrum (figure 4-6) the presence of two amino groups at the end of chain is confirmed by the signal at 39.3 ppm and by the absence of the signals related to the terminal ethyl or methyl ester groups. Besides, the formation of the product is confirmed by the signals at 174.0 and 175.0 ppm (CONH) and 38.5 ppm (CH_2NHCO); a signal at 72.3 ppm is present related to the CH-OH and a signal related to the CH_2 of the succinic unit is present at 31.0 ppm (CH_2CONH).

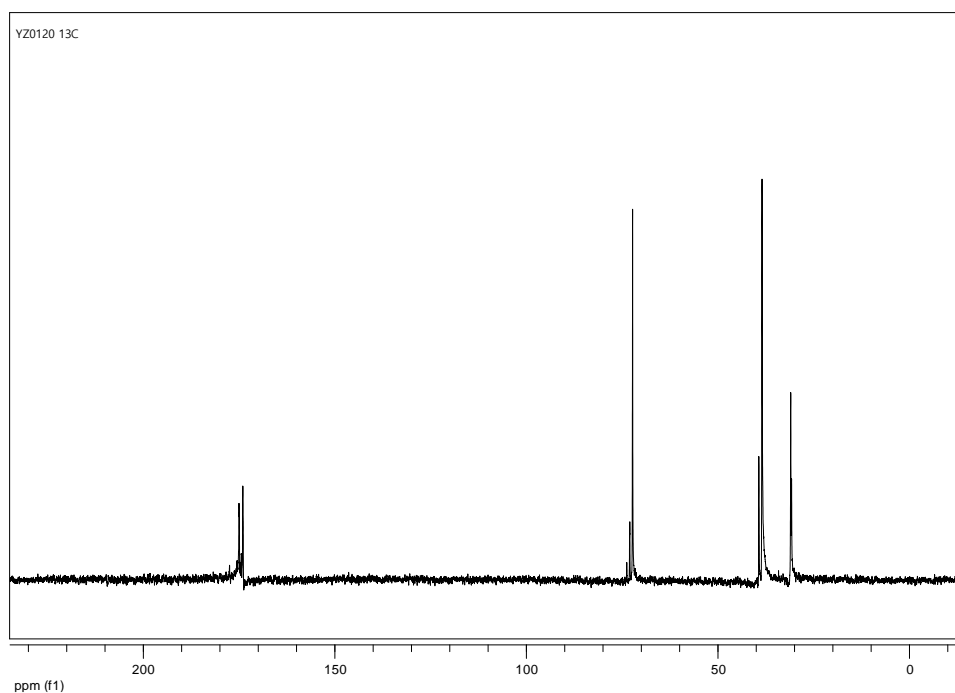


Figure 4-6: ^{13}C -NMR spectrum in D_2O of oligoamide 2 (EST)

- Synthesis of oligoamide 2 (EST)

Considering the molecular complexity and the average molecular weight increase with reaction time in the step-growth polymerization, and the requirement to obtain an oligoamide with lower molecular weight but a better ability to penetrate inside a stone or painting structure, the reaction time of the next synthesis was reduced to 24 h instead of 72 h keeping the other reaction conditions and work-up procedure keeping unchangeable. The integrals of signal area obtained in the ^1H -NMR spectrum (figure 4-7) were,

$$\int -\text{CH}_2\text{NH}_2 = 11.51 \text{ ascribing to } 4\text{H}$$

$$\int -\text{CHOH} = 12.55 = 2x \text{ ascribing to } 2\text{H for } x \text{ tartaric units}$$

$\int -\text{CH}_2\text{NHCO} = 53.43 = 4y+4$ ascribing to 4H for y internal diamido units + 4H for two amido in terminal diamine units

$$\int -\text{CH}_2\text{CONH} = 15.73 = 4z \text{ ascribing to } 4\text{H for } z \text{ succinic units}$$

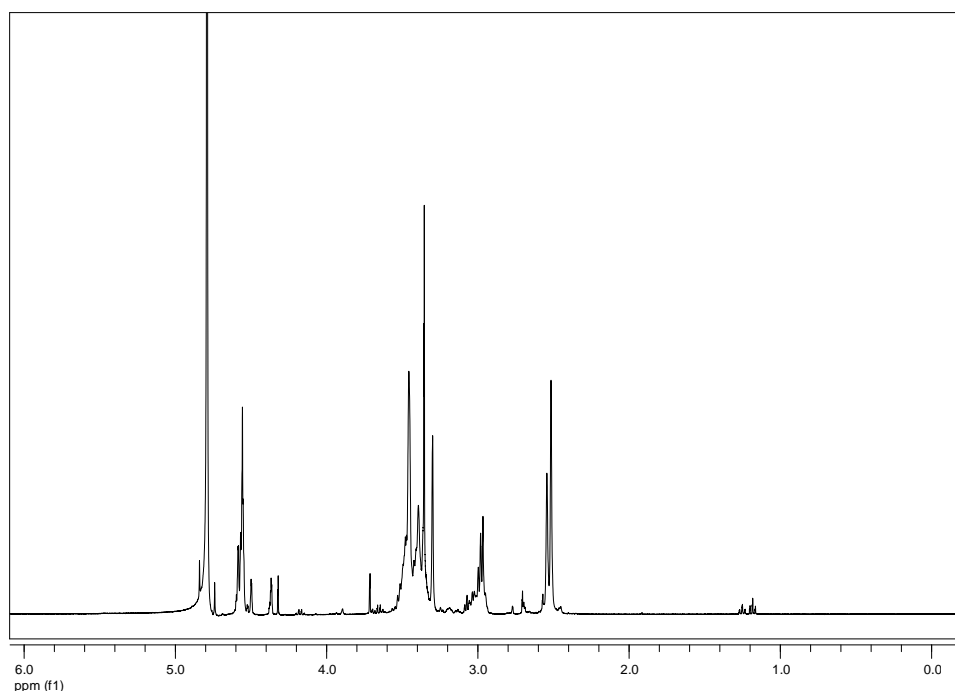


Figure 4-7: $^1\text{H-NMR}$ spectrum in D_2O of oligoamide 2 EST

In the synthesis with reaction time of 24 hours, the integrals in ^1H NMR spectrum permits to evaluate that the product recovered as solid at the end of reaction (72 % yield) is composed by repeating units having an average of 2.18 L-tartrate units and 1.37 of succinate units, 4.55 ethylenediamine, with two amino groups at the end of the chain: consequently, the average molecular weight is 633.86 g/mol (figure 4-8). The lower yield observed after 24 hours compared to that after 72 hours is in agreement with a lower degree of polymerization. In particular, a smaller quantity of succinic units is observed in the smaller quantity of insoluble fraction which is richer in tartaric units. In accordance with these evaluations, the molecular weight is also lower.

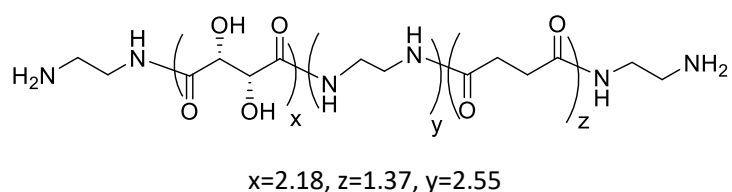


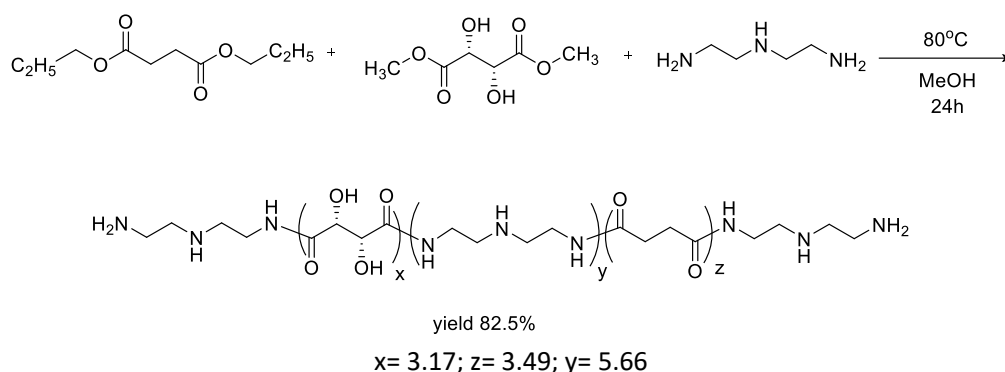
Figure 4-8: Oligoamide 2 EST

Considering the need for easy penetration, 24 h is a suitable reaction time to obtain a lower average molecular weight. As a result, oligoamide 2 with 633.86 g/mol was selected for the successive reaction with perfluorinated compound.

- Synthesis of oligoamide 3 (DST)

Instead of using ethylenediamine, diethylenetriamine was used in the next synthesis with

dimethyl L-tartrate and diethyl succinate under the same reaction conditions. The molar ratio of diethyl succinate/dimethyl L-tartrate /diethylenetriamine was 1:1:2, and a very small excess of the amine was generally used with respect to the stoichiometric ratio. The reaction mixture was heated at 80 °C in methanol for 24 hours. At the end of the reaction a yellow brown liquid was obtained due to the presence of triamine which increases the solubility of the oligoamide. The product was obtained as a yellow oil after the evaporation under vacuum with 82.5 % yield. (scheme 4-11)



Scheme 4-11: Synthesis of oligoamide **3 DST**

The synthesis of the oligoamide was confirmed by characterization by NMR spectroscopy. In $^1\text{H-NMR}$ spectrum (figure 4-9),

- i. The presence of signals between 3.2 and 3.5 ppm attributable to the CH_2 group in α position to the amide group confirms the formation of an amide bond: CH_2NHCO (2 methylene groups adding 2 amide groups in the middle of the chain next to tartrate units and succinate units $\text{CO-NH-CH}_2\text{-CH}_2\text{-NH-CH}_2\text{-CH}_2\text{-NH-CO}$, and the CH_2 next to terminal amido groups $\text{CO-NH-CH}_2\text{-CH}_2\text{-NH-CH}_2\text{-CH}_2\text{-NH}_2$)
- ii. Signal at 4.56 ppm is attributable to protons of tartrate units CO-CHOH-CHOH-CO
- iii. The presence of a signal at 2.86 ppm can be attributed to the CH_2 in α position to the terminal amino group $\text{CO-NH-CH}_2\text{-CH}_2\text{-NH-CH}_2\text{-CH}_2\text{-NH}_2$
- iv. The signal between 2.73 and 2.77 ppm is attributable to protons of $\text{CH}_2\text{-NH-CH}_2$
- v. Signal at 2.54 ppm is attributable to protons of 2 methylene groups in α position of 2 carbonyl groups $\text{NH-CO-CH}_2\text{-CH}_2\text{-CO-NH}$

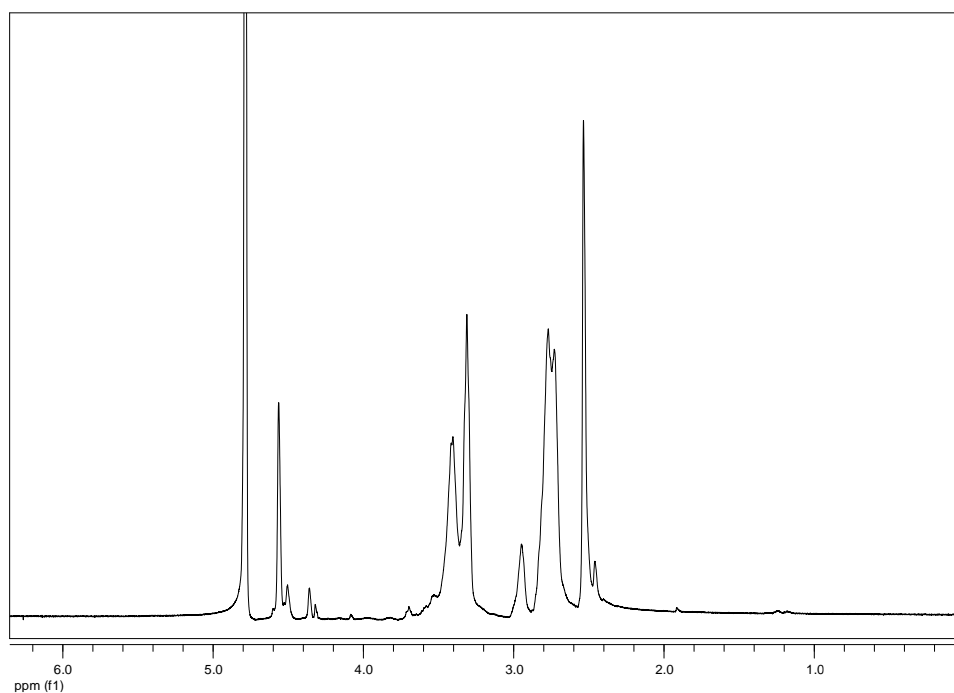


Figure 4-9: $^1\text{H-NMR}$ spectrum in D_2O of oligoamide 3 DST

gCOSY spectrum (figure 4-10) confirms this assignment, thanks to the couplings between CO-NH-CH_2 (from 3.20 and 3.50 ppm) and $\text{CH}_2\text{-NH-CH}_2$ (from 2.73 and 2.77 ppm)

The same methodology was used for M_n calculation.

$$\int -\text{CH}_2\text{NH}_2 = 4.27 \text{ ascribing to } 4\text{H};$$

$$\int -\text{CHOH} = 7.48 = 2x \text{ ascribing to } 2\text{H for } x \text{ tartaric units}$$

$\int -\text{CH}_2\text{NHCO} = 31.43 = 4y+4$ ascribing to 4H for y internal diamido units + 4H for two amido in terminal diamine units

$\int -\text{CH}_2\text{NHCH}_2 = 35.41 = 4y+8$ ascribing to 4H for y internal diamido units + 8H for two amine in terminal diamine units

$$\int -\text{CH}_2\text{CONH} = 16.49 = 4z \text{ ascribing to } 4\text{H for } z \text{ succinic units}$$

Therefore, the product is composed by repeating units having an average of 3.17 L-tartrate units and 3.49 of succinate units, 7.66 diethylenetriamine, with two amino groups at the end of chain: consequently, the average molecular weight is 1436.54 g/mol.

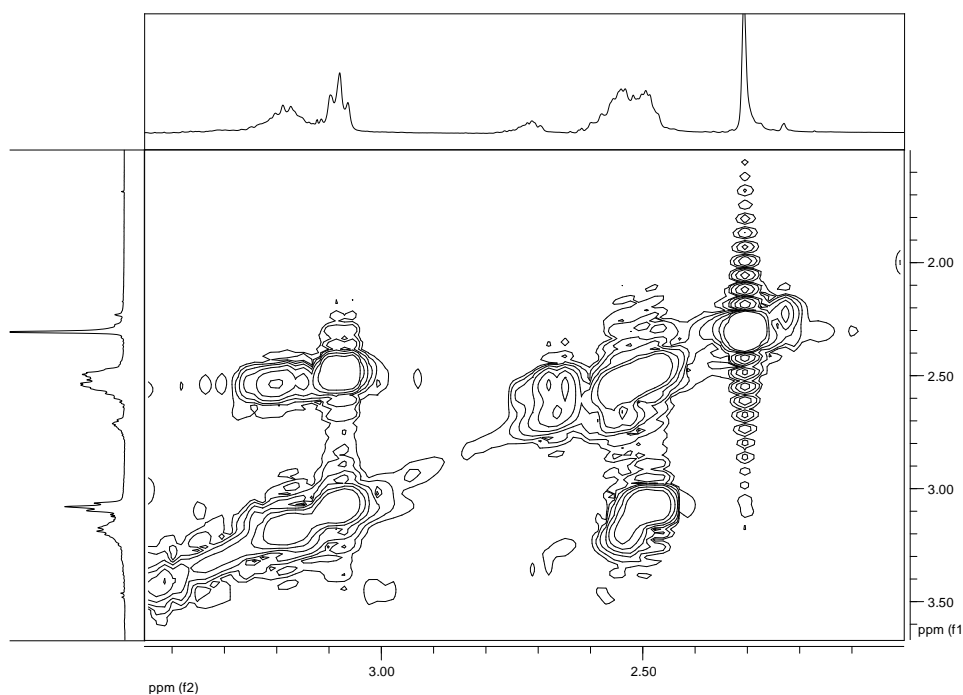


Figure 4-10: gCOSY spectrum in D_2O of oligoamide 3 DST

In ^{13}C -NMR spectrum (figure 4-11) the presence of two amino groups at the end of chain is confirmed by the signal at 38.4 ppm and by the absence of the signals related to the terminal ethyl or methyl ester groups. Besides, the formation of the product is confirmed by the signals at 174.0 and 174.9 ppm (CONH) and 37.9 ppm (CH_2NHCO); signals at 72.4 and 73.1 ppm are present related to the CH-OH, while the signals at 47.0 and 45.7 ppm are attributable to $CH_2-NH-CH_2$ and a signal related to the CH_2 of the succinic unit is present at 30.8 ppm (CH_2CONH). gHSQC spectrum (figure 4-12) confirms this assignment.

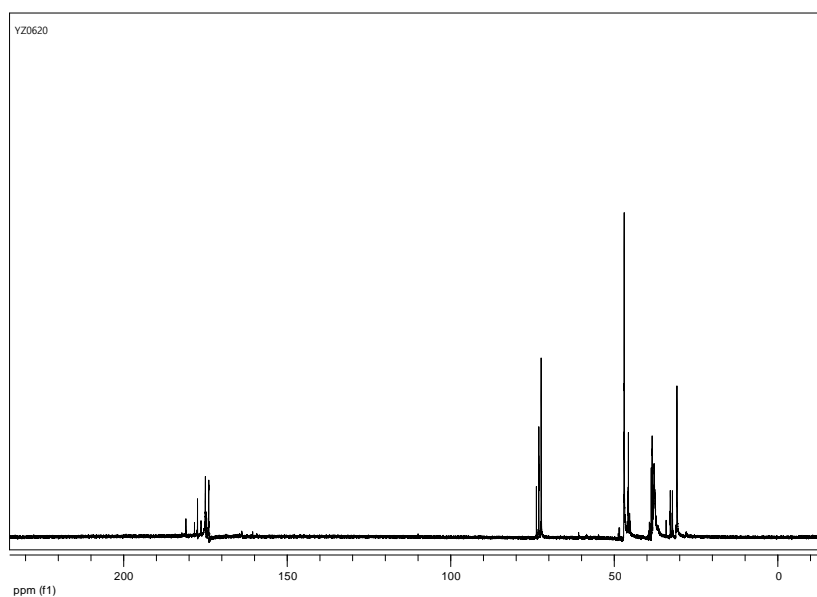


Figure 4-11: ^{13}C -NMR spectrum in D_2O of oligoamide 3 DST

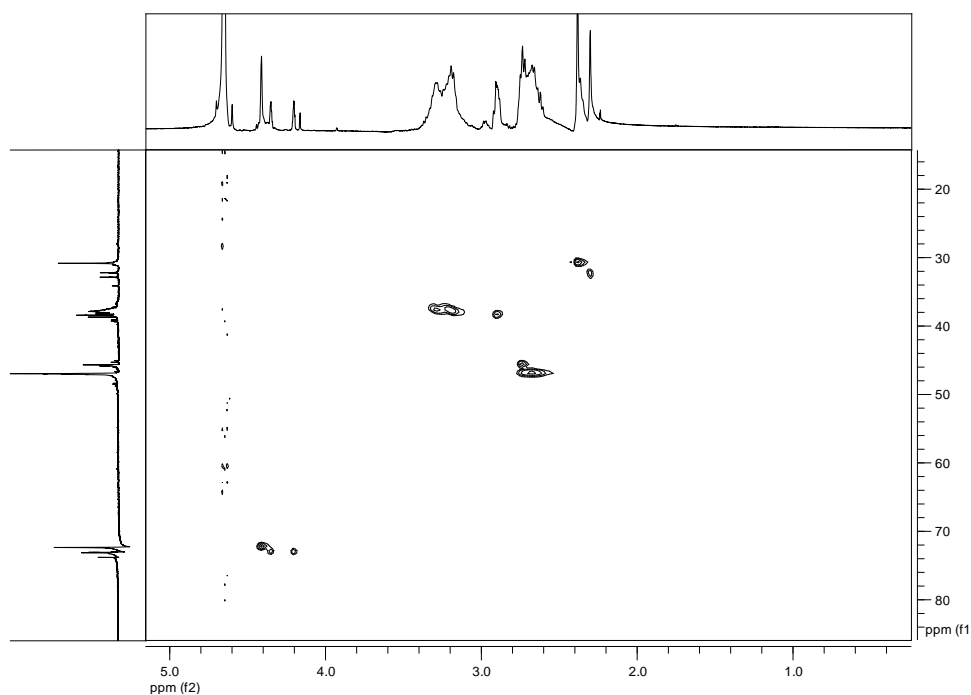
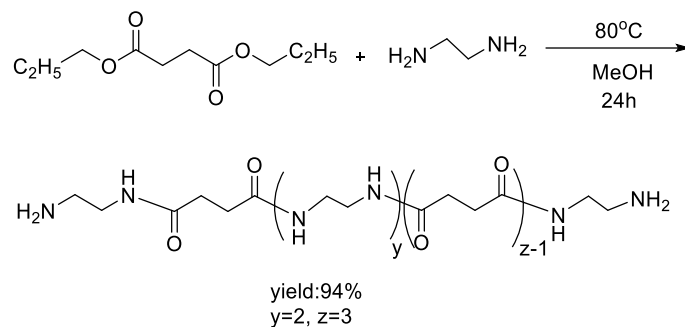


Figure 4-12: gHSQC-NMR spectrum in D_2O of oligoamide 3 *DST*

In order to expand the possibilities of application on stone protection and blanching painting restoration, and understand the roles of functional groups in the applicative performance, especially the hydroxyl groups, it was decided to carry out similar synthesis by modulating the structural characteristics by modifying the initial monomers. Particularly, the two synthesis were designed with poly condensation between amine source and diethyl succinate, but without dimethyl L-tartrate. That means the next two oligomers are less polar and hydrophilic without hydroxyl functional groups. Therefore, comparing the applicative performance (*i.e.* the solubility in environmentally friendly solvents, hydrophobic and adhesion properties) between hydroxylated oligomers and non-hydroxylated will help to understand the role of OH groups and optimize the structure of molecule.

- Synthesis of oligoamide 4 (ES)

Ethylenediamine and diethyl succinate were reacted through the poly condensation reaction using the similar procedure with the synthesis of previous hydroxylated oligoamides. However, as optimized in previous studies [42], for this compound the molar ratio of diethyl succinate/ethylenediamine was 1:2, and a very small excess of the diamine was generally used to obtaining oligoamides with terminal amine groups. The reaction mixture was heating at 80 °C in methanol for 24 hours obtaining the formation of a solid compound. The work-up was carried on filtering by büchner funnel and washing the remained solid by ethyl ether; the residual solid was dried under reduced pressure at room temperature and was isolated giving a 94 % yield. The product is a white solid. (scheme 4-12)



Scheme 4-12: Synthesis of oligoamide 4 ES

This oligoamide has already been synthesized in the past using THF as a solvent and different molar ratio between diethyl succinate and ethylenediamine (1:1, 1:2 or 1:3) and its structure has already been characterized [42]. The greater simplicity compared to the previous oligoamides in terms of monomer units and a reduced chain growth observed using THF as solvent allow a more detailed definition of the signals present in the ^1H NMR spectrum.

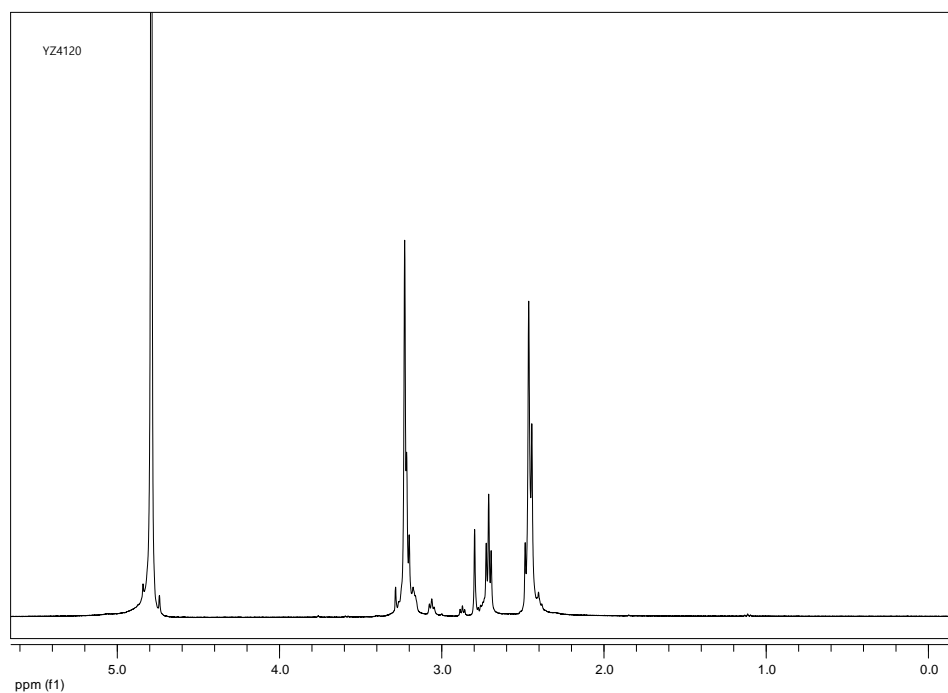
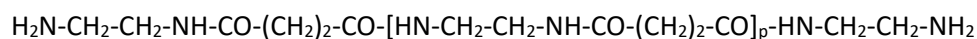


Figure 4-13: ^1H -NMR spectrum in D_2O of oligoamide 4 ES

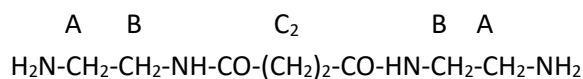
The general structure is:



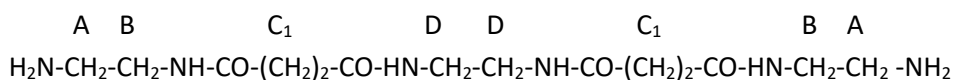
where p is the repeating number or polymerization degree.

In this oligoamide, comparing the spectroscopic data with those described in the literature [42], it is possible to identify the presence of oligomers with $p = 0$ or 1 or ≥ 2 .

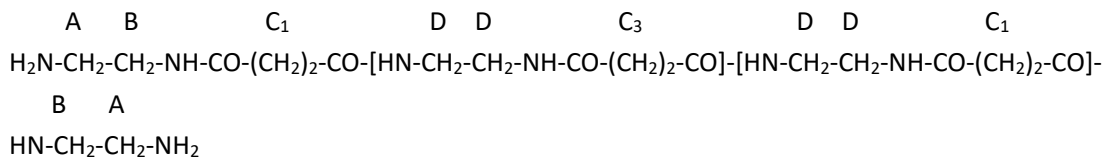
When $p=0$, the structure is:



When p=1, the structure is:



When p=2, the structure will be:



Similarly for $p > 2$

If capital letters A, B, C... are used to denote groups of protons in the structural scheme, it is possible to assign the singlet at 3.27 ppm (D) to $NH-CH_2-CH_2-NH$ inside the repeating unit; the triplet at 3.24 ppm (B) to $CH_2-NH-CO$ at the end of chain; the triplet at 2.77 ppm (A) to H_2N-CH_2 at the end of chain; the singlet at 2.48 ppm (C_2) to $CO-(CH_2)_2$ when $p=0$; the singlet at 2.45 ppm (C_1) to $CO-(CH_2)_2-CO$ when $p=1$ and 2; the singlet at 2.43 ppm (C_3) to $CO-(CH_2)_2$ in the middle of chain when $p \geq 2$.

However, using methanol as a solvent, a higher molecular weight oligoamide was obtained and consequently, a partial overlap of the signals was observed. For this reason, also in this case, the PM was calculated with an equation similar to that of the previous oligoamides. Considering the general formula of the oligoamides and the information provided by the 1H -NMR spectrum (figure 4-13), it is possible to evaluate the degree of polymerization and hence molecular weight.

In particular, the integrals of the signals present between 3.14-3.31 ppm (CH_2NHCO), between 2.38-2.51 ppm (CH_2CONH) and of the triplet at 2.71 ppm (4H, CH_2NH_2) were used for the calculation. The attribution of this last signal is in agreement with the chemical shift of group A mentioned above.

Since the integral of signal area is proportional to the number of protons, the number of each type of protons is calculable based on the following equations:

$$\int -CH_2NH_2 = 1 \text{ attributable to 4H of group A ;}$$

$$\int -CH_2NHCO = 3.09 = 4y+4 \text{ ascribing to 4H for } y \text{ internal diamido units + 4H for two amido (protons of group B) in terminal diamine units}$$

$$\int -CH_2CONH = 3.04 = 4z \text{ ascribing to 4H (protons of groups } C_1, C_2, C_3) \text{ for } z \text{ succinic units}$$

Therefore, the product is composed by repeating units having an average of 3 succinate units, 4 ethylenediamine, with two amino terminations: consequently, the average molecular weight is 486 g/mol (yield 94 %).

In ^{13}C -NMR spectrum (figure 4-14) the presence of two amino terminations is confirmed by the signal at 39.7 ppm and by the absence of the signals related to the terminal ethyl or methyl ester groups. Besides, the formation of the product is confirmed by the signal at 175.0 ppm ($CONH$), 41.3 (in terminal diamine unit CH_2NHCO) and 38.6 ppm (internal CH_2NHCO); a signal related to the CH_2 of the succinic unit present at 31.1 ppm (CH_2CONH).

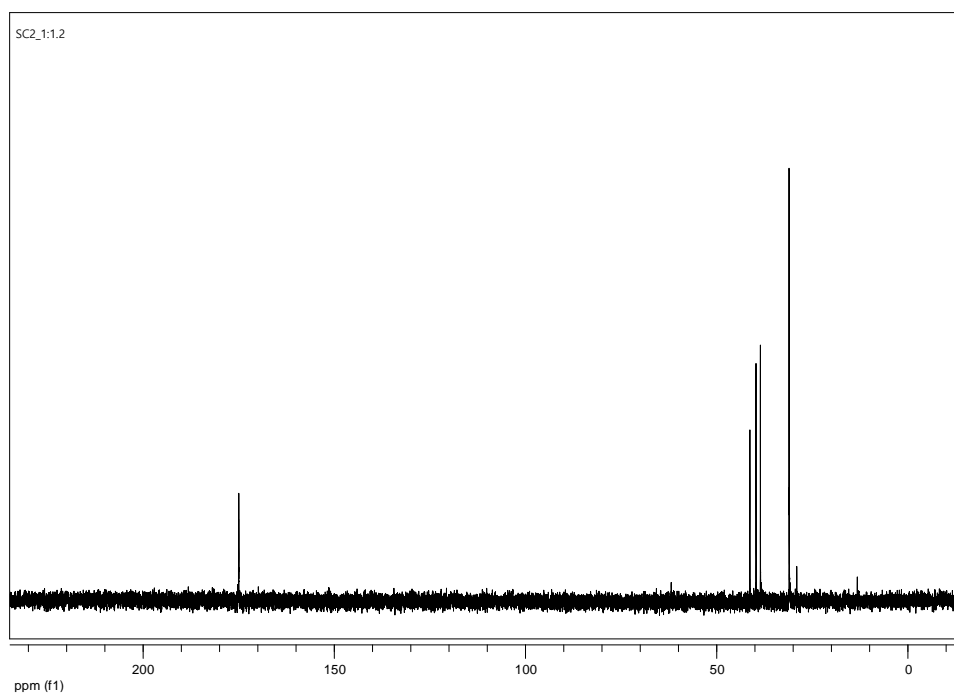
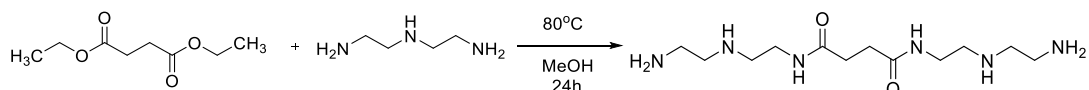


Figure 4-14: ^{13}C -NMR spectrum in D_2O of oligoamide 4 ES

- Synthesis of oligoamide 5 (DS)

The last synthesis of non-fluorinated oligoamide is realized through the poly condensation reaction between diethylenetriamine and diethyl succinate at 80 °C in methanol for 24 hours. diethyl succinate /diethylenetriamine was 1:2 and a very small excess of the amine was used to obtaining oligoamides with terminal amine groups. (scheme 4-13)



Scheme 4-13: Synthesis of oligoamide 5 DS

At the end of the reaction a yellow brown liquid was obtained. The product was obtained as a yellow oil after the evaporation under vacuum with 82.5 % yield.

The synthesis of the oligoamide was confirmed by characterization by NMR spectroscopy. In ^1H NMR spectrum (figure 4-15),

- The presence of a signal at 3.31 ppm is attributable to the CH_2 group in α position to the amide group confirms the formation of an amide bond: CH_2NHCO
- The signal at 2.72 ppm is attributable to protons of $\text{CH}_2\text{-NH-CH}_2$
- The presence of a signal that can be attributed to the CH_2 in α position to the terminal amino group at 2.65 ppm: $\text{CO-NH-CH}_2\text{-CH}_2\text{-NH-CH}_2\text{-CH}_2\text{-NH}_2$
- Signal at 2.53 ppm is attributable to protons of 2 methylene groups in α position of 2 carbonyl groups: $\text{NH-CO-CH}_2\text{-CH}_2\text{-CO-NH}$;

$$\int -\text{CH}_2\text{NHCH}_2\text{CH}_2\text{NH}_2 = 24,17 \text{ ascribing to } 4\text{H};$$

$$\int -\text{CH}_2\text{NHCH}_2\text{CH}_2\text{NH}_2 = 48,35 = 4y+8 \text{ ascribing to } 4\text{H for } y \text{ internal diamido units } +8\text{H for two}$$

amido in terminal diamine units (for this product $y=0$);

$\int -\text{CH}_2\text{NHCO} = 23.58 = 4y+4$ ascribing to 4H for y internal diamido units + 4H for two amido (protons of in terminal diamine units (for this product $y=0$))

$\int -\text{CH}_2\text{CH}_2\text{CONH} = 23 = 4z$ ascribing to 4H for z succinic units

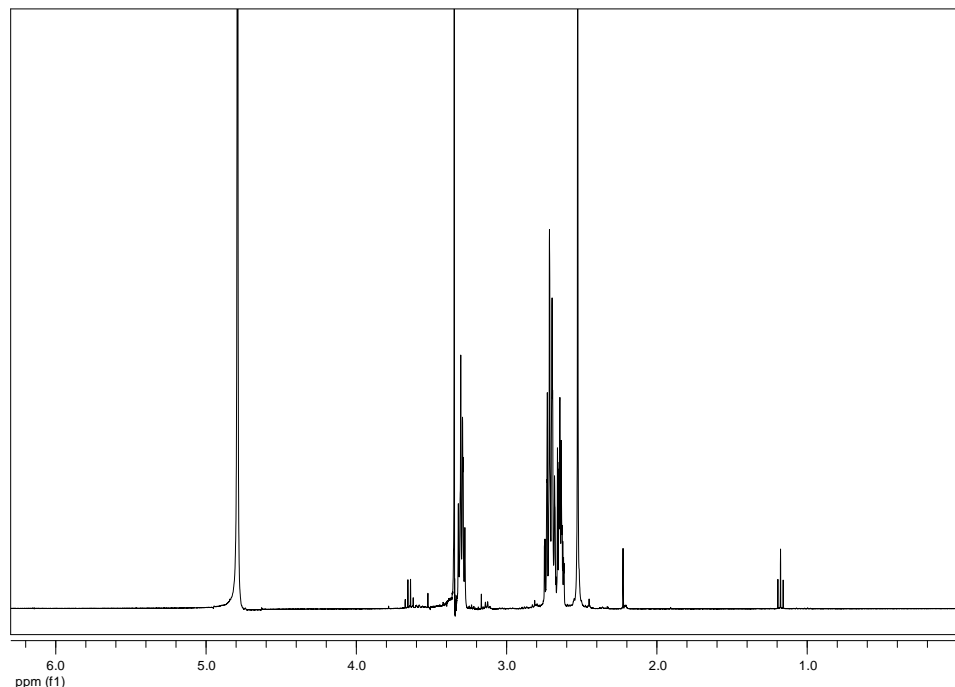


Figure 4-15: ^1H NMR spectrum in D_2O of oligoamide 5 DS

Therefore, the compound is composed by 1 succinate unit, 2 diethylenetriamine, with two amino groups at the end of chain: consequently, the average molecular weight is 288 g/mol (yield 100 %)

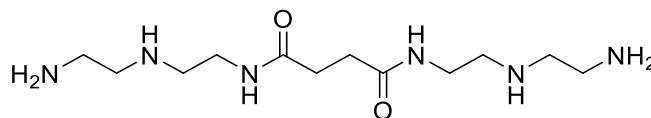


Figure 4-16: Oligoamide 5 DS

4.2.2 Synthesis of partially perfluorinated oligoamides

4.2.2.1 Methodology

The synthesis of perfluorinated derivatives was carried out by the ring open reaction between the terminal amino groups of oligoamides and a perfluorinated epoxy derivative (3-perfluorohexyl-1,2-epoxypropane, figure 4-17). The perfluoroepoxy shows good solubility in 2-propanol while the oligoamide is soluble in H_2O . The synthesis with 2-propanol as solvent in the presence of the dispersed oligoamide can cause low conversion. The solubilization of both reactants can be achieved by working with a mixture of 2-propanol/water favoring the conversion however the presence of water requires an excess

of reagents for the competitive reaction of epoxy group with water. Then the mixtures of water and 2-propanol in different ratio (1: 1 or 1: 3) were tested as solvent to optimize the conversion using a molecular ratio between oligoamides and perfluoroepoxy 1:4. The reaction mixture was heating at 70 °C for 48 hours.

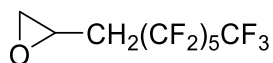


Figure 4-17: 3-perfluorohexyl-1,2-epoxypropane

In the general work up procedure, the solvent and the excess epoxide were removed by evaporation, then water was firstly used to wash the residue to remove the remained starting oligoamide. Subsequently, cold acetone (-20 °C) was used to wash the residue, in order to remove the by-product caused by the reaction of the epoxy with water.

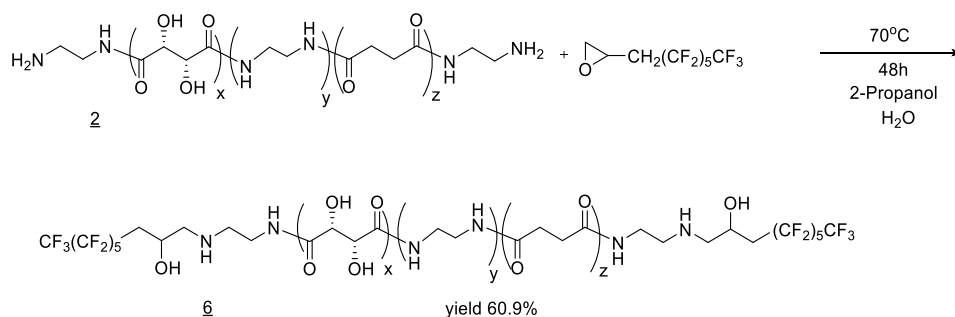
4.2.2.2 Synthesis

- Synthesis of partially perfluorinated oligoamide 6 (**ESTF**)

As mentioned above, the solvent for the ring open reaction needs attention because of the different solubility of the starting reagents. With the aim to find the suitable solvent, two different solvents (2-propanol and H₂O/2-propanol) were investigated in the synthesis of fluorinated oligoamide 6 (ESTF).

- Synthesis of **ESTF** in mixture of 2-propanol and H₂O

Firstly, oligoamide EST was reacted with 3-perfluorohexyl-1,2-epoxypropane (perfluoroepoxy), *via* ring open reaction at 70 °C. The reaction was performed in the mixture of 2-propanol and H₂O with volume ratio 1:1 for 48 h. The molecular ratio between EST and epoxy is 1:4 (scheme 4-14). The final product was obtained as a yellow solid with 60.9 % yield.



Scheme 4-14: Synthesis of partially perfluorinated oligoamide 6 **ESTF**

In the ¹H NMR spectrum recorded in CD₃OD (figure 4-18), the presence of the fluorine chain is confirmed by the signals between 2.10 and 2.80 ppm attributable to CH₂ in CH₂NHCH₂CH(OH)CH₂(CF₂)₅CF₃. The signal at 4.10 ppm attributes to CH in the

$\text{CH}_2\text{CH}(\text{OH})\text{CH}_2(\text{CF}_2)_5\text{CF}_3$, which is formed by the opening of the epoxy group with the amino group. The signals ascribable to hydroxylated oligoamide fragment are also present. The signals between 3.0-3.5 ppm attributes to CH_2NHCO and the signal at 4.47 ppm is assigned to CHOHCHOH . The signal at 2.46 ppm is ascribable to $\text{COCH}_2\text{CH}_2\text{CO}$. The signals at 3.50 and 4.04 ppm are assigned to a low amount of diol as impurity. Starting from oligoamide 2 (EST), the integral ratio between the signal at 4.10 (ascribing to 1H) and 4.47 ppm (ascribing to 2H for 2.18 tartaric units on average in each oligoamide chain) allows to evaluate a degree of functionalization of 3.57 for the two terminal amino groups. This result is also in agreement with previous data obtained in the UNIFI and IGG-CNR laboratories for the synthesis of perfluorinated derivatives of diamines for which the chemical shift of $\text{CH}(\text{OH})$ due to the presence of two perfluorinated groups on amine was 4.08 ppm while the monosubstituted one had a higher chemical shift (about 4.20 ppm).

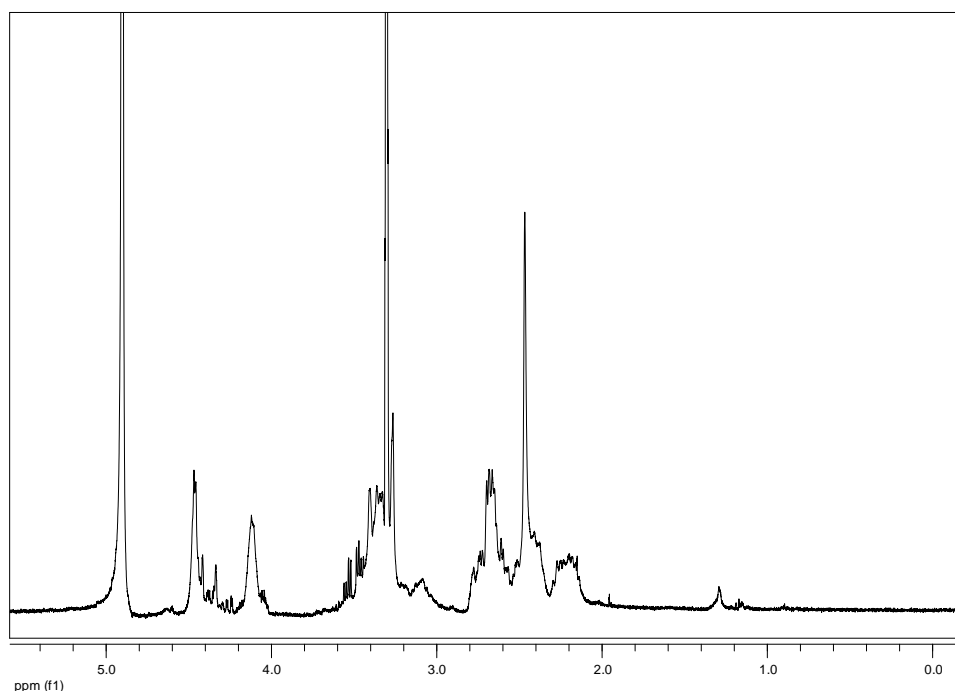


Figure 4-18: ^1H NMR spectrum in CD_3OD of oligoamide 6 ESTF

gCOSY (figure 4-19) also confirms the assignment, thanks to the couplings between CH at α position (at 4.10 ppm) and CH_2 at β position (between 2.55-2.80 ppm) of hydroxyl group in fluorochain, and the coupling between CH_2NHCO (3.0-3.5 ppm) and CH_2 at β position respect amido group $\text{CONHCH}_2\text{CH}_2\text{NHCH}_2$ (between 2.55-2.80 ppm).

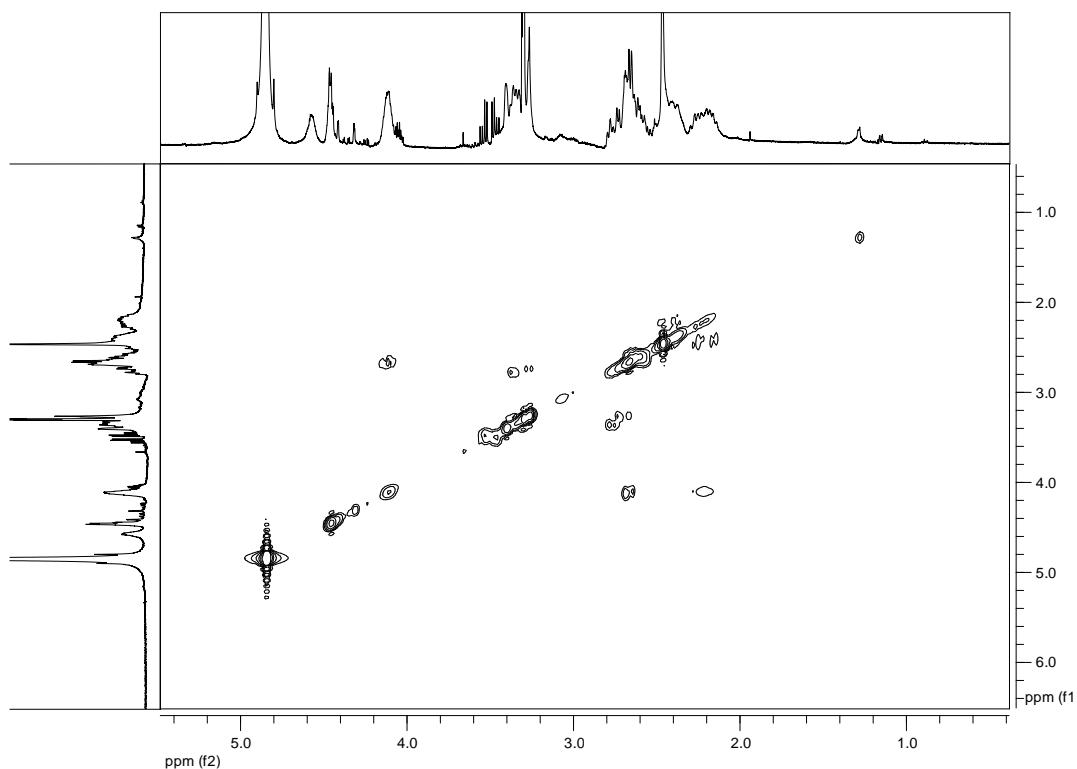


Figure 4-19: gcosy NMR spectrum in CD_3OD of oligoamide 6 ESTF

^{19}F NMR spectrum confirms the presence of perfluorochain for the presence of signals at -82.5 (CF_3), -122.9, -124.0, -124.6 ($CH_2(CF_2)_4CF_2CF_3$) and -127.5 ($CH_2(CF_2)_4CF_2CF_3$) ppm. (figure 4-20)

In ^{13}C -NMR spectrum (figure 4-21), formation of the product is confirmed by the presence of signals at 30.7 ($COCH_2$), 35.5 ($CH_2CH(OH)CH_2(CF_2)_5CF_3$), 38.5 (CH_2NHCO), 54.7 (CH_2NH), 60.9 and 65.4 ($CH_2CH(OH)CH_2(CF_2)_5CF_3$), 61.9, 63.5 63.5 ($CH_2CH(OH)CH_2(CF_2)_5CF_3$), 72.7 ($COCHOHCHOHCO$), 108.3, 111.5, 113.5, 115.7, 118.4, 121.0 ($CF_3(CF_2)_5$), 173.8 ($CONH$) ppm.

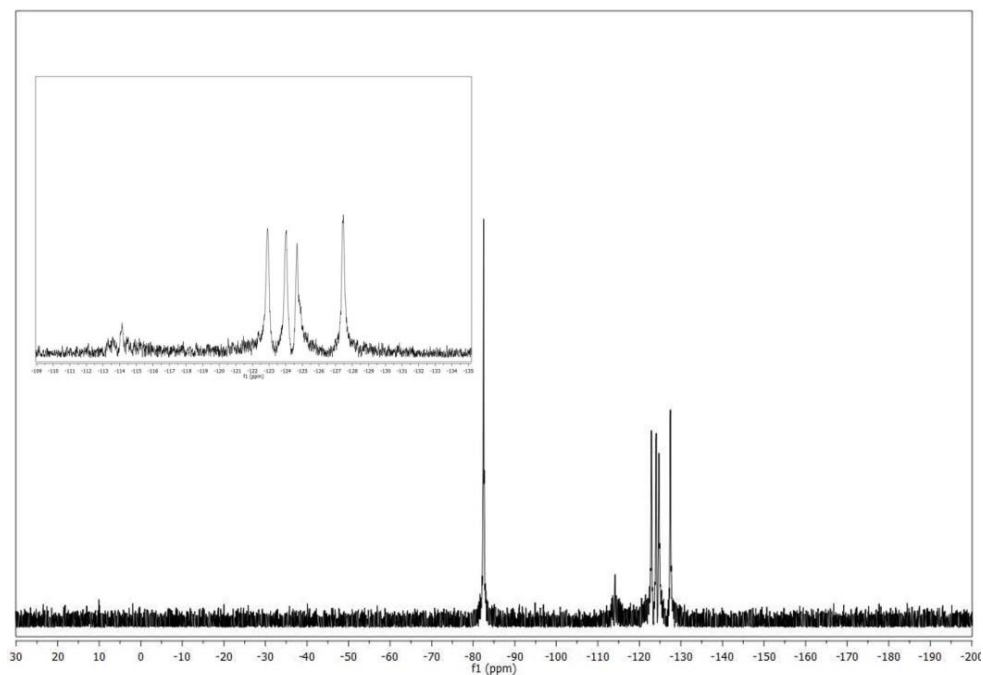


Figure 4-20: ^{19}F NMR spectrum in CD_3OD of oligoamide 6 ESTF

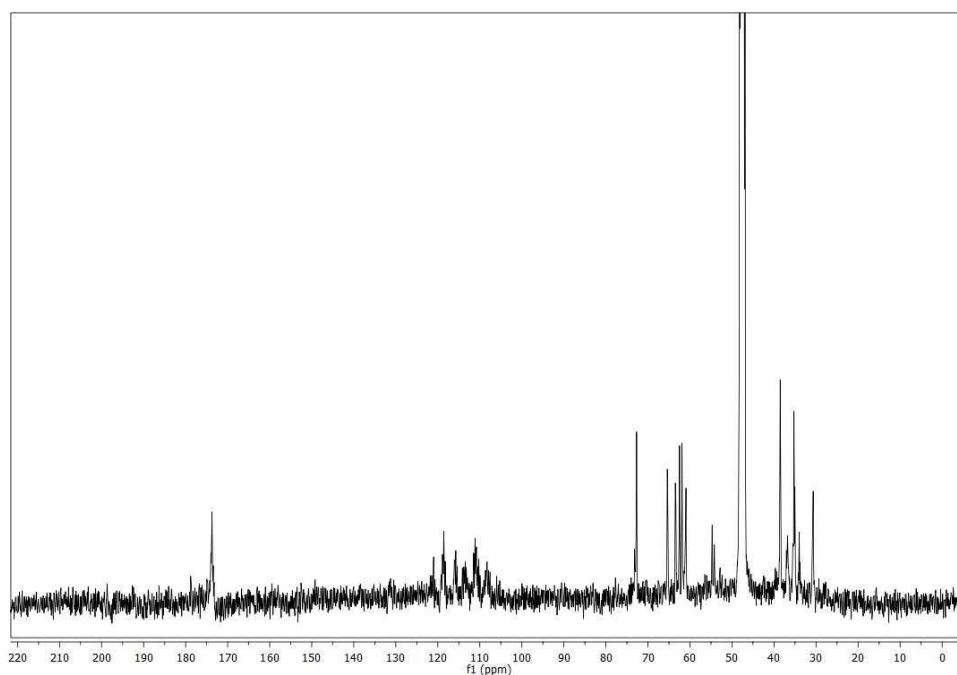


Figure 4-21: ^{13}C NMR spectrum in CD_3OD of oligoamide 6 ESTF

In the work-up procedure, the reaction residue was firstly washed by water to remove the unconverted oligoamide. Then cold acetone ($-20\text{ }^\circ\text{C}$) was used to wash the residue to remove the diol product, which came from the reaction between water and perfluoroepoxy. In the ^1H NMR of acetone soluble part (figure 4-22), signal of diol can be observed at 3.50 ($-\text{CH}_2\text{OH}$) and 4.04 ($-\text{CHOH}$) ppm. Signals attributable to $-\text{CH}_2-\text{CF}_2$ were also present between 2.25 and 2.65 ppm overlapped to those attributable to the

presence of a small amount of oligoamide 6 (ESTF).

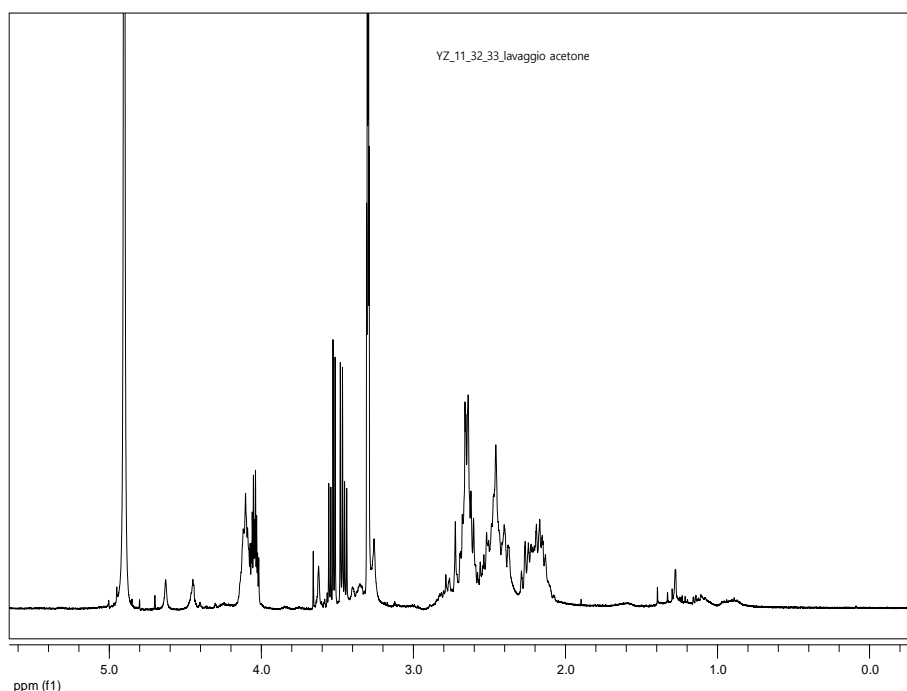


Figure 4-22: ^1H NMR spectrum in CD_3OD of fraction soluble in acetone at -20°C of oligoamide 6 ESTF

- Synthesis of **ESTF** in 2-propanol

In order to avoid side reaction between water and 3-perfluorohexyl-1,2-epoxypropane, the synthesis with the same reagents was performed using 2-propanol as solvent instead of the mixture of water and 2-propanol. Other reaction conditions were kept unchanged as in the previous synthesis. However only trace amount of product 6 was obtained due to the poor solubility of starting oligoamide EST in 2-propanol which may cause the low yield. Signals attributable to pure product were present in ^1H NMR spectrum (figure 4-23). Although in this case, the integral ratio between the signal at 4.10 (ascribing to 1H) and 4.47 ppm (ascribing to 2H for each tartatic unit) is higher, it is in agreement with a reduced number of tartaric units compared to succinic in the chains soluble in pure 2-propanol which reacted with the epoxide. No signal related to diol was observed.

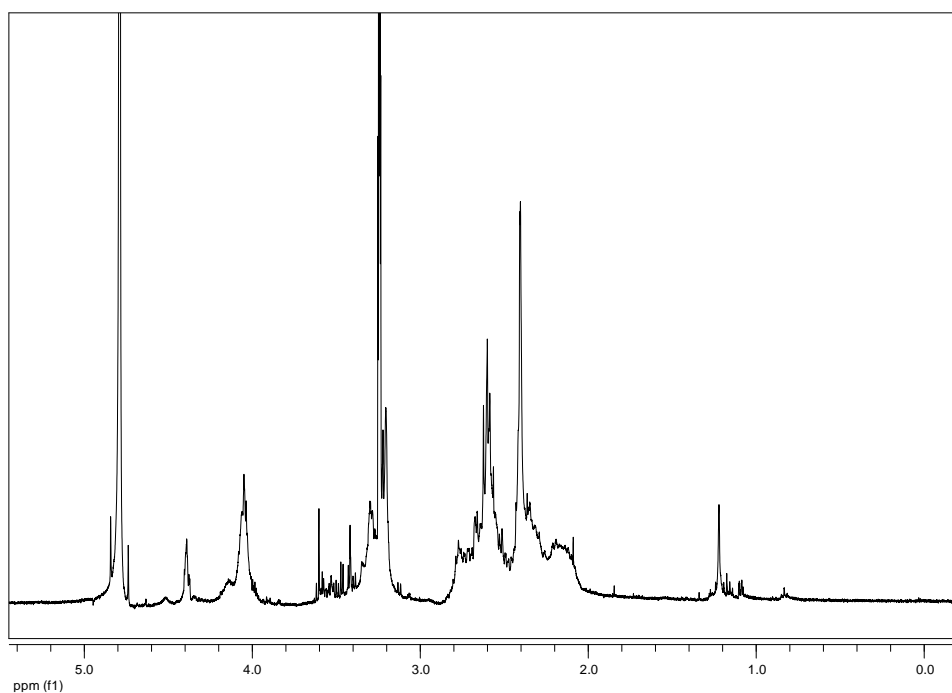
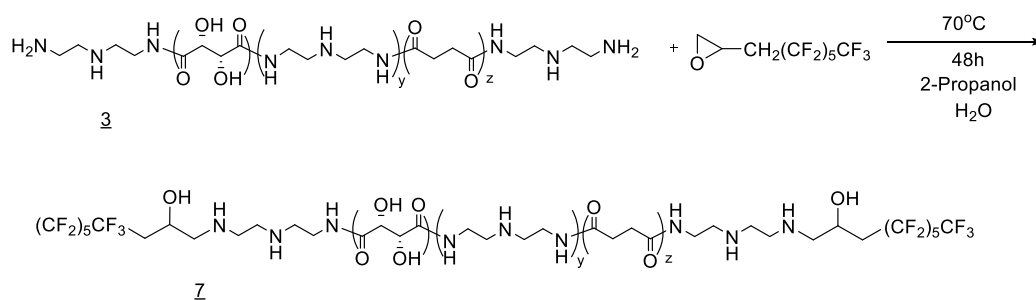


Figure 4-23: ^1H NMR spectrum in CD_3OD of oligoamide 6 ESTF (synthesis in 2-propanol)

- Synthesis of partially perfluorinated oligoamide 7 (DSTF)

The corresponding perfluorinated derivative of the oligoamide 3 (DST) was obtained by reaction with 3-perfluorohexyl-1,2-epoxypropane, molar ratio 1:4, in mixture of 2-propanol and water with volume ratio 1:1 at 70 °C for 48 h. The same work-up procedure was performed. Orange oil was obtained as the final product with 100 % yield. (scheme 4-15)



Scheme 4-15: Synthesis of partially perfluorinated oligoamide 7 DSTF

In the ^1H NMR (figure 4-24), the signal between 3.2-3.6 ppm is assigned to CH_2NHCO . The signal at 4.11 ppm is ascribable to CH in the $\text{CH}_2\text{CH}(\text{OH})\text{CH}_2(\text{CF}_2)_5\text{CF}_3$. The signal at 4.51 ppm is assigned to CHOHCHOH and the signals between 2.06-3.10 ppm are ascribable to $\text{CH}_2\text{NHCH}_2\text{CH}(\text{OH})\text{CH}_2(\text{CF}_2)_5\text{CF}_3$ overlapped to the signal at 2.49 ppm assigned to $\text{COCH}_2\text{CH}_2\text{CO}$ and to the signals between 2.5-3.0 ppm assigned to CH_2NHCH_2 .

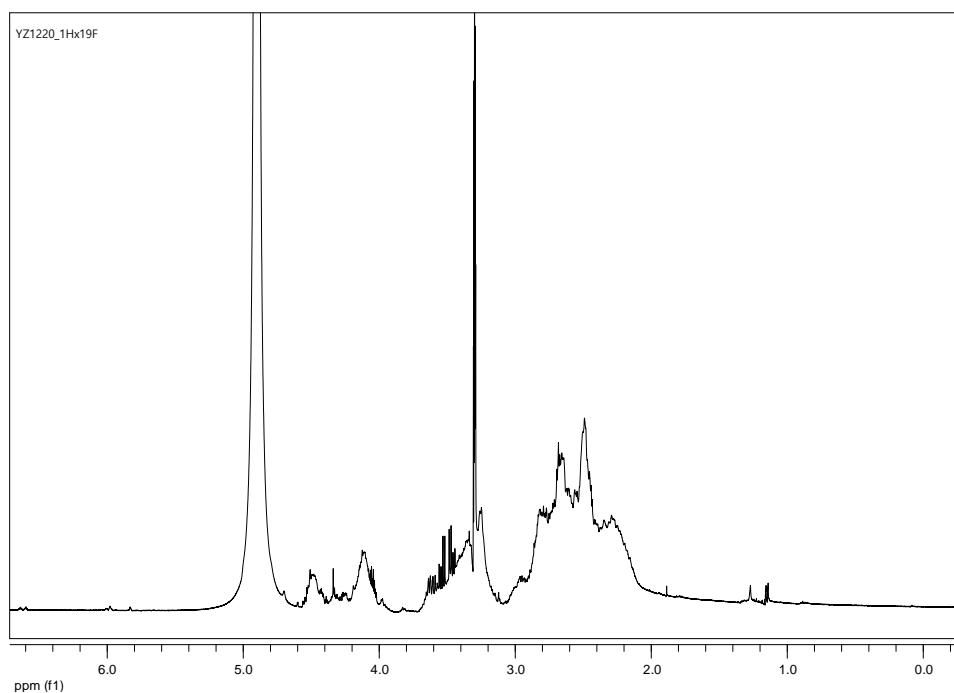


Figure 4-24: ¹H NMR spectrum in CD₃OD of oligoamide **Z DSTF**

These assignments are confirmed by gCOSY spectrum (figure 4-25), for the presence of the coupling between signals at 4.11 ppm (**CH**) and at 2.4-2.8 ppm attributable to CH₂ in CH₂NHCH₂CH(OH)CH₂(CF₂)₅CF₃, while the signals between 2.5-3.0 ppm assigned to CH₂NHCH₂ show a coupling with signals between 3.2-3.6 ppm (CH₂NHCO). The overlap between numerous signals even in the area around 4.1-4.6 ppm does not allow for an evaluation of the degree of functionalization for this compound which, however, appears to be very high. In fact, based on the relative intensity of the signal at 4.11 ppm compared to that at 4.51 ppm, it is possible to hypothesize the presence of amino groups with two substituent groups and therefore a high degree of functionalization.

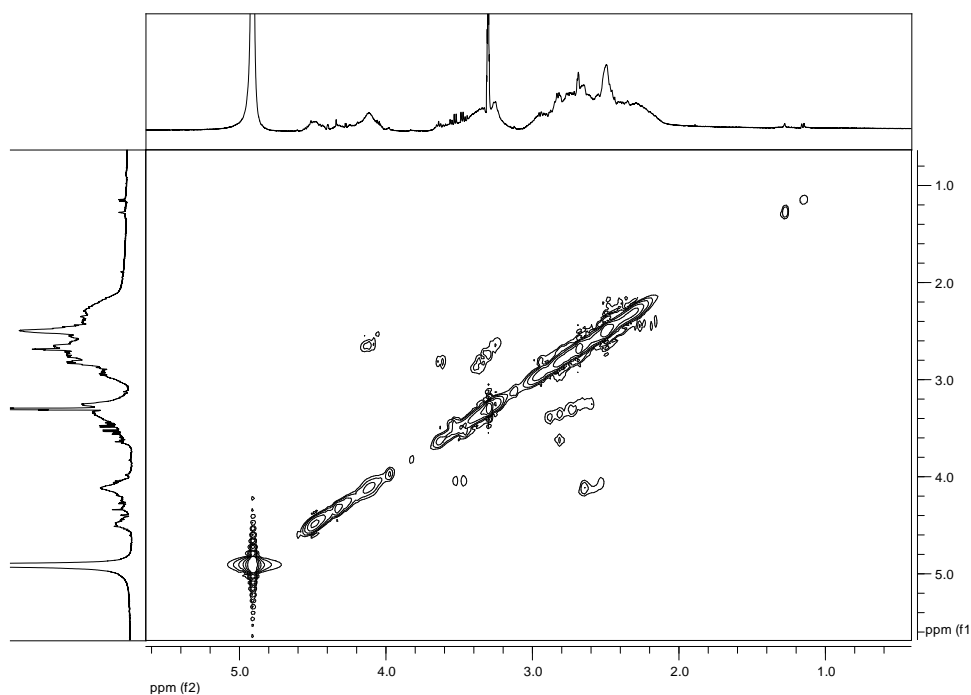


Figure 4-25: gCOSY NMR spectrum in CD_3OD of oligoamide **Z DSTF**

^{19}F NMR spectrum confirms the presence of perfluorochain for the presence of signals at -82.5 (CF_3), -122.9, -124.0, -124.7 ($CH_2(CF_2)_4CF_2CF_3$) and -127.4 ($CH_2(CF_2)_4CF_2CF_3$) ppm. (figure 4-26)

In ^{13}C -NMR spectrum (figure 4-27), the formation of the product is confirmed by the presence of signals at 31.0 ($COCH_2$), 35.2 (CH_2NHCH_2) and ($CH_2CH(OH)CH_2(CF_2)_5CF_3$), 37.0 (CH_2NHCO), 53.5 (CH_2NH), 60.8 and 65.2 ($CH_2CH(OH)CH_2(CF_2)_5CF_3$), 62.5 ($CH_2CH(OH)CH_2(CF_2)_5CF_3$), 73.0 ($COCHOHCHOHCO$), 108.1, 110.5, 113.5, 115.7, 118.1, 121.3 ($CF_3(CF_2)_5$), 173.2 ($CONH$) ppm. These assignments are confirmed by gHSQC spectrum (figure 4-28).

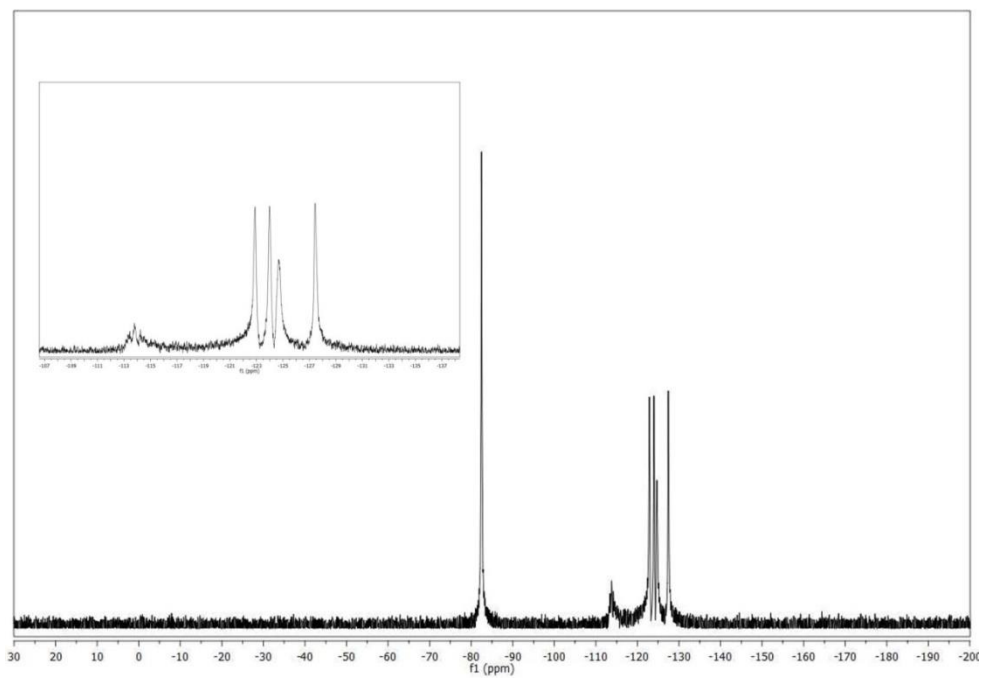


Figure 4-26: ^{19}F NMR spectrum in CD_3OD of oligoamide Z *DSTF*

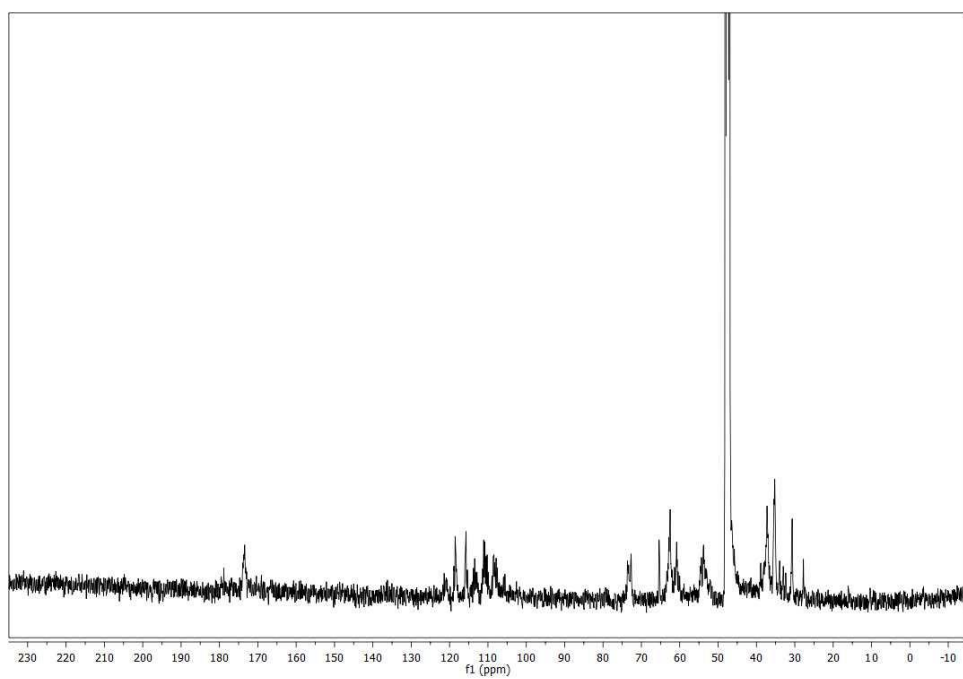


Figure 4-27: ^{13}C NMR spectrum in CD_3OD of oligoamide Z *DSTF*

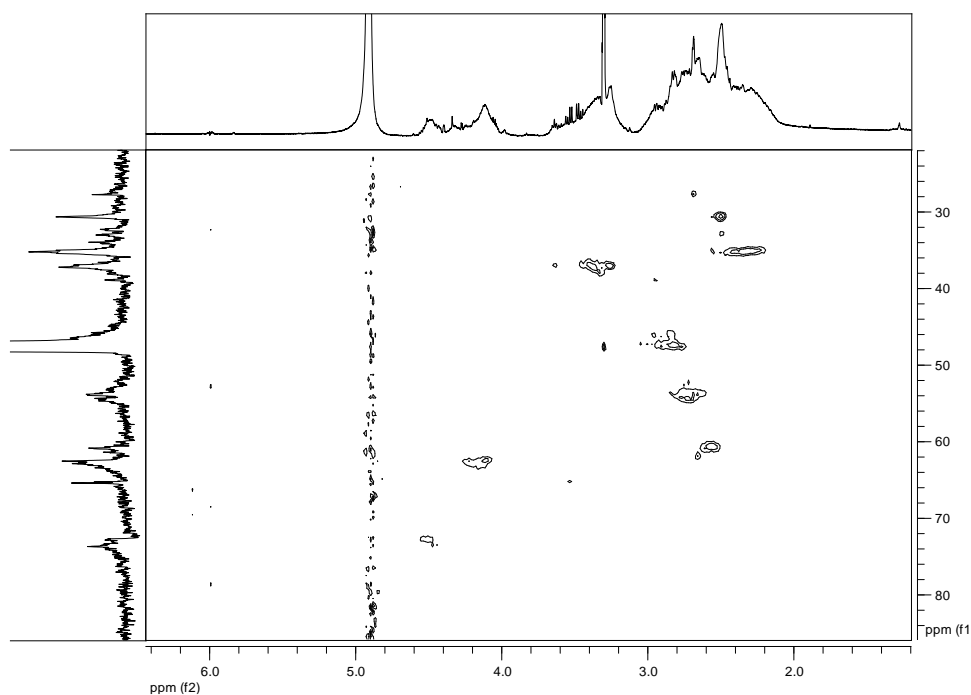
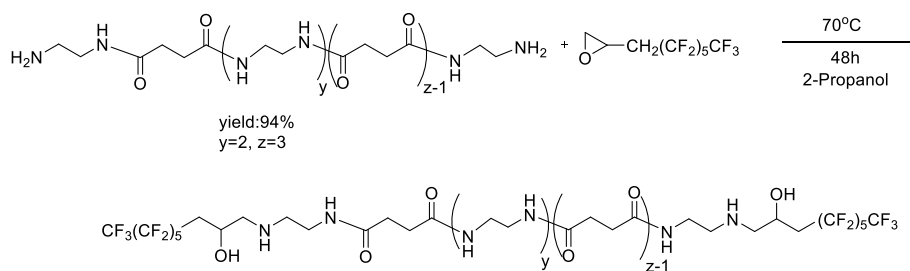


Figure 4-28: gHSQC NMR spectrum in CD_3OD of oligoamide Z DSTF

- Synthesis of partially perfluorinated oligoamide 8 (ESF)

In the synthesis of oligoamide 4 (ES) with the perfluoroepoxy, *via* ring open reaction, pure 2-propanol was used as solvent (scheme 4-16). In fact, the solubility of the starting oligoamides in alcohol increases when the ratio of alkyl groups increases in its structures and when tartaric units are not present. So in this synthesis, 2-propanol was used as the reaction solvent instead of the mixture 2-propanol/water. Molar ratio between the reagents and reaction conditions has been kept unchanged. Finally, the target partially perfluorooligoamide was obtained as white solid with 95 % yield.



Scheme 4-16: Synthesis of partially perfluorinated oligoamide 8 ESF

Based on the data present in the 1H NMR and gCOSY spectra (figure 4-29, 4-30), the signal at 4.11 ppm is ascribable to CH in the $CH_2CH(OH)CH_2(CF_2)_5CF_3$, and the signals between 2.05 and 2.77 ppm are attributable to CH_2 in $CH_2NHCH_2CH(OH)CH_2(CF_2)_5CF_3$ overlapped to the signal at 2.46 ppm which is assigned to $COCH_2CH_2CO$. Finally, the signal at 3.26 ppm is attributable to CH_2NHCO . The overlap between numerous signals does not allow for an

evaluation of the degree of functionalization for this compound. However, also in this case the presence of the signal at 4.11 ppm and the considerations reported on the characterization of the previous perfluorinated oligoamides (ESTF and DSTF) allow to hypothesize the presence of amino groups with two substituent groups and therefore a high degree of functionalization.

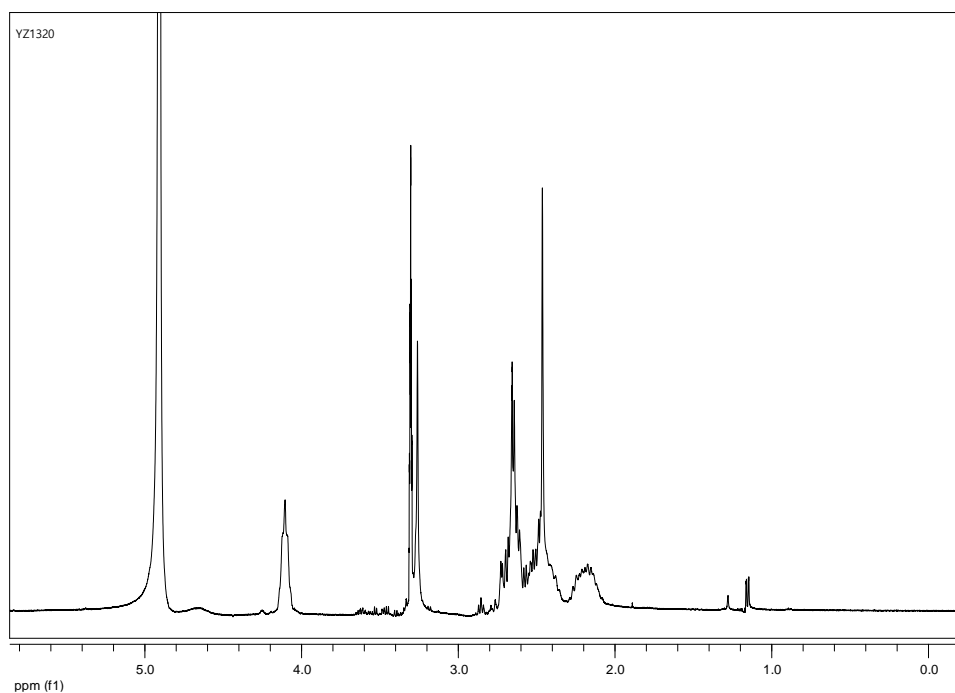


Figure 4-29: ^1H NMR spectrum in CD_3OD of oligoamide **8** ESF

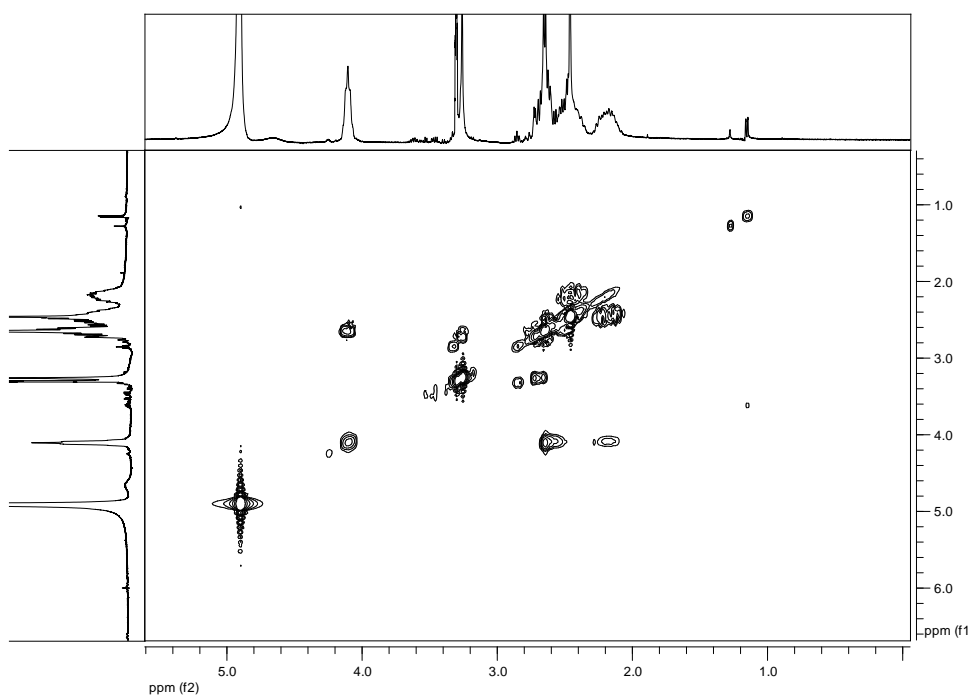


Figure 4-30: gCOSY NMR spectrum in CD_3OD of oligoamide **8** ESF

^{19}F NMR spectrum confirms the presence of perfluorochain for the presence of signals at -82.5 (CF_3), -122.9, -124.1, -124.6, -124.9 ($\text{CH}_2(\text{CF}_2)_4\text{CF}_2\text{CF}_3$) and -127.6 ($\text{CH}_2(\text{CF}_2)_4\text{CF}_2\text{CF}_3$) ppm. (figure 4-31)

In ^{13}C -NMR spectrum (figure 4-32), formation of the product is confirmed by the presence of signals at 30.7 (COCH_2), 34.6 ($\text{CH}_2\text{CH}(\text{OH})\text{CH}_2(\text{CF}_2)_5\text{CF}_3$), 38.2 (CH_2NHCO), 52.6 and 54.1 (CH_2NH), 61.1 and 61.2 ($\text{CH}_2\text{CH}(\text{OH})\text{CH}_2(\text{CF}_2)_5\text{CF}_3$), 62.3 and 63.2 ($\text{CH}_2\text{CH}(\text{OH})\text{CH}_2(\text{CF}_2)_5\text{CF}_3$), 108.4, 110.8, 112.9, 114.7, 118.9, 121.3 ($\text{CF}_3(\text{CF}_2)_5$), 173.6 (CONH) ppm. These assignments are confirmed by gHSQC spectrum (figure 4-33).

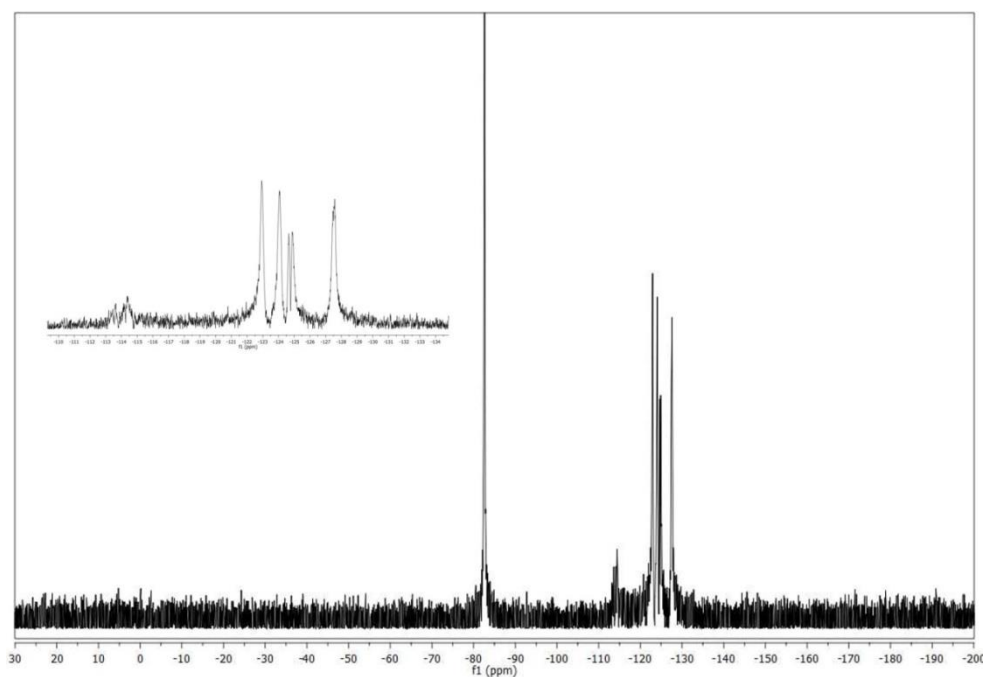


Figure 4-31: ^{19}F NMR spectrum in CD_3OD of oligoamide 8 ESF

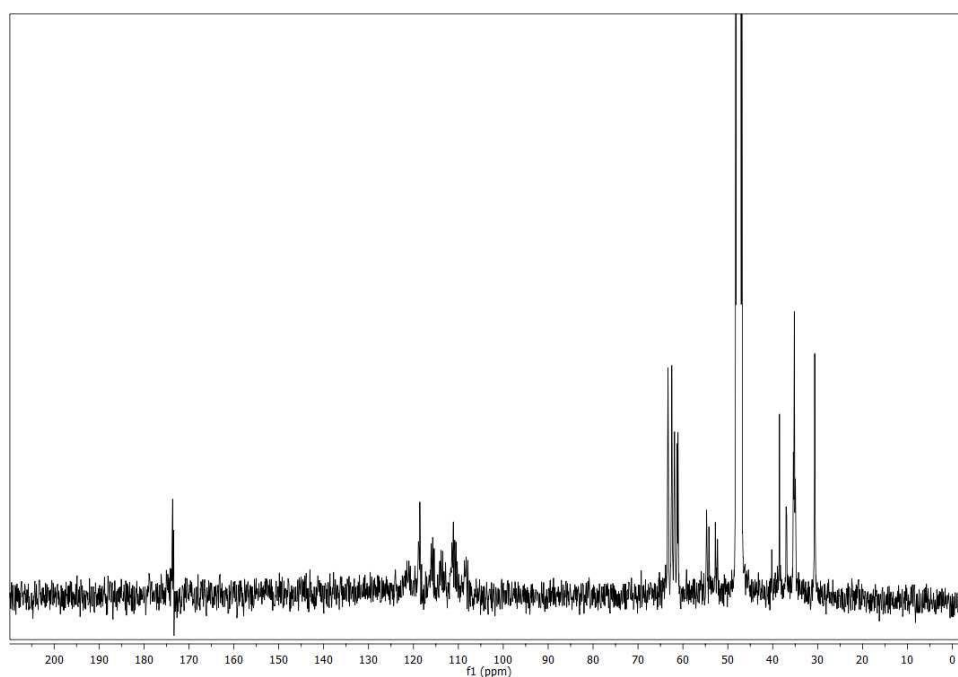


Figure 4-32: ^{13}C NMR spectrum in CD_3OD of oligoamide 8 ESF

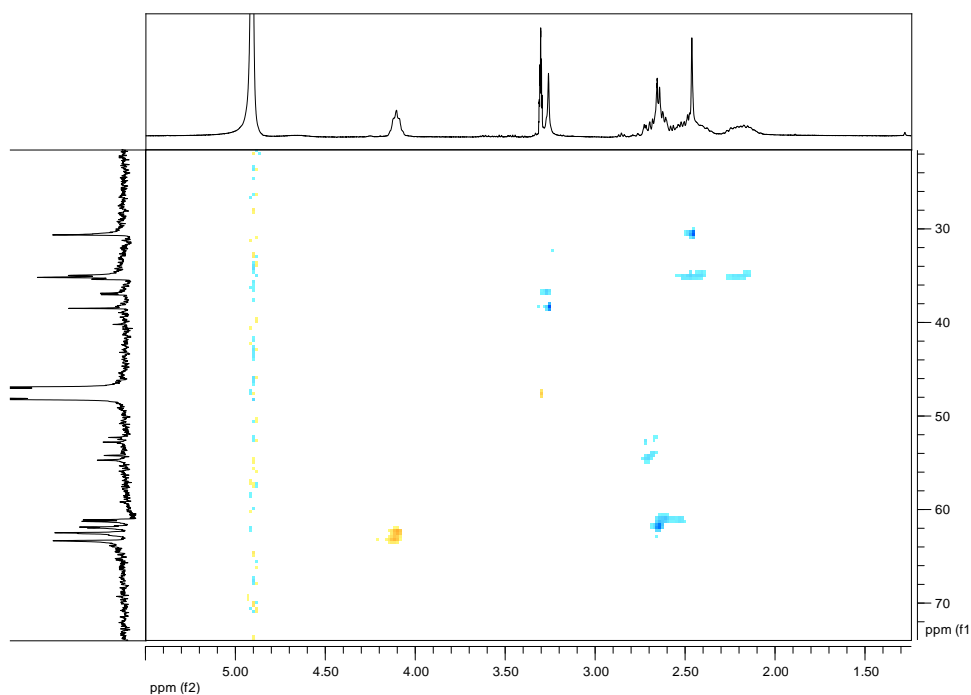
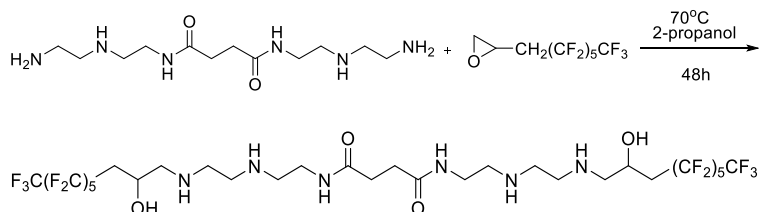


Figure 4-33: gHSQC NMR spectrum in CD_3OD of oligoamide 9 *ESF*

- Synthesis of partially perfluorinated oligoamide 9 (*DSF*)

The synthesis between oligoamide 5 (*DS*) and perfluoroepoxy was carried out in 2-propanol at 70 °C for 48 h. The final product was obtained as orange oil with 100 % yield. (scheme 4-17)



Scheme 4-17: Synthesis of partially perfluorinated oligoamide 9 *DSF*

In the 1H NMR spectrum (figure 4-34), the signal at 4.12 ppm is ascribable to CH in the $CH_2CH(OH)CH_2(CF_2)_5CF_3$ and the signal at 3.25 ppm is assigned to CH_2NHCO . The signal between 2.07-2.90 ppm is assigned to CH_2NH and $CH_2CH(OH)CH_2(CF_2)_5CF_3$, and the overlapped signal at 2.48 ppm is attributable to $COCH_2CH_2CO$. The overlap between numerous signals does not allow for an evaluation of the degree of functionalization for this compound. However, also in this case the presence of the signal at 4.12 ppm and the considerations reported on the characterization of the oligoamide ESTF allow to hypothesize the presence of amino groups with two substituent groups and therefore a high degree of functionalization.

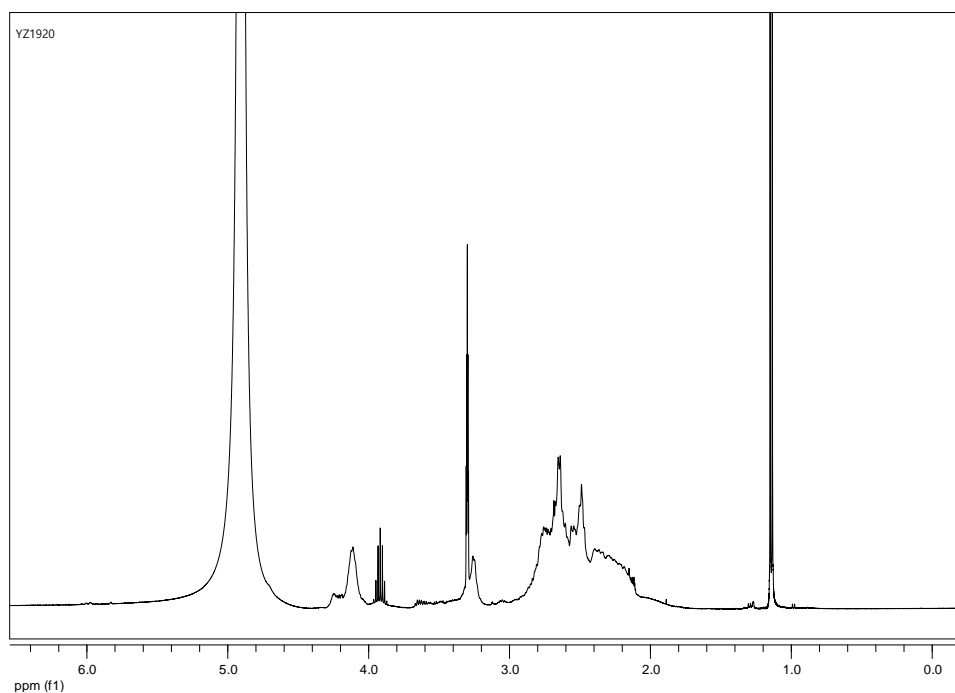


Figure 4-34: ^1H NMR spectrum in CD_3OD of oligoamide 9 DSF

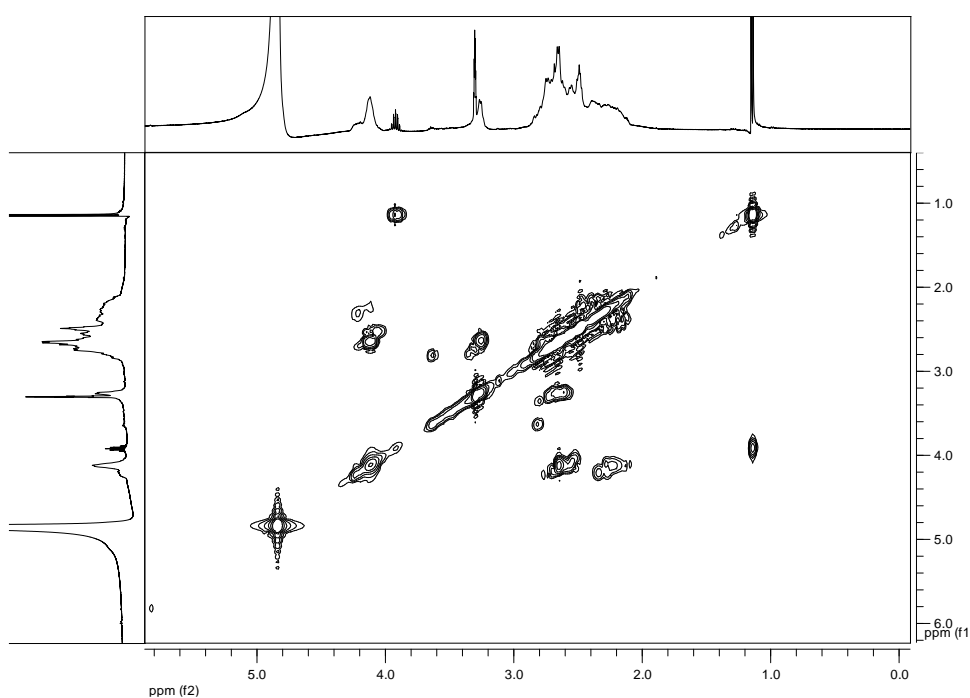


Figure 4-35: gCOSY NMR spectrum in CD_3OD of oligoamide 9 DSF

^{19}F NMR spectrum confirms the presence of perfluorochain for the presence of signals at -82.4 (CF_3), -122.9, -124.1, -124.8 ($\text{CH}_2(\text{CF}_2)_4\text{CF}_2\text{CF}_3$) and -127.5 ($\text{CH}(\text{OH})\text{CH}_2(\text{CF}_2)_4\text{CF}_2\text{CF}_3$) ppm. (figure 4-36)

In ^{13}C -NMR spectrum (figure 4-37), formation of the product is confirmed by the presence of signals at 30.7 (COCH_2), 34.9 $\text{CH}_2\text{CH}(\text{OH})\text{CH}_2(\text{CF}_2)_5\text{CF}_3$, 37.0 (CH_2NHCO), 53.5 (CH_2NH), 61.0, 62.5 ($\text{CH}_2\text{CH}(\text{OH})\text{CH}_2(\text{CF}_2)_5\text{CF}_3$), 63.3 ($\text{CH}_2\text{CH}(\text{OH})\text{CH}_2(\text{CF}_2)_5\text{CF}_3$), 105.7, 108.8, 110.8, 113.5,

115.9, 118.3, 121.0 (CF₃(CF₂)₅), 173.6 (CONH) ppm.

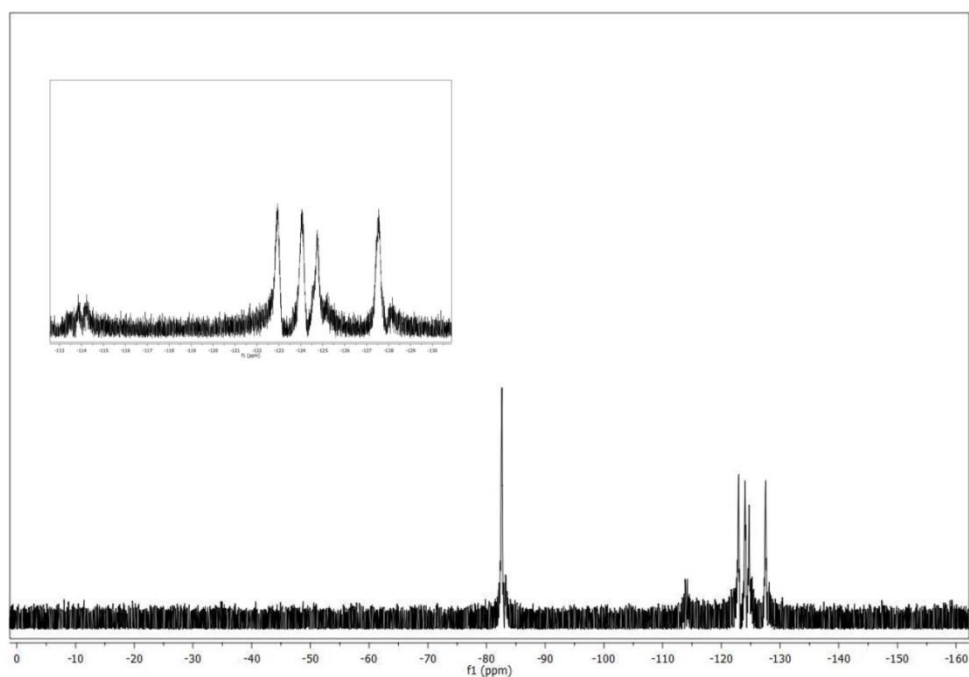


Figure 4-36: ¹⁹F NMR spectrum in CD₃OD of oligoamide 9 DSF

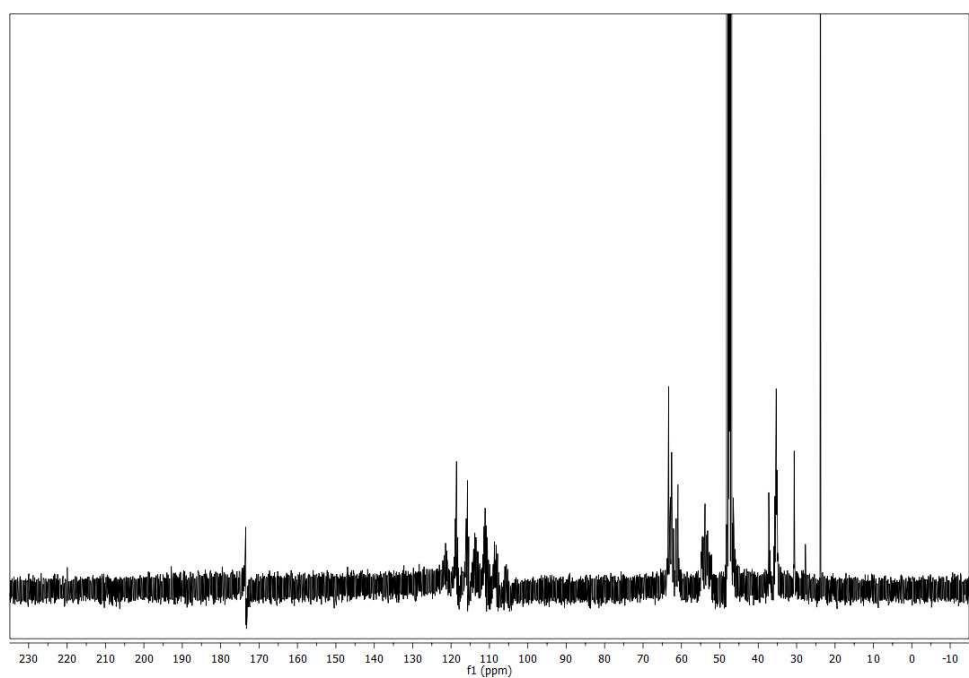
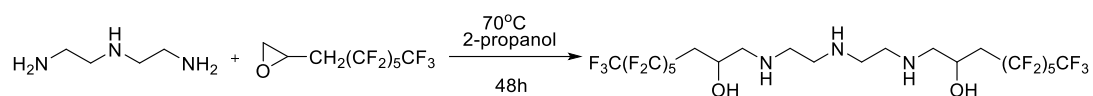


Figure 4-37: ¹³C NMR spectrum in CD₃OD of oligoamide 9 DSF

- Synthesis of partially perfluorinated diethylenetriamine 10 (DF)

In order to understand the role of amide group on the application behavior of new partially perfluorinated products, the last synthesis was performed using diethylenetriamine

and perfluoroepoxy in 2-propanol with molar ratio 1:4 using the same reaction conditions as for oligoamido synthesis. Yellow oil was obtained as final product with 100 % yield. (scheme 4-18)



Scheme 4-18: Synthesis of partially perfluorinated diethylentriamine **1Q DF**

In ¹H NMR spectrum (figure 4-38), the signals at 4.11 and 4.19 ppm are ascribable to CH in the CH₂CH(OH)CH₂(CF₂)₅CF₃. Signals between 2.07 and 2.83 ppm are attributable to NHCH₂CH(OH)CH₂(CF₂)₅CF₃ overlapped with the signals ascribable to CH₂NH. The presence of two signals attributable to CH₂CH(OH)CH₂(CF₂)₅CF₃ and the considerations reported on the characterization of the ESTF oligoamide allow to hypothesize the prevalent presence of amino groups with two substituent groups together a low amount of amino groups with only one substituent in a ratio of approximately (2:1). The gCOSY spectrum (figure 4-39) confirms the coupling between both signals at 4.11 and 4.19 ppm and signals between 2.07 and 2.83 ppm.

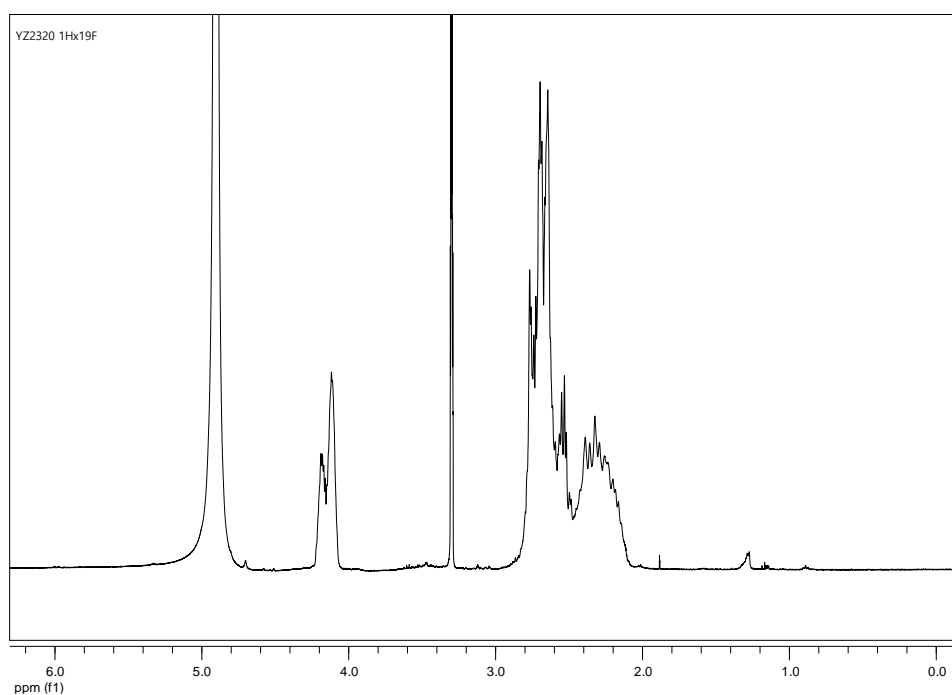


Figure 4-38: ¹H NMR spectrum in CD₃OD of perfluorinated diethylentriamine **1Q DF**

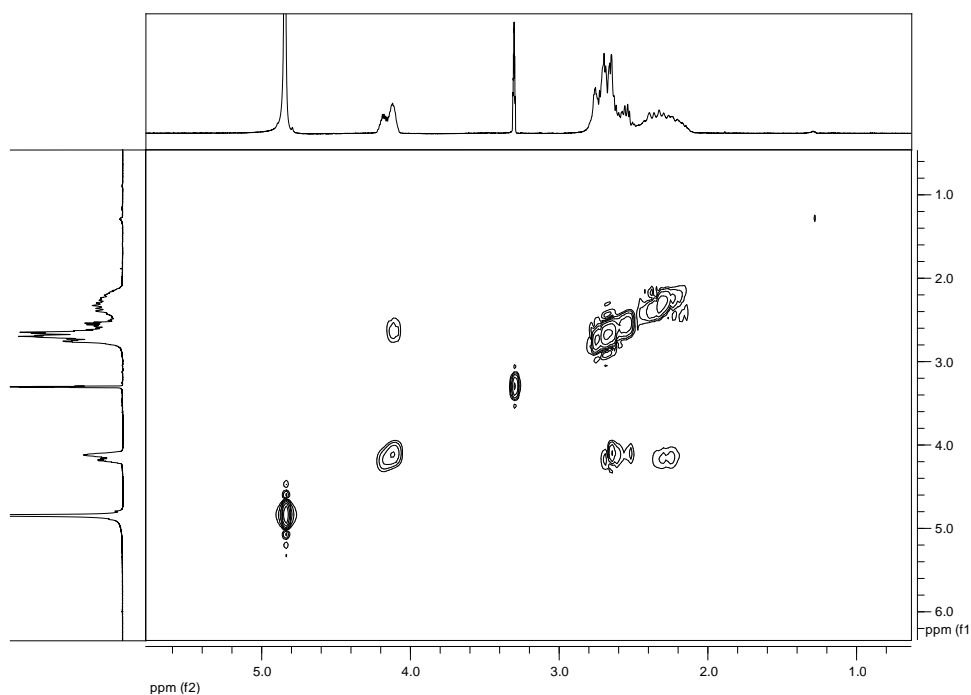


Figure 4-39: gCOSY NMR spectrum in CD_3OD of perfluorinated diethylentriamine 1Q DF

^{19}F NMR spectrum confirms the presence of perfluorochain for the presence of signals at -82.6 (CF_3), -123.0, -124.1, -124.8 ($CH_2(CF_2)_4CF_2CF_3$) and -127.5 ($CH(OH)CH_2(CF_2)_4CF_2CF_3$) ppm. (figure 4-40)

In ^{13}C -NMR spectrum (figure 4-41), formation of the product is confirmed by the presence of signals at 35.4 $CH_2CH(OH)CH_2(CF_2)_5CF_3$, 55.0 (CH_2NH), 61.0 ($CH_2CH(OH)CH_2(CF_2)_5CF_3$), 63.1 ($CH_2CH(OH)CH_2(CF_2)_5CF_3$), 108.8, 111.7, 113.5, 115.9, 118.6, 121.0 ($CF_3(CF_2)_5$) ppm.

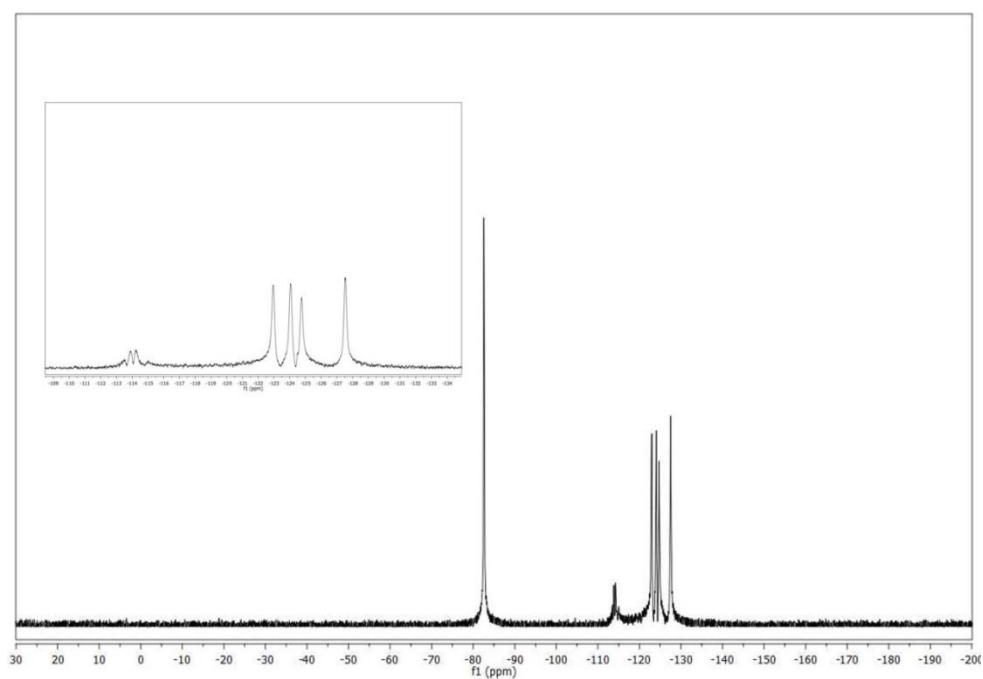


Figure 4-40: ^{19}F NMR spectrum in CD_3OD of perfluorinated diethylentriamine 1Q DF

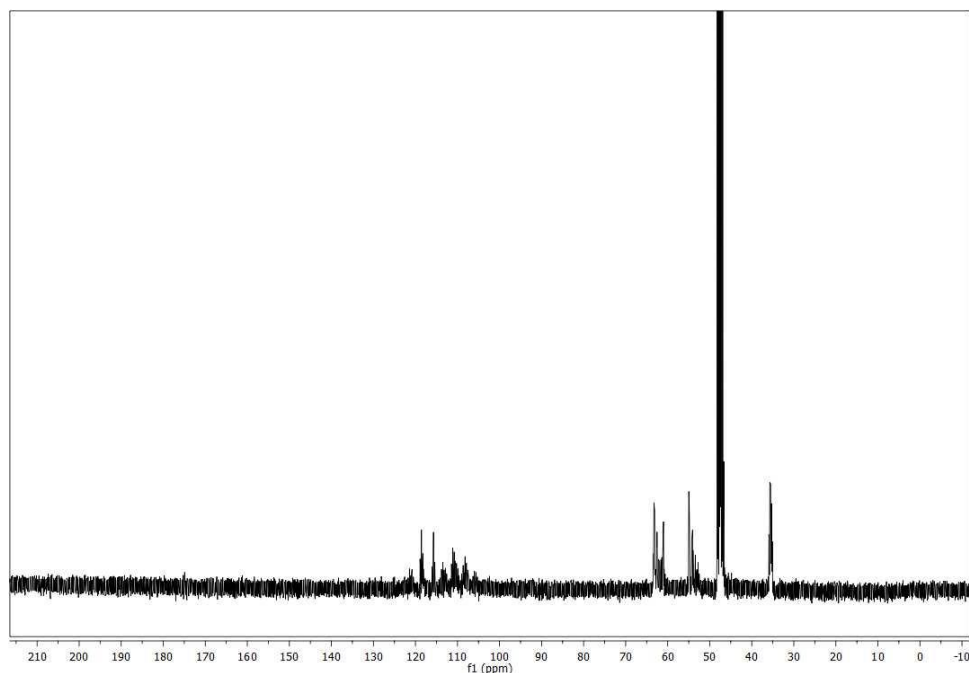


Figure 4-41: ^{13}C NMR spectrum in CD_3OD of perfluorinated diethylenetriamine **1Q DF**

4.3 Conclusion

With the aim to find suitable partially perfluoroderivatives for stone protection and blanching painting restoration, four new partially perfluorinated compounds with different structures and properties (*i.e.* solubility, hydrophilicity, different chain length, molecular weight, and *etc.*) were obtained. Among them, two partially perfluorinated oligoamides contain also hydroxyl groups. In order to understand the roles of hydroxyl groups in the applicative performance, two partially perfluorinated oligoamides with no hydroxyl groups, but with the unchanged amine and succinate sources were synthesized. Also a partially perfluoroamine was obtained in order to compare its applicative performance with the compounds containing amide functional groups.

In particular, oligoamides, which are named as **EST**, **DST**, **ES**, **DS**, starting from different monomers (dimethyl L-tartrate, diethyl succinate, diethylenetriamine or ethylenediamine) were successfully obtained *via* polycondensation reaction. The choice of monomers was made in order to balance the presence of polar groups to favour interactions with polar substrates. Among those oligoamides, **EST** and **DST** are containing hydroxyl groups due to the presence of L-tartrate units. The different amine sources (diethylenetriamine and ethylenediamine) formed the amide groups in **DST** and **EST**. The oligoamides without hydroxyl groups, **ES** and **DS**, were synthesized as controls to investigate the role of OH groups on stone protection and blanching painting restoration.

Target partially perfluorinated oligoamides, **ESTF**, **DSTF**, **ESF**, **DSF**, were obtained by introducing perfluorinated chains into **EST**, **DST**, **ES** and **DS** through ring open reactions with good yield. Besides, partially perfluorinated amine **DF** was synthesized to investigate the function of amide groups in restoration performance. Therefore, the partially perfluorinated

oligoamides and amine, which have different average molecular weight, polarity, solubility and physical states, were obtained.

In the molecules of hydroxylated oligoamides with perfluorinated chains (**ESTF** and **DSTF**), the hydroxyl groups, amide groups and amine groups could give interactions by hydrogen bonding or dipolar interaction with the stones or painting materials. That could help increase the adhesion to stones and fill the pores in blanching paintings. For **ESF** and **DSF**, the amide and amine groups could interact with the substrates. For **DF**, the amine groups could interact with the substrates by hydrogen bonding. On the other hand, the perfluorinated chains could contribute hydrophobicity to the molecules for stone protection and blanching easel painting restoration.

All the compounds above described containing perfluorochains were synthesized and tested for the research of stone protection and blanching painting restoration.

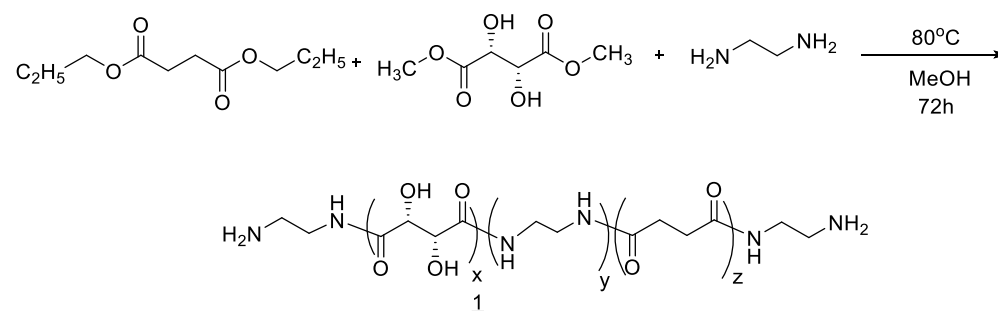
4.4 Experimental part

¹H-NMR analysis was performed with a Varian Mercury VXR400 spectrometer operating at a frequency of 399.921 MHz. Spectra are reported in chemical shift (ppm) relative to tetramethylsilane (TMS) at 0 ppm. The processing of the spectra was performed using Mestre-C 4.3.2.0.

The ¹³C-NMR spectra were recorded Varian Mercury VXR400 spectrometer operating at a frequency of 100.571 MHz. All spectra are reported in ppm using TMS as external standard (0 ppm). Spectra processing was done by using Mestre-C 4.3.2.0.

¹⁹F-NMR spectra were recorded with a Bruker Avance III spectrometer operating at a frequency of 376.5 MHz. CCl₃ is referred to as external standard (0 ppm) for all spectra. The processing of spectra was done by using software Mestre-C 4.3.2.0.

Oligoamide 1 (**EST**)



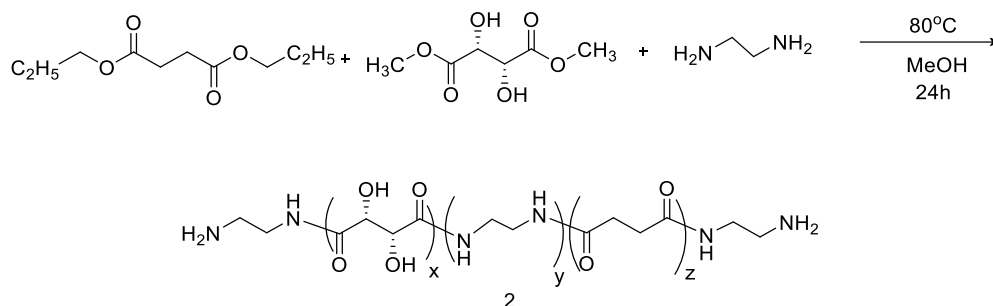
Diethyl succinate (0.35 g, 2 mmol), ethylenediamine(0.24 g, 4 mmol) and methanol (1.5 ml) were added under nitrogen atmosphere to (0.36 g, 2 mmol) dimethyl L-tartrate in the Sovirel® tube. After stirring at 80 °C for 72 h, the disappearance of the liquid phase and the formation of a lightly yellow solid were observed. In the work up process, the reaction mixture was transferred by adding one pipette of methanol, then filtered on a Büchner Funnel, washed by ethyl ether, and then dried at a reduce pressure giving 0.5846 g product. The product is light yellow crystalline solid, water soluble. The average molecular weight is 887.92 g/mol, 100 % yield.

¹H-NMR(D₂O)δ:2.52 and 2.54 (m, 4H, COCH₂CH₂CO), 2.97 (m, 2H, CH₂NH₂), 3.2-3.5 (m, 2H,

CH_2NHCO), 4.56 (m, 1H, CHOH) ppm

$^{13}\text{C-NMR}(\text{D}_2\text{O})\delta$: 31.0 (CH_2CONH), 38.5 (CH_2NHCO), 39.3 (m, 2H, CH_2NH_2), 72.3 (CH-OH), 174.0 and 175.0 (CONH) ppm

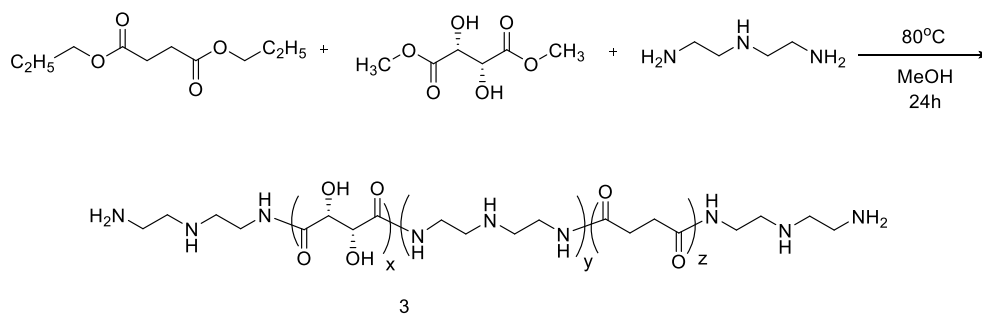
Oligoamide 2 (EST)



Diethyl succinate (0.35 g, 2 mmol), ethylenediamine (0.24 g, 4 mmol) and methanol (1.5 ml) were added under nitrogen atmosphere to (0.36 g, 2 mmol) dimethyl L-tartrate in the Sovirel[®] tube. After stirring at 80 °C for 24 h and with the same work-up as 1, a lightly yellow crystalline solid (Oligoamide 2, 0.4922 g), water soluble, was obtained. The average molecular weight is 633.86 g/mol, 72.4 % yield.

$^1\text{H-NMR}(\text{D}_2\text{O})\delta$: 2.52 and 2.54 (m, 4H, $\text{COCH}_2\text{CH}_2\text{CO}$), 2.97 (m, 2H, CH_2NH_2), 3.2-3.5 (m, 2H, CH_2NHCO), 4.56 (m, 1H, CHOH) ppm.

Oligoamide 3 (DST)

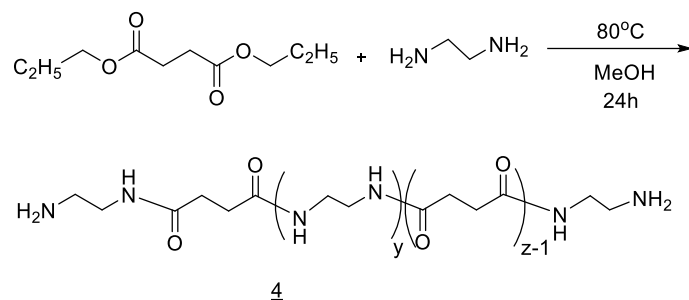


The synthesis between diethyl succinate (0.35 g, 2 mmol), dimethyl L-tartrate (0.36 g, 2 mmol) and diethylenetriamine (0.41 g, 4 mmol) was performed under stirring with methanol (1.5 ml) as solvent in a Sovirel[®] tube, at 80 °C for 24 h. Lightly orange solid (0.49 g) was obtained after evaporating the solvent.

$^1\text{H-NMR}(\text{D}_2\text{O})\delta$: 2.54 (m, 4H, $\text{COCH}_2\text{CH}_2\text{CO}$), 2.73 and 2.77 (m, 4H, CH_2NHCH_2), 2.86 (m, 2H, CH_2NH_2), 3.20-3.50 (m, 2H, CH_2NHCO), 4.56 (m, 1H, CHOH) ppm.

$^{13}\text{C-NMR}(\text{D}_2\text{O})\delta$: 30.8 (CH_2CONH), 37.9 (CH_2NHCO), 38.4 (CH_2NH_2), 47.0 and 45.7 ($\text{CH}_2\text{-NH-CH}_2$), 72.4 and 73.1 (CH-OH), 174.0 and 174.9 (CONH) ppm.

Oligoamide 4 (ES)

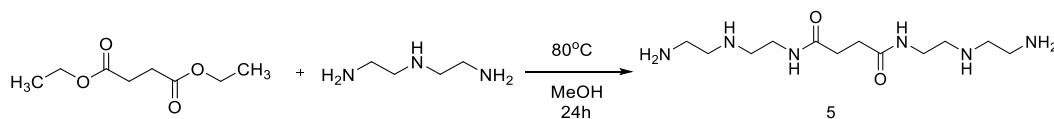


In a Sovirel® tube, diethyl succinate (0.35 g, 2 mmol), ethylenediamine (0.24 g, 4 mmol) and methanol (1.5 ml) were added under nitrogen atmosphere. After stirring at 80 °C for 24 h and with the same work-up as 1, a white solid was obtained. The average molecular weight is 486 g/mol, 94 % yield.

¹H-NMR(D₂O)δ:2.38, 2.51 (m, 4H, COCH₂CH₂CO), 2.71 (m, 2H, CH₂NH₂), 3.14, 3.31 (m, 2H, CH₂NHCO) ppm.

¹³C-NMR(D₂O)δ:31.1 (CH₂CONH), 38.6 and 41.3 (CH₂NHCO), 39.7 (m, 2H, CH₂NH₂), 175.0 (CONH) ppm.

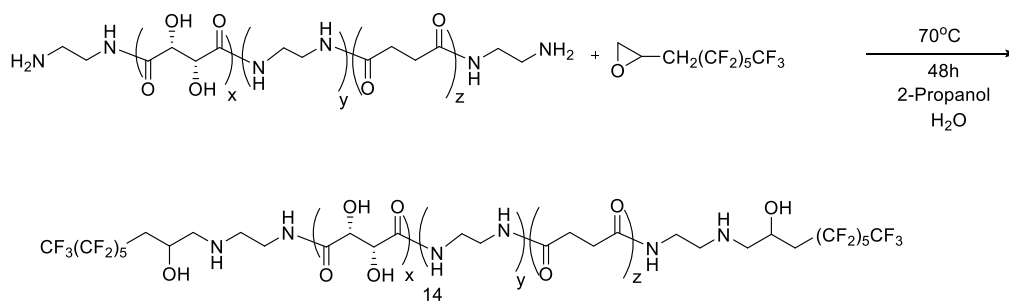
Oligoamide 5 (DS)



In a Sovirel® tube, diethyl succinate (0.35 g, 2 mmol), diethylenetriamine (0.41 g, 4 mmol) and methanol (1.5 ml) were added under nitrogen atmosphere. After stirring at 80 °C for 24 h, the reaction mixture was cooled at r.t. Light yellow sticky oil, 0.7757 g (100 % yield), was obtained after the evaporation of the solvent in the reaction mixture. The average molecular weight is 288.4 g/mol.

¹H-NMR(D₂O)δ:2.53 (m, 4H, COCH₂CH₂CO), 2.72 (m, 4H, CH₂NHCH₂), 2.65 (m, 2H, CH₂NH₂), 3.31 (m, 2H, CH₂NHCO) ppm.

Fluorinated Oligoamide 6 (ESTF)



In a Sovirel® tube, oligoamide 2 (0.12 g, 0.189 mmol), 3-perfluorohexyl-1,2-epoxypropane (0.19 mg, 0.706 mmol), 2-propanol (2 ml) and water (2 ml) were added under nitrogen atmosphere. The reaction mixture was allowed to react at 70 °C for 48 h. Reaction mixture

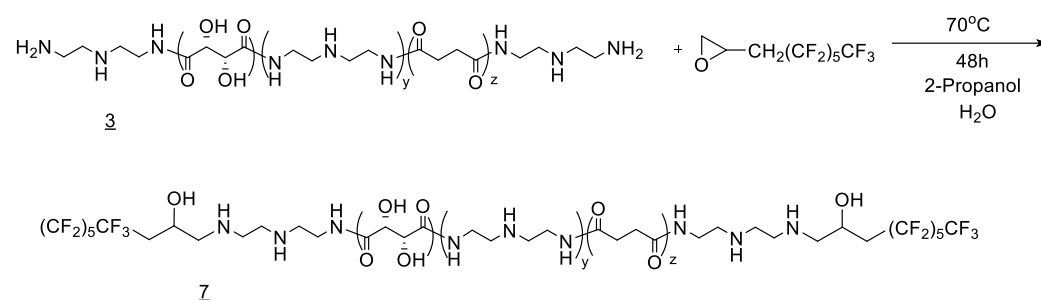
was evaporated and washed by water, then the cold acetone (-20 °C). Final target product is 0.1827 g (yield 69.7 %) as a yellow solid.

$^1\text{H-NMR}(\text{CD}_3\text{OD})\delta$: 2.46 (m, 4H, $\text{COCH}_2\text{CH}_2\text{CO}$), 2.10-2.80 (m, 4H, $\text{CH}_2\text{CH}(\text{OH})\text{CH}_2(\text{CF}_2)_5\text{CF}_3$), 2.8 (m, 2H, $\text{CH}_2\text{NHCH}_2\text{CHOHCH}_2(\text{CF}_2)_5\text{CF}_3$), 3.0-3.5 (m, 2H, CH_2NHCO), 4.10 (m, 1H, $\text{CH}_2\text{CH}(\text{OH})\text{CH}_2(\text{CF}_2)_5\text{CF}_3$), 4.47 (m, 2H, CHOHCHOH) ppm.

$^{13}\text{C-NMR}(\text{CD}_3\text{OD})\delta$: 30.7 (COCH_2), 35.5 ($\text{CH}_2\text{CH}(\text{OH})\text{CH}_2(\text{CF}_2)_5\text{CF}_3$), 38.5 (CH_2NHCO), 54.7 (CH_2NH), 60.9 and 65.4 ($\text{CH}_2\text{CH}(\text{OH})\text{CH}_2(\text{CF}_2)_5\text{CF}_3$), 61.9, 63.5 63.5 ($\text{CH}_2\text{CH}(\text{OH})\text{CH}_2(\text{CF}_2)_5\text{CF}_3$), 72.7 (COCHOHCHOHCO), 108.3, 111.5, 113.5, 115.7, 118.4, 121.0 ($\text{CF}_3(\text{CF}_2)_5$), 173.8 (CONH) ppm

$^{19}\text{F-NMR}(\text{CD}_3\text{OD})\delta$: -82.5 (CF_3), -122.9, -124.0, -124.6 (CF_2), -127.5 (CF_2CF_3) ppm

Fluorinated Oligoamide 7 (DSTF)



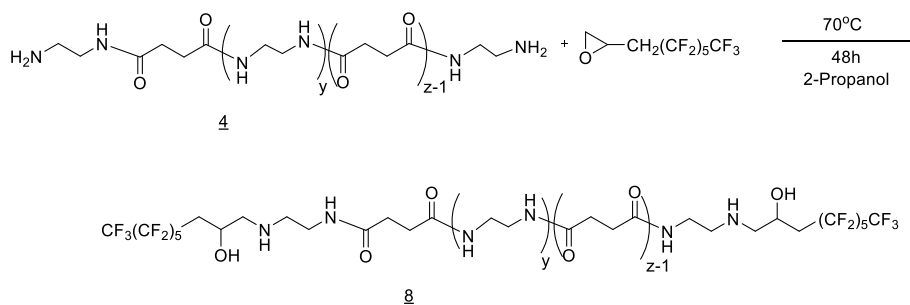
In a Sovirel® tube, oligoamide 3 (0.15 g, 0.105 mmol), 3-perfluorohexyl-1,2-epoxypropane (0.16 g, 0.42 mmol), 2-propanol (2 ml) and water (2 ml) were added under nitrogen atmosphere. The reaction mixture was allowed to react at 70 °C for 48 h. Using the similar work-up process with 6, the perfluorinated derivative was obtained with the mass of 0.3314 g, as an orange solid.

$^1\text{H-NMR}(\text{CD}_3\text{OD})\delta$: 2.49 (m, 4H, $\text{COCH}_2\text{CH}_2\text{CO}$), 2.06-3.10 (m, 4H, $\text{CH}_2\text{CH}(\text{OH})\text{CH}_2(\text{CF}_2)_5\text{CF}_3$), 2.5-3.0 (m, 4H, CH_2NHCH_2 and $\text{NHCH}_2\text{CH}_2\text{NHCH}_2\text{CH}(\text{OH})\text{CH}_2(\text{CF}_2)_5\text{CF}_3$), 3.2-3.6 (m, 2H, CH_2NHCO), 4.11 (m, 1H, $\text{CH}_2\text{CH}(\text{OH})\text{CH}_2(\text{CF}_2)_5\text{CF}_3$), 4.51 (m, 2H, CHOHCHOH) ppm.

$^{13}\text{C-NMR}(\text{CD}_3\text{OD})\delta$: 31.0 (COCH_2), 35.2 (CH_2NHCH_2) and ($\text{CH}_2\text{CH}(\text{OH})\text{CH}_2(\text{CF}_2)_5\text{CF}_3$), 37.0 (CH_2NHCO), 53.5 (NHCH_2), 60.8 and 65.2 ($\text{CH}_2\text{CH}(\text{OH})\text{CH}_2(\text{CF}_2)_5\text{CF}_3$), 62.5 ($\text{CH}_2\text{CH}(\text{OH})\text{CH}_2(\text{CF}_2)_5\text{CF}_3$), 73.0 (COCHOHCHOHCO), 108.1, 110.5, 113.5, 115.7, 118.1, 121.3 ($\text{CF}_3(\text{CF}_2)_5$), 173.2 (CONH) ppm

$^{19}\text{F-NMR}(\text{CD}_3\text{OD})\delta$: -82.5 (CF_3), -122.9, -124.0, -124.7 (CF_2), -127.4 (CF_2CF_3) ppm

Fluorinated Oligoamide 8 (ESF)



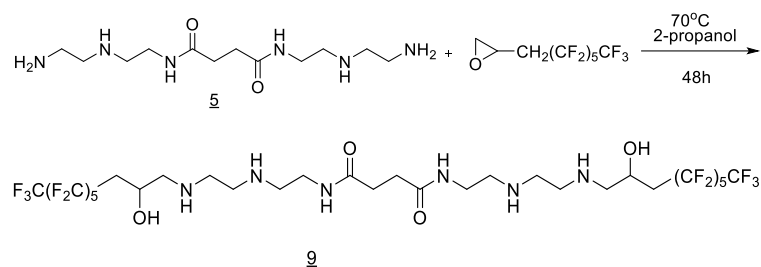
In a Sovirel® tube, oligoamide **4** (0.12 g, 0.247 mmol), 3-perfluorohexyl-1,2-epoxypropane (0.68 g, 1.809 mmol), 2-propanol (2 ml) were added under nitrogen atmosphere. The reaction mixture was allowed to react at 70 °C for 48 h. White dispersion was observed at the end of the reaction. After evaporating the reaction mixture, the residue was washed by water in order to remove the starting oligoamide. Lightly yellow solid (0.438 g) was obtained with 95 % yield.

¹H-NMR(CD₃OD)δ:2.46 (COCH₂CH₂CO), 2.05-2.77 (m,4H,CH₂CH(OH)CH₂(CF₂)₅CF₃), 2.6-2.7 (m,2H,CH₂NHCH₂CH(OH)CH₂(CF₂)₅CF₃), 3.26 (m, 2H, CH₂NHCO), 4.11 (m, 1H, CH₂CH(OH)CH₂(CF₂)₅CF₃) ppm

¹³C-NMR(CD₃OD)δ:30.7 (COCH₂), 34.6 (CH₂CH(OH)CH₂(CF₂)₅CF₃), 38.2 (CH₂NHCO), 52.6 and 54.1 (CH₂NH), 61.1 and 61.2 (CH₂NHCH₂CH(OH)CH₂(CF₂)₅CF₃), 62.3 and 63.2 (CH₂CH(OH)CH₂(CF₂)₅CF₃), 108.4, 110.8, 112.9, 114.7, 118.9, 121.3 (CF₃(CF₂)₅), 173.6 (CONH) ppm

¹⁹F-NMR(CD₃OD)δ:-82.5 (CF₃), -122.9, -124.1, -124.6, -124.9 (CF₂), -127.6 (CF₂CF₃) ppm

Fluorinated Oligoamide **9** (DSF)



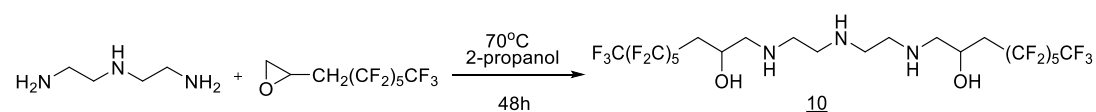
In a Sovirel® tube, oligoamide **5** (0.15 g, 0.52 mmol), 3-perfluorohexyl-1,2-epoxypropane (0.78 g, 2.08 mmol), 2-propanol (2 ml) were added under nitrogen atmosphere. The reaction mixture was allowed to react at 70 °C for 48 h. Yellow solution was observed at the end of the reaction. After evaporating the reaction mixture, the residue was washed by water. Orangeoil (0.913 g, 100 % yield) was obtained.

¹H-NMR(CD₃OD)δ:2.48 (COCH₂CH₂CO), 2.07-2.90 (m,4H,CH₂CH(OH)CH₂(CF₂)₅CF₃) and (m,2H,CH₂NHCH₂CH(OH)CH₂(CF₂)₅CF₃), (CH₂NHCH₂), 3.25 (m, 2H, CH₂NHCO), 4.12 (m, 1H, CH₂CH(OH)CH₂(CF₂)₅CF₃) ppm

¹³C-NMR(CD₃OD)δ:30.7 (COCH₂), 34.9 (CH₂CH(OH)CH₂(CF₂)₅CF₃), 37.0 (CH₂NHCO), 53.5 (CH₂NHCH₂), 61.0, 62.5 (CH₂CH(OH)CH₂(CF₂)₅CF₃), 63.3 (CH₂CH(OH)CH₂(CF₂)₅CF₃), 105.7, 108.8, 110.8, 113.5, 115.9, 118.3, 121.0 (CF₃(CF₂)₅), 173.6 (CONH) ppm

¹⁹F-NMR(CD₃OD)δ:-82.4 (CF₃), -122.9, -124.1, -124.8 (CH₂(CF₂)₄CF₂CF₃) and -127.5 (CH(OH)CH₂(CF₂)₄CF₂CF₃) ppm

Fluorinated amine **10** (DF)



In a Sovirel® tube, diethylenetriamine (0.02 g, 0.194 mmol), 3-perfluorohexyl-1,2-epoxypropane (0.29 g, 0.788 mmol), 2-propanol (4 ml) were added under nitrogen atmosphere. The reaction mixture was allowed to react at 70 °C for 48 h. Yellow solution was observed at the end of the reaction. After evaporating the reaction mixture, the residue was washed by water. Light orange oil (0.268 g, 100 % yield) was obtained.

$^1\text{H-NMR}(\text{CD}_3\text{OD})\delta$: 2.07-2.83 (m, 2H, $\text{CH}_2\text{CH}(\text{OH})\text{CH}_2(\text{CF}_2)_5\text{CF}_3$), (m, 8H, $\text{NHCH}_2\text{CH}_2\text{NHCH}_2\text{CH}_2\text{NH}$) and (m, 2H, $\text{NHCH}_2\text{CH}(\text{OH})$), 4.11 and 4.19 (m, 1H, $\text{CH}_2\text{CH}(\text{OH})\text{CH}_2(\text{CF}_2)_5\text{CF}_3$) ppm

$^{13}\text{C-NMR}(\text{CD}_3\text{OD})\delta$: 35,4 ($\text{CH}_2\text{CH}(\text{OH})\text{CH}_2(\text{CF}_2)_5\text{CF}_3$), 55.0 (CH_2NH), 61.0 ($\text{CH}_2\text{CH}(\text{OH})\text{CH}_2(\text{CF}_2)_5\text{CF}_3$), 63.1 ($\text{CH}_2\text{CH}(\text{OH})\text{CH}_2(\text{CF}_2)_5\text{CF}_3$), 108.8, 111.7, 113.5, 115.9, 118.6, 121.0 ($\text{CF}_3(\text{CF}_2)_5$) ppm

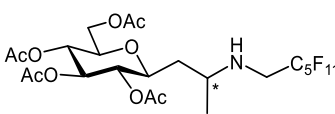
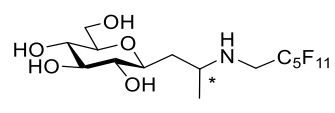
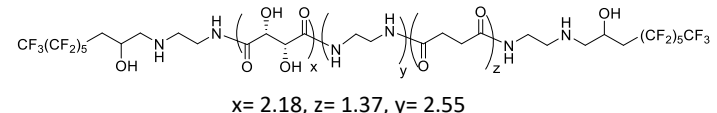
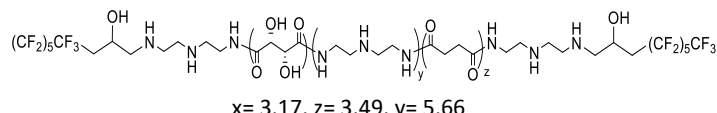
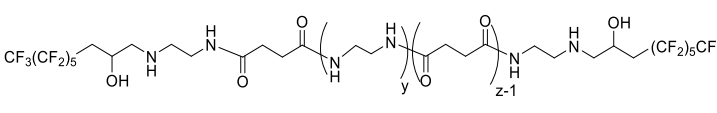
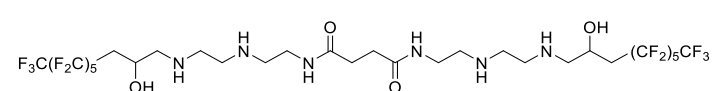
$^{19}\text{F-NMR}(\text{CD}_3\text{OD})\delta$: -82.6 (CF_3), -123.0, -124.1, -124.8 (CF_2), -127.5 (CF_2CF_3) ppm

Chapter 5

Stone protection

5.1 Introduction

After the proposed partially perfluorinated derivatives were successfully obtained, the next step of this research was focused on investigating their performance on stone protection and blanching easel painting restoration. Particularly, this part of the thesis evaluates the performance of the seven compounds that were synthesized during this PhD research project, such as partially perfluorinated C-glycosides, oligoamides and amine as protective agents, by a series of measurements on different stone materials (Lecce stone, sandstone, and marble) with different porosity and chemical composition. In the following table 5-1, the compounds used in the stone protection and their simplified names are presented, in order to clarify the measurements.

Name	Compound	M _n / M _w
C-Glc-OAc		671.16
C-Glc-OH		503.31
ESTF		1386.1
DSTF		2188.8
ESF		1238.22
DSF		1040.2

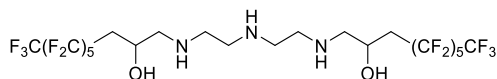


Table 5-1: Products used for stone protection

When faced with decaying stone artefacts, conservation treatment is primarily divided into two categories: preventive conservation (or “Preservation”) and active conservation. Preservation, defined as “the activities that avoid something alteration over time” or “Treatment procedures intended to maintain the integrity of cultural property and to minimize deterioration” by AIC (American Institute for Conservation of historic and artistic works), is generated and developed based on the principal of minimum intervention. [209] Preservation as routine maintenances, such as temperature, relative humidity, pollution, traffic and visitor management for indoor artworks, and groundwater control, shelters, wind fences, reburial for immovable stone heritage, are of vitally importance.

As the other kind of conservation methods, active conservation can mitigate decay processes. The active conservation treatments are deliberate intervention, specifically designed to operate on objects in order to reduce the rate of damage. Surface cleaning, desalination, consolidation and protection are the major active treatments for stone conservation. Among them, protection of stone is one topic that this thesis dealt with. By definition, protection of stone surfaces is an active conservation treatment, which mainly involves historical buildings and other stone artifacts. [210] The understanding of decay mechanisms with scientific methodologies and techniques can help to realize the deliberate intervention. In our case, the analysis of the mechanisms of stone degradation has led to the conclusion about the need to protect the stone especially from liquid water. That means stone protective agents are supposed to protect stone material against the chemical-physical processes of degradation caused by water. In fact, protection treatments for stone can be differentiated by whether they are totally impermeable to water or whether they are only impermeable to liquid water. In the first case the treatment is called waterproofing, and in the second, water-repelling or hydrophobization. The last treatment prevents liquid water from entering the treated surface, but is permeable to water vapor. This thesis addresses water-repelling coating which prevents water from entering the treated surface but permits the migration of water vapor through the stone. Although being very important, high water repellency is not the only requirement for a protective agent on stone surfaces. [211] A series of criteria shall be considered when selecting appropriate products. According to the Committee for Stone Material Normalization recommendations, the essential requirements for a substance to be considered a protective agent for stone artifacts include [212]:

(1) hydrophobicity; (2) good adhesion to stone substrates; (3) good permeability to water vapor; (4) good chemical and physical compatibility with stone substrates; (5) good chemical, physical, thermal, and photo-oxidative stability; (6) good solubility in environmentally benign and healthy solvents; (7) no perceivable color change of substrates; (8) reversibility, *etc.*

Based on those requirements, the behaviour of the synthesized compounds including solubility, and photo-oxidative stability were investigated. Moreover, water repellency, wetting properties, vapour permeability and chromatic effect after the application of the synthetic products on the stone materials, are examined as parameters of their protection

performance.

5.2 Experimental part

5.2.1 Materials

Stone materials

Lecce stone, Pietra Serena (sandstone), and Carrara marble specimens that demonstrated constant water absorptivity were chosen. Samples were previously cut into 5x5x2 cm³ slabs

5.2.2 Ultraviolet (UV) irradiation

The solution or suspension of the 5 fluorinated compounds, **DSF**, **DF**, **ESF**, **ESTF** and **DSTF**, (concentration w/w: 4.8%) was applied uniformly on a transparent glass slice by pipette (table 5-2). Before submitting the compounds to irradiation, the solvents (2-propanol and water) were evaporated at room conditions for 4 days. The aging process was performed under UV (long wave ultraviolet, 365 nm) for 24 days. The light was on for 12 hours on each day, 254 h in total.

#	Glass 1	Glass 2	Glass 3	Glass 4	Glass5
Compound	DSF	DF	ESF	ESTF	DSTF
Solvent	2-propanol	2-propanol	2-propanol	H ₂ O/2-propanol	H ₂ O/2-propanol

Table 5-2: Conditions of UV irradiation tests.

5.2.3 Stone sample selection

Prismatic Lecce stone, Pietra Serena (sandstone), and Carrara marble samples (5x5x2 cm³) were washed with water. After being dried overnight at room temperature, samples were transferred to oven at 60 °C for 24 hours and then cooled to room temperature in desiccator with silica gel for 2 h. The dry weight of samples was registered through a balance with an accuracy of 0.001 g. Stones samples were put on about 1 cm thick stacks of wet filter paper. The marked face of samples was placed on the wet paper, enabling the absorption by capillarity (figure 5-1) [213]. The wet weight of samples was measured every 60 mins. After 4 h, the 1st set of capillarity absorption process was considered completed, and all the samples were dried at room temperature and then moved to oven at 60 °C until the dry weight was reached again. The procedure dry weight-capillary absorption was repeated 3 times to obtain a total of 3 sets of capillary absorption test.

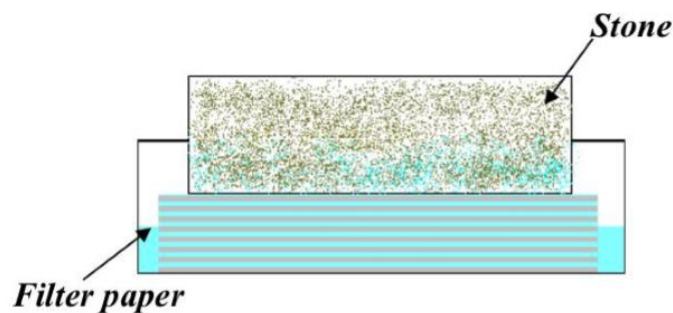


Figure 5-1: Water capillary tests [214]

5.2.4 Coating procedure

To fabricate the coating, the solution or suspension of all the tested compounds was prepared with 2.5 % (w/w) concentration at disposal. (table 5-3)

Compound	Solvent	Physical state (conc. 2.5%w/w)
C-Glc-OAc	Ethyl acetate	Transparent solution
C-Glc-OH	2-propanol	Transparent solution
ESTF	2-propanol/H ₂ O (v/v=1/1)	Yellow solution
ESF	2-propanol	White suspension
DSTF	2-propanol/H ₂ O (v/v=1/1)	Yellow solution
DSF	2-propanol	Yellow solution
DF	2-propanol	Yellow solution

Table 5-3: Solution and suspension prepared for treatments

15 g/m², 10 g/m² and 5 g/m² product amounts were theoretically adopted for Lecce stone, sandstone and marble samples respectively. The solution was deposited on the stone sample by a pipette with the method “wet on wet”, avoiding overloading the stone surface with an excess of solution. The same face used for water capillary absorption test was treated. To start, a suitable amount of solution, *e.g.*, 1 ml was firstly distributed on the targeted face homogeneously and gently by a pipette. Subsequent additions were made once all liquid was absorbed. Application continued in this way till all the fixed amount of solution was used. The solvent was evaporated at laboratory conditions. At the same time, blank stone samples without treatment (three for each lithotype) and used as references were put near treated samples (three stone samples for each compound and for each stone material). After 12 hours, all the samples were transferred to the desiccator, until the dry weight was reached.

5.2.5 Methods for treatment evaluation

5.2.5.1 FT-IR spectroscopy

The infrared spectra of **DSF**, **DF**, **ESF**, **ESTF**, and **DSTF** in Fourier Transform Infrared

Spectroscopy (FT-IR) were recorded before and after the UV irradiation by the FT-IR Spectrometer Perkin Elmer Spectrum 1000 and processed by the software Spectrum v.3.0202.

5.2.5.2 Colorimetric analysis

The colorimetric analysis on the coated glass slices by **DSF**, **DF**, **ESF**, **ESTF** and **DSTF**, was performed before and after UV irradiation. The colorimetric analysis on stone surfaces was performed before and after products application.

For each sample, 5 spots were selected by using a mask prior to analysis. Measurements were conducted by exploiting a portable reflection colorimeter XRite SP60 according to Norm UNI-EN 15886-2010 [215]. The color variations are defined by the colorimetric or chromaticity coordinates CIE L^* a^* b^* , established by Commission Internationale de l'Eclairage (CIE, 1986) [216]. The colorimetric coordinates can be used for expressing the colorimetric measurements in the open and isotropic color space. It allows to determine the hue, lightness and saturation of a color. It is therefore well suited to the characterization of the colors of opaque objects like stones and easel paintings. Three spacial coordinates L^* , a^* and b^* express the colors in numerical terms. L^* indicates the brightness and has values between 0 (black) to 100 (white); a^* represents tint and varies from -60 (green) to +60 (red); b^* signifies the saturation and varies from -60 (blue) to +60 (yellow). (figure 5-2)

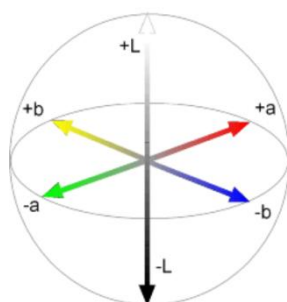


Figure 5-2: CIE Lab color space [71]

The method was used to evaluate the color changes after UV ageing on the coated glass slides and after the compound application on the stone samples. The parameters color change was calculated as $\Delta X^* = X^*_{\text{after}} - X^*_{\text{before}}$, where ΔX^* after is the L^* , a^* , b^* and E^* value after UV irradiation or treatments, and X^*_{before} is the same parameter before UV irradiation or treatment.

The color change ΔE^* was evaluated, according to the formula:

$$\Delta E^* = \sqrt{\Delta L^{*2} + \Delta a^{*2} + \Delta b^{*2}}$$

where ΔL^* is the lightness variation, Δa^* and Δb^* are the chromaticity indices. When ΔE^* is equal to or less than 3, the chromatic change is not perceptible to the human eye. [217]

5.2.5.3 Protection efficacy

The water capillary absorption of stone samples, before and after protective treatment, were performed under the guidance of Norm UNI-EN 15801-2010 [213]. The two partially perfluorinated C-glycosides were applied on the Lecce stone samples, while other 5 partially perfluorinated oligoamides or amine were applied on three stones (Lecce, sandstone and marble). Every compound was applied on three samples of the same kind of stone to increase the accuracy of the test. Also 3 references without any treatment were set for each stone material. This capillary absorption procedure was repeated at regular intervals of time, using the same absorption times adopted for the untreated specimens.

The results were processed and reported as Protection Efficacy (PE%) as described by Camaiti M *et al.* [43]

PE% was calculated as:

$$PE\% = \frac{A_0 - A_1}{A_0} \times 100,$$

where A_0 and A_1 are the amount of water absorbed before and after treatment.

5.2.5.4 Contact angle (CA)

CA of neat and coated Lecce stone, sandstone and Carrara marble samples was measured using a Ramè-Hart Model 190 CA Goniometer. Static CA of 5 μ l sessile droplets of liquid on stone surfaces was measured. Deionized water was employed as liquid for CA measurements.

For each treatment three specimens were tested, and eight measurements were done on each specimen. The contact angle is the average value and it was not corrected on the basis of the stone surface roughness. All measurements were done after the capillary absorption test.

5.2.5.5 Vapor diffusivity test

The residual vapor permeability of polymeric film on treated stone samples was evaluated by the "Cup" method according to Norm UNI-EN 15803-2010 [218]. The "Cup" was placed in a closed PVC container at controlled temperature (30 °C) and controlled humidity (5 % by silica gel). It was weighed at every 24 h to record the change in weight as the function of time (typically 9 days). Three samples for each treatment and each lithotype were used for vapor permeability test.

The results are expressed as Residual Permeability percentage (RP %). RP % is calculated according to the formula:

$$RP\% = \frac{P_1}{P_0} \times 100$$

where P_0 is the average permeability of untreated specimens, while P_1 is the permeability of the treated ones. The permeability P_0 and P_1 are calculated by the ratio between the weight change of "Cup" between two successive measurements (24 h) and the surface of the

sample. For the calculation of P_0 , three untreated specimens were considered and the value was calculated from the following equation:

$$P_0 = \frac{\sum_{i=1,2,3}^i \frac{\Delta m_i}{s}}{3}$$

where Δm_i is the weight change of “Cup” with the untreated specimens in 24 h; “s” is the free surface of the specimen through which vapor passes from the inside to outside. P_1 was calculated for each sample through the formula:

$$P_1 = \frac{\Delta m_x}{s}$$

where Δm_x is the weight change of “Cup” with the treated specimen x in 24 h.

5.3 Results and discussion

5.3.1 Solubility of the partially perfluorinated derivatives

The first characteristic of the synthesized products to be evaluated is their solubility. From the practical point of view, a protective agent is supposed to be soluble in environment-friendly solvents. Besides, a suitable solubility can help to control the amount of product during coating process, and eventually help to avoid oversaturated and non-uniform distribution of the product on the stone surfaces.

Firstly, the solubility of the 2 partially perfluorinated C-glycosides was tested in 2-propanol and ethyl acetate with different concentration (w/w) at different temperature. The results are shown in the following table 5-4. **C-Glc-OH** shows good solubility in 2-propanol with 2.5 % concentration at r.t, while **C-Glc-OAc** shows good solubility in ethyl acetate with 2.5 % concentration at r.t.

Name	Solvent	Conc. W/W (%);T	Solubility
C-Glc-OH	2-propanol	5; 50 °C	Partially soluble
		2.5; r.t	Soluble
C-Glc-OAc	Ethyl acetate	2.5; r.t	Soluble
	2-propanol	2.5; 50 °C	Not soluble

Table 5-4: Solubility of partially perfluorinated C-glycosides

For the partially perfluorinated oligoamides and amine, their solubility was firstly investigated in H₂O, 2-propanol and ethanol. However, for **ESTF** and **DSTF** which contain OH groups from tartrate and alkyl moieties from succinate, they showed poor solubility in H₂O or alcoholic solvents. Considering the mixed solvent system has been widely used for many years, especially in the industry of coating [219], hydro-alcoholic solvents have been tested for **ESTF** and **DSTF**. The mixture of H₂O and alcohol is in the volume ratio 1:1. The solubility results are shown in the table 5-5 below. **ESTF** and **DSTF** are more soluble in the hydro-alcoholic solvent, which may be due to the succinate moiety, which improve the solubility of the products in alcohol by the alkyl chain, while tartrate units have higher

affinity with H₂O. Compared with **ESF**, the evident improved solubility of **DSF** and **DF** in alcohol is probably due to the more intermolecular hydrogen bonds created between the diethylenetriamine and the alcohol.

Name	Solubility					Conc. W/W (%); T
	H ₂ O	2-propanol	ethanol	H ₂ O /2-propanol	H ₂ O /ethanol	
ESTF	Partially soluble	unsoluble	unsoluble	soluble	soluble	1; 50 °C
DSTF	suspension	Partially soluble	Partially soluble	soluble	soluble	2; r.t
ESF	unsoluble	suspension	suspension	unsoluble	unsoluble	1; 50 °C
DSF	Partially soluble	Soluble	Soluble	Soluble	Partially Soluble	1; r.t
DF	Partially soluble	Soluble	Soluble	Partially soluble	Partially soluble	1; r.t

Table 5-5: Solubility of 5 partially perfluoro compounds

Therefore, the 5 synthetic compounds such as the partially perfluorinated oligoamides and amine that were prepared during the PhD research project, are soluble in alcohols and/or hydro-alcoholic solvents.

In summary, all the synthetic partially perfluorinated products prepared, are soluble in environmentally benign and safe solvents.

5.3.2 Resistance to photodegradation

The long-term efficiency of the protective treatments is mainly influenced by the direct action of sunlight in promoting oxidation reactions, whose effects may be exacerbated by temperature, moisture, and especially by the presence of atmospheric pollutants. [220] The complexity of natural ageing of materials may be reproduced in the laboratory only by considering a simplified approach by simulation with convenient short-term experiments. Lifetime prediction and mechanistic studies of the outdoor degradation processes are in general carried out by means of accelerated ageing experiments involving temperature and/or light treatments. The light sources which can be efficiently employed for such purposes must have high power output and the closest resemblance to the solar light spectrum, particularly in the UV range. Lower-wavelength radiations must be removed, as it has been shown that they can cause the occurrence of reactions which do not take place outdoors. [221][222]

Most polymer products break down slowly through a combination of environmental processes, but light, especially UV light, can be a significant source of photodegradation. Photodegradation is the degradation of a photodegradable molecule caused by the absorption of photons, particularly those wavelengths found in sunlight, such as infrared

radiation, visible light, and ultraviolet light. It alters paintings and other artifacts. Photodegradation may occur in the absence of oxygen (chain breaking or cross-linking) and the presence of oxygen (photooxidative) degradation. Photooxidative degradation can result in breaking of the polymer chains, produces radicals and reduces or increases the molecular weight, causing deterioration of mechanical properties and leading to useless materials, after an unpredictable time. [223]

In our case, the investigation of the stability of the partially perfluorinated oligoamides and amine after laboratory aging, especially using light source, can give the clue about the long-term efficiency of the protective treatments. Therefore, the stability of the partially perfluorinated oligoamides and amine was estimated by means of accelerated aging tests exploiting UV radiations (wavelength of 365 nm). And their behavior was followed *via* ^1H NMR, FT-IR spectroscopy and colorimetric measurements. The weight change was also recorded, in order to track the change of the compounds after the UV exposure test.

5.3.2.1 Weight variation

Weight variation was evaluated through the weight measurements of the glass slide with the 5 partially perfluorinated compounds, during the irradiation (table 5-6). Significant changes in weight (between 1 and 2 mg in the interval 32 h-254 h of irradiation) were observed in all compounds during the aging process. A decrease of weight in all compounds can be observed after 32 h of aging. However, compounds **ESTF**, **DSTF**, **DSF** and **DF** showed an increase of weight (around 1-2 mg) from 72 h aging to 204 h aging. From 204 h to 254 h, the weight of **DSF** and **DF** almost stayed no change, while **ESTF** and **DSTF** showed the decrease of weight. For the compound **ESF**, its weight has decreased since the beginning of the aging process (2.1 mg in total).

5.3.2.2 Color variation

Firstly, a camera was used to record, through a photo, the change in the appearance of the sample before and after UV aging (figure 5-3, background is white). The samples of **DSF** and **DF** were slightly yellow before aging, while the other samples were transparent and colorless. After aging, the yellowing of compounds **DSF**, **DF**, **DSTF** was observed, while compound **ESF** turned white and the compound **ESTF** did not show an obvious change. Subsequently, colorimetric measurements were used to give more specific investigation of the color variations.

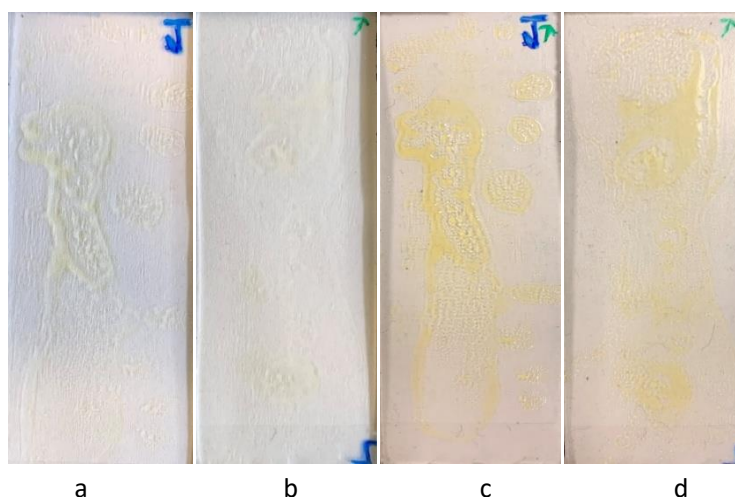


Figure 5-3: a) **DSF** before aging; b) **DF** before aging; c) **DSF** after aging; d) **DF** after aging

The colorimetric measurements were made before and after irradiation to evaluate the color variations due to the interaction between the partially perfluorinated compounds and the UV radiation. The results of the colorimetric measurements on UV irradiated glass slices are shown in the table 5-6 below.

Compound	Glass #	Δm (g)				ΔE^*			
		$\Delta t=32h$	$\Delta t=72h$	$\Delta t=204h$	$\Delta t=254h$	$\Delta t=32h$	$\Delta t=72h$	$\Delta t=204h$	$\Delta t=254h$
DSF	1	-0.0008	-0.0001	0.0005	0.0005	5.59	8.68	10.20	9.96
DF	2	-0.0008	-0.0003	0.0002	0.0003	2.22	5.87	9.44	9.14
ESF	3	-0.0011	-0.0013	-0.0019	-0.0021	2.77	3.33	0.54	0.97
ESTF	4	-0.0006	-0.0003	0.0003	0	0.93	1.59	1.49	1.07
DSTF	5	-0.0015	-0.0003	0.0005	0	3.15	10.72	15.60	14.16

Table 5-6: Color and weight changes during UV aging

ΔE^* of **DSF**, **DF**, **DSTF**, which contain diethylenetriamine units, shows a big difference after 254 h UV aging. While, ΔE^* of both **ESF** and **ESTF**, which contain ethylenediamine units, is around 1. In order to give the specific information about chromatic changes, data of ΔL^* , Δa^* and Δb^* is shown in table 5-7. Δb^* of **DSF**, **DF**, **DSTF** has a significant increase, which means the samples became yellowing under UV radiations after 254 hours.

Compound	Glass #	254 h UV aging			
		ΔL^*	Δa^*	Δb^*	ΔE^*
DSF	1	-1.80	-1.95	9.60	9.96
DF	2	-1.27	-2.27	8.76	9.14
ESF	3	0.06	-0.20	-0.95	0.97
ESTF	4	-0.62	-0.23	0.85	1.07
DSTF	5	-2.35	-2.93	13.65	14.16

Table 5-7: ΔL^* , Δa^* and Δb^* of compounds after UV aging

5.3.2.3 FT-IR and ^1H NMR spectroscopy

^1H NMR and Fourier Transform Infrared (FT-IR) spectroscopy were used to investigate the possible chemical change behind the yellowing.

- **DSF**

In the ^1H NMR after UV irradiation (figure 5-4), for **DSF** (Glass 1, G-1), new signals near hydroxyl groups (4.4 ppm) and near CONH (3.0, 3.4 ppm) appear. Also the signals of CHNH area has slightly modified in relative strength of signals. The overlap of the signals does not allow to evaluate exactly the reciprocal relationships between the signals or to identify new ones. The observed variations may be in agreement with a partial oxidation of triamine units. The FTIR spectrum of **DSF** after UV irradiation (figure 5-5) shows:

- a slight decrease of the signal intensity at 3300 cm^{-1} and/or an increase at 3344 cm^{-1} (region of OH/NH stretching);
- a broadening of the peak at 1654 cm^{-1} (C=O stretching of Amide I) and
- a very slight decrease in the intensity of the signals assigned to $-\text{CH}_2-$ symmetric stretching (2840 cm^{-1}) and wagging/twisting deformation (1319 cm^{-1}).

These spectral modifications are in agreement with the oxidation of the diethylenetriamine units.

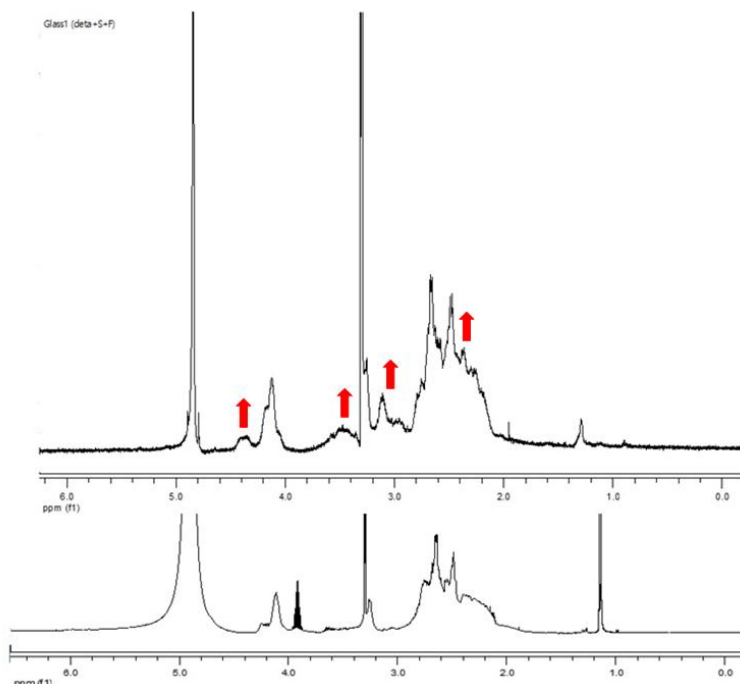


Figure 5-4: ^1H NMR spectra of **DSF** before and after (with red arrows) aging.

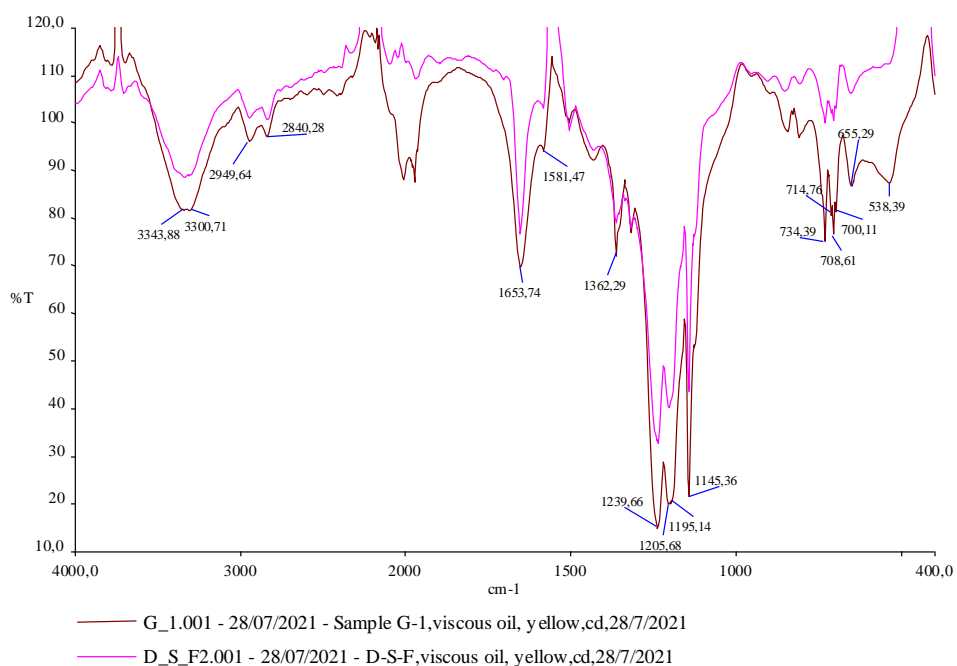


Figure 5-5: FT-IR spectrums of DSF before (pink) and after (black) UV aging

- **DF**

The same behaviour was observed for DF (Glass 2, G-2) in the FT-IR spectrum (figure 5-6), which sustains the hypothesis formulated of a partial oxidation on the triamine units. Also for this compound in the ¹H NMR spectrum (figure 5-7), the variation of the shape and relative intensity of the signals of CHNH in the 2-3 ppm zone can be observed. In particular, a new signal at 3.0 ppm appeared and the shape of original CHNH area also changed.

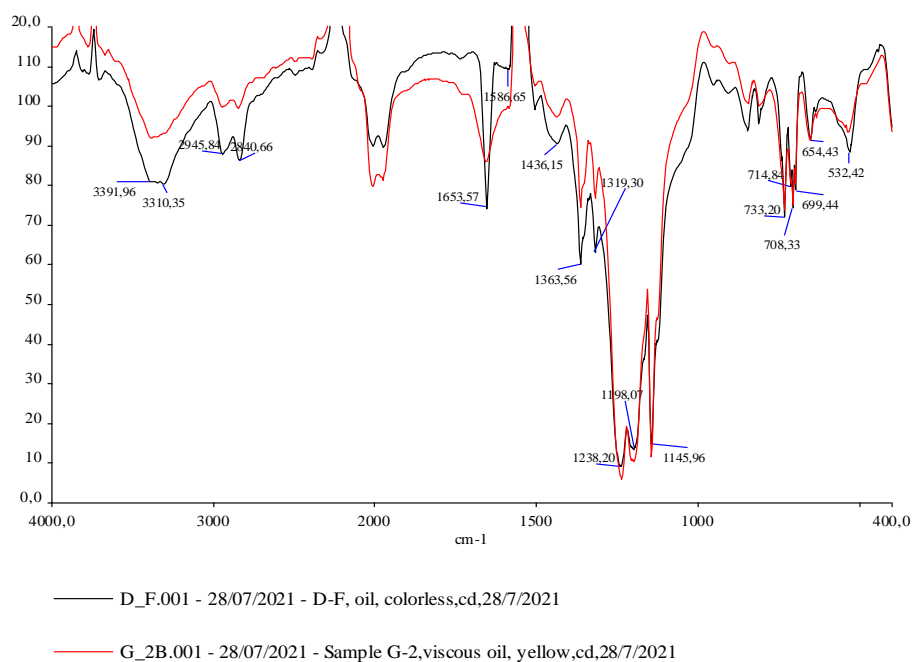


Figure 5-6: FT-IR spectrums of DF before (black) and after (red) UV aging

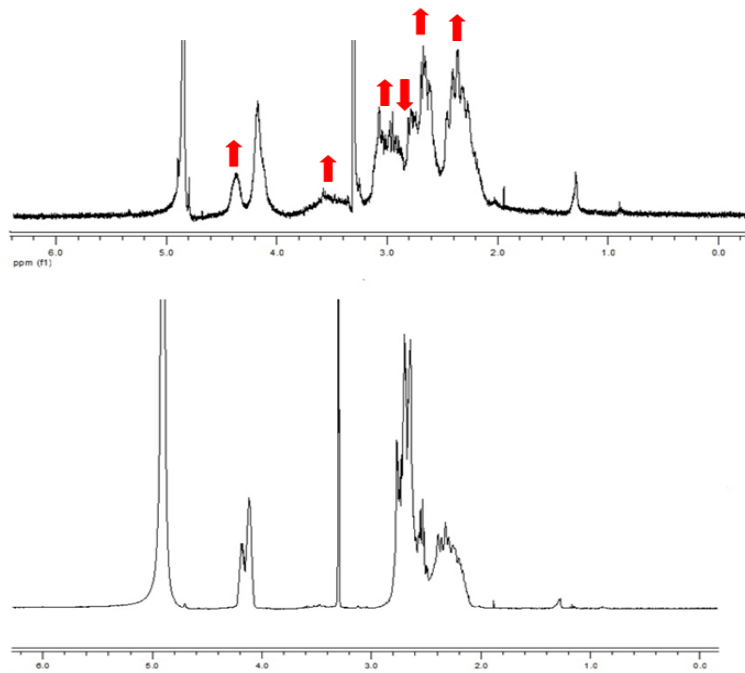


Figure 5-7: ¹H NMR spectrums of DF before and after (with red arrows) aging

- **DSTF**

Similar change attributable to the oxidation of triamine units, can be also observed in the ¹H spectrums of **DSTF** (Glass 5, G-5) (figure 5-8). Furthermore, comparing the ¹H NMR spectra of **DSTF** before and after aging, new signals near hydroxyl groups (4.4 ppm), and near CONH (3.6 ppm) appears. The superposition of the signals does not allow to evaluate these transformations in detail.

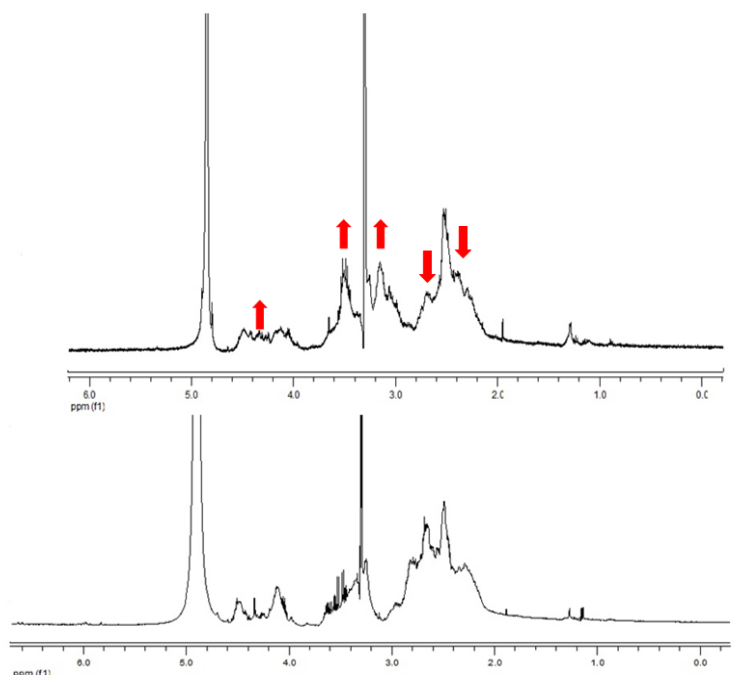


Figure 5-8: ¹H NMR spectrums of DSTF before and after (with red arrows) aging

For FT-IR spectrum, **DSTF** (figure 5-9), which contains both diethylenetriamine and tartaric units, shows more evident modifications compared to **DSF**, as the tartaric units has a synergic effect on the oxidation of the diethylenetriamine units. The decrease of the peak intensity at 2846 and 1320 cm^{-1} is also associated to the decrease of the peaks at 2949 ($-\text{CH}_2-$ asymmetric stretching), 1362 ($-\text{CH}_2-$ bending), 735 and 709 cm^{-1} ($-\text{CH}_2-$ rocking deformation), and to the increase of the intensity of the peak intensity at 1648 cm^{-1} . This signal at 1648 cm^{-1} , as in the case of DSF, shows also a slight broadening due to the formation of carbonyl groups (e.g. acid or ketone groups). In the ^1H NMR spectrum (figure 5-8), there are variations in the signals and their intensities in the area between 2 and 3 ppm. A new signal appears at 3.5 ppm while the signal is reduced in intensity to 4.11 ppm. These variations can be in agreement with oxidations of the amino groups but also with a reduction of solubility for hydrogen bonds between the OH and NH groups present in the compound.

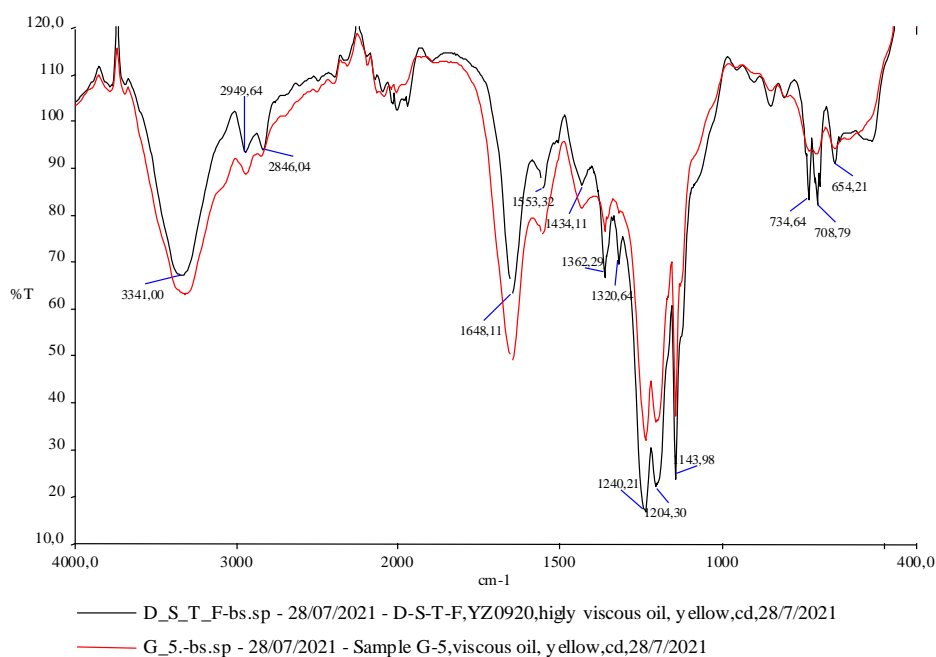


Figure 5-9: FT-IR spectrums of **DSTF** before (black) and after (red) UV aging

- **ESF**

Contrary to what was observed for compounds with diethylenetriamine units, the FT-IR spectrum of **ESF** after irradiation (Glass 3, G-3) (figure 5-10), does not show similar changes, as well no other modifications in the spectrum. Also in the ^1H NMR spectrum no changes were observed (figure 5-11).

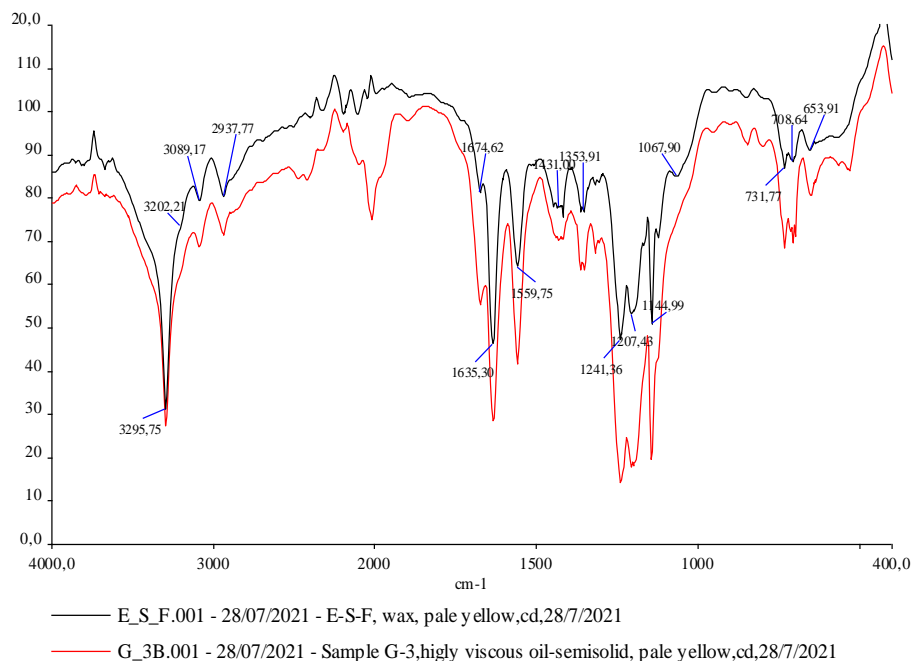


Figure 5-10: FT-IR spectrums of *ESF* before (black) and after (red) UV aging

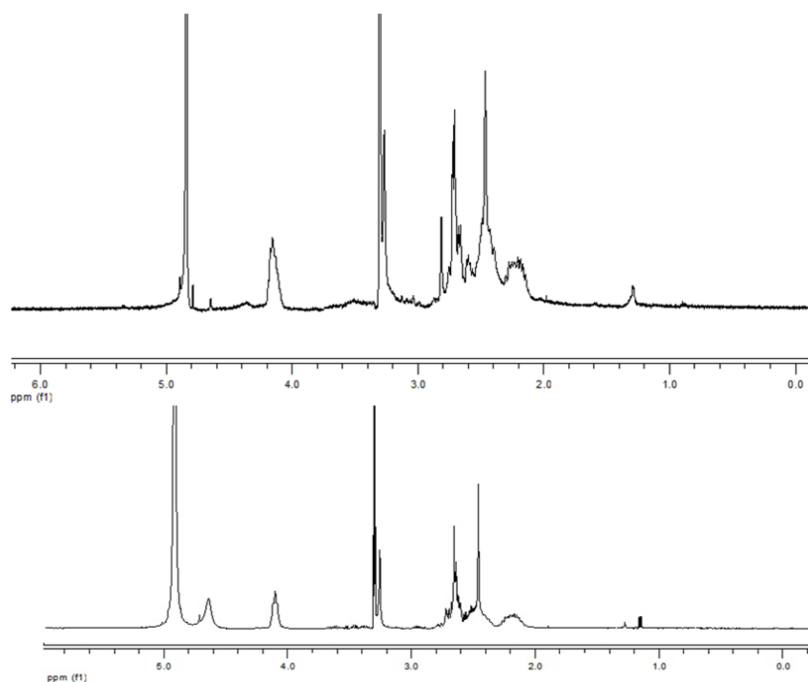


Figure 5-11: ^1H NMR spectrums of *ESF* before (down) and after (up) aging

- **ESTF**

Also in the presence of tartaric units, when the diethylenetriamine is substituted by ethylenediamine (**ESTF**, Glass 4, G-4) (figure 5-12), the peaks associated to $-\text{CH}_2-$ are unchanged, while the signals at about 3300 cm^{-1} ($-\text{OH}$ and $-\text{NH}$ stretching) and 1550 cm^{-1} ($-\text{NH}$ bending, Amide II) are slightly shifted in respect to the corresponding not irradiated compound. This modification may be justified with hydrogen bonding involving mainly $-\text{OH}$

and -NH groups. ESTF did not show a significant yellowing, however, in the ^1H NMR spectrum, the reduction of signal intensity to 4.11 ppm and of signals between 2.6 and 3.0 ppm was observed (figure 5-13). These variations can be in agreement with a reduction in solubility for hydrogen bonds between the OH and NH groups present in the compound.

In summary, for the compounds (**DSF**, **DF** and **DSTF**) containing diethylenetriamine units, the changes can be observed in the similar areas of the ^1H NMR and FT-IR spectras, while a reduction of solubility is observed above all in the presence of tartaric units.

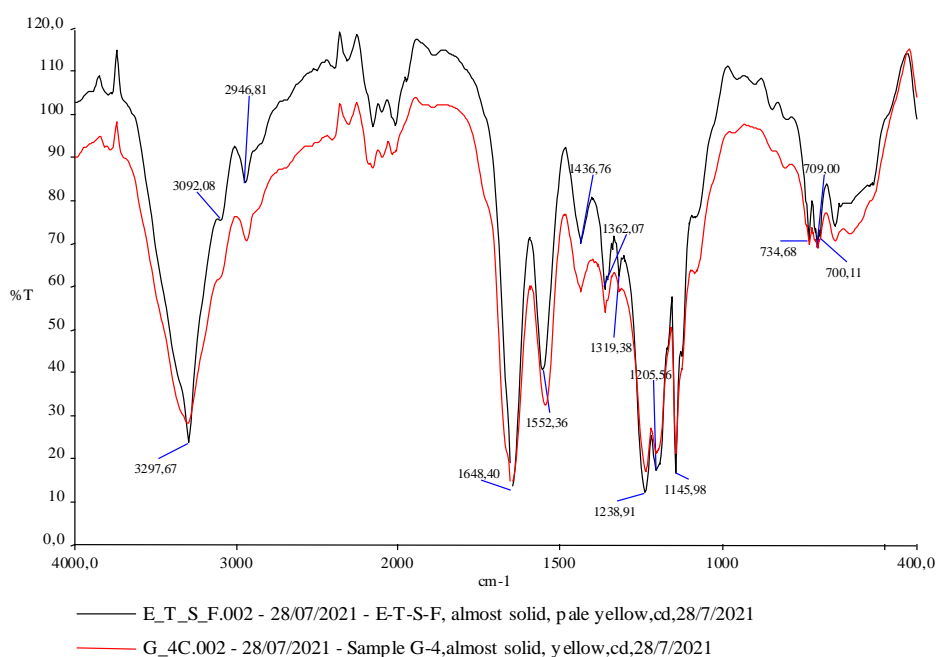


Figure 5-12: FT-IR spectrums of **ESTF** before (black) and after (red) UV aging

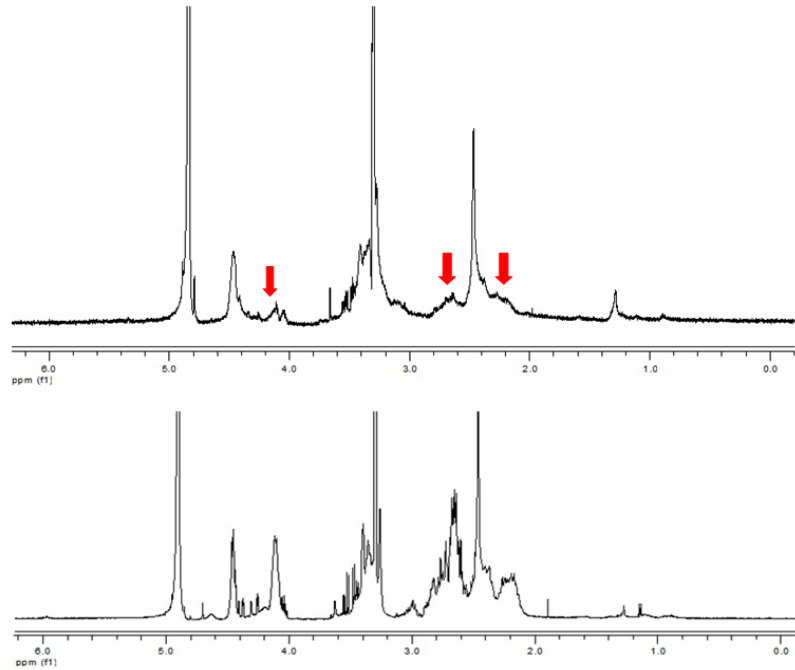


Figure 5-13: ^1H NMR spectrums of *ESTF* before and after (with red arrows) aging

5.3.3 Stone sample selection

Three types of natural stones with distinct chemical and physical properties *i.e.* Lecce stone, sandstone (Pietra Serena) and Carrara marble were used as coating substrates.

Lecce stone is a kind of beige, fine bio-calcarene with high porosity (water accessible porosity ranging from 35 to 47 %, pore size ranging from 0.01 to 2 μm). Owing to its high workability, golden and warm color, Lecce stone was broadly employed for Baroque architectures during the 17th and 18th century in southern Italy. [12]

Pietra Serena, a light grey sandstone, is mainly constituted by sandy fraction, clay matrix and a small amount of calcite. Owing to its workability and relative compactness, Pietra Serena was frequently used during the Renaissance period for ornamental purposes (*e.g.* as capitals, columns) and also as road paving, household furnishing nowadays in central Italy. Varied from quarry to quarry, Pietra Serena has a water accessible porosity around 3–6 %, with pores size ranging from 0.004 to 0.3 μm . [224]

Carrara marble, quarried from north Tuscany and used since ancient Roman times, is very compact (water accessible porosity about 2 %, pore size < 1 μm). Predominantly constituted of calcite, there is also a small amount of accessory minerals that affect color (grey to blue color) and veining. Lecce stone, sandstone and Carrara marble samples were all cut as slabs in dimension 5x5x2 cm^3 to use for the coating process.

Prior to product application and subsequent tests, Lecce stone, sandstone and Carrara marble samples were selected based on three sequences of water capillary absorption tests conducted following the standard method. [213] In our case, water capillary absorption is depicted by the uniaxial penetration of water into a 5x5 cm^2 surface for 2 cm-distance, indicated as numerical value of wet weight changes.

The collected data were processed after all the absorption tests. Average amount of water

absorption every 60 min until 4 h was calculated for each sample, as well as the value “(max-min)/max*100” (referred to water absorption amount) of each sample was determined. When the “(max-min)/max*100” value < 1, the sample is considered suitable for the hydrophobicity test evaluation and other further experiments (*i.e.* the sample shows reproducible absorption properties). In the end, 27 Lecce stone samples were selected. The water absorbed in 4 h for those samples tested, along with the average values, standard deviations and (Max-Min)/Max % values are reported in table 5-8. There were also 18 sandstone samples and 18 Carrara marble samples selected for the product application and subsequent tests, based on three sequences of water absorption tests previously conducted following the standard method [213].

Sample#	Water absorption after 4 h (g)			Average (g)	SD	(Max-Min)/Max*100
	1 st test	2 nd test	3 rd test			
YZ003	13.381	13.365	13.382	13.376	0.010	0.127
YZ006	13.439	13.357	13.431	13.409	0.045	0.610
YZ007	13.136	13.125	13.136	13.132	0.006	0.084
YZ008	13.33	13.33	13.344	13.335	0.008	0.105
YZ009	13.117	13.131	13.136	13.128	0.010	0.145
YZ010	12.779	12.799	12.816	12.798	0.019	0.289
YZ011	13.239	13.179	13.234	13.217	0.033	0.453
YZ023	12.904	12.848	12.879	12.877	0.028	0.434
YZ024	13.397	13.314	13.349	13.353	0.042	0.620
YZ029	13.28	13.325	13.292	13.299	0.023	0.338
YZ030	12.959	12.993	12.968	12.973	0.018	0.262
YZ033	13.19	13.216	13.177	13.194	0.020	0.295
YZ034	13.222	13.247	13.211	13.227	0.018	0.272
YZ036	13.149	13.163	13.121	13.144	0.021	0.319
YZ038	12.976	12.989	12.965	12.977	0.012	0.185
YZ039	13.519	13.544	13.533	13.532	0.013	0.185
YZ040	13.056	13.095	13.069	13.073	0.020	0.298
YZ042	13.267	13.296	13.267	13.277	0.017	0.218
YZ043	13.112	13.138	13.134	13.128	0.014	0.198
YZ044	13.353	13.387	13.373	13.371	0.017	0.254
YZ046	13.051	13.116	13.12	13.096	0.039	0.526
YZ047	12.926	13	12.991	12.972	0.040	0.569
YZ048	13.029	13.091	13.083	13.068	0.034	0.474
YZ049	12.873	12.851	12.881	12.868	0.016	0.233
YZ050	13.347	13.225	13.345	13.306	0.070	0.914
YZ051	12.966	12.9	12.965	12.944	0.038	0.509
YZ052	13.181	13.115	13.17	13.155	0.035	0.501

Table 5-8: Water capillary absorption of Lecce stone samples (after 4 h); SD= standard deviation

Moreover, in order to evaluate the maximum water absorbed by the untreated samples (water saturation under capillary absorption), kinetics of water uptake until 7 days for the 25 selected Lecce stone samples have been reported in figure 5-14. The wet weight of each sample was recorded every hour up to 8 h and then every 24 h for a total of 7 days of capillary absorption. After 4 days, the wet weight slightly increased and saturation was considered almost reached after 168 hours (7 days).

In summary, 25 Lecce stone samples, 18 sandstone samples and 18 Carrara marble with “constant” water absorptivity were selected for the coating procedure and subsequent tests.

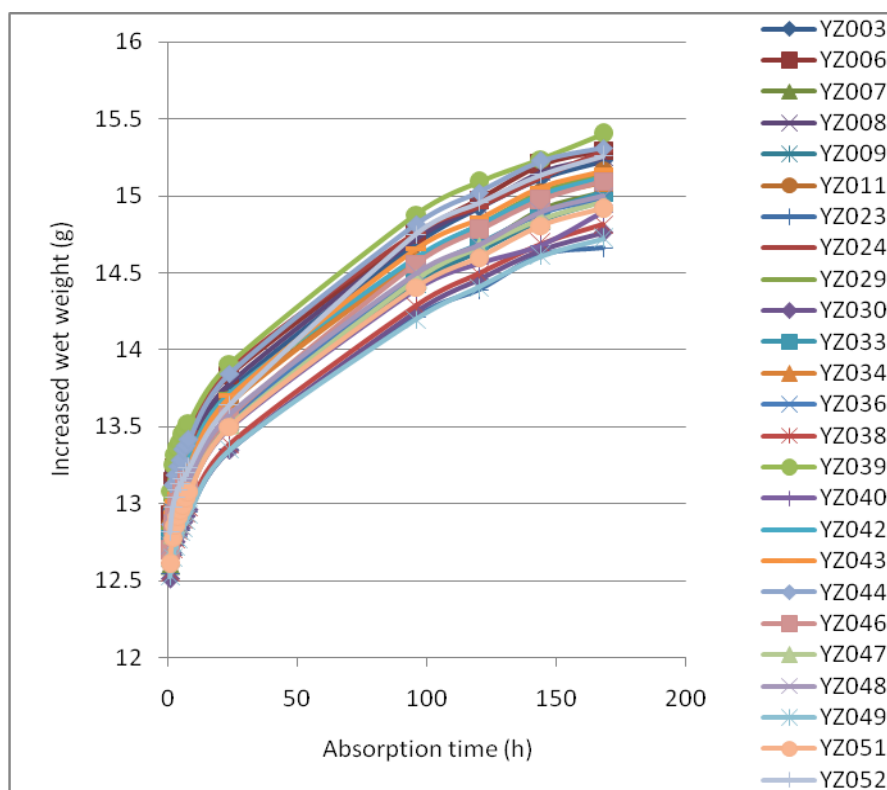


Figure 5-14: Kinetics of water capillary absorption on untreated Lecce stone samples

5.3.4 Coating procedure

To test their performance as water repellent coating, the seven partially perfluorinated derivatives that were synthesized in this PhD research project, were applied on the selected stone samples with solution or suspension (2.5 % w/w) forms.

The quantities of all the products to be applied were determined based on the concept obtaining good hydrophobic effect without over saturation. According to the generally referred amount of polymer application, determined mainly by porosity and water absorption properties of stones, 15 g/m², 10 g/m² and 5 g/m² product amounts were theoretically adopted for Lecce stone, sandstone and marble samples respectively. The details of the coating on Lecce stone are shown in table 5-9, as well as on the sandstone and marble in table 5-10. The actual and dry mass (before treatment) of those samples was used for calculating the mass of active product actually applied. The mass of active product was corrected on the basis of the actual weight of the untreated samples in respect to the

previous dry weight. For several samples, the mass is less than 0 due to the correction. Most of the “less than 0” mass was observed on sandstone samples, probably due to the difficulty of having a uniform drying process for all samples.

Lecce stone					
Theoretical Quantity of Applied Compound (TQAM): 0.00375 g, 15 g/m ²					
Treatment	Sample	Quantity applied g (g/m ²)	Treatment	Sample	Quantity applied g (g/m ²)
C-Glc-OAc	YZ003	0.036 (14.4)	ESF	YZ043	0.042 (16.8)
	YZ006	0.034 (13.6)		YZ044	0.054 (21.6)
	YZ007	0.029 (11.6)		YZ046	0.044 (17.6)
	Average	0.033 (13.2)		Average	0.047 (18.8)
C-Glc-OH	YZ023	0.025 (10.0)	ESTF	YZ050	-0.008 (-3.2)
	YZ024	0.026 (10.4)		YZ051	0.032 (12.8)
	YZ029	0.027 (10.8)		YZ052	0.046 (18.4)
	Average	0.026 (10.4)		Average	0.039 (15.6)
DSF	YZ038	0.045 (18)	DSTF	YZ047	0.033 (13.2)
	YZ040	0.053 (21.2)		YZ048	0.030 (12)
	YZ042	0.042 (16.8)		YZ049	0.025 (10)
	Average	0.047 (18.7)		Average	0.029 (11.6)
DF	YZ010	0.003 (1.2)	NT	YZ030	0
	YZ036 ^a	0.056 (22.4)		YZ033	0
	YZ039 ^b	0.052 (20.8)		YZ034	0
	Average ^{ab}	0.054 (21.6)			

Table 5-9: Coating on Lecce stone samples

Treatment	Sand stone TQAM: 0.025 g, 10 g/m ²		Marble TQAM: 0.0125 g, 5 g/m ²	
	Sample	Quantity applied g (g/m ²)	Sample	Quantity applied g (g/m ²)
DSF	AP 025	0.020 (8)	AP071	0.014 (5.6)
	AP 038	0.036 (14.4)	AP096	0.012 (4.8)
	AP 096	0.040 (16)	AP098	0.015 (6)
	Average	0.032 (12.8)	Average	0.0137 (5.47)
DF	AP 027	0.027 (10.8)	AP073	0.012 (4.8)
	AP 053	0.015 (6)	AP090	0.001 (0.4)
	AP 062	0.014 (5.6)	AP093	0.013 (5.2)
	Average	0.0187 (7.47)	Average	0.0087 (3.47)
ESF	AP 030	0.022 (8.8)	AP026	0.004 (1.6)
	AP 046	0.042 (16.8)	AP077	0.012 (4.8)
	AP 087	-0.013 (-5.2)	AP084	0.008 (3.2)
	Average	0.032 (12.8)	Average	0.008 (3.2)
ESTF	AP 073	0.003 (1.2)	AP028	-0.009 (-3.6)
	AP 083	-0.012 (-4.8)	AP072	0.011 (4.4)
	AP 094	-0.005 (-2)	AP088	0.014 (5.6)
	Average	0.003 (1.2)	Average	0.0125 (5)
DSTF	AP 095	0.012 (4.8)	AP038	0.010 (4)
	AP 097	0.022 (8.8)	AP061	0.007 (2.8)
	AP 098	0.007 (2.8)	AP083	-0.001 (-0.4)

	Average	0.0137 (5.47)	Average	0.0085 (3.4)
NT	AP 045	0	AP016	0
	AP 064		AP076	
	AP 070		AP095	

Table 5-10: Coating on sandstone and marble samples

5.3.5 Water repellency

Water repellency was determined through the standard method of capillary absorption, mainly used in the field of stone protection. This method was applied to verify the water absorption inhibition as well as the adhesion stability of the fluorinated compounds when applied on a polar substrate (*i.e.*, Lecce stone, a carbonate sedimentary rock). [213]

The capillary absorption was considered to demonstrate the hydrophobic properties of compounds applied. The water repellency results of all the compounds on different stone material were calculated and shown as PE % and discussed as following.

5.3.5.1 On Lecce stone

All the seven partially perfluorinated compounds were tested for the water repellency on Lecce stone samples. Three no-treated samples (named as N.T) were used as references. The results (average values on 2 absorption tests except samples coated by C-glycosides) are shown in the table 5-11.

Treatment	Sample #	Amount of compound (g)	Lecce stone					
			1h	SD	PE (%) 2h	SD	3h	SD
C-Glc-OAc	YZ003	0.036	9.1	-	-	-	2.5	-
	YZ006	0.034	19.7	-	-	-	2.5	-
	YZ007	0.029	18.6	-	-	-	2.5	-
C-Glc-OH	YZ023	0.025	19.2	-	-	-	6.6	-
	YZ024	0.026	19.1	-	-	-	6.6	-
	YZ029	0.027	32.1	-	-	-	6.5	-
DSF	YZ038	0.045	58.1	7.9	28.1	10.8	11.5	4.9
	YZ040	0.053	68.0	7.7	43.8	12.1	25.2	12.3
	YZ042	0.042	57.9	10.4	24.5	16.0	8.8	6.8
DF	YZ010	0.003	84.4	4.6	65.1	3.5	46.8	1.3
	YZ036	0.056	78.1	4.0	55.4	2.4	34.7	0.2
	YZ039	0.052	78.3	0.1	57.2	3.2	38.4	5.4

ESF	YZ043	0.042	89.8	1.1	80.6	1.2	71.6	1.1
	YZ044	0.054	88.1	3.3	78.3	4.3	68.9	4.9
	YZ046	0.044	87.1	3.5	76.5	5.1	66.1	5.7
ESTF	YZ050	-0.008	30.0	18.6	7.2	3.3	5.0	0.4
	YZ051	0.032	24.6	14.8	4.9	0.9	4.2	0.0
	YZ052	0.046	29.5	18.5	5.2	1.6	4.2	0.3
DSTF	YZ047	0.033	81.5	8.4	62.9	12.2	47.2	10.7
	YZ048	0.03	65.4	17.2	33.3	23.9	15.7	14.8
	YZ049	0.025	59.1	28.8	30.4	35.3	18.6	20.4
N.T	YZ030		5.1	0.7	1.4	0.1	1.3	0.0
	YZ033	–	2.8	0.0	1.4	0.2	1.4	0.1
	YZ034		5.1	1.4	1.9	0.2	1.8	0.2

Table 5-11: Water repellency of partially perfluorinated compounds coated Lecce stone; SD= standard deviation

The obtained protective efficacy of different compounds is very different. Firstly, for the data of efficacy after 1 h water capillary absorption test, three groups can be divided according to their protective performance. **DF** and **ESF** show high protective efficacy, both around 80 %. Compound **DSF** shows medium PE % around 60 %, and the PE % of **DSTF** is from 59 % to 82 % with poor reproducibility on the three samples. While, two **C-glycosides** and **ESTF** show low water repellency below 30 %.

After another 2 hours of water absorption, PE % of all the compounds shows dramatic decrease, except **ESF**. **ESF** shows the best protective efficacy among all the tested compounds even after 3 h water absorption, and the PE % is still medium high (between 66 % and 72 %). The second highest protective efficacy is contributed by **DF**, which is medium (between 35 % and 47 %). While other compounds only show low protective efficacy on Lecce after 3 h of water absorption.

DSTF shows higher PE % on sample YZ047 than on the other two samples. This may probably be due to its high average molecular weight compared with other compounds. The molecules can form a no homogeneous distribution on the external surface of the samples and/or inside the pores with a rearrangement of the polymeric film, poorly adhered at the surface, during the drying step from measurement to measurement.

C-Glc-OAc and **C-Glc-OH** both show low PE %, however, PE % of **C-Glc-OH** is slightly higher than **C-Glc-OAc**. Probably the interaction between the OH groups in **C-Glc-OH** and stone contributed to a better adhesion of the compound, and consequently to the slight increase of protective efficacy.

ESTF shows low protective efficacy around 4 % on Lecce, compared with the medium high PE % of **ESF**. The dramatic decrease could be due to the affinity of the OH groups to water. The different behaviors among the two groups of compounds (**C-Glc-OAc**, **C-Glc-OH**; **ESTF**, **ESF**), probably mean the OH groups can not only increase the PE % by helping adhere to stone, but also can decrease the PE % by attracting water. So a suitable percentage of OH groups in the molecule can keep the balance between good adhesion and hydrophobicity.

5.3.5.2 On sandstone (Pietra Serena)

Five partially perfluorinated oligoamides and amine were tested for their water repellency on sandstone samples. Three no-treated samples (N.T) were used as references. The results (average values on 2 absorption tests) are shown in the table 5-12.

	Sample #	m(g)	Sandstone PE (%)							
			1h	SD	2h	SD	3h	SD	4h	SD
DSF	AP 025	0.020	78.0	1.5	77.2	0.9	75.9	1.2	73.5	1.5
	AP 038	0.036	78.8	1.9	77.8	1.0	76.3	1.0	73.7	0.7
	AP 096	0.040	83.4	1.0	80.3	2.2	76.3	3.4	72.0	4.3
DF	AP 027	0.027	78.9	1.3	80.7	1.1	80.8	1.0	78.6	1.1
	AP 053	0.015	79.6	0.7	81.1	0.8	81.9	0.9	80.3	0.6
	AP 062	0.014	84.9	0.4	82.5	0.5	80.2	0.5	77.7	0.5
ESF	AP 030	0.022	51.6	2.8	46.7	2.1	39.1	3.5	28.9	3.5
	AP 046	0.042	68.7	2.4	59.6	3.8	44.8	5.2	30.6	5.9
	AP 087	-0.013	67.4	1.7	47.9	2.6	33.4	2.5	15.9	2.6
ESTF	AP 073	0.003	40.7	10.7	27.9	11.2	14.1	11.7	2.0	10.6
	AP 083	-0.012	38.5	10.9	26.3	10.4	15.4	10.0	5.1	9.5
	AP 094	-0.005	42.7	8.9	41.2	7.3	31.3	7.5	18.2	8.2
DSTF	AP 095	0.012	25.0	16.5	25.7	14.3	25.8	13.3	22.7	13.0
	AP 097	0.022	33.8	19.4	17.7	17.8	5.7	13.7	-4.7	9.0
	AP 098	0.007	26.6	4.0	10.3	4.7	0.0	3.7	-8.7	1.7
N.T	AP 045		10.1	6.2	10.1	5.2	9.1	5.1	7.4	4.4
	AP 064	—	30.2	8.3	18.8	7.4	4.5	7.0	-7.9	5.0
	AP 070		31.7	6.7	25.7	6.0	9.0	6.4	-6.4	4.2

Table 5-12: Water repellency of partially perfluorinated compounds on sand stone; SD= standard deviation; m: amount of compound

The compound **DF** shows a protective efficacy at around 79-85 %, and **DSF** shows a similar PE % at around 78-83 % as average value after 1 hour of absorption. Moreover, those two compounds show stable water repellency from 1 h to 4 h of water absorption, while other compounds show a clear decrease on protective efficacy as the absorption time increases. **ESF** shows a medium low protective efficacy after 4 hours of absorption (between 16 % and 31 %). The higher PE % of **DSF** compared with **ESF**, probably is due both to the extra NH group, which can enhance the adhesion between the protective agent and stone, and to its better solubility which favors a uniform distribution of the low amount of product on the stone surface.

However, compounds containing tartrate units in the molecules (**ESTF** and **DSTF**) show in general low protective efficacy. This may probably be due to the hydrophilicity of OH groups.

5.3.5.3 On Carrara marble

Five partially perfluorinated oligoamides and amine were tested for their water repellency on Carrara marble samples. Three no-treated samples (N.T) were used as references. The results (average values on 2 absorption tests) are shown in the table 5-13. Due to the low porosity of marble compared with Lecce and sandstone (fast saturation with water), the water absorption test lasted 1 hour.

Treatment	Sample #	Marble		
		Amount of compound (g)	PE (%) 1h	SD
DSF	AP071	0.014	64.4	6.4
	AP096	0.012	50.1	12.1
	AP098	0.015	51.6	6.4
DF	AP073	0.012	69.0	8.6
	AP090	0.001	64.1	5.1
	AP093	0.013	60.5	12.1
ESF	AP026	0.004	23.7	6.7
	AP077	0.012	15.2	0.00
	AP084	0.008	22.1	3.2
ESTF	AP028	-0.009	36.0	2.1
	AP072	0.011	43.0	7.4
	AP088	0.014	10.5	0.6
DSTF	AP038	0.010	37.0	11.7
	AP061	0.007	34.1	11.2
	AP083	-0.001	14.2	4.7
N.T	AP016		-0.4	6.0
	AP076		4.6	1.8
	AP095		7.1	1.1

Table 5-13: Water repellency of partially perfluorinated compounds coated on marble; SD= standard deviation; m: amount of compound

Compounds **DF** and **DSF** show medium high water repellency, between 61 % and 69 %, and from 50 % to 64 % respectively, but with low reproducibility. While the PE % of compounds **ESTF** and **DSTF** are around 40 % and 30 % respectively, with poor reproducibility. **ESF** shows medium low water repellency with an average PE % value at 20 %.

Like observed in sandstone, the higher PE % of **DSF** compared with **ESF**, is probably due to the extra NH group which can enhance the adhesion between the protective agent and stone. The higher solubility of **DSF** compared to **ESF** is another factor that influences the uniformity of the coating, and therefore the PE % value. As the amount of product applied on marble is much lower than that on sandstone, the solubility of the protective agent can be more relevant to achieve a good coating on marble than on sandstone. In accordance with this explanation, the PE % of **ESF** on marble is in fact lower than that on sandstone.

The slightly higher PE % of **ESTF** than **ESF** probably is because the OH groups can enhance the adhesion between the molecules of the protective agent and the stone. While the quite low reproducibility observed in the specimens treated with **DSTF** and **ESTF** is probably due to the inhomogeneous distribution of the product, rather than to the difference in product applied on each specimen. Because of the low porosity of marble (which means low ability to absorb the treatment solution), the accumulation of the coating agent along the edges of the sample due to the faster evaporation of the solvent is favored. This fact can easily lead to the inhomogeneous distribution on the external surface of the stone.

5.3.5.4 Summary

In summary, different partially perfluorinated compounds have different water repellency on three stone materials with different porosity. **ESF** has the highest PE % (between 66 %-72 %) after the 3 hours of absorption on Lecce stone, among all the 7 tested compounds. **DF** and **DSF** show the highest PE %, 80 % - 82 % and 76 % respectively on Pietra Serena after 3 hours of absorption, among all the tested 5 partially perfluorinated oligoamides and amine. **DF** and **DSF** also give the highest PE % on marble among all the 5 partially perfluorinated oligoamides and amine, which is between 61 % and 69 %, and from 50 % to 64 % respectively after 1 hour of absorption.

5.3.6 Chromatic effect

The results on the chromatic change on different stone materials, which is caused by the treatments of different compounds, are shown in the tables below.

5.3.6.1 On Lecce stone

In the table 5-14, ΔE^* of the two partially perfluorinated C-glycosides, **ESF**, and **DSTF** are less than 3 on Lecce stone, which means is imperceptible chromatic change (except sample YZ043 by **ESF**).

Treatment	Sample #	Lecce stone		
		Amount of compound (g)	ΔE^*	SD
C-Glc-OAc	YZ003	0.036	0.4	0.04
	YZ006	0.034	0.5	0.19
	YZ007	0.029	0.3	0.01
C-Glc-OH	YZ023	0.025	0.9	0.57
	YZ024	0.026	1.3	0.53
	YZ029	0.027	1.1	0.47

DSF	YZ038	0.045	5.15	0.01
	YZ040	0.053	5.33	0.19
	YZ042	0.042	5.27	0.05
DF	YZ010	0.003	4.43	0.02
	YZ036	0.056	3.67	0.11
	YZ039	0.052	4.31	0.03
ESF	YZ043	0.042	3.37	0.06
	YZ044	0.054	2.90	0.03
	YZ046	0.044	2.49	0.12
ESTF	YZ050	-0.008	5.62	0.02
	YZ051	0.032	6.25	0.08
	YZ052	0.046	5.80	0.04
DSTF	YZ047	0.033	2.10	0.03
	YZ048	0.03	2.50	0.06
	YZ049	0.025	1.63	0.03
N.T	YZ030		0.22	0.12
	YZ033	-	0.59	0.02
	YZ034		0.53	0.05

Table5-14: Chromatic effect by partially perfluorinated compounds coated on Lecce; SD= standard deviation

5.3.6.2 On sandstone

While for sandstone, **DSF**, **DF** and **ESF** show clear increase of ΔE^* , which is around 10. ΔE^* of **ESTF** is between 5 and 6.4. Only compound **DSTF** show a ΔE^* at around 3, which can be almost imperceptible for human eye. (table 5-15)

5.3.6.3 On Carrara marble

For marble, **ESF** shows the lowest chromatic change, whose ΔE^* is from 0.9 to 1.8. **ESTF** and **DSTF** has the ΔE^* which is slightly higher than 3. While, **DF** gives a significant chromatic change with ΔE^* from 7.0 to 7.8. Also **DSF** shows the ΔE^* close to 9, which is perceptible for human eye. (table 5-15)

	Sandstone				Marble			
	Sample #	m(g)	ΔE^*	SD	Sample #	m(g)	ΔE^*	SD
DSF	AP 025	0.02	11.79	0.07	AP071	0.014	8.80	0.09
	AP 038	0.036	10.39	0.29	AP096	0.012	8.74	0.04
	AP 096	0.04	11.15	0.46	AP098	0.015	8.66	0.08
DF	AP 027	0.027	10.46	0.07	AP073	0.012	7.62	0.13
	AP 053	0.015	10.55	0.19	AP090	0.001	6.99	0.06
	AP 062	0.014	9.48	0.19	AP093	0.013	7.75	0.03

ESF	AP 030	0.022	1.31	0.20	AP026	0.004	1.83	0.05
	AP 046	0.042	10.82	0.27	AP077	0.012	0.88	0.03
	AP 087	-0.013	8.80	0.05	AP084	0.008	1.37	0.03
ESTF	AP 073	0.003	5.03	0.44	AP028	-0.009	1.70	0.13
	AP 083	-0.012	5.55	0.06	AP072	0.011	3.19	0.02
	AP 094	-0.005	6.36	0.04	AP088	0.014	3.53	0.04
DSTF	AP 095	0.012	3.78	0.09	AP038	0.010	4.61	0.09
	AP 097	0.022	4.93	0.16	AP061	0.007	3.14	0.06
	AP 098	0.007	2.22	0.10	AP083	-0.001	3.48	0.03
N.T	AP 045		11.79		AP016		8.80	
	AP 064	–	10.39		AP076	–	8.74	
	AP 070		11.15		AP095		8.66	

Table 5-15: Chromatic effect by partially perfluorinated compounds coated on sandstone and marble; SD= standard deviation; m: amount of compound

5.3.7 Contact angle

As a common interface phenomenon, the wetting of a solid surface by a liquid is mainly determined by the microstructure of the solid surface and the surface chemical composition (surface free energy). [225][226]

Contact angle (CA) quantifies the wettability of a solid surface by a liquid *via* Young's equation.

$$\gamma_{LV} \cos \theta_Y = \gamma_{SV} - \gamma_{SL}$$

Where γ is the interfacial tension, subscripts SV, SL, and LV denote the solid–vapor (gas), solid-liquid, and liquid-vapor (gas) interfaces, respectively, and θ_Y (Young's CA) is the equilibrium CA at the three-phase point [227]. Surfaces are defined as hydrophilic when the water CA is less than 90° . If the CA ranges from 90° to 150° , the surface is hydrophobic, while surfaces are superhydrophobic when $CA > 150^\circ$ [228]. (figure 5-15)

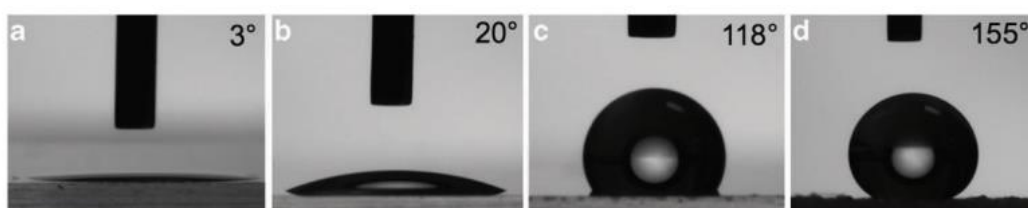


Figure 5-15: Surface classification based on contact angles. (a) Superhydrophilic, (b) hydrophilic, (c) hydrophobic and (d) superhydrophobic surfaces display $\theta \approx 0^\circ$, $\theta < 90^\circ$, $\theta > 90^\circ$ and $\theta > 150^\circ$, respectively. [229]

Therefore, CA was used here for investigating the hydrophobicity of the stone surface treated with the 5 partially perfluorinated oligoamides and amine. The results are reported in the following content and table 5-16.

5.3.7.1 On Lecce stone

All the 5 tested compounds give the $CA > 90^\circ$ on Lecce stone, which means all the surface is hydrophobic after coating. CA of **ESTF** coated surface is the lowest, which is around 95° . This result is consistent with the low PE % of **ESTF** on Lecce stone. Compound **ESF** contributes to the highest CA, with one value at 117.9° and two values at around 130° . Which means it has one of the best hydrophobic performance among the 5 tested compounds on Lecce stone. Compound **DF** gives CA at around 116° , which is slightly higher than the CA (between 101 and 109°) obtained with **DSF**. Also the PE % results show that **DF** has a slightly higher PE % value than **DSF**. While **DSTF** is the second compound with the highest CA (121 - 135°), which does not correspond to the PE % result in the water repellency test. It is probably due to the highest molecular weight of **DSTF** which reduces its penetration into the stone. Therefore, most molecules were deposited on the external surface of the sample and contribute to the high CA, but not to the inhibition of water absorption during prolonged contact with liquid water.

5.3.7.2 On sandstone

Compound **ESTF** does not provide a hydrophobic surface after being applied on the sandstone samples having a CA ranging from 70.4° to 80.5° . While, the other 4 tested compounds provide hydrophobic surface after being coated on sandstone. The CA of **ESF** treated surfaces is the highest at around 125° , which is followed by that of **DF** (114 - 121°) and **DSF** (101 - 115°). However, in the protective efficacy test, the PE % of **DF** and **DSF** (72% - 80%) are significantly higher than that of **ESF** (16% - 31%). This contradiction is probably due to the solubility property. **ESF**, being a suspension, had been mainly distributed on the external surface providing high hydrophobic effect. While the dilute solution of **DF** and **DSF** could diffuse inside the substrate reducing the actual quantity of product on the surface, but improving the water inhibition for prolonged contact with liquid water. Therefore, the PE % of **DF** and **DSF** is higher than **ESF** while CA of **DF** and **DSF** is smaller than **ESF**. Compound **DSTF** gives the CA between 97° and 103° , which corresponds to its low PE % on sandstone.

5.3.7.3 On Carrara marble

ESF gives the highest CA on marble, which ranges from 101° to 139° . **DSF** and **DF** give similar CA, which is slightly higher than 90° on most samples. These results also contradict the PE % values. The explanation of this is probably the same as that reported for sandstone, *i.e.* the fact that the suspension of **ESF** is mainly precipitated on the external surface, which is not sufficient to protect against prolonged contact with water. Two of the three specimens show **DSTF** can provide hydrophobic surface with CA at around 95° , however, one specimen shows the CA is 69° , which means the surface is still hydrophilic. Compound **ESTF** failed to give marble a hydrophobic surface with the $CA < 90^\circ$.

5.3.7.4 Summary

In summary, the compound **ESF** provides the highest CA to each stone material, which ranges from 101° (minimum) to 139° (maximum). However, that does not mean it can give the best water repellency, especially on stones with lower porosity like sandstone and marble. The compounds **DSF** and **DF** also provide hydrophobic property on Lecce stone and sandstone, with CA > 90°. The compound **DSTF** generally gives hydrophobic surfaces on Lecce stone, sandstone and marble, while **ESTF** can contribute to hydrophobic property only on Lecce stone.

Coating	Lecce stone			Sandstone			Marble		
	Sample	Average CA(°)	SD	Sample	Average CA(°)	SD	Sample	Average CA(°)	SD
DSF	YZ038	101.0	7.5	AP025	115.2	12.9	AP071	91.3	1.4
	YZ040	104.7	4.8	AP096	100.6	8.1	AP098	90.7	2.9
	YZ042	109.8	7.1	AP038	109.2	7.9	AP096	87.1	5.9
DF	YZ036	118.1	6.9	AP027	120.8	7.7	AP090	94.3	4.2
	YZ039	113.6	8.4	AP053	114.0	7.9	AP073	89.6	4.5
	YZ010	116.4	7.4	AP062	115.8	5.3	AP093	95.6	4.4
ESF	YZ043	117.9	6.3	AP046	124.1	5.1	AP026	139.3	2.7
	YZ044	130.9	11.5	AP087	124.8	13.3	AP077	101.0	10.7
	YZ046	132.9	5.3	AP030	129.1	8.4	AP084	112.6	3.8
ESTF	YZ050	95.8	3.5	AP094	70.4	8.7	AP028	69.6	5.9
	YZ051	96.4	5.1	AP073	74.8	10.1	AP072	76.1	6.1
	YZ052	95.5	4.8	AP083	80.5	5.3	AP088	67.6	12.9
DSTF	YZ047	127.4	10.4	AP095	99.3	9.3	AP083	94.3	3.7
	YZ048	135.0	8.1	AP097	97.0	3.5	AP038	96.3	6.1
	YZ049	121.1	16.5	AP098	103.4	6.6	AP016	69.0	1.3
N.T	YZ030	23.4	6.3	AP045	115.6	12.2	AP095	59.9	10.4
	YZ033	16.6	5.7	AP070	106.5	11.6	AP076	71.7	8.9
	YZ034	26.1	7.7	AP064	98.9	10.2	AP061	85.3	7.9

Table 5-16: CA of stone surface after the treatment by partially perfluorinated compounds

5.3.8 Vapor permeability

One requirement for stone protection agents is good permeability to water vapor. After the application of the protective product, the surface must be completely water repellent, but the petrophysical properties of the material, such as the permeability to water vapour, should not change drastically, in order to avoid the damages due to the entrapment of liquid water inside the stone. A drastic reduction of the water vapor permeability may occur when superficial polymeric films are formed or a high number of pores are filled with the conservation materials. [12] Therefore, the vapor permeability was tested after treatments

with the 5 partially perfluorinated compounds on stone materials. The RP parameter gives a rough idea of how much the original pores, pore structures have been modified (or damaged) by the applied compounds.

The results on vapor permeability are shown on the table 5-17

Treatment	Residual Permeability (%)					
	Lecce stone	SD	Sand stone	SD	Marble	SD
DSF	106	8.80	87	3.76	57	5.08
DF	101	2.21	82	8.35	71	12.11
ESF	99	5.42	93	5.15	123	41.46
ESTF	101	3.11	93	5.72	106	32.84
DSTF	103	4.28	100	5.76	92	7.52

Table 5-17: Residual permeability (%) after treatments

The original vapor permeability of Lecce stone almost has no decrease after the treatments by 5 partially perfluorinated oligoamides and amine. It is worthy to observe that for **ESF** (which gives the highest PE % on Lecce), the residual permeability is 99 %. For the sandstone, the original vapor permeability was slightly decreased for **DSF** and **DF** treatments, but always good and acceptable values. This slightly decreased vapor permeability corresponds to the highest PE % value of **DSF** and **DF** on sandstone. On marble, there is a significant decrease for **DSF** treatment whose RP % is only at 57 %. The **DF** treatment also decreased the vapor permeability of marble (71 % RP). However, PE % of **DF** is higher than **DSF** on marble. This means **DSF** did not change the porosity and it is distributed along the pore walls. However, in the case of very low porous stone (*i.e.* marble), the pore blockage could be significant, or a hydrophobic effect may occur along several pore walls inside the stone, causing a reduced vapor permeability.

In summary, all the 5 tested compounds can give a good maintenance of the original porosity and pore structures after treatment on Lecce stone. On sandstone, slightly decreased vapor permeability was observed for **DSF** and **DF** treatments, while their RP % values are still higher than 80 %. While a dramatic decrease of vapor permeability was observed for **DSF** treatment on marble. That is probably due to the partial or total pore blockage by **DSF**. **DF** also decreased the vapor permeability of marble with 71 % RP.

5.4 Conclusion

The performance of the seven partially perfluorinated derivatives that were synthesized during this PhD research project, was evaluated by a series of measurements on different stone materials (Lecce stone, sandstone, and marble) with different porosity. **C-Glc-OAc** shows good solubility in ethyl acetate, and all the other 6 compounds show good solubility in alcohols and hydro-alcoholic solvents *e.g.* ethanol, 2-propanol, H₂O/2-propanol, except **ESF** which is less soluble. Solubility in common solvents is of essential importance for the wide application of protective coatings, and additionally, using alcoholic or hydro-alcoholic solvents, the conservation treatments are not only healthy to human beings but also environmentally friendly.

The resistance to photodegradation test was also performed by the radiation of long wave ultraviolet 365 nm. Comparing with the partially perfluorinated derivatives containing diethylenetriamine moiety, the compounds with ethylenediamine units show better stability under UV aging.

In the water repellency test on Lecce stone, **C-Glc-OAc** and **C-Glc-OH** show low protective efficacy, however, PE % of **C-Glc-OH** is slightly higher than **C-Glc-OAc** which has no OH groups. **ESF** shows medium high protective efficacy and **DF** contributes a medium protective efficacy. As for the water repellency test on sandstone with lower porosity compared with Lecce, **DF** and **DSF** both show medium high PE % values. On marble, which has the lowest porosity, **DF** and **DSF** also show medium high PE % values.

Concerning the chromatic effect test, the two partially perfluorinated **C-glycosides**, **ESF**, and **DSTF** show imperceptible chromatic change on Lecce. On sandstone, **DSF**, **DF** and **ESF** show clear increase of ΔE^* , which is around 10. Only compound **DSTF** show a ΔE^* at around 3, which is imperceptible for human eyes. On marble, **DF** and **DSF** give a significant chromatic change around 8, while the chromatic change of treatments by the other compounds is imperceptible (**ESF**) or close to imperceptible (**ESTF**, **DSTF**).

Compound **ESF** can give the highest CA to each stone material, which is from 101° (minimum) to 139° (maximum), while **ESTF** failed to contribute hydrophobic surface on sandstone and marble.

In the vapor permeability test, all the 5 tested partially perfluorinated oligoamides and amine can give a good maintenance of the original porosity and pore structures after treatment on Lecce stone. On sandstone, slightly decreased vapor permeability was observed for **DSF** and **DF** treatments (RD % over 80 %). Dramatic decrease of vapor permeability was observed for **DSF** treatment (RD % at 57 %) on marble.

Considering all the performance of each compound in all the tests, **ESF** is a suitable protective agent on Lecce stone with acceptable solubility in 2-propanol, good stability under UV, high PE %, high CA and ability to maintain the original porous structure and chromatic features. **DSF** and **DF** could be the potential protective agents on sandstone if the chromatic change can be decreased after coating. **DF** can be also considered as a potential protective agent if the chromatic change can be decreased after coating on marble.

Chapter 6

Blanching easel painting restoration

6.1 Introduction

The blanching phenomenon mostly appears in old master easel paintings painted between the 16th and 18th century. [71] From the history point of view, those paintings showed the features of society, nature, and religion in their time. Thus, the old master easel paintings are important materials to record and remember the life of people in the history. However, when blanching appeared on the paintings, the paint composition can be hidden partially or totally by the whiten opacification. [84] The blanching significantly disrupts the readability of paintings and makes it more difficult to comprehend the expression of the paintings. From the aesthetics point of view, blanching gives different degree of damage on the beauty of the old master easel paintings. It affects the aesthetics expression by the artists. For example, blanching could modify the presentation of chiaroscuro initially desired by the painter in the paintings. Moreover, the survival of those old master paintings is important to the generations in future.

Therefore, restoration treatments which could decrease or eliminate blanching in easel painting are highly desired. During centuries, different traditional restoration treatments for blanching paintings have been developed. Those methods include rubbing the surface of paintings with egg yolk or oil, scraping off the top layer of the paint, or the “Pettenkofer” method (using solvents like alcohol in vapor or liquid form to restore the damaged works) [79b]. Among those restoration treatments mentioned, the use of solvent in liquid form was reported as the technique currently practiced in French restoration workshops [8]. It is important to note that the restoration of blanching varnish layer can give a satisfied performance by using volatile solvents (2-propanol, ethanol) in liquid form. Because the solvent can either directly remove the blanching varnish layer or, dissolve the varnish material again and make the pores resorb. [8] Thus, blanching varnish layer does not present major challenge for restoration work.

However, when it comes to blanching paint layers, the traditional restoration treatments show low efficacy and poor durability during the practical process. Blanching was not decreased obviously or eliminated by those treatments and remains as a challenging problem in the easel painting restoration field. [8] Thus developing effective and durable restoration treatments to overcome the blanching of paint layer in easel oil paintings and reconstitute their past glory is necessary.

Fortunately, revealing the porous structures has a major impact for the development of appropriate and durable restoration treatments to overcome the blanching. [84] Indeed, restoration treatments will be effective and sustainable only if they resorb or durably fill the pores, to reduce the light scattering. Using solvents in liquid form to treat the blanching paint

layer is not effective, because the pores did not be filled after the solvent evaporated. [71]

Recently, Genty *et al.* proposed an innovative methodology for blanching painting restoration: using a synthetic compound to fill the pores in paint layer permanently. The used compound is partially perfluoropolyetheric diamide, which is synthesized from isobutyl ester of perfluoropolyetheric monocarboxylic acid and hexamethylenediamine. This compound is chemically inert, long-term stable, non-toxic, and also has been used as water repellency product for stone material. The research shows that the perfluoropolyether diamide could decrease the blanching effectively by filling the pores in blanching paintings. Besides, reversibility of this treatment is realized by using perfluorooctane to remove the compound. Therefore, this partially perfluorinated diamide is considered promising for the restoration of blanching paintings. [8][71]

Inspired by those previous research results, in this thesis we proposed to use the new partially perfluorinated derivatives that were synthesized in this PhD research project for the blanching painting restoration. In particular, the restoration object in this chapter is blanching paint layer. Considering the external humidity could cause the blanching, the molecules are designed to be water repellent by the perfluorinated chains as hydrophobic ends. Meanwhile, concerning the porous structures and polarity of paint layers, hydroxyl groups as polar ends were especially introduced into the molecules to help the molecules fill the pores to improve their restoration performance. Besides, the partially perfluorinated compounds, without hydroxyls or containing different amine monomers (*e.g.* ethylenediamine and diethylenetriamine), were also designed to synthesize. In this way, a library of partially perfluorinated derivatives, which present different molecule structures, different solubility, different average molecular weight, was built.

The aim of the research presented in this chapter, is to examine the efficacy of those synthetic compounds on blanching paint-layer restoration, and select one or several compounds as promising products. Therefore, an applicative study on mock-up samples of blanching paint layers was developed, to assess if the partially perfluorinated compounds could weaken or eliminated blanching effectively.

Considering the object of restoration (paint layers), the visual appearance of blanching, the nature of blanching and the treatment process, four parameters were proposed to evaluate if the fluorinated compounds that were synthesized in this PhD research project, could act against blanching effectively. And different analysis methods in macro and micro scales, were established to examine the behaviours of the compounds on each parameter. The four parameters and examining methods corresponding to each parameter were listed as followed:

- **Parameter 1**

The applied compounds should not cause any physical or chemical degradation of the pigments in blanching areas of paint layers, like the appearance of darkening, crystallization *etc.* on the pigments. For example, dimethyl sulfoxide (DMSO) was reported to cause crystallization on verdigris and thus, it is not an ideal restoration product for paintings which contain verdigris.

Method: All the compounds would be tested on the pure pigments, which were reported sensitive to blanching. Optical microscopy and complementary method ^1H NMR and

FT-IR were used for the examination for the changes of pigments.

- **Parameter 2**

In macro scale, the restoration results should be visually satisfying. That means the blanching areas can receive the original gloss and color after treatments. The chromatic change after restoration treatments could be quantified and presented directly by CIE L* a* b* Coordinates. By comparing the chromatic change before and after restoration, the performance of restoration on visual aspect can be evaluated.

- Method: Spectro-colorimetric analysis would be performed before and after the treatments of the compounds on the blanching mock-up samples.

- **Parameter 3**

In micro scale, the pores which cause the blanching in the paint layers, should be filled by the compounds after the restoration treatments. In this way, the treatment could be expected as effective and durable. To investigate if the pores are filled, morphological study of the micro structures and the distribution study of the compounds in treated samples would be performed.

Method: Field emission gun scanning electron microscopy (FEG-SEM) would be used for morphological study in micro samples of treated and blanching mock-ups. As complementary methods, optical microscopy and scanning electron microscopy - energy dispersive X-ray spectrometry (SEM-EDS) would be used to investigate the distribution of the partially perfluorinated derivatives in the treated samples.

- **Parameter 4**

The restoration treatments by the compounds should be reversible. Reversibility is a cardinal requirement for the restoration treatments. In our case, the compounds applied in paint layers of old master paintings, are expected to be removable. Reversibility could be evaluated in macro scale (chromatic change) and micro scale (morphological appearance and compound distribution).

Method: The compounds would be removed by solvents. The reversibility of the treatments would be evaluated by spectro-colorimetric analysis, FEG-SEM, SEM-EDS and optical microscopy.

Concerning the tested compounds, the seven new partially perfluorinated derivatives including partially perfluorinated C-glycosides, oligoamides and amine were all investigated as blanching painting restoration products. Those compounds are named as **C-Glc-OAc**, **C-Glc-OH**, **ESTF**, **DSTF**, **ESF**, **DSF** and **DF**, and their corresponding structures are shown in the table 6-1. The 7 tested compounds were also used for stone protection in chapter 5. The partially perfluoropolyetheric diamide (named as **DC6G900**) used by Genty A *et al.* is included in the tests as a reference [71].

6.2 Experiment

6.2.1 Materials

- **Pigments**

White lead, Calcium carbonate, Ivory black genuine, Raw umber (greenish dark), Green earth, Ultramarine blue, Copper (II) acetate monohydrate, Blue Verditer (synthetic azurite), Azurite natural standard, Lapis Lazuli natural ultramarine, Ultramarine Ash, Red ochre, Vermilion, Natural Cinnabar, Madder Lake genuine, Red Lead minium, Carmine, Lead tin yellow II, and Lead oxide yellow were selected. Among those pigments, Copper (II) acetate monohydrate is the product of ACROS ORGANICS, Red ochre is the product from Sennelier, and all other pigments are products of Kremer pigmente GmbH & Co.

- **Glass slides**

Two kinds of glass slides were used for pigments and mock-up samples. Single depression concave slides with the size 26 mm x 75 mm x 1 mm. Standard microscope slides the size 26 mm x 75 mm x 1 mm.

- **Other materials**

Walnut oil (HMB-BDA, France), PbO (Merck-Eurolab-Prolabo, France), 2-propanol, and 2,2,2-Trifluoroethanol (TFE), Styrene (E.S.C.I.L.), Catalyst SODY33 C (ELF ATOCHEM)

6.2.2 Sample preparation

6.2.2.1 Paint-layer mock-up samples

Mock-up paint-layer samples were prepared by mixing the binder (containing walnut oil, water and PbO), two different pigments (green earth, and raw umber greenish dark) and the drier CaCO_3 . Binder was made from walnut oil, water, and PbO in the mass proportions 10-10-1. PbO was first ground with oil. This mixture was heated for 40 min at 60 °C. After adding water, it was heated at 100 °C for 180 min.

Green earth, and raw umber (greenish dark) were chosen as pigments for mock-up sample. Binders were ground with pigment, and CaCO_3 and then the ground mixture was applied on microscope glass slides. The relative mass quantities of binder, pigment, and chalk used for the preparation of the painting mock-ups are shown in table 6-2.

The colored mixtures were applied uniformly on standard microscope slides by brush. All the mock-up samples were dried for 1 month in laboratory conditions. One green earth sample and one raw umber sample were selected as reference samples, named Ref. GE and

Ref. RU.

Green earth mock-up samples	Raw umber mock-up samples
	
Binder: 40%	Binder: 39% w/w
Green earth pigment: 30 %	Raw umber (greenish dark): 30.5%
CaCO ₃ :30%	CaCO ₃ : 30.5%

Table 6-2: Paint-layer mock-up samples and the relative mass portions of binder, pigment, and chalk

6.2.2.2 Blanching paint-layer mock-up samples

In order to produce blanching areas, an ageing test consisting in “wet-dry” cycles and UV radiation was performed on the mock-up paint samples using a climate chamber and a UV lamp.

Two sets of mock-up samples above consisted of 11 green earth samples and 11 raw umber samples, were used for the accelerated aging process. The target of the accelerated aging process is to reproduce the blanching phenomenon on those selected mock-up samples in a relatively short time to simulate as well as possible natural aging. The selected 22 samples were put in a climatic chamber (MPC 2001) with alternately humid and dry conditions, and also radiated under ultraviolet (UV) light (Philip) in the 300–400 nm range. The details of aging conditions were presented in the table 6-3. After the accelerated aging process, 22 blanching paint-layer mock-up samples were obtained, and ready for the restoration treatment by using the partially perfluorinated derivatives.

Ageing cycle	Conditions	Ageing time (hours)
Cycle 1	T= 40 °C and RH= 40 %	168
Cycle 2	T= 40 °C and RH= 70 %	288
Cycle 3	UV radiation in laboratory conditions	696
Cycle 4	T= 50 °C and RH= 80 %	337
	UV radiation	818

Table 6-3: Aging conditions

6.2.3 Preparation of partially perfluorinated derivatives for restoration treatments

The solution or suspension of the seven new synthetic partially perfluorinated derivatives were prepared for the blanching painting restoration, and also the perfluoropolyetheric diamide (**DC6G900** tested by Genty *et al.* [71]) was prepared as a reference compound during the series of tests. Information (solvent, concentration, and physical state) about the solution or suspension of the compounds for the restoration treatments are reported in the following table 6-4.

Compound	Solvent	Concentration (w/w %)	Physical state
C-Glc-OAc (white solid)	Ethyl acetate	30	Transparent solution
C-Glc-OH (lightly yellow oil)	2-propanol	30	Transparent solution
ESTF (yellow solid)	TFE	19	White suspension
DSTF (orange oil)	TFE	30	Yellow solution
ESF (white solid)	2-propanol	13	White suspension
DSF (orange oil)	2-propanol	30	Lightly yellow solution
DF (yellow oil)	2-propanol	30	Lightly yellow solution
DC6G900 (transparent oil)	TFE	30	Transparent solution

Table 6-4: Solution or suspension of the partially perfluorinated compounds for the restoration treatments

6.2.4 Treatments

6.2.4.1 Treatments on pure pigments

The seven synthetic partially perfluorinated compounds (in solution or suspension form), the reference compound (solution form), and walnut oil were mixed with different pure pigments. 19 kinds of pigments which are frequently used in the old master easel paintings from the 16th to 18th century were chosen for the test of interaction between pigments and compounds. As a reminder, the names, color and chemical composition of the studied pigments were reported table 6-5, as previously presented in Introduction section.

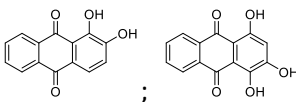
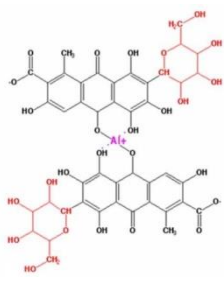
Color	Pigment	Chemical composition
White	White lead	$2\text{PbCO}_3 \cdot \text{Pb}(\text{OH})_2$
	Calcium Carbonate	CaCO_3
Black	Ivory Black, genuine	$\text{Ca}_3(\text{PO}_4)_2, \text{C}$
Brown	Raw Umber, greenish dark	$\text{Fe}_2\text{O}_3, \text{MnO}_2$
Green	Green earth	$(\text{K}, \text{Na})(\text{Fe}^{3+}, \text{Al}, \text{Mg})_2(\text{Si}, \text{Al})_4\text{O}_{10}(\text{OH})_2$
Blue	Ultramarine blue	$\text{Na}_{8-10}\text{Al}_6\text{Si}_6\text{O}_{24}\text{S}_{2-4}$
	Copper(II) acetate monohydrate	$\text{Cu}_2(\text{OAc})_4 \cdot 2\text{H}_2\text{O}$
	Blue Verditer, synthetic azurite	$2\text{CuCO}_3 \cdot \text{Cu}(\text{OH})_2$
	Azurite natural, standard	$2\text{CuCO}_3 \cdot \text{Cu}(\text{OH})_2$
	Lapis Lazuli, natural ultramarine	$(\text{Na}, \text{Ca})_8[(\text{SO}_4, \text{S}, \text{Cl})_2(\text{AlSiO}_4)_6]$
	Ultramarine Ash	$(\text{Na}, \text{Ca})_8[(\text{SO}_4, \text{S}, \text{Cl})_2(\text{AlSiO}_4)_6]$
Red	Red ochre	$\text{Fe}_2\text{O}_3, \text{FeTiO}_3$
	Vermilion	HgS
	Natural Cinnabar	$\text{HgS}(\text{mineral})$
	Madder Lake, genuine	Alizarin ;Purpurin 
	Red Lead, Minium	Pb_3O_4
	Carmine	
Yellow	Lead Tin Yellow II	$\text{Pb}(\text{Sn}, \text{Si})\text{O}_3$
	Lead oxide yellow	PbO

Table 6-5: The pigments used for the test of interaction between pigments and compounds

Firstly, clean depression concave slides were divided into 9 groups, and 19 slides for each group. Next, a small amount (around 10 mm diameter) of each pigment was placed on the 19 slides of each group respectively. Then one or two drops of prepared solution/ suspension of partially perfluorinated derivatives (according to table 6-4) and walnut oil would add to every slide in each group respectively, and one product was used for one group. (figure 6-1)



Figure 6-1: 19 pigments mixed with walnut oil

6.2.4.2 Treatments on the blanching paint-layer mock-up samples

8 blanching green earth mock-up samples and 8 blanching raw umber mock-up samples were selected for the treatments. The prepared solution or suspension of 8 partially perfluorinated compounds (including the reference compound) were applied uniformly on 8 green earth mock-up blanching samples respectively by a brush. The treated area was confined to the upper half of each sample. Subsequent additions were made once all liquid was absorbed. Application continued in this way till the surface became glossy like the paint samples without artificial aging. The same materials and treatment process were also performed on 8 raw umber mock-up blanching samples.

Micro samples were taken from treated blanching paint-layer mock-ups, to prepare as cross-sections. Those samples were mounted in a block of polyester resin and then ground and polished.

6.2.5 Methods of treatment evaluation

6.2.5.1 Optical binocular microscopy

Optical binocular microscope with a Nikon DS Fi1 camera in C2RMF was used to observe the 19 pure pigments before and after adding the partially perfluorinated compounds and walnut oil. The light source is ZLED CLS6000 with 40 % intensity. The observation of the samples was performed under magnification 3x and 8x.

Optical binocular microscope Nikon Eclipse LV 100ND with reflected visible light and fluorescence filter B2A (excitation filter and dichromatic mirror cut-on are 450–490 nm/500 nm) was used for cross-section sample study to investigate the distribution of compounds.

6.2.5.2 Spectro-colorimetry analysis

The no-contact NCS-RUBY spectrometer was used for chromatic measurements of 3 sets of samples. The first set was two reference paint-layer mock-up samples (Ref. GE, Ref. RU); the second is the blanching paint-layer mock-up samples; the third is the treated blanching paint-layer mock-up samples. NCS-RUBY spectrometer is with a tungsten halogen light source, using a spot of 6 mm diameter, a detection angle of 22° and the standard illuminant D65. The software used to export data was RUBY Manager (STIL). Spectra were measured with a wavelength λ situated between 400 and 800 nm. The coordinates used (the same with stone protection) were L^* , a^* , b^* (CIE 1986) [216]. In addition to L^* , a^* , b^* , ΔE^* which were already used in stone protection part (chapter 5), C^* and ΔC^* were also used to represent and discuss the results in the blanching easel painting restoration part.

Chroma C^* is derived from chromaticity parameters (a^* , b^*). C^* is defined by following mathematical function:

$$C^* = \sqrt{(a^{*2} + b^{*2})}$$

The parameters color change was calculated as $\Delta X^* = X^*_{\text{altered}} - X^*_{\text{reference (non-aged)}}$, where $\Delta X^*_{\text{altered}}$ is the L^* , a^* , b^* , E^* and C^* value after aging or treatments, and $X^*_{\text{reference (non-aged)}}$ is the same parameter before aging. ΔE^* value less than or equal to 3 implies an imperceptible chromatic change. [217]

6.2.5.3 Field emission gun scanning electron microscopy (FEG-SEM)

FEG-SEM was used for morphological study to observe and record the porous structures in reference paint-layer mock-ups, blanching paint-layer mock-ups and treated blanching paint-layer mock-ups. FEG-SEM was performed on a JSM-7800F with the PC-SEM version 5.1.0.1 software (JEOL). Samples were observed without any preparation and without coating. Secondary electron (SE) images were collected at 1 kV with a probe current of ca. 18–20 pA and a working distance of ca. 6–7 mm.

6.2.5.4 Scanning electron microscopy - Energy dispersive X-ray spectrometry (SEM-EDS)

SEM-EDS was used for evaluating the distribution of the perfluorinated derivatives in the treated blanching paint-layer samples by investigating the distribution of the Fluorine element in different areas of the treated samples. SEM-EDS was performed on JSM-7800F with energy-dispersive X-ray spectrometer (EDS) (Brucker, Esprit). Samples were observed without any preparation and without coating. Elemental compositions were obtained at 20 kV and a working distance of ca. 9–10 mm. SEM-EDS was also performed on FEI Philips XL30 CP with energy-dispersive X-ray spectrometer (EDS) (Oxford, Inca). The cross-section samples were carbon coated and the distribution of the chemical elements of interest was obtained at 15 kV and a working distance of ca. 10 mm.

6.2.6 Removal of the treatment (Reversibility test)

One half of the treated area of the mock-up samples was rubbed slowly by cotton swabs, which had been wet using different solvents. The solvents used for removing compounds were the same with the solvents used for treatment. For compounds **ESTF**, **DSTF**, **DC6G900**, the solvent TFE was used for the removal process. 2-propanol was used for removing **C-Glc-OH**, **ESF**, **DS** and **DF**. Ethyl acetate was used to remove **C-Glc-OAc**.

6.2.7 Evaluation of the reversibility

6.2.7.1 Spectro-colorimetry analysis

The no-contact NCS-RUBY spectrometer was used for chromatic measurements of the removal part of treated area. All the measurements parameters and conditions stayed the same with evaluation on the treated parts. The coordinates used were also $L^* a^* b^*$ (CIE 1986).

6.2.7.2 Field emission gun scanning electron microscopy (FEG-SEM)

FEG-SEM was used for observing and recording the porous structures on the removal parts. The preparation process and measurement conditions stayed the same with evaluation on the treated parts.

6.2.7.3 Scanning electron microscopy - Energy dispersive X-ray spectroscopy (SEM-EDS)

SEM-EDS was used for evaluating the reversibility of the treatments, by investigating the change on quantity of Fluorine element on the removal parts and treated parts. SEM-EDS was performed on JSM-7800F with energy-dispersive X-ray spectrometer (EDS) (Brucker, Esprit). Samples were observed without any preparation and without coating. Elemental compositions were obtained at 20 kV and a working distance of ca. 9–10 mm.

6.3 Results and discussion

6.3.1 Treatments on the pure pigments

The blanching phenomenon was reported to appear on blue, green, brown, red, dark, and grey and yellow areas in the blanching paintings [71]. Pigments were usually used separately, or several pigments were mixed together for creating those colors in the easel painting

between 16th to 18th centuries. For example, the blanched green trees of the 15 paintings from Dughet and Claude, were composed mostly by green earth, ochre, bone black, chalk, lead tin yellow. [76] For a restoration product especially used for paint layers of those old master paintings, it should not cause any additional degradation, like darkening, crystallization *etc.* Therefore, each partially perfluorinated compound was directly added on the pure pigments which are sensitive to blanching. The compound which can cause degradation of the pigment will not be considered as a qualified product for blanching restoration. The compounds and pigments which show the physical or chemical degradation after being mixed, were reported in the following:

- **C-Glc-OAc**

For the compound **C-Glc-OAc**, its physical state is white solid. A transparent solution can be obtained, when **C-Glc-OAc** is dissolved in ethyl acetate with 30 % w/w concentration. With adding one or two drops of its solution, the white solid can reappear on the all pigments' surface in less than 1 day after the treatment. Under optical binocular microscope, the white solid can be observed clearly. For example, the white solid can be obviously identified from the original green earth pigment. (figure 6-2)

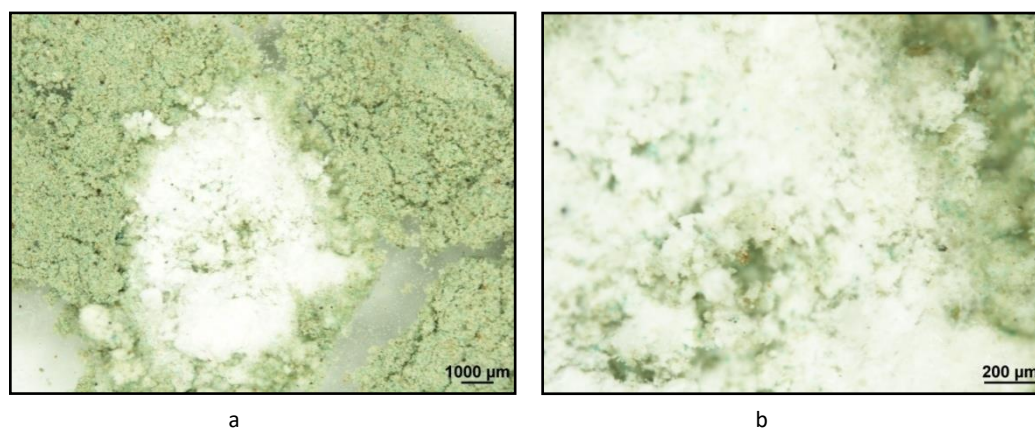


Figure 6-2: Green earth pigment after adding C-Glc-OAc under optical microscope a) With magnification 3×; b) With magnification 8×

Considering the physical state of **C-Glc-OAc**, the white solid appeared on the pigments could be the deposit of the original compound after the solvent evaporated. In order to confirm this hypothesis, the white solid on the pigment was examined by FT-IR. Comparing the spectrums (figure 6-3) of the original compound **C-Glc-OAc** (in pink) and the white solid (in blue), no significant differences (characteristic peaks of N-H and C=O, and the fingerprint area) have been brought to light between the original compound and the white solid on green earth. Thus, the investigation from FT-IR indicates the white solid is the original compound.

From the results of testing **C-Glc-OAc** on pure pigments, the white deposit could appear in a short time and create the obvious visual change on the pigments. As a result, **C-Glc-OAc** could make the paint layer become a more complicated system. Also, the white solid itself would not help decrease the blanching. Therefore **C-Glc-OAc** is not a suitable product for blanching painting restoration, based on the results from testing it on pure pigments.

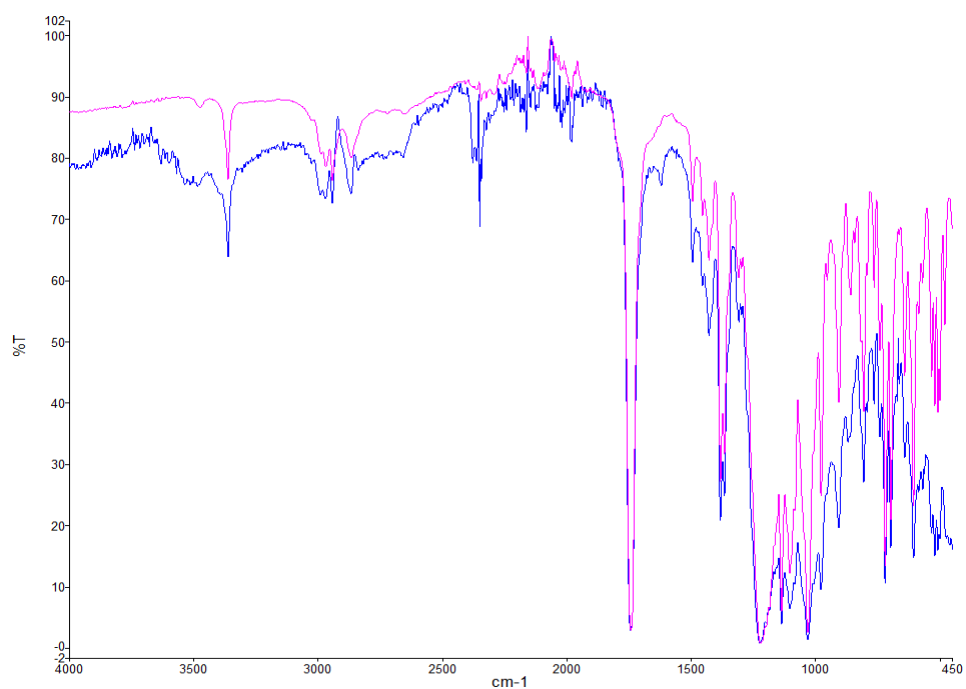
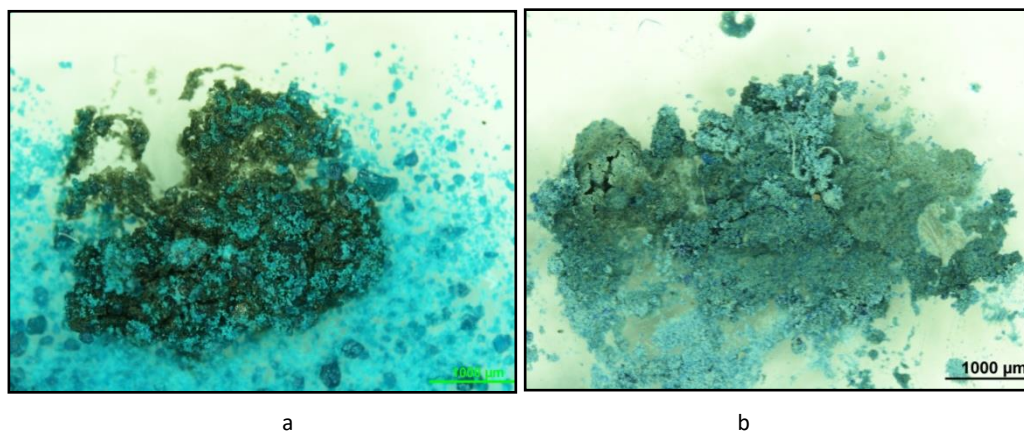


Figure 6-3: FTIR spectrum of the original compound C-Glc-OAc (pink), and the white solid appearing on green earth (blue)

- **C-Glc-OH**

C-Glc-OH is a lightly yellow oil, and it becomes a transparent solution after dissolving in 2-propanol with a 30 % w/w concentration. One or two drops of the solution were added to all the tested pigments. After the examination under optical binocular microscope, obvious darkening can be observed on the pigments Copper (II) acetate monohydrate, and Azurite (synthetic and natural) after 12 days. (figure 6-4)



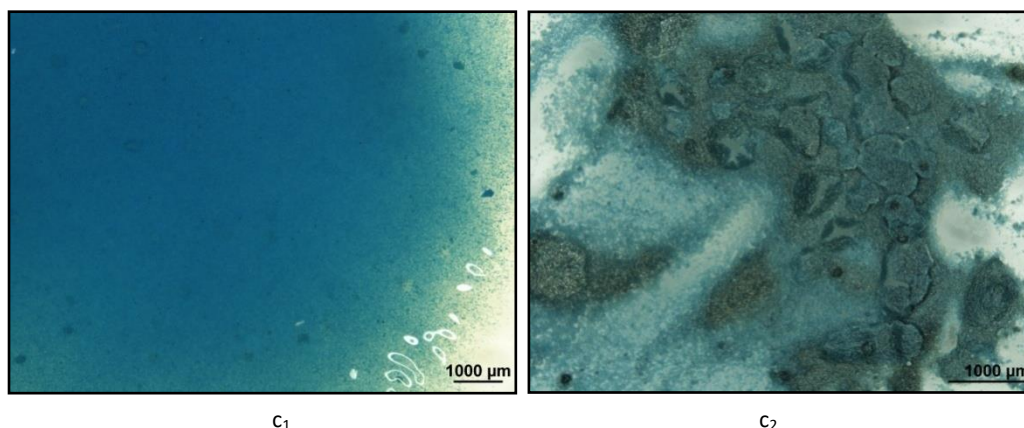


Figure 6-4: a) Copper (II) acetate monohydrate with C-Glc-OH; b) Azurite natural with C-Glc-OH; c₁) Synthetic azurite with walnut oil; c₂) Synthetic azurite with C-Glc-OH; All the observation were under optical microscope with magnification 3×

In the figure 6-4 a), the severely darkening is clearly observed in the part where the Copper (II) acetate monohydrate mixed with **C-Glc-OH**. And in figure 6-4 b), a weaker darkening is easily identified from the original pigment Azurite natural. Figure 6-4 c₁) shows the mixture of Synthetic azurite and walnut oil. This mixture was set as a reference, in order to get a visually contrast from the mixture of synthetic azurite and **C-Glc-OH** under the optical microscope (figure 6-4 c₂). Comparing figure 6-4 c₁) and c₂), the darkening could be identified in the mixture of Synthetic azurite and **C-Glc-OH**.

Copper (II) acetate monohydrate ($\text{Cu}_2(\text{OAc})_4 \cdot 2\text{H}_2\text{O}$) is a bimetallic green copper pigment used in easel paintings around the 15th to 18th centuries in Europe. Its use was quickly given up because of their tendency to progressively darken with time. Alter M *et al.* reported that the darkening is induced by ambient light and atmospheric oxygen. The bimetallic Cu (II) complexes are photodissociated by the dissociation of bridging carboxylate ligands. The resulting bimetallic Cu (I) complexes are re-oxidized by molecular oxygen molecules, giving a peroxy-bimetallic Cu (II) complex responsible for the darkening. [230]

Azurite ($2\text{CuCO}_3 \cdot \text{Cu}(\text{OH})_2$) was the most diffused blue pigment during Middle Ages and before, and darkening also reported on Azurite in paintings. Humidity, chloride ions and hot alkali were reported to cause the formation of black copper oxide and as a result the darkening can be observed on Azurite. [231]

In our case, the hydroxyl groups of **C-Glc-OH** probably can act as ligands to form the hydroxo bridging or alkoxo bridging in Cu (II) complexes after **C-Glc-OH** mixed with Cu (II) pigments. The change of the structure could lead to the darkening on those pigments.

Based on the results from optical microscope, the confirmed conclusion is that partially perfluorinated C-glycoside **C-Glc-OH** could cause darkening in Copper (II) acetate monohydrate, Synthetic azurite and Azurite natural.

Except the pigments mentioned above, Carmine shows darkening under microscope on the 3rd day, after mixed with **C-Glc-OH**. (figure 6-5)

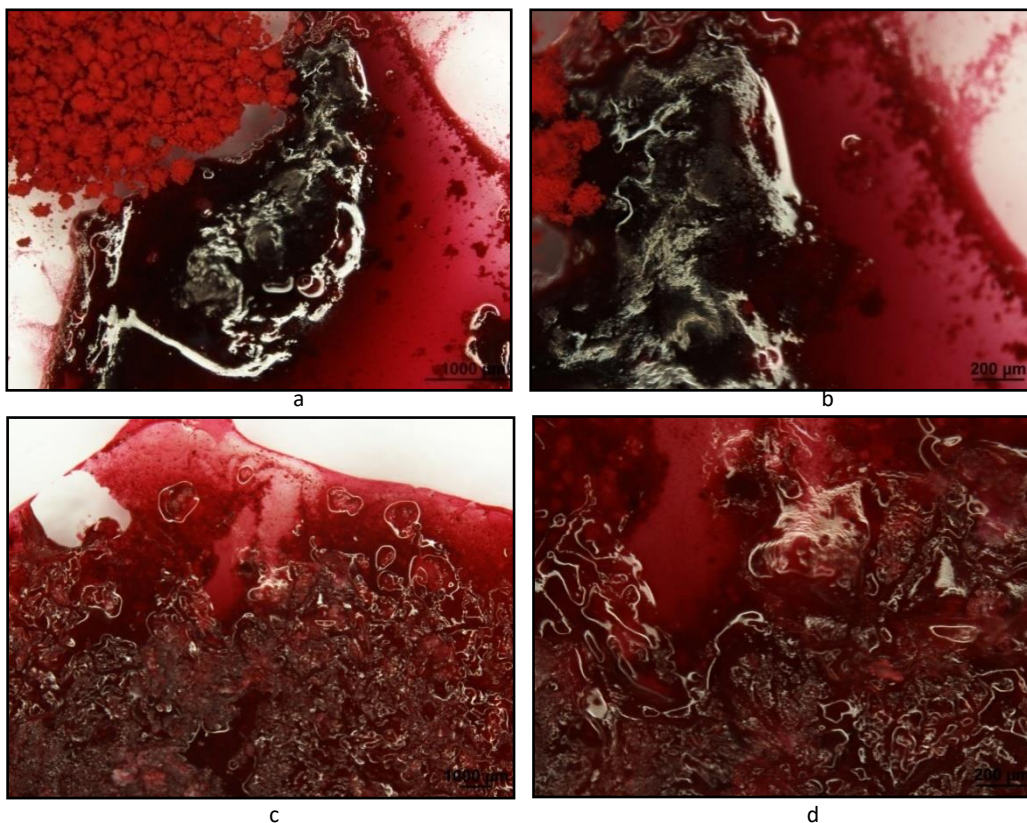


Figure 6-5: a) Carmine with C-Glc-OH under optical microscope with magnification 3x; b) Carmine with C-Glc-OH under optical microscope with magnification 8x; c) Carmine with walnut oil under optical microscope with magnification 3x; d) Carmine with walnut oil under optical microscope with magnification 8x

Comparing with the mixture of walnut oil and Carmine, the darkening appeared in some area of the mixture of **C-Glc-OH** and Carmine. Carmine is a metal coordination complex involving aluminium and glucosidal hydroxylanthrapurin. Two molecules of glucosidal hydroxanthrapurin coordinately bound to a single aluminum atom at carbonyl-hydroxyl pairs. [232] (figure 6-6) In order to investigate if there is chemical change of the Carmine and **C-Glc-OH** in the darkening area, ^1H NMR of **C-Glc-OH**, Carmine and the darken mixture was performed in D_2O .

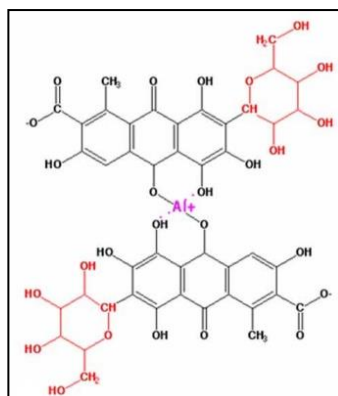


Figure 6-6: Structure of Carmine

Comparing the ^1H NMR spectrums (figure 6-7) of the original compound **C-Glc-OH** (in blue), the darken mixture (in green) and Carmine (red), no significant chemical shift change has been brought to light between the original compounds and the darken mixture. The signals attributed to **C-Glc-OH** can be clearly observed in the spectra of the darken mixture, it indicates that no chemical change of the **C-Glc-OH** could be detected. Concerning Carmine, there are signals with similar shape and chemical shift (around 3.8 ppm) can be found in both Carmine (attributed to H in C2) and darken mixture's spectras. [233][234] However, Carmine's signals could not be clearly and fully observed due to the overlaps with signals of **C-Glc-OH** and the relatively lower amount in the tested sample. Therefore, no interaction between **C-Glc-OH** and Carmine could be detected by ^1H NMR. However, D_2O used as a solvent in NMR experiment could break the interaction between Carmine and **C-Glc-OH** has to be considered.

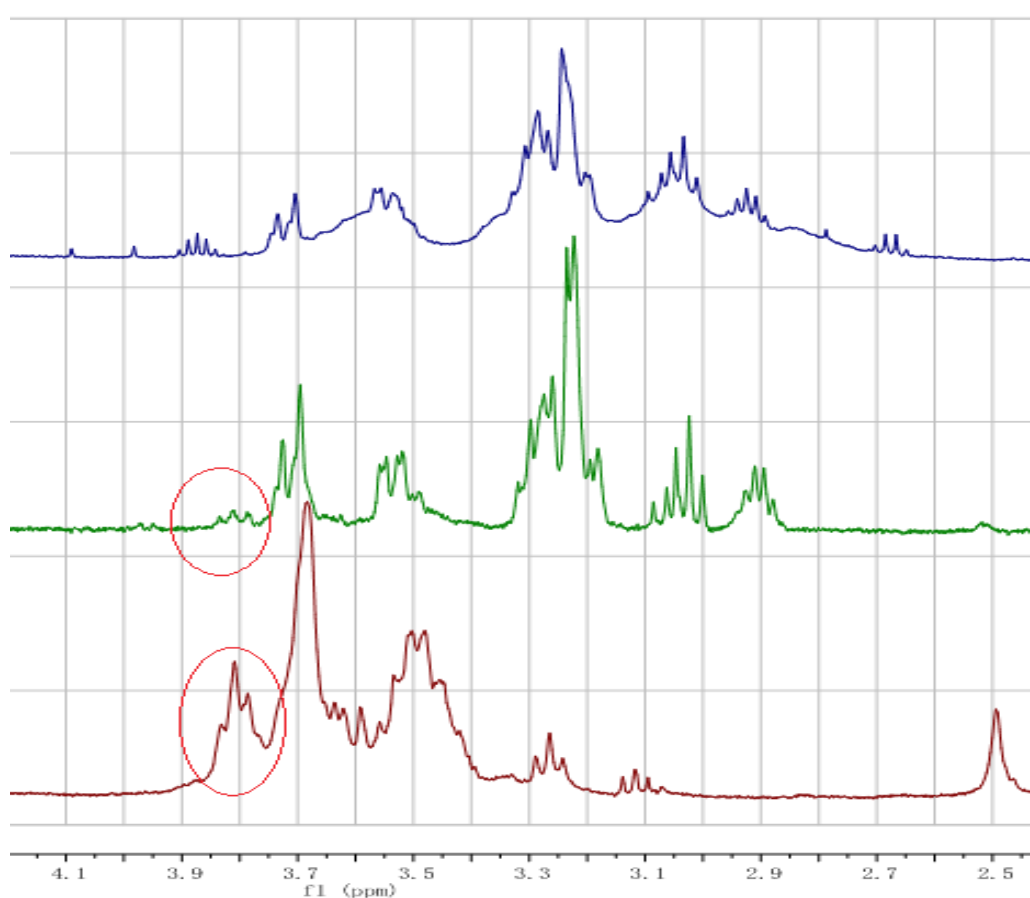


Figure 6-7: ^1H NMR (D_2O) spectras of C-Glc-OH (blue), the darken mixture (green) and Carmine (red)

In summary, according to the results of optical microscopy, **C-Glc-OH** would cause the darkening in Cu (II) pigments: Copper (II) acetate monohydrate, Synthetic azurite and Azurite natural. Also it could cause darkening in Carmine. Although the reasons behind the darkening are not fully understood, it is risky to use **C-Glc-OH** on the restoration of the blanching paintings, especially for the paintings containing those pigments.

- **ESF**

ESF is white solid and becomes white suspension in 2-propanol with 13 % w/w concentration.

One or two drops of the suspension were added into the tested pigments. After 23 days, white solid appeared on Carmine (figure 6-8). The white solid could probably be the deposit

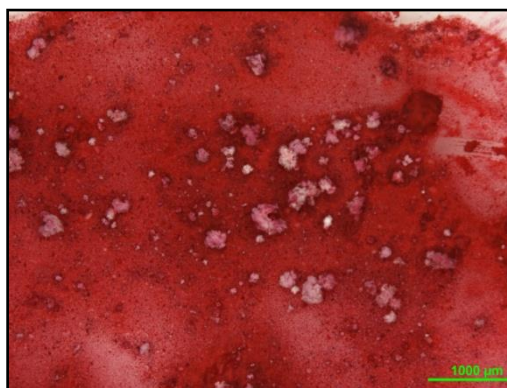


Figure 6-8: Carmine with **ESF** under optical microscope with magnification 3X

of the **ESF** after the solvent evaporated. However, there is no sign that white solid appeared on other pigments. In conclude, **ESF** is not a suitable restoration compound for easel paintings, especially the paintings with Carmine as a pigment.

To summarize, white deposit (**C-Glc-OAc**) was observed on the 19 tested pigments after added the solution of **C-Glc-OAc**. **C-Glc-OH** would cause the darkening in Cu (II) pigments: Copper (II) acetate monohydrate, Synthetic azurite and Azurite natural, and Carmine. White solid was observed on Carmine after added the suspension of **ESF**. Although those physical or chemical degradations are not fully understood, the results based on optical microscopy indicate that it should be avoided to use **C-Glc-OAc**, **C-Glc-OH** and **ESF** as blanching restoration compounds, especially when it comes to the paintings consisted of Cu (II) pigments and Carmine.

6.3.2 Treatments on blanching paint-layer mock-up samples

6.3.2.1 Paint-layer mock-up samples and their artificial aging

In our research of blanching easel painting restoration, the basis of the restoration practical is to reproduce the blanching in mock-up paint samples. The synthesized compounds could be tested and checked if they were effective for blanching restoration, only if the blanching mock-up samples were obtained. According to the research of Genty *et al.*, the binder, pigments, extender and their relative quantity of paint-layer mock-up are important factors for obtaining blanching. The appropriate conditions of aging the mock-ups are also essential for reproducing blanching. [84] Based on the successful conditions explored in previous research, green earth and raw umber paint-layer mock-ups were

prepared in glass slides, and aged by “wet-dry” cycles and UV light. The altered green earth and raw umber mock-up samples were obtained using similar preparation and aging conditions with Genty. *et al.* [84] The paint-layer mock-up samples without aging were set as references and the altered mock-up samples after artificial aging, were recorded by photography (visible imaging). Figure 6-9 shows the green earth mock-up without aging, which is marked as “Reference”, and the other 11 aged mock-ups.

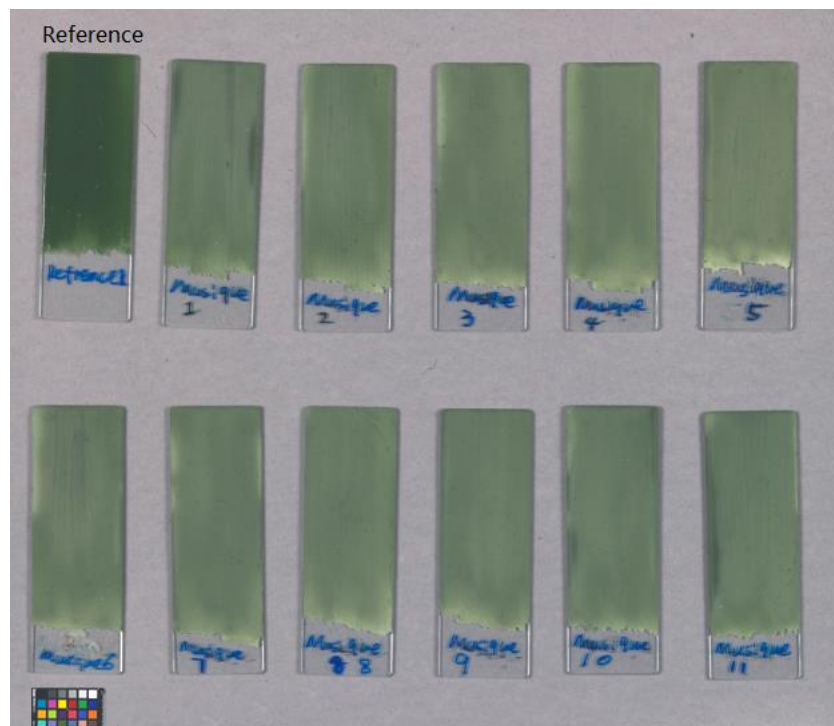


Figure 6-9: Mock-up reference (without aging) and 11 aged mock-up samples ©C2RMF/Anne Maigret

From figure 6-9, the alteration of whitening can be obviously observed in the 11 samples by human eyes. And it shows that the alteration is not homogeneous. More altered, less unaltered and no-altered areas can coexist within a same color range. For example, the bottom parts of the alteration sample show more obvious whitening than other parts in the same sample.

Figure 6-10 shows the raw umber mock-up without aging, which is marked as “Reference” on the photo, and the other 11 aged mock-ups. After the same aging process, the 11 aged samples show less obvious alteration than aged green earth samples.

The altered raw umber samples seemed less glossy and less dark than the reference.

However, it is difficult to confirm the alteration of the aged paint-layer mock-ups is blanching only through human eyes and the photography. Therefore, characterization of the reference and altered samples by colorimetry analysis and micro structure analysis is necessary, and it is reported in the following part.

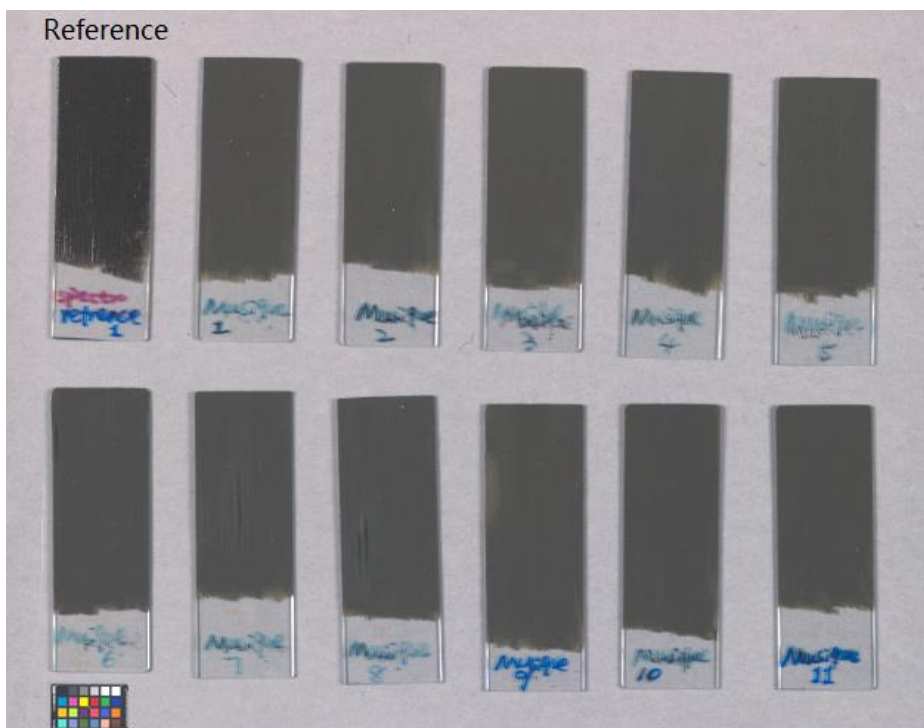


Figure 6-10: Mock-up reference (without aging) and 11 aged mock-up samples ©C2RMF/Anne Maigret

6.3.2.2 Characterizations of no-treated paint-layer mock-up samples

Characterizations of the no-treated paint-layer mock-up samples were realized by two methods: colorimetric measurements in macro scale and morphological study in micro scale.

- **Colorimetric measurements**

Genty *et al.* reported the value variation in brightness parameter L^* is related to blanching. The L^* value increases significantly, while the change in chromaticity parameters a^* and b^* are weak after the colorimetric analysis on the blanching painting *L'Aurore* from the Louvre museum. Later, they reported more specific information of the colorimetric analysis on blanching paint-layer mock-up samples: a maximum $\Delta C^* = 3.11$ and a maximum $\Delta L^* = 18.6$ in blanching green earth mock-ups; a maximum $\Delta C^* = 2.09$ and a maximum $\Delta L^* = 17.25$ for blanching raw umber mock-ups. Moreover, the increase of the pore concentration induces the increase of L^* parameter in the blanching paint mock-ups. [86] Therefore, the L^* is a significant parameter to characterize blanching.

In our case, the colorimetric measurements were performed on the reference paint-layer mock-up samples (non-aged) and the altered mock-up samples (after aging), which were presented in the figures 6-9 and 6-10. Three measurements were performed in the same area. Average values of L^* , a^* , b^* of the reference (non-aged) and altered samples and the calculated ΔL^* , ΔC^* of the altered samples comparing with reference were reported in table 6-6. As all the altered samples were prepared by the same process and have been aged under the same conditions, the colorimetric measurement results of each altered sample

using the same pigment were highly similar. The “altered” in the table, represents one altered sample of green earth or raw umber.

Comparing the altered and reference green earth mock-ups, a significant increase of L* at 19.16 was reported while the C* value slightly decreased after the aging process. Those results fit in previous research on blanching painting and mock-ups. [71] That means the alteration of the aged green earth mock-ups is visually blanching in the macro scale. For the raw umber mock-ups, similar results were obtained. Comparing with the reference sample, L* value of aged sample is 10.42 more than the reference sample while the C* value only increases at 0.1. Thus, in the macro scale, the alteration of the aged raw umber mock-ups is blanching.

In summary, the alteration of the aged green earth and raw umber mock-ups was characterized by colorimetric measurements. And the results indicate the aging process reproduced blanching successfully in the macro scale. The alteration visually fit the features of blanching.

Samples		Color view	L*	a*	b*	ΔL^*	ΔC^*
Green earth mock-ups	Reference (non-aged)		28.47	-11.84	9.46	19.16	-0.68
	Altered		47.63	-8.05	12.03		
Raw umber mock-ups	Reference (non-aged)		16.07	3.2	2.37	10.42	0.1
	Altered		26.49	2.31	3.37		

Table 6-6: Chromatic characteristics of reference paint-layer mock-up samples (without aging) and the altered mock-up samples (after aging); $\Delta L^* = L^* - L^*_{reference}$; $\Delta C^* = C^* - C^*_{reference}$

- **Morphological study in micro scale**

In micro scale, porous is the significant morphological feature of the blanching area in easel paintings. In fact, like mentioned in the Instruction chapter, the presence of porosity leads to a scattering of the light and as a consequence leads to blanching of the paint surface. Therefore, a blanching sample is supposed to have porous structure in micro scale. In order to characterize the paint-layer mock-ups and investigate if the blanching was reproduced successfully in micro scale, the reference samples (without aging) and the altered samples (artificial aged) were studied by FEG-SEM. It is necessary to note that the traditional sample preparation approach (*i.e.*, embedding in resin and polishing a sample cross-section) would render the proper observation impossible. That is because the resin would change the original structure in the sample by resin penetration [235]. However, it has been proved an innovative approach requiring no sample preparation could ensure the non-modification of

the internal structure of the sample. And in this way, the porous structures can be successfully observed in the blanching easel paintings. Therefore, in our study, the observation with no sample preparation was performed by FEG-SEM on the reference and altered mock-ups. The observation results of reference and altered green earth mock-ups by FEG-SEM were reported in figure 6-11.

In figure 6-11, the micro structures of reference green earth samples are shown in image a) and b) with different magnifications. The pigment particles are well agglomerated in the binder. No porous structure can be observed in those images. That means no artificial aged and no altered green earth mock-up sample does not have porous structure in micro scale. While, obvious micro structure modifications can be seen in images c) and d), which show the micro structures of altered green earth mock-ups. The observations by FEG-SEM in images c) and d), reveal that pores present in the altered mock-up samples. The pores are not in the exactly spherical shape due to spatial constraints imposed by the presence of pigments. The pore sizes are around 1-5 μm in figure 6-12, which is the image of altered green earth mock-up with different magnification under FEG-SEM. These observation results correspond well to the observations on blanching ancient paintings and blanching mock-ups reported by Genty *et al.* [84]. Therefore, the characterizations on the reference and altered green earth mock-ups by FEG-SEM morphological study indicate the alteration in the micro scale is blanching, which means blanching was reproduced successfully in the altered green earth samples.

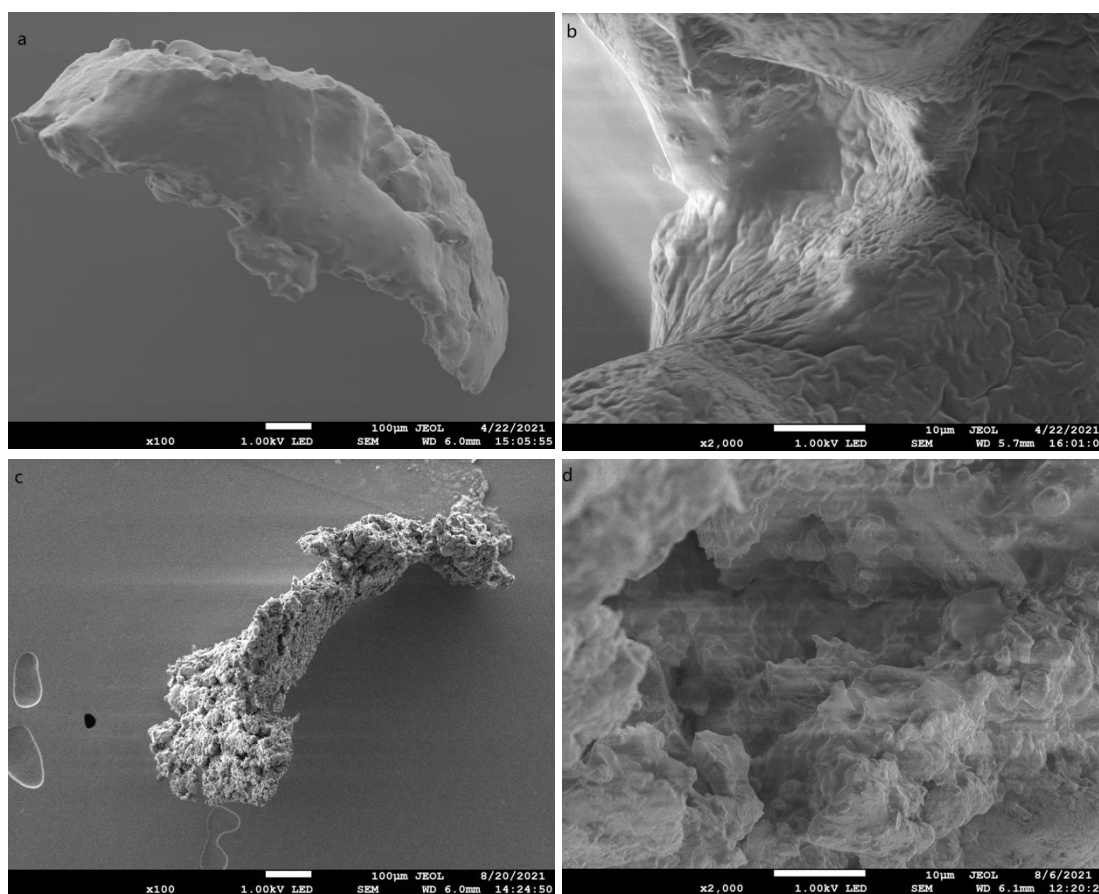


Figure 6-11: FEG-SEM images at 1 kV. Scale bar 10 μm a) Reference green earth mock-up; b) Zoom of the reference green earth sample; c) Altered green earth mock-up; d) Zoom of the altered green earth mock-up.

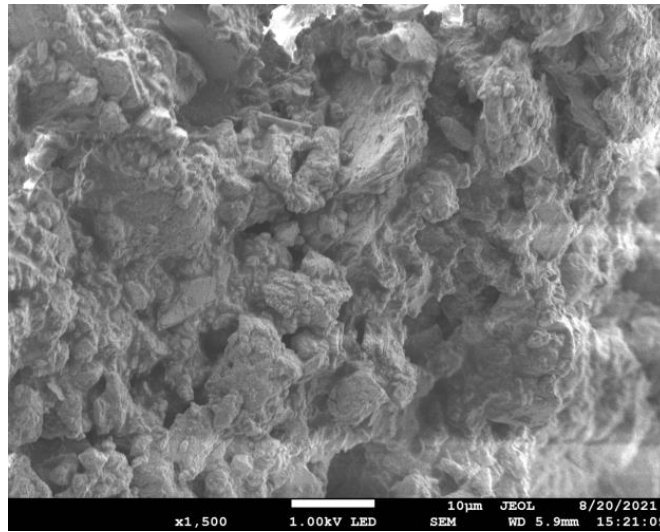
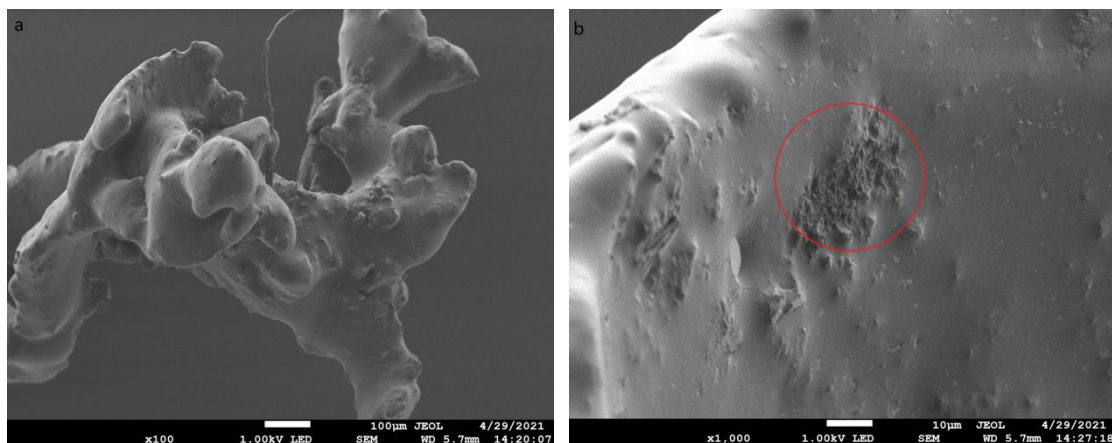


Figure 6-12: FEG-SEM image of altered green earth mock-up at 1 kV. Scale bar 10 μ m

Similar micro structure modifications were observed, comparing the FEG-SEM images of reference and altered raw umber mock-ups.

Firstly, the observations were on reference raw umber mock up sample with FEG-SEM. The results were reported in figure 6-13. In image a), which was obtained with magnification 100X, the pigment particles are agglomerated in the binder and no porous structure observed. In the image b), which was zoomed with 1000X magnification, there is no pore can be observed. However, there is one part (in red circle of image b)) where seems more non-uniform than other areas. In order to confirm there is no pore in this area, this part was zoomed at 2000X and 10000X magnifications. Those images show that this part is not porous. Their presence could probably be due to the inhomogeneous grounding process of binder, pigment and extender. Therefore, no artificial aged and no altered raw umber mock-up sample have no pores from the morphological study by FEG-SEM.



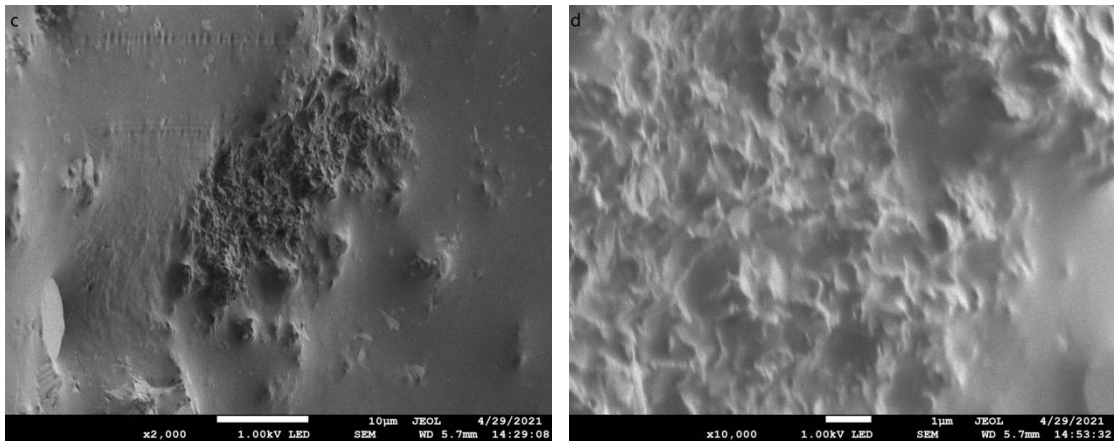


Figure 6-13: FEG-SEM image of reference raw umber mock-up at 1 kV. Scale bar 10 μm . a) Image under magnification 100X; b) Image under magnification 1000X; c) Zoom of image under magnification 2000X; c) zoom of image under magnification 10000X

Next, observation by FEG-SEM was performed on the altered raw umber mock-ups and the results were reported in figure 6-14. Significant micro structure modifications can be seen in the FEG-SEM images of the altered raw umber mock-up, comparing with reference raw umber sample. Like the altered green earth mock-up, the porous structure of altered raw umber sample is also revealed by FEG-SEM. The observed pore size is around 1-2 μm . Those observations also correspond to the results of observing blanching ancient paintings and mock-ups reported by Genty *et al.* [84]

Therefore, the characterizations on the reference and altered raw umber mock-ups by FEG-SEM morphological study indicate the alteration in the micro scale is blanching, which means blanching was reproduced successfully raw umber samples.

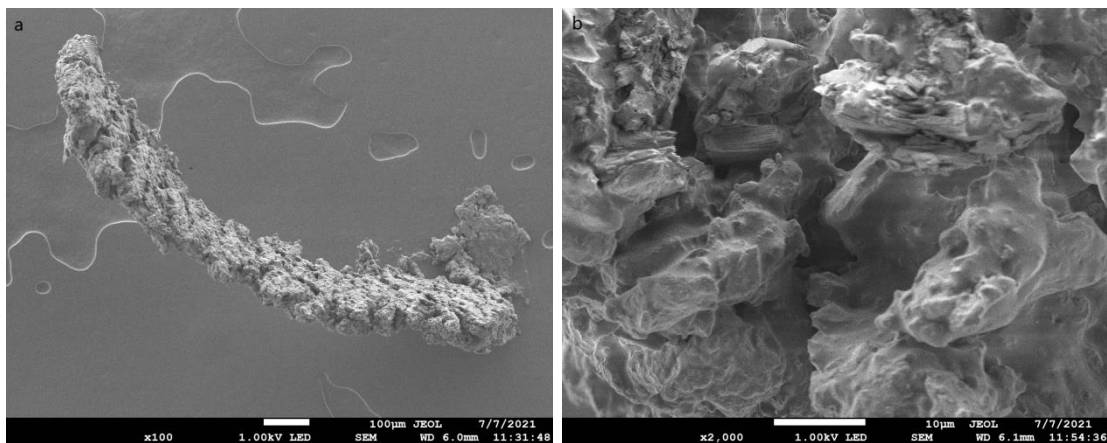


Figure 6-14: FEG-SEM images at 1 kV. Scale bar 10 μm a) Altered raw umber mock-up; b) Zoom of the altered raw umber mock-up.

Thus, the characterizations of micro structures in reference, and altered green earth and raw umber mock-ups by FEG-SEM, confirmed the presence of pores and the alteration consequently is blanching in all those two groups of mock-ups. Blanching was successfully reproduced in aged green earth and raw umber mock-ups in micro scale.

To be summarized, characterizations were performed on the reference and aged mock-up

samples through the colorimetric measurements in macro scale and FEG-SEM morphological observations in micro scale. The results indicate that the alteration in the aged samples is blanching. And those blanching mock-up samples in green earth and raw umber can be, therefore, used as objects in the restoration by partially perfluorinated derivatives.

6.3.2.3 Evaluation of the restoration treatments on blanching paint-layer mock-up samples

The new seven partially perfluorinated derivatives, and the reference compound **DC6G900** were applied on the blanching mock-up samples. Volatile solvents: 2-propanol, TFE, ethyl acetate, were used for the solvents in the treatments process. For all the products except C-glycosides, their solutions or suspensions with respective maximum concentration were used for the treatment. This choice of volatile solvent and maximum concentration was due to avoiding the uptake of extra solvent and long retention time of solvent in paint layer. The extra solvent may result in the migration (redistribution) of soluble components between paint layers. The migration of soluble paint components can enhance the rate of degradation reactions inside oil paint [236]. Therefore, volatile solvents and the maximum concentration are the priority options in the treatment process design. As for C-glycosides, they are highly soluble in 2-propanol or ethyl acetate. Keeping the same concentration used for C-glycoside solution with other products, could help for the comparison of restoration efficacy against blanching. Therefore, 30% w/w was set for C-glycoside solutions, like other 4 compounds reported in table 6-4.

The solution or suspension of each compound was applied several times on the blanching sample, until the treated sample was observed glossy as the non-aged reference sample. In order to give a clear contrast between the treated and untreated parts in the same sample, the treatment was only confined to the upper half of each sample. Photography (visible imaging) documented the treated blanching samples after the first treatment and the last treatment. Figure 6-15 a) shows the treated green earth samples after the first application of compounds, and sample treated by DSTF looked glossier than other treated samples. Figure 6-15 b) shows the treated green earth samples after the last application of compounds, and the significant differences could be observed on the treated samples comparing the first application.

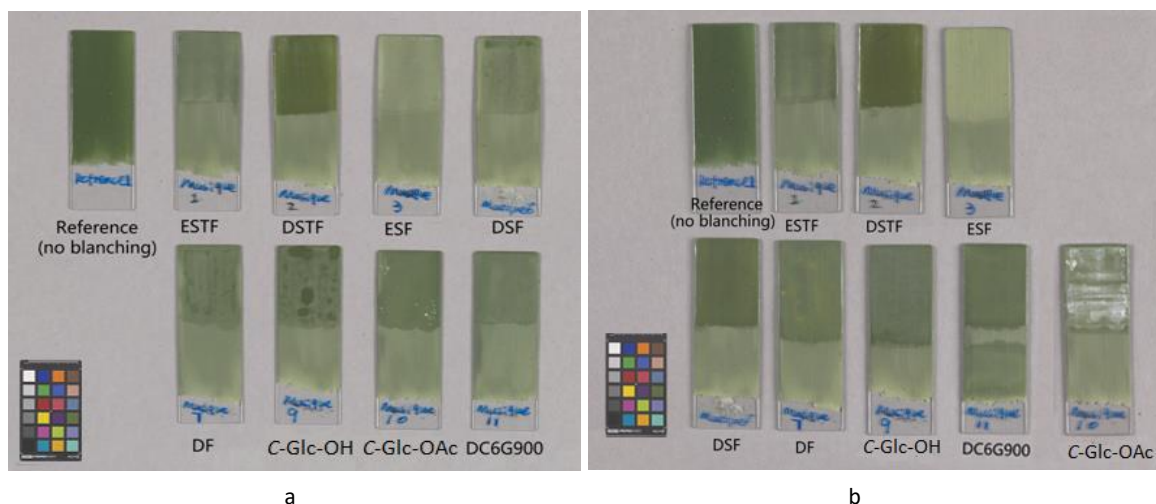


Figure 6-15: Photography of treated green earth samples. The sample was named as the compound applied on it. Reference is the no aged and no blanching sample. a) The photo after 1st treatment; b) The photo after the last treatment. ©C2RMF/ Anne Maigret

In particular, an obvious improvement of gloss appeared on the samples treated by **DSTF**, **DSF**, **DF**, **C-Glc-OH** and **DC6G900**. The samples treated by **ESF** and **C-Glc-OAc**, the treated upper-half looked more whitening than the non-treated half after applying more amount of compounds (figure 6-16). In fact, white deposit can be observed on those two samples.

That is because the extra white solid **ESF** and **C-Glc-OAc** was deposited on the mock-ups, after the solvent evaporated. This result on **ESF** and **C-Glc-OAc** is corresponding to the result observed on pure pigments, and indicates **ESF** and **C-Glc-OAc** are not suitable restoration products on blanching paintings.



Figure 6-16: The samples treated by **ESF** and **C-Glc-OAc** after the last application of compounds.

For the blanching raw umber mock-ups, the compounds were applied on the samples once and the obvious increase of gloss can be observed in the samples treated by **C-Glc-OH**, **DF**, **DSF**, **DSTF** and **DC6G900** (figure 6-17).

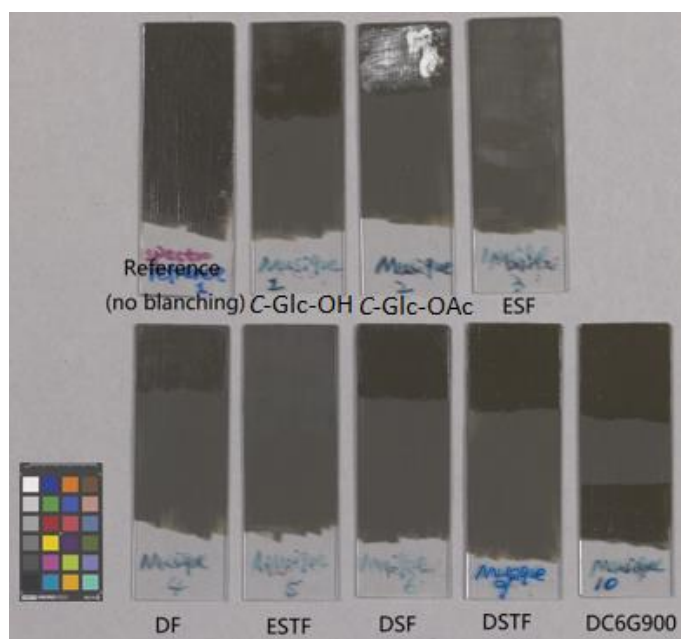


Figure 6-17: Photography of treated raw umber samples ©C2RMF/ Anne Maigret

White solid can be observed on the samples treated by **ESF** and **C-Glc-OAc**, similar with on green earth samples. Therefore, this result is also indicating **ESF** and **C-Glc-OAc** are not suitable restoration products.

By the preliminary evaluation through photography of treated green earth and raw umber samples, **ESF** and **C-Glc-OAc** are not suitable restoration products on blanching paintings. **C-Glc-OH**, **DF**, **DSF**, **DSTF** and **DC6G900** gave an obvious improvement of gloss on the blanching samples. **ESTF** did not give an obvious increase of gloss on the treated samples.

- **Colorimetric measurements**

Colorimetric measurements were performed on the treated green earth and raw umber mock-ups. The measurement result corresponding to each product on treated green earth sample was presented in the table 6-7, also the measurement results of non-aged reference and blanching reference were presented. The change of L^* was firstly investigated, as it is significantly related to the blanching. In order to obtain a clear contrast of the data, ΔL^* of each sample was presented in the figure 6-18. In this case, ΔL^* means the difference of L^* between the treated sample and non-aged reference, and its calculation cited the results from the table 6-7. From the figure 6-18, the sample treated by **DSTF** has the least ΔL^* , which means its luminance is closest to the non-aged sample. And **DSTF** is effectively against blanching, as it has significantly decreased the value of L^* comparing with blanching sample. Thus, it has the best performance to revive the original luminance of the blanching sample, and decrease the degree of blanching. Compounds **C-Glc-OH** and **DSF** also give good performance with ΔL^* below 5. Compounds **DC6G900**, **ESTF** and **DF** also help to decrease L^* of treated samples, comparing with the blanching sample.

Although, the sample treated by **ESF** becomes obviously white shown on the photography

image, the colorimetric measurement was performed. Compound **ESF** gives a higher L* value than blanching sample, which means it is not effectively against blanching. The high L* value is due to the white product depositing after the solvent evaporated.

In order to investigate how the color changed, their colorimetric results were presented in CIE a* b* space (figure 6-19)

Sample (treated by compounds)	L*	a*	b*	ΔL^* (compared with non-aged)	ΔE^* (compared with non-aged)
Non-aged	27.79	-11.67	9.3	-	-
Blanching	43.28	-8.92	12.82	15.48	16.12
ESTF	36.44	-9.45	11.04	8.65	9.15
DSTF	28.77	-9.14	14.75	0.97	6.09
ESF	53.72	-9.41	18.36	25.93	27.56
DSF	32.74	-9.88	13.67	4.94	6.83
DF	36.47	-9.76	12.38	8.68	9.40
C-Glc-OH	32.21	-8.27	9.93	4.42	5.61
DC6G900	35.83	-10.89	13.81	8.04	9.25

Table 6-7: Results of colorimetric measurements of treated green earth samples, non-aged green earth sample, and non-treated blanching sample.

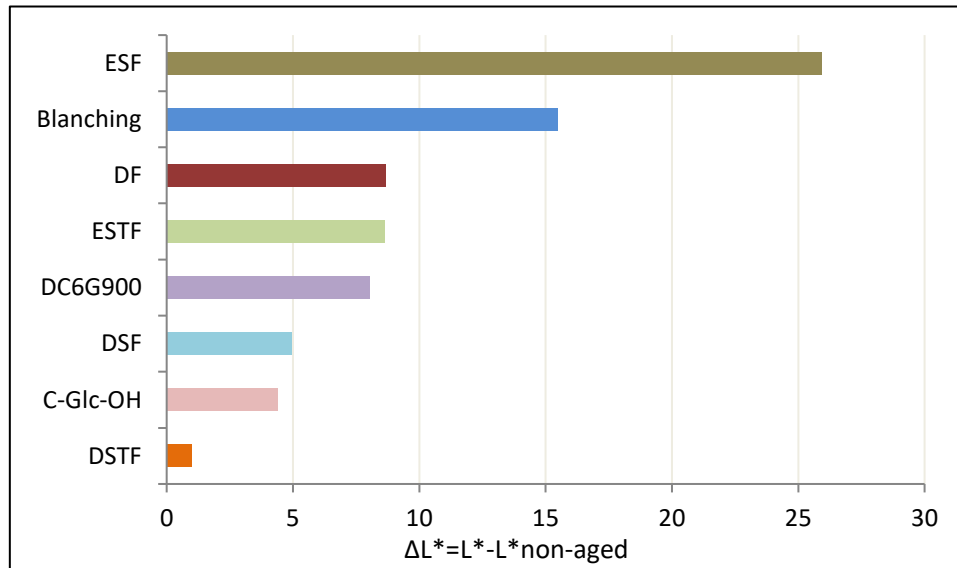


Figure 6-18: ΔL^* of the treated and blanching green earth samples compared with non-aged green earth sample

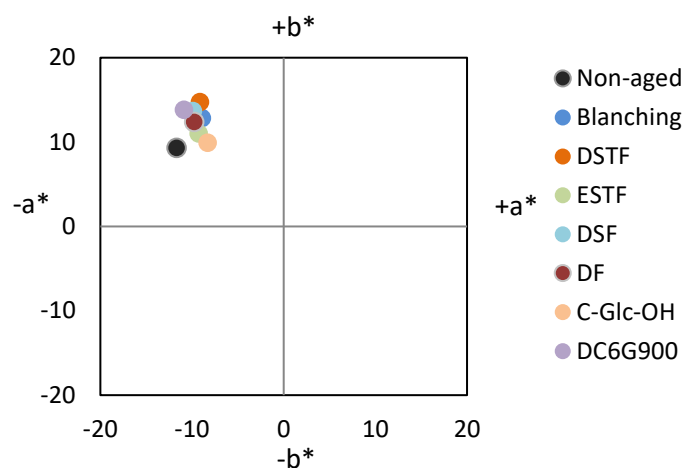


Figure 6-19: CIE a^*b^* space of green earth samples

From the CIE $a^* b^*$ space (figure 6-19), all the treated samples have increased a^* and b^* value, which means the colour of the treated samples become more red and yellow. Among those compounds, **DSTF** gave the most increase in b^* value, followed by **DC6G900** and **DSF**. Compound **C-Glc-OH** gave the most increase in a^* value. Compounds **DF** and **ESTF** gave slightly chromaticity change, similar with the blanching samples.

ΔE^* , which represents the total color change, was listed in the table 6-7. **C-Glc-OH** gave the least ΔE^* at 5.61, followed by **DSTF** (6.09) and **DSF** (6.83). For **DF**, **ESTF**, **DC6G900**, ΔE^* are around 9. That is due to the L^* of samples treated by those compounds is relatively higher. Except **ESF**, all the tested samples show less ΔE^* than non-treated blanching sample. That means, although the total color variant between the treated samples and non-aged samples is perceptible for human eyes, the restoration treatment decreased the color variant between blanching sample and non-blanching sample.

In summary, concerning L^* parameter, partially perfluorinated compounds **DSTF**, **C-Glc-OH**, **DSF**, **DC6G900**, **ESTF** and **DF** could visually decrease blanching on green earth samples. And among those compounds, **DSTF** has the closet L^* with non-blanching sample, followed by **C-Glc-OH** and **DSF**. Concerning the total colour variant ΔE^* , **C-Glc-OH**, **DSTF**, **DSF**, **ESTF**, **DC6G900** and **DF** could decrease the colour variant between blanching sample and non-blanching green earth sample. **C-Glc-OH**, **DSTF**, **DSF** have the lowest ΔE^* around 6.

The colorimetric measurement results of treated raw umber samples were reported in table 6-8.

Sample (treated by compounds)	L*	a*	b*	ΔL^* (compared with non-aged)	ΔE^* (compared with non-aged)
Non-aged	15.88	3.46	1.64	-	-
Blanching	25.31	2.21	2.83	9.43	9.59
ESTF	23.02	2.33	2.49	7.14	7.28
DSTF	17.59	2.69	5.08	1.71	3.92
ESF	28.28	1.98	3.37	12.40	12.61
DSF	17.50	3.81	2.89	1.62	2.07
DF	19.39	2.64	3.99	3.51	4.30
C-Glc-OH	16.74	3.86	3.45	0.86	2.04
DC6G900	18.53	3.33	3.88	2.66	3.47

Table 6-8: Results of colorimetric measurements of treated raw umber samples, non-aged raw umber sample, and non-treated blanching sample.

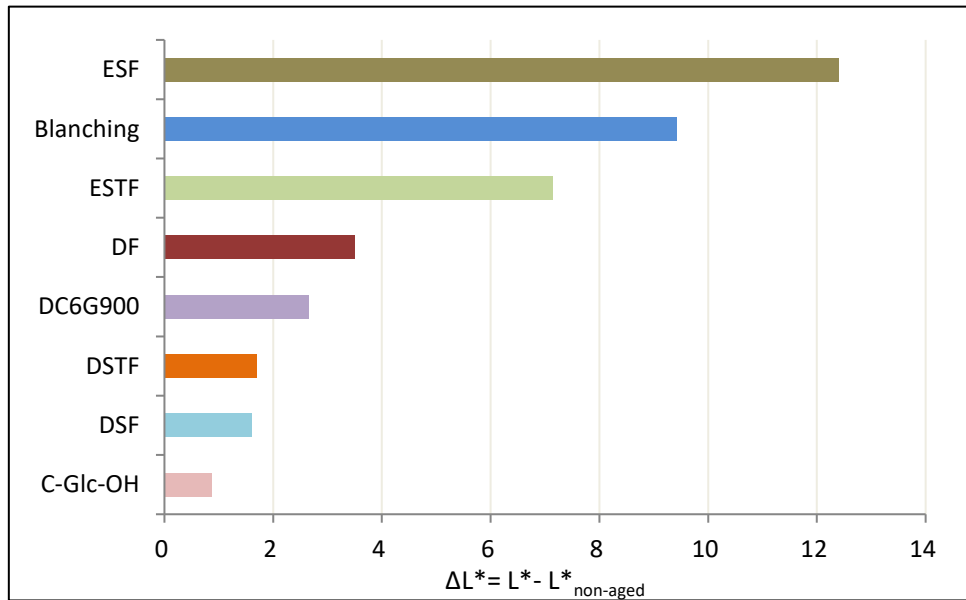


Figure 6-20: ΔL^* of the treated and blanching raw umber samples compared with non-aged raw umber sample

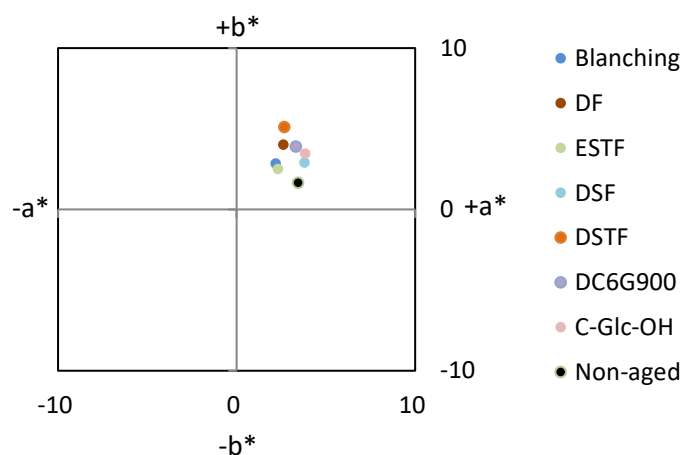


Figure 6-21: CIE a^*b^* space of raw umber samples

ΔL^* of each sample was presented in the figure 6-20. ΔL^* means the difference of L^* between the treated sample and non-aged reference and its calculation cited the results from the table 6-8. Compound **C-Glc-OH** shows the closest L^* to the non-aged-sample, followed by **DSF** and **DSTF**. Compounds **DC6G900** and **DF** also effectively decreased L^* value comparing with the L^* of blanching sample. Compound **ESTF** can slightly decrease the L^* . However, compound **ESF** gave the sample a higher L^* value than blanching sample, which means it is not suitable for the restoration.

From the CIE a^*b^* space (figure 6-21), **DSTF** gave the most increase in b^* value, followed by **DC6G900** and **DF**. Compounds **DSF** and **ESTF** gave slightly chromaticity change, similar with the blanching samples. Concerning the total color variant, the difference between the samples treated by **C-Glc-OH** and **DSF**, and non-blanching sample is imperceptible for human eyes. Compounds **DSTF**, **DC6G900** and **DF** give the sample ΔE^* around 4. Compound **ESTF** can also decrease the ΔE^* between treated sample and blanching sample. However, **ESF** gave a bigger total color variant than blanching.

In summary, concerning L^* parameter, partially perfluorinated compounds **C-Glc-OH**, **DSF**, **DSTF**, **DC6G900**, **DF** and **ESTF** could visually decrease blanching on raw umber samples. And among those compounds, **C-Glc-OH** has the closet L^* with non-blanching sample, followed by **DSF** and **DSTF**. Concerning the total colour variant ΔE^* , **C-Glc-OH**, **DSF**, **DSTF**, **DC6G900**, **DF** and **ESTF** could decrease the colour variant between blanching sample and non-blanching raw umber sample. And **C-Glc-OH** and **DSF** have the lowest ΔE^* less than 3 comparing with non-blanching sample.

Therefore, compounds **DSTF**, **C-Glc-OH**, and **DSF** could significantly decrease the blanching on both green earth and raw umber samples, according to the results of colorimetric measurements. Those compounds also show a better efficacy than **DC6G900**, which was reported as promising product. Among those compounds, **DSTF** shows the best performance on blanching green earth sample.

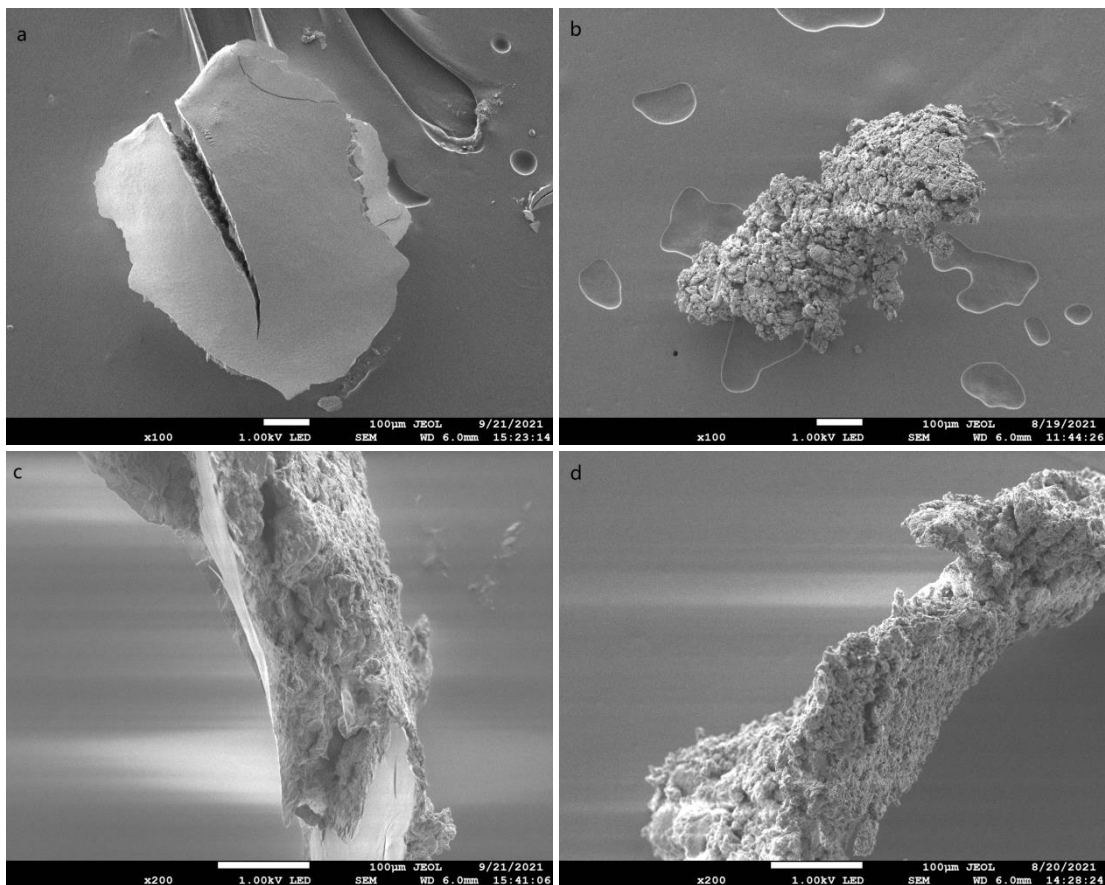
The colorimetric measurements were not performed on green earth or raw umber samples treated by **C-Glc-OAc**, because the obvious white deposit can be seen from the photography images. That means they are not suitable for restoration of blanching painting.

- **Morphological study and compound distribution study**

- **DSTF**

FEG-SEM was used in morphological study to investigate the porous structure modifications in the treated mock-up samples.

Figure 6-22 a) presents the surface of green earth sample treated by **DSTF** under FEG-SEM observation. Comparing with image b) which is the surface of blanching green earth sample, the pores were filled after treating by **DSTF** and the surface became obviously smooth. Image c) presents the lateral direction of the treated sample by **DSTF**, while image d) shows the lateral direction of the blanching sample under 200X magnification. Comparing those two images, it seems the porous structure modification in lateral direction is not as obvious as the surface. By zooming the lateral area with 500X and 1500X magnification, image e) and g) indicate the treated sample has the modified and less porous structure in the area near surface, than the blanching sample presented by images f) and h). It means the compound **DSTF** penetrates into the sample with a limited depth. Comparing with the non-aged sample (figure 6-11 a)), the sample treated by **DSTF** is not a well agglomerated structure. And the pores of deeper area in lateral direction remain unfilled.



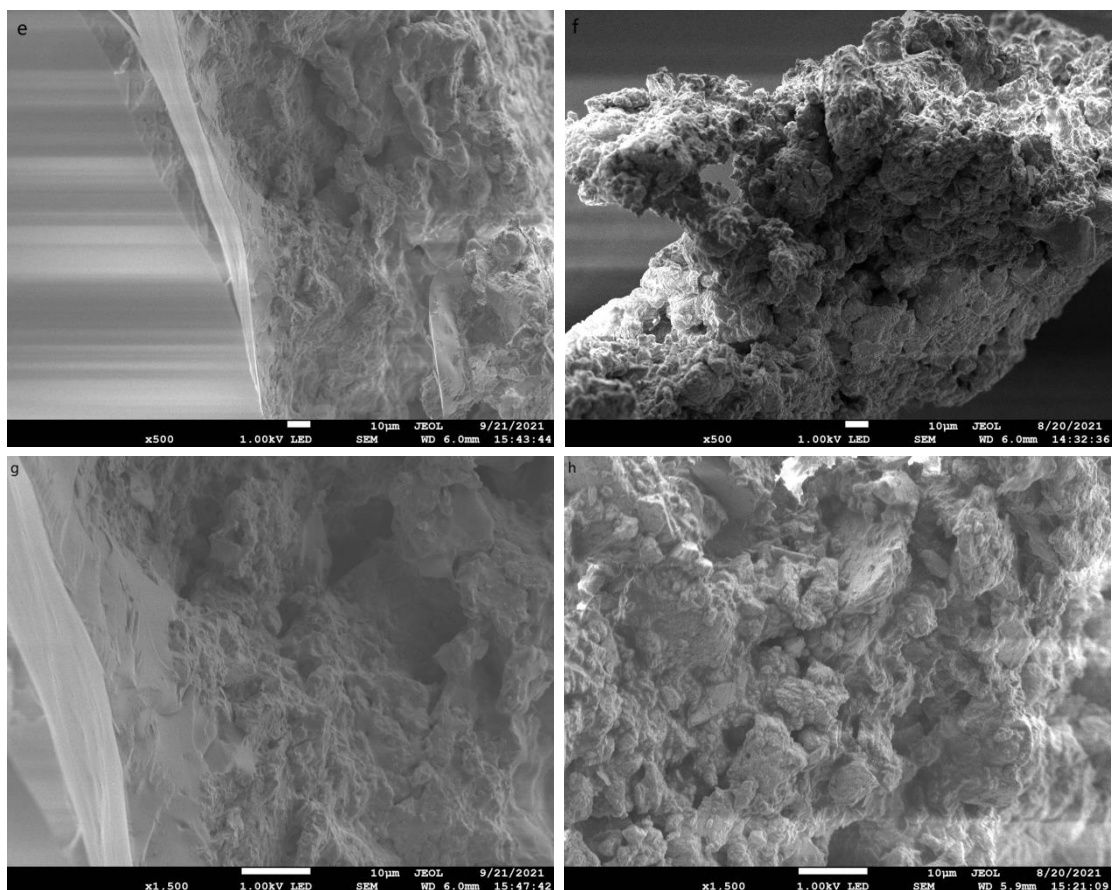


Figure 6-22: Images a), c), e), g) FEG-SEM images of green earth sample treated by **DSTF**. b), d), f), h) FEG-SEM images of blanching green earth samples.

The micro sample taken from the treated green earth sample by **DSTF** was prepared as a cross-section. Optical microscope with fluorescence filter B2A revealed the obviously fluorescent area, which is located from surface to the upper of the sample (figure 6-23 b)). Considering some compounds with perfluorinated chains are fluorescent compounds [237], the fluorescent area could probably present the distribution of **DSTF** in the sample.

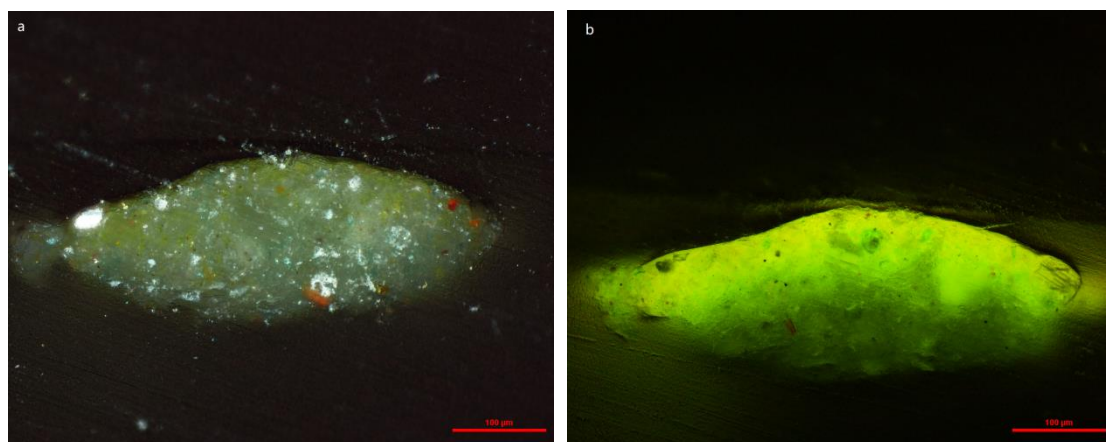


Figure 6-23: Cross-section from green earth sample treated by **DSTF**; a) Visible light; b) Blue Excitation: B-2A

In order to confirm this hypothesis, the fluorescent area (figure 6-24 a), 1) and non-fluorescent area (figure 6-24 a), 2) were analyzed by SEM-EDS. The results of SEM-EDS area analysis confirm the presence of Fluorine in the fluorescent area 1 which is near the surface. It also shows that no Fluorine in the non- fluorescent area 2 which is near the bottom. The results are corresponding to the hypothesis based on the investigation from optical microscope. That means the fluorescent area could present the distribution of **DSTF** in the sample and **DSTF** indeed shows limited penetration.

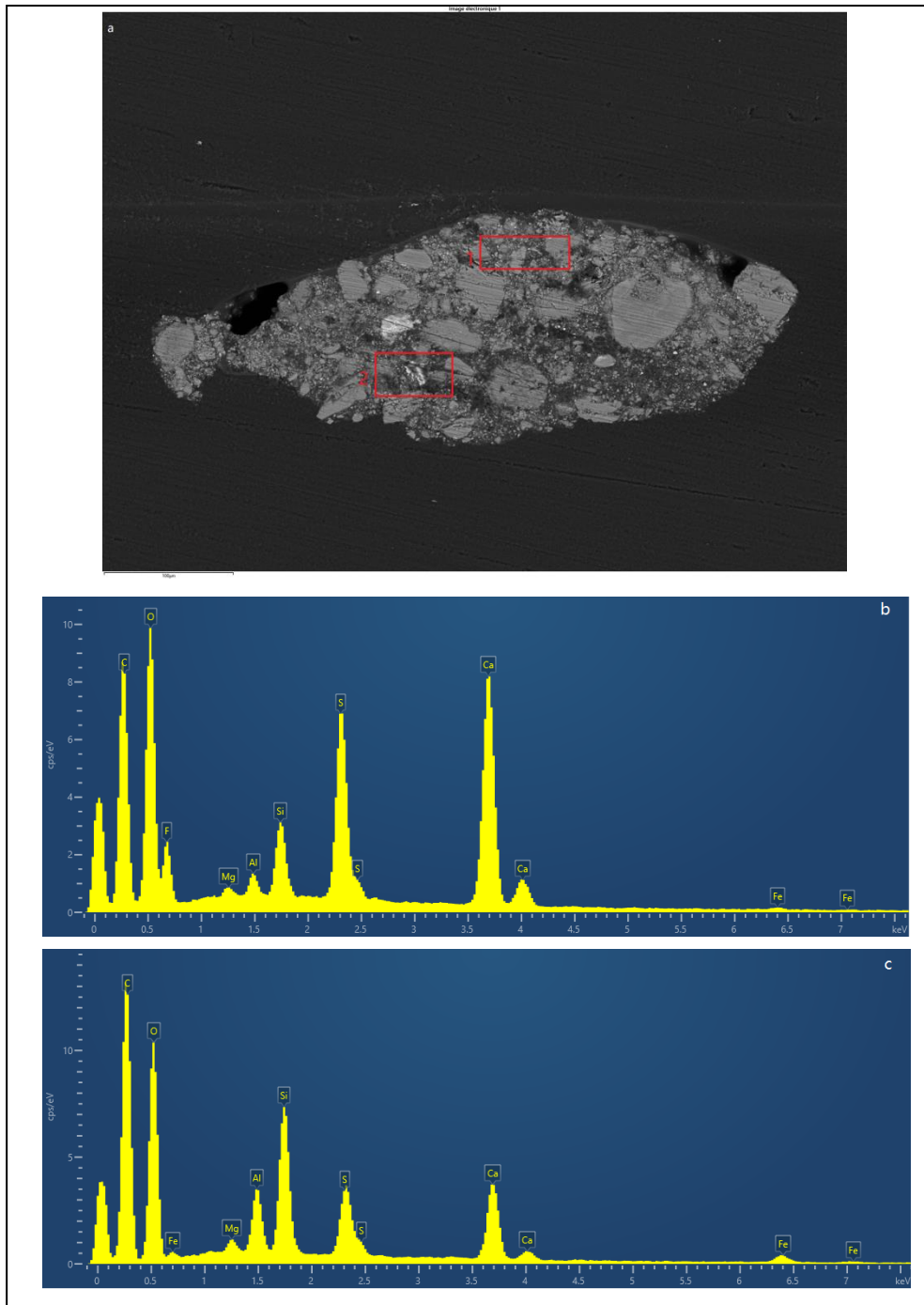


Figure 6-24: SEM-EDS area analysis of cross-section from green earth sample treated by **DSTF**; a) SEM backscattered electron image of the cross section; b) SEM-EDS spectrum of element composition in fluorescent area 1; c) SEM-EDS spectrum of element composition in non-fluorescent area 2.

Moreover, line profile analysis of the same cross-section sample was performed. The result (figure 6-25) shows that the quantity of Fluorine decreases as the increase of the depth in the sample.

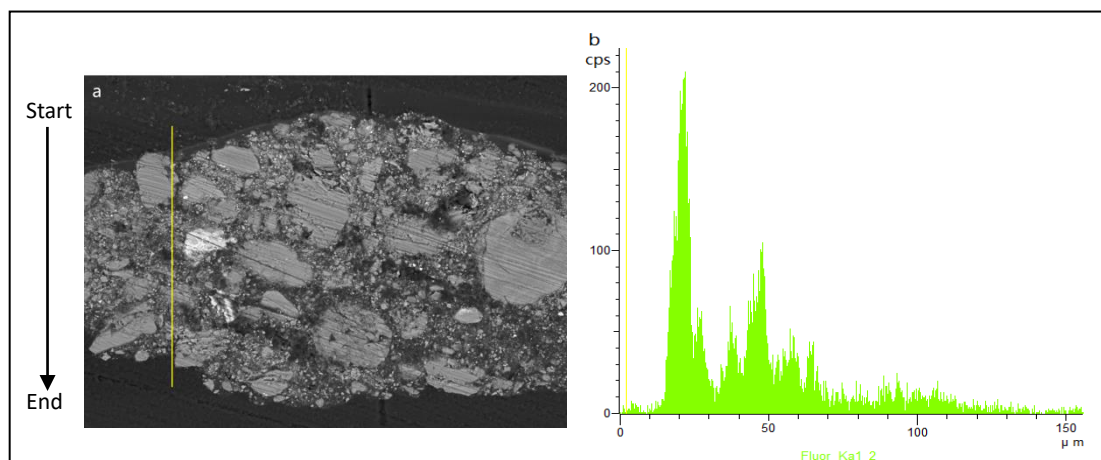
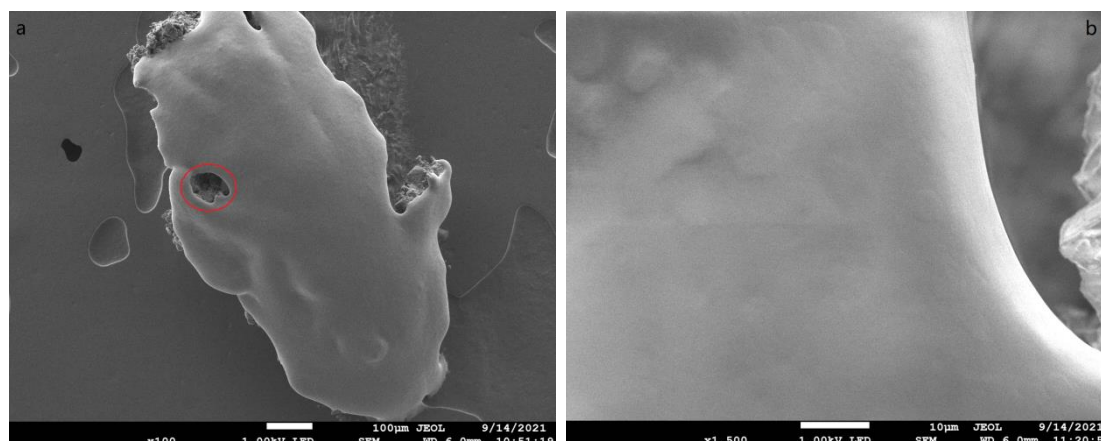


Figure 6-25: SEM-EDS line profile analysis in **DSTF** treated green earth sample; a) Selected area for SEM-EDS line profile analysis, analysis direction shown as the arrow; b) SEM-EDS line profile of F K α in the sample.

The morphological study of the raw umber sample treated by **DSTF** was presented (figure 6-26). In image a) and b), the pores were filled on the surface of the treated sample, and the pigment, binder and **DSTF** were well agglomerated in the structure (except the area in red circle). On the lateral direction (image c) and d)), **DSTF** shows a limited penetration which is confined to the area near the surface of the sample. And the pores of deeper area in lateral direction remain unfilled.

In summary, morphological study by FEG-SEM, optical microscopy observation and distribution of **DSTF** study by SEM-EDS all indicate that **DSTF** could fill the pores in blanching mock-up samples but with a limited penetration.



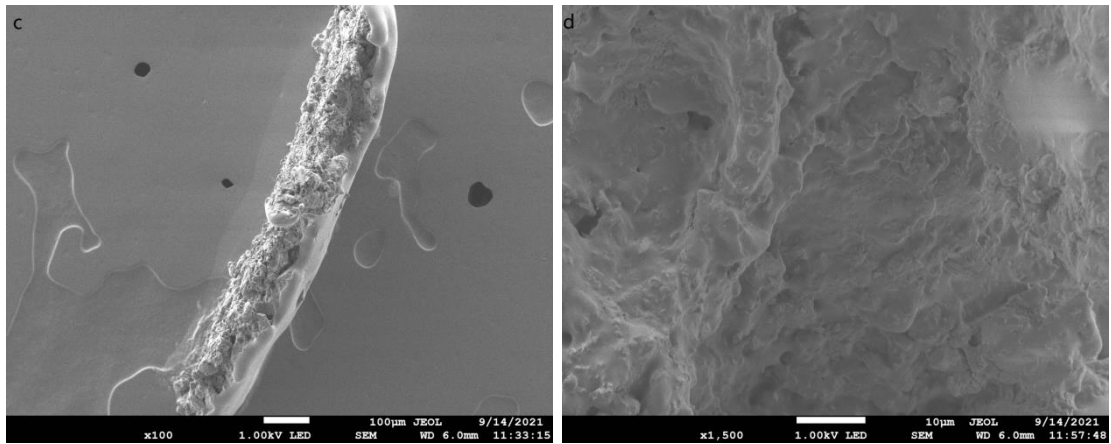
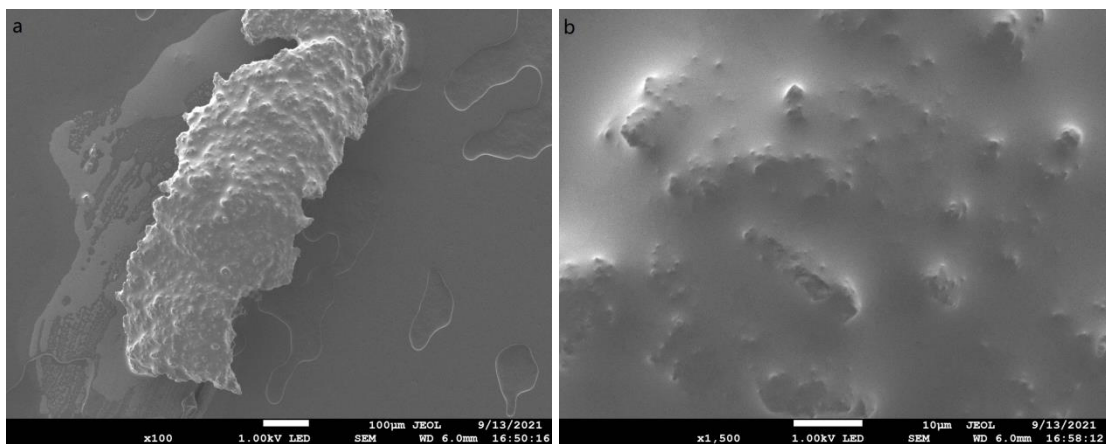


Figure 6-26: FEG-SEM images of raw umber sample treated by **DSTF**. a) and b) The surface of the sample; c) and d) The lateral side of the sample.

- **DC6G900**

The sample treated by **DC6G900**, which has been reported to penetrate in the depth of the sample, was also investigated by FEG-SEM. Figure 6-27 presents the micro structure of the raw umber sample treated by **DC6G900**. The pores were filled both on the surface (image a) and b)) and in the lateral direction of the sample (image c) and d)). The surface is not as smooth as the sample treated by **DSTF**, but it is similar with structure of the non-aged sample. On the lateral direction, **DC6G900** shows a different behaviour on penetration compared with **DSTF**. It gives a better penetration into the pores in depth of the altered sample and the structure was well agglomerated after treatment, like in the non-aged sample.



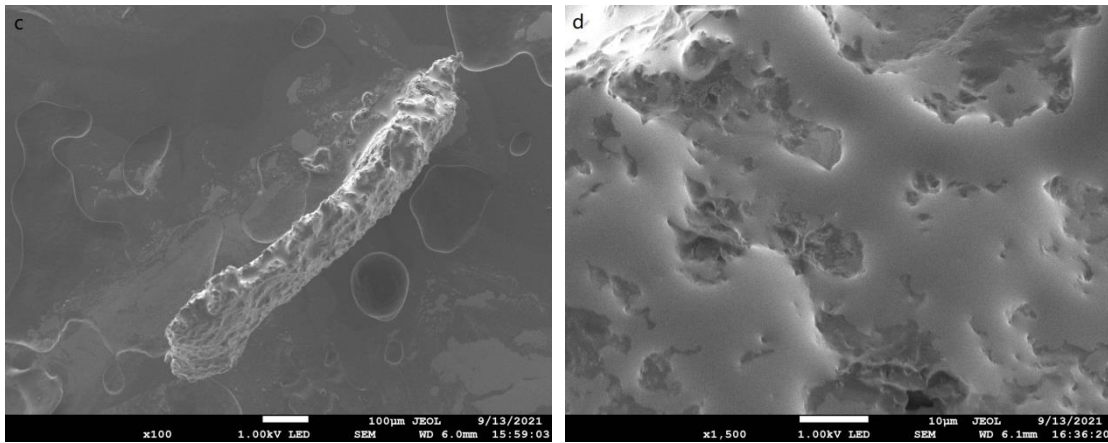


Figure 6-27: FEG-SEM images of raw umber sample treated by **DC6G900**. a) and b) The images of the surface; c) and d) The images of the lateral direction.

Optical microscope with fluorescence filter B2A also revealed **DC6G900** had a good penetration, as the fluorescence in the area near bottom can be detected (figure 6-28).

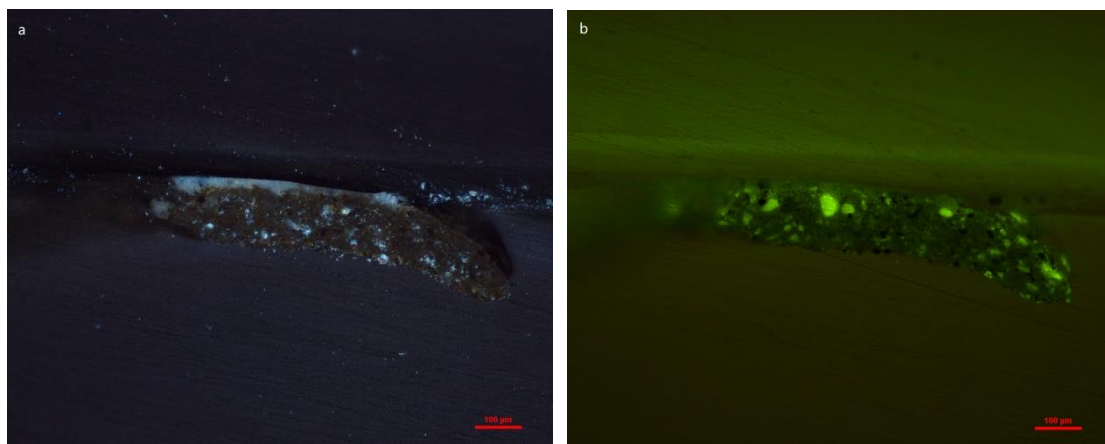


Figure 6-28: Cross-section from raw umber sample treated by **DC6G900**; a) Visible light; b) Blue Excitation: B-2A

- ESTF

Figure 6-29 presented the morphological modification by **ESTF** in the treated blanching green earth sample. The treated surface has a similar micro structure modification with the sample treated by **DSTF** (figure 6-22 a)). The pores were filled and it became smoother than the surface of blanching sample. In the lateral direction, it showed a more limited penetration than **DC6G900** (figure 6-27 d)). However, it has a better penetration performance than **DSTF** by comparing the FEG-SEM images with the same magnification (figure 6-22 g)). Those different results from FEG-SEM could contribute to discussion the relation between the molecule structures and their penetration behaviours in the blanching paint mock-ups.

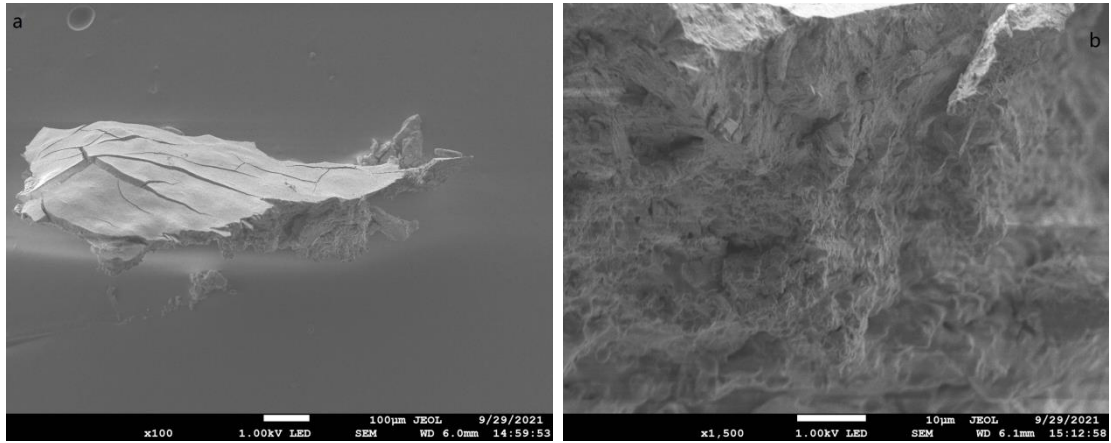


Figure 6-29: FEG-SEM images of the green earth sample treated by **ESTF**. a) The surface and lateral side of the sample under 100X magnification; b) Zooming the lateral side of the sample with 1500X magnification.

- **DSF**

Figure 6-30 showed the FEG-SEM images of green earth sample treated by **DSF**. The treated surface is similar with the surface treated by **DC6G900**, while, not as smooth as the surface treated by **DSTF**. Concerning the lateral direction of the treated sample, the limited penetration was observed in the **DSF** treated sample which was similar with **DSTF**.

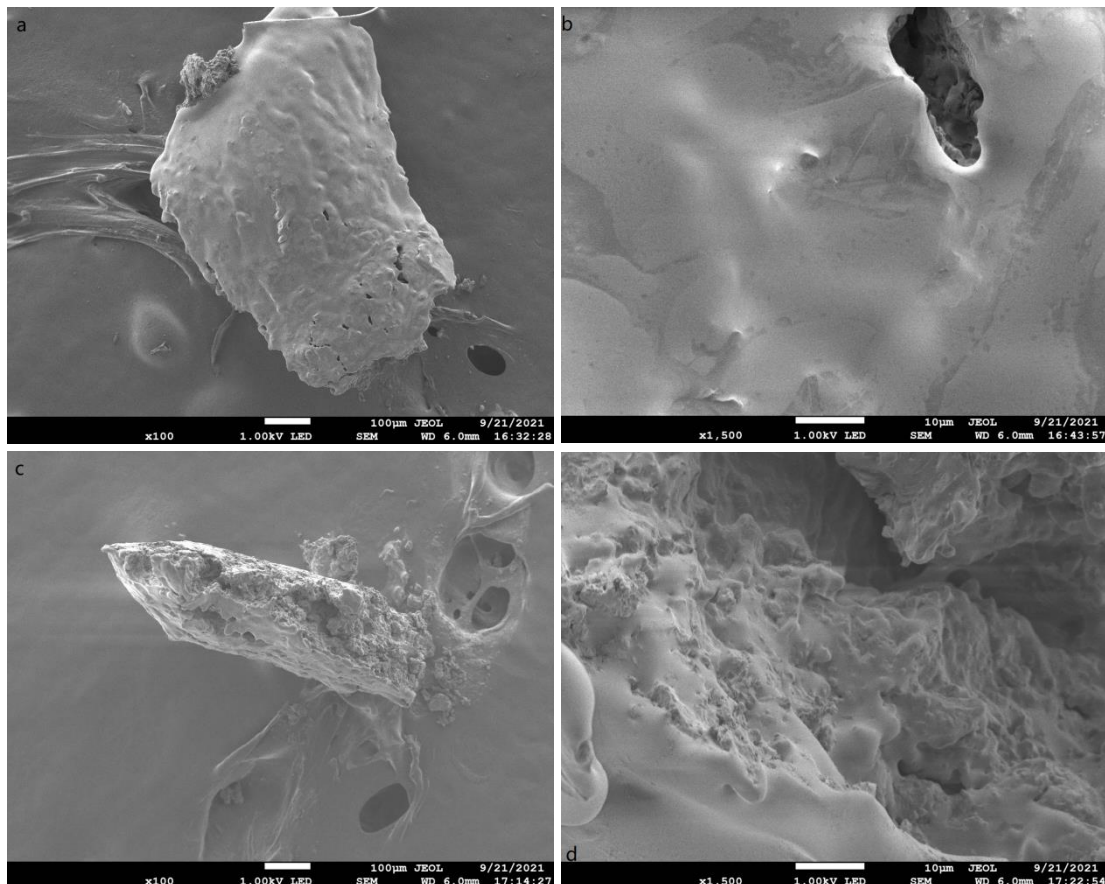


Figure 6-30: FEG-SEM images of green earth sample treated by **DSF**. a) and b) The treated surface; c) and d) The lateral side of the treated sample.

The limited penetration was also presented by optical microscope observation (figure 6-31), as **DSF** was distributed near the surface of the sample.

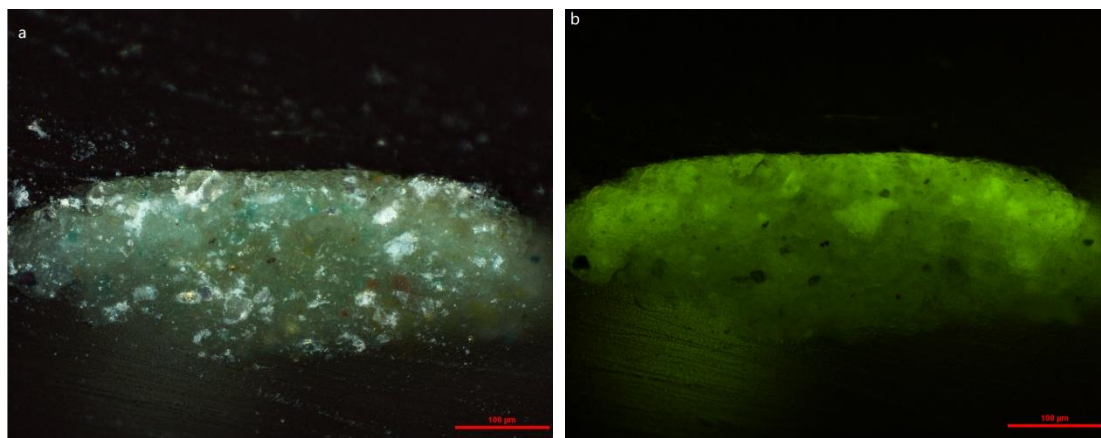
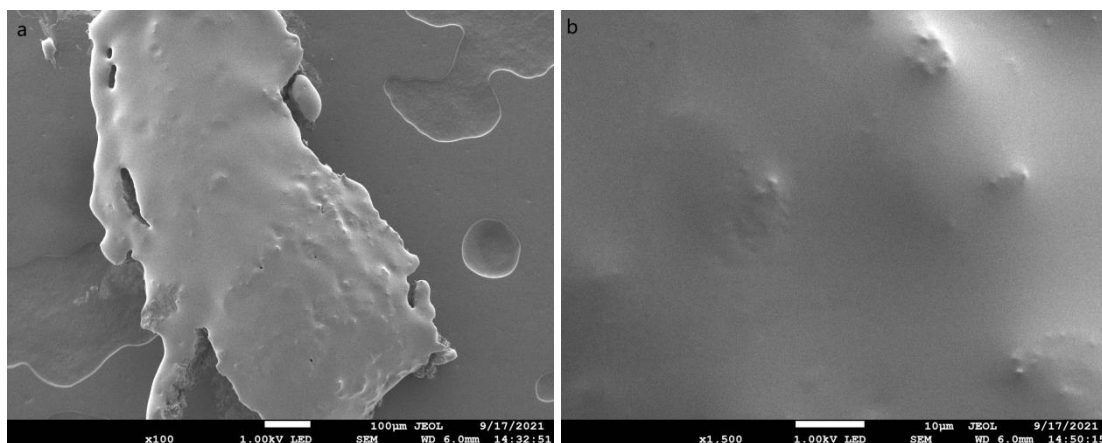


Figure 6-31: Cross-section from green earth sample treated by **DSF**; a) Visible light; b) Blue Excitation: B-2A

- **DF**

For compound **DF**, figure 6-32 reported the FEG-SEM observation results of the treated raw amber sample. Image a) and b) showed the treated surface by **DF**. The pores were filled and the structure was well agglomerated. The distribution of the compound is similar with **DSF**. On the other hand, the compound also showed a limited penetration which is similar with **DSTF**.



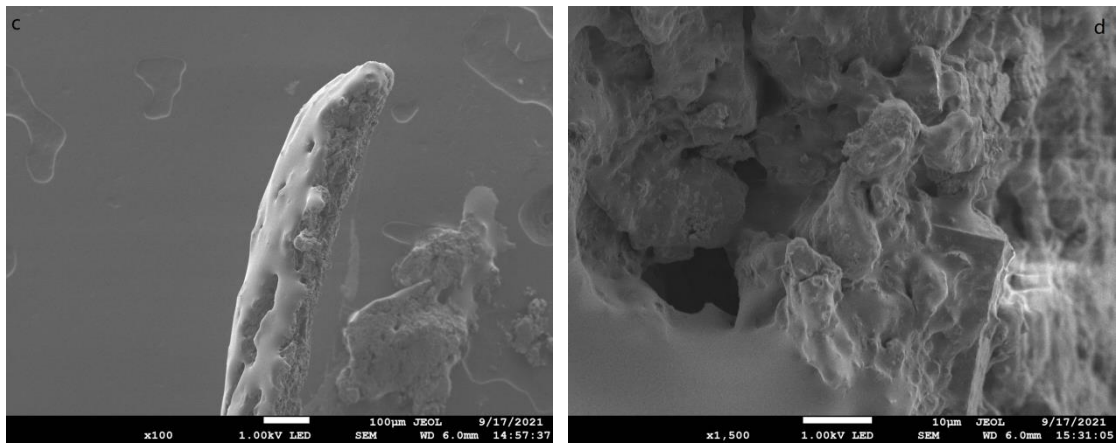


Figure 6-32: FEG-SEM images of raw umber sample treated by **DF**. a) and b) The surface of the treated sample; c) and d) The lateral side of the treated sample.

- **C-Glc-OH**

For the sample treated by **C-Glc-OH**, most pores on the surface were filled but there was some area not filled by the compound (figure 6-33 a) and b)). On the lateral side, compound **C-Glc-OH** showed limited penetration, which seemed similar with **DSTF** and **DF** (figure 6-33 c) and d)).

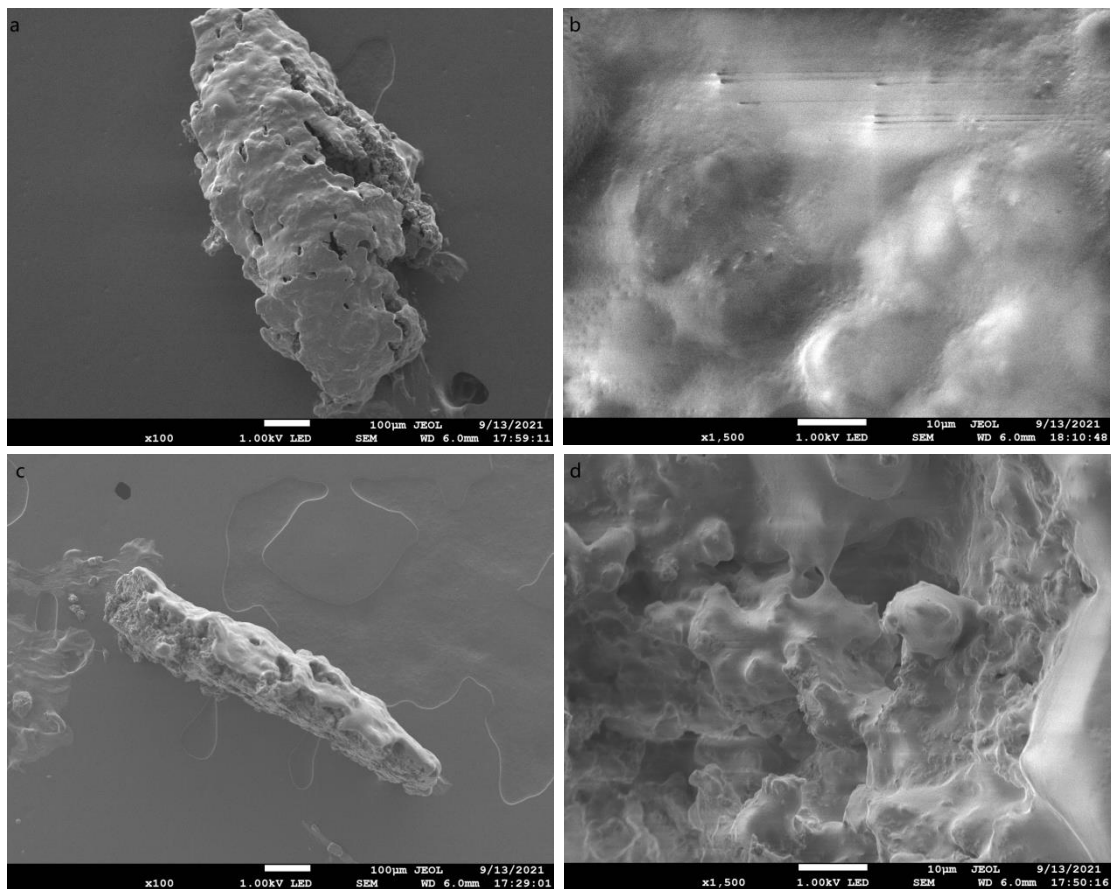


Figure 6-33: FEG-SEM images of treated raw umber sample by **C-Glc-OH**. a) and b) The images of treated surface. c) and d) The images of lateral side.

To summarize, in the FEG-SEM observation part, all those images showed morphological modification were modified in the treated samples by different perfluorinated derivatives, from both the treated surface and the lateral direction.

On the treated surface, compounds **DSTF**, **ESTF**, **DSF**, **DF**, **DC6G900** and **C-Glc-OH** can fill the pores. Among them, compound **DSTF** and **ESTF** can give a relatively smooth surface to the treated sample. **DSF** and **DF** gave a less smooth surface, but they are similar with the non-aged surface. Compound **DC6G900** show a different distribution on the surface and it seems that the molecules were not accumulated on the surface. Compound **C-Glc-OH** also could fill the pores on the surface, but there was still area of surface where the compound, pigment and binder were not well agglomerated.

According to morphological micrographs, lateral side of the treated sample, compound **DC6G900** showed good penetration and the pores in depth were also filled. The total micro structure of the treated sample of **DC6G900** was similar with the non-aged sample. However, compound **DSTF** showed limited penetration. The pores near surface were filled but the pores located deeper in lateral direction were not filled. The similar limited penetration could also be observed in the sample treated by **DSF**, **DF** and **C-Glc-OH**. While, the compound **ESTF** showed a slightly better penetration than **DSTF**. Moreover, this conclusion also has been confirmed by the distribution of compounds study in lateral direction using optical microscopy observation and SEM-EDS analysis of the cross-section samples.

Regarding the different behaviours of compounds on the surface and lateral side, possible reasons could be proposed and they could be divided into 2 main categories.

The first category is the concentration of solutions and suspension applied on the sample. The relatively smooth surface and the limited penetration of **DSTF**, **DSF**, **DF**, **ESTF** and **C-Glc-OH** could indicate that the molecules were accumulated on the surface. Accumulation could be a result of relatively high concentration (30 %) and not enough solvent brought the molecules into the pores in the depth. But **DC6G900** which shows good penetration ability, was the same concentration with **DSTF**, **DSF**, **DF** and **C-Glc-OH**. That means the structure of molecule could be the other category of reasons: the properties of the molecules.

The properties of the molecules, which have an influence on the penetration, could be their average molecular weight and structure.

Firstly, the average molecular weight of partially perfluorinated oligoamide **DSTF** is 2188.8 g/mol, which is higher than 1840 g/mol than **DC6G900**. The high molecular weight could influence the penetration in the painting layer.

Secondly, considering the lower average molecule weight in **ESTF**, **DSF**, **DF** and **C-Glc-OH** compared with **DC6G900**, another possible reason of the limited penetration is the polar groups in the molecules (NH, CONH and OH) could form intermolecular hydrogen bonds, or hydrogen bonding/dipolar interaction with the paint material. Those non-covalent interactions would hinder the molecules to penetrate into the deeper area in paint layer. Also, the different penetration performance between **DSTF** and **ESTF** is worth to note. The monomer in **ESTF** is ethylenediamine instead of the diethylenetriamine in **DSTF**, could contribute a better penetration of **ESTF** than **DSTF**. That could a result of the decreased degree of hydrogen bonding due to decreased amount of NH groups. Besides, the better penetration could also relate to the lower average molecular weight of **ESTF** than **DSTF**.

Therefore, all those reasons could lead to a different penetration performance of each

compound in the treated mock-up samples. In order to improve the penetration, a lower concentration of the solution or suspension could be used. Or the molecule structure could be modified with less polar groups.

Summary

In summary, the performance of partially perfluorinated compounds on blanching restoration would be evaluated by the results of their treatments on pure pigments and blanching mock-ups. Regarding the treatments on pure pigments, compounds **C-Glc-OH**, **C-Glc-OAc** and **ESF** are not suitable products. Compound **C-Glc-OH** could cause darkening in Copper (II) pigments and Carmine. Compounds **C-Glc-OAc** and **ESF** could become white deposit on the pigments after the solvent evaporated.

Regarding the treatments on blanching mock-ups, compounds **DSTF**, **C-Glc-OH**, **DSF**, **DC6G900**, **DF** and **ESTF** could give a less blanching visual effect by the colorimetric results. In particular, **DSTF**, **C-Glc-OH** and **DSF** obviously decrease the blanching visually. Compounds **DSTF**, **C-Glc-OH**, **DSF**, **DC6G900**, **DF** and **ESTF** could fill the pores in the blanching mock-ups. **DC6G900** shows a good penetration in the lateral direction, while other compounds show the limited penetration. The limited penetration could be a result of high concentration, molecular weight and highly polar molecular structure.

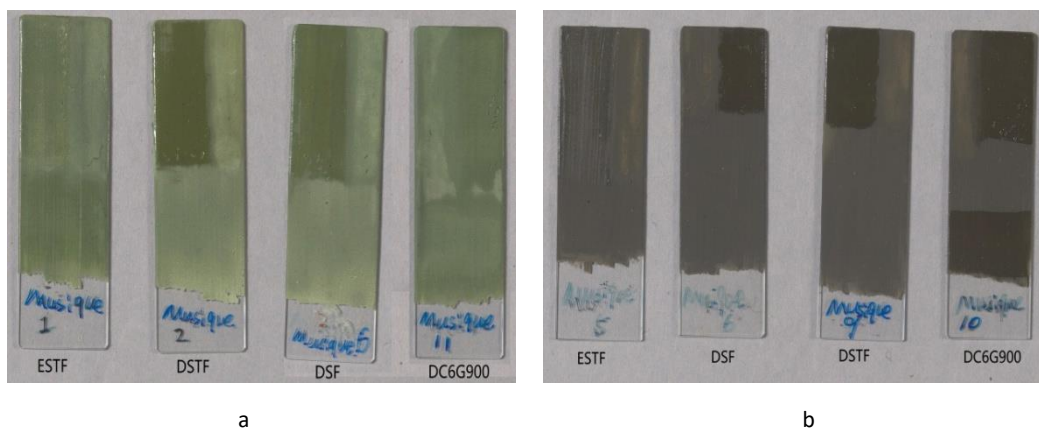
Based on all these results, compounds **DSTF**, **DSF** and **DC6G900** are considered as the most promising restoration compounds for blanching restoration. However, **ESTF** is also worth to consider as a promising compound, because it can fill the pores on the surface and can show a better penetration than **DSTF**. Its relatively poor performance in the colorimetric measurements could be due to the white colour of its suspension. The modification of its colour could possibly be realized by using decolorizing carbon.

Next, the reversibility tests of those interesting products were reported and discussed in the following part.

6.3.2.4 Evaluation of the reversibility of treatments on blanching paint-layer mock-up samples

The reversibility test was performed on the samples treated by **ESTF**, **DSTF**, **DSF** and **DC6G900**. TFE was used to remove **ESTF**, **DSTF** and **DC6G900**, and 2-propanol was used to remove **DSF**.

Figure 6-34 showed the results of removal by photography. The removal part is confined to one half of the treated part on each sample. From the photograph, the removed part of the sample became blanching again and seemed like the untreated blanching part (the down half of each sample). That means the removal of the compounds was realized visually.



Figures 6-34: Photographs of the samples after the compounds removed ©C2RMF/ Anne Maigret

Next, colorimetric measurements were performed on the removal part. Figure 6-35 presented the L* value of the treated, removal, and blanching raw umber samples. An obvious increase of L* can be observed after the compounds were removed from the treated samples. That indicates the reversibility of treatment is realizable. A slightly increased L* can be observed in the removed sample compared with the blanching sample. That is due to the pigment attached to the cotton swab during the removal practical process.

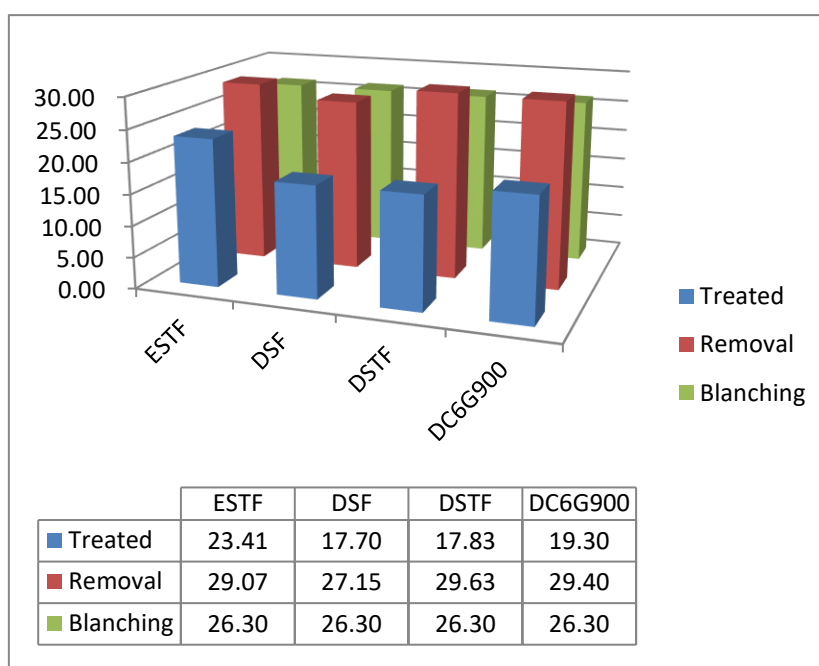


Figure 6-35: L* value of treated, removal and blanching raw umber sample.

The decrease of a* value after removing the compounds can be observed in figure 6-36, which reported a* value of treated, removal and blanching raw umber samples. The value of a* in the removal samples also became closer to the blanching samples. Those results also indicated the reversibility of the treatments.

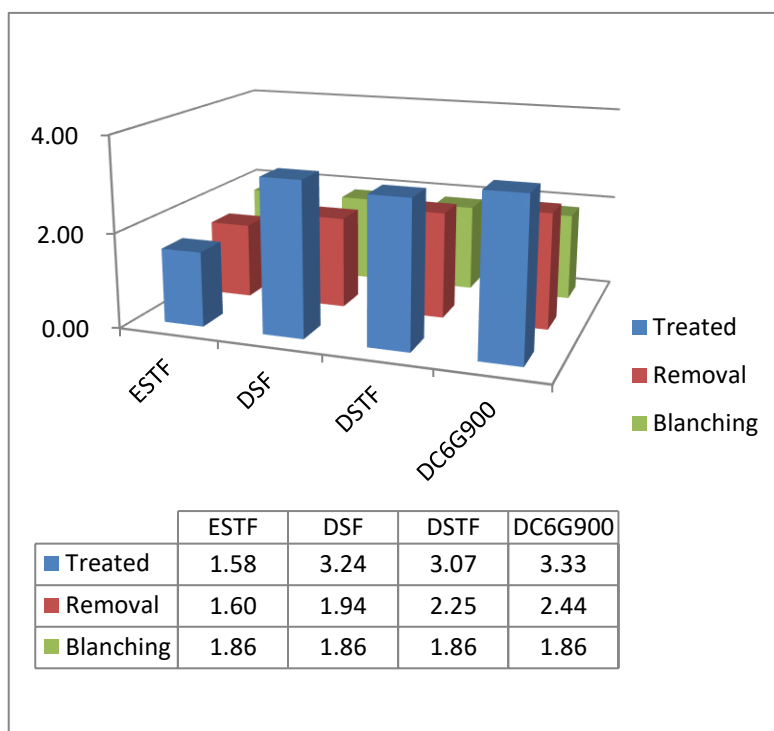


Figure 6-36: a^* value of treated, removal and blanching raw umber sample.

The value of b^* of the treated sample was slightly lower than the blanching sample (figure 6-37). After the removal of the compounds, b^* is eventually higher than b^* value of the blanching sample. That could be also due to the extra attached pigment on the cotton swab during the removal practical process.

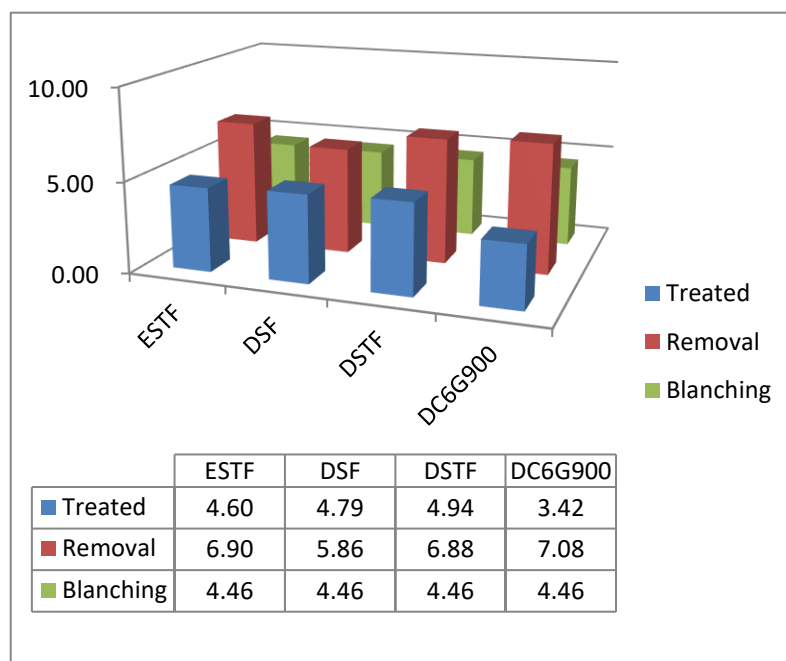


Figure 6-37: b^* value of treated, removal and blanching raw umber sample.

All those results indicated that the removal of the treatments by partially perfluorinated compounds could be realized by using the solvents (TFE, 2-propanol). The optimization of the practical process, especially to avoid removing extra pigment, could be needed.

FEG-SEM also revealed the micro structure of the samples after the compounds removed (figure 6-38). Image a) presented the micro structure of green earth sample after **DSTF** was removed. Image b) presented the micro structure of raw umber sample after the removal of **DC6G900**. The porous structures reappeared after the treated compounds were removed from the samples. Those observations under FEG-SEM also indicated the treatment could be removed.

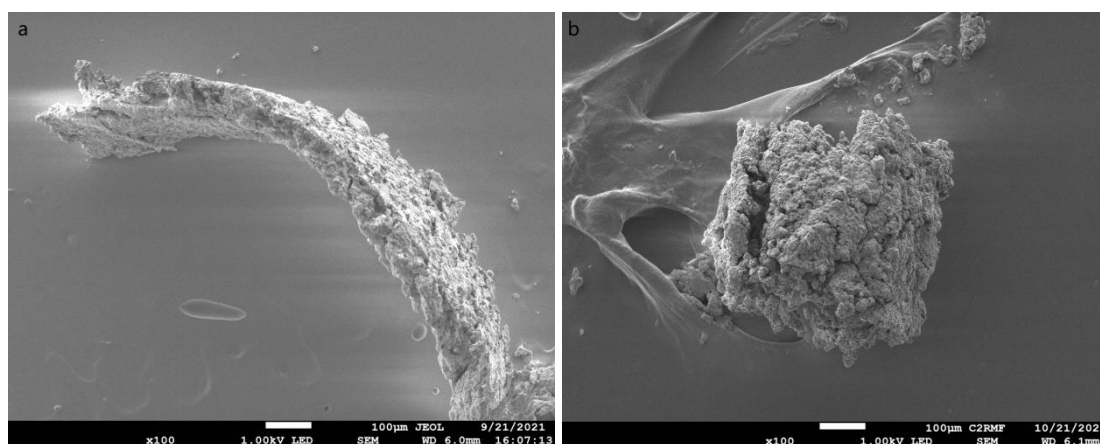


Figure 6-38: FEG-SEM images of the samples after removal of the compounds. a) Green earth sample after **DSTF** was removed; b) Raw umber sample after **DC6G900** was removed.

Moreover, the removal of the compounds from the treated sample was proved by the SEM-EDS element analysis, especially by the different quantity of Fluorine in treated samples and removal samples. The results of SEM-EDS investigated were reported in figure 6-39. S_04 1 in blue represents the element spectrum of the green earth sample treated by **DSTF**. S_05 1 in pink presents the element spectrum of the green earth sample after the removal of **DSTF**, and S_06 1 in dark shows the element spectrum of untreated sample. Comparing those three element maps, the quantity of Fluorine dramatically decreased in S_05 1, and closer to 0 in S_06 1. The compounds can be removed after treatment by TFE. That means the treatment could be reversible.

In summary, the reversibility of the restoration treatment by partially perfluorinated derivatives was evaluated by colorimetric measurements, FEG-SEM observation and SEM-EDS elemental analysis. The L^* value could be dramatic increased after the removal of the perfluorinated compounds. The highly porous structures reappear after the compounds were removed. The quantity of Fluorine was decreased effectively after the removal of the compounds. The results indicated that the compounds could be removed by TFE or 2-propanol. Thus, the restoration treatments by partially perfluorinated derivatives seem promising to be reversible. The optimization of the practical process and further tests concerning the reversibility could be developed in the future.

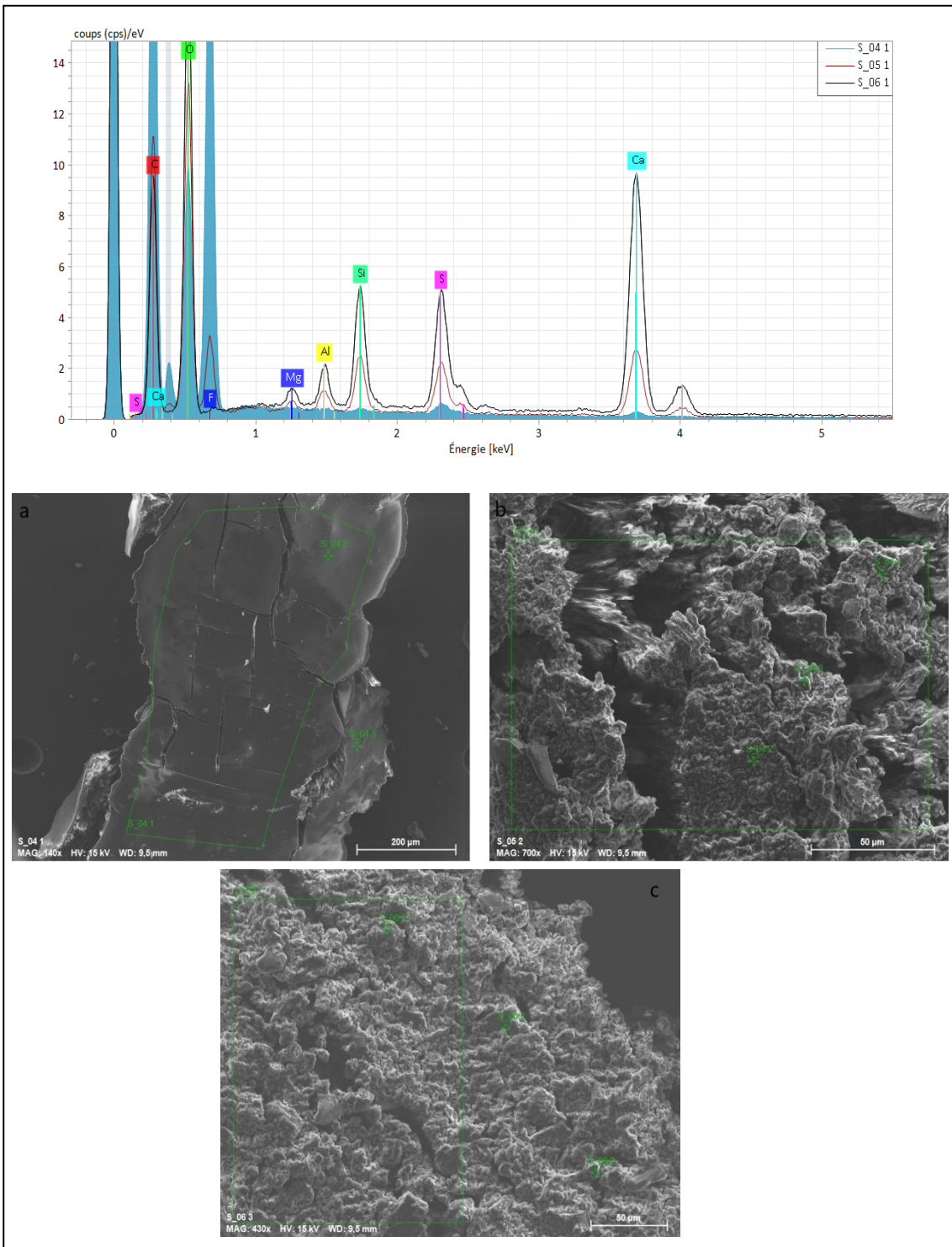


Figure 6-39: SEM-EDS results of green earth sample. a) SEM image of the treated sample by DSTF; b) SEM image of green earth sample after removal of DSTF; c) SEM image of untreated blanching sample; The element map was shown in the up of the figure.

6.4 Conclusion

The partially perfluorinated derivatives **DSTF**, **DSF**, **DF**, **ESTF**, **ESF**, **C-Glc-OH**, **C-Glc-OAc** and **DC6G900** were tested on the pure 19 pigments and blanching paint-layer mock-up samples. During the treatment on pure pigments, **C-Glc-OH** could cause darkening in Copper (II) pigments and Carmine. Compounds **C-Glc-OAc** and **ESF** could become white deposit on the pigments after the solvent evaporated. Therefore, those three compounds are not suitable for blanching painting restoration.

During the treatment on blanching green earth and raw umber samples, the colorimetric measurements showed that **DSTF**, **C-Glc-OH**, **DSF**, **DC6G900**, **DF** and **ESTF** could give a less blanching visual effect. In particular, **DSTF**, **C-Glc-OH**, and **DSF** obviously decrease the blanching, with a dramatic decrease of L^* value in the treated samples. That could indicate the pores, which would change the light scattering leads to the different L^* a^* b^* values, have been possibly filled. While, it is worth to note that the color of the compounds themselves and their solution of suspension would have influence on the color variant of the treated samples.

Next, the morphological study by FEG-SEM revealed that **DSTF**, **C-Glc-OH**, **DSF**, **DC6G900**, **DF**, and **ESTF** could fill the pores in the blanching mock-ups. Morphological study and compound distribution study reveal that **DC6G900** shows a good penetration in the lateral direction, while other compounds show the limited penetration. The limited penetration could be a result of high concentration, molecular weight and the hydrogen bonding/dipolar interaction by the polar groups in molecular structures. An optimized concentration could be developed in the future. The partially perfluorinated derivatives with less polar groups could be designed and synthesized in the future.

According to the FEG-SEM investigation, **ESTF** could fill the pores on the surface and show a better penetration on lateral direction than **DSTF**. Therefore, the relatively high L^* value in the **ESTF** treated sample could be due to the white colour of its suspension. Decolorizing carbon could be used for the modification of its colour in the future.

The reversibility of the restoration treatments was evaluated by colorimetric measurements, FEG-SEM, and SEM-EDS. The results indicated that the compounds in the treated samples could be removed by using TFE or 2-propanol. The L^* value could be dramatic increased after the removal of the perfluorinated compounds. The highly porous structures reappear after the compounds were removed. The quantity of Fluorine was decreased effectively after the removal of the compounds. Those results indicate the restoration treatments by partially perfluorinated derivatives could be promising for reversibility. The optimization of the practical process and related tests could be developed in the future.

In order to clearly and easily present the results on each parameter, the performance of each compound is shown in table 6-9. “√” represents the compound fulfils basic requirement on each parameter. More “√” means better performance. While, no “√” means the compound does not fulfil the requirement.

Compounds	Pigment test	Decreased L* value	Filling the pores	Penetration	Reversibility
C-Glc-OAc					
C-Glc-OH		✓ ✓ ✓	✓	✓	✓
ESTF	✓	✓	✓	✓ ✓	✓
DSTF	✓	✓ ✓ ✓ ✓	✓	✓	✓
ESF					✓
DSF	✓	✓ ✓ ✓	✓	✓	✓
DF	✓	✓ ✓	✓	✓	✓
DC6G900	✓	✓ ✓	✓	✓ ✓ ✓ ✓	✓

Table 6-9: Restoration performance of partially perfluorinated derivatives

Therefore, based on the results of tests on pure pigments and blanching mock-up samples, **DSTF**, **DSF**, **DC6G900**, **DF** and **ESTF** could be considered as promising restoration compounds for blanching painting restoration by acting against blanching effectively. It is necessary to point that it is difficult to find a perfect product that could fulfil all the requirements in restoration practices of artworks, as in the blanching painting restoration. Balancing those compounds performance on all the parameters, **DSTF**, **DSF** and **DC6G900** are recommended as restoration products for blanching paintings. This is because **DSTF** and **DSF** could dramatically decrease the L* value and **DC6G900** demonstrated a good penetration. Although those compounds could cause slight chromatic change of the treated samples (more red and yellow), it is acceptable comparing with the damage caused by blanching in paintings (ΔE^* caused by those compounds less than ΔE^* caused by blanching).

Besides, based on the structure of those molecules, modifications could be considered by controlling the number of polar groups and molecular weight. The optimized concentration for treatment solution or suspension could be developed. All of those could contribute to improve the restoration efficacy on blanching paintings.

Chapter 7

Conclusions

On the basis of the results presented and discussed in the previous chapters, the following conclusions, regarding the synthesis of partially perfluorinated derivatives and their properties and performance of the partially perfluorinated derivatives on stone protection and blanching painting restoration, can be drawn.

7.1 Synthesis of partially perfluorinated derivatives

7.1.1 Partially perfluorinated C-glycosides

Starting from the unprotected carbohydrate, the natural, renewable, and low cost D-glucose, β -C-glycosidic ketone as the direct C-glycosidation product was successfully obtained *via* Lubineau reaction following a green-chemistry process. The target compound, i.e, the partially perfluorinated C-glycoside (**C-Glc-OH**, figure 7-1) was successfully obtained through the convenient one-pot reductive amination reaction with medium yield.

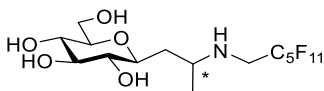


Figure 7-1: C-Glc-OH

In this target molecule, hydroxyl groups are expected to be compatible with polar substrates, stones, and porous blanching paintings through non-covalent interactions. As a result, the compound is supposed to give good adhesion properties and long-term durability on stones. It could also enter into the pores and decrease the blanching in easel paintings. Meanwhile, the perfluorinated tail introduced into the molecule is supposed to form a coating on stones with efficient water repellency, and contributing to the hydrophobicity in the blanching painting restoration.

Moreover, the protected partially perfluorinated C-glycoside (**C-Glc-OAc**, figure 7-2) was also successfully obtained by the similar synthetic route. **C-Glc-OAc** was synthesized as a control, in order to investigate if hydroxyl groups in C-glycosides can improve the restoration efficacy as expected. Also different physical properties like physical states, solubility, and color could have influence on the restoration performance.

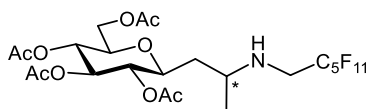


Figure 7-2: C-Glc-OAc

7.1.2 Partially perfluorinated oligoamides

Oligoamides, which are named **EST**, **DST**, **ES**, **DS**, starting from different monomers (dimethyl L-tartrate, diethyl succinate, diethylenetriamine or ethylenediamine) were successfully obtained *via* polycondensation reaction. The choice of the monomers was made in order to balance the presence of polar groups to favour interactions with polar substrates. Among those oligoamides, **EST** and **DST** contain hydroxyl groups due to the presence of L-tartrate units. Different amine sources (diethylenetriamine and ethylenediamine) formed the amide groups in **DST** and **EST**. The oligoamides without hydroxyl groups, **ES** and **DS**, were synthesized as controls to investigate the role of OH groups on stone protection and blanching painting restoration.

The target partially perfluorinated oligoamides, **ESTF**, **DSTF**, **ESF**, **DSF**, were obtained by introducing perfluorinated chains into **EST**, **DST**, **ES** and **DS** through ring open reactions with good yield. Moreover, partially perfluorinated amine **DF** was synthesized to investigate the function of amide groups in restoration performance. Therefore, the partially perfluorinated oligoamides and amine, which have different average molecular weight, polarity, solubility and physical state, were obtained. Their different properties due to the different molecular structures would highly influence their efficacy on stone protection and blanching painting restoration. Moreover, the rich molecular structures can give clues about the optimization of the molecules based on their restoration performance.

7.2 Restoration performance

7.2.1 Stone protection

The protection performance of the seven synthetic partially perfluorinated derivatives developed in this PhD thesis, was evaluated through a series of measurements on different stone materials (Lecce, sandstone, and marble) with different porosity.

Those compounds show different solubility due to their structures. **C-Glc-OAc** shows good solubility in ethyl acetate, and all the other six compounds show good solubility in alcohols and hydro-alcoholic solvents *e.g.* ethanol, 2-propanol, H₂O/2-propanol, except **ESF** that is less soluble. Comparing with the partially perfluorinated derivatives containing diethylenetriamine moiety, the compounds with ethylenediamine units show better resistance to photodegradation under UV aging.

In the water repellency test on Lecce stone, **C-Glc-OAc** and **C-Glc-OH** show low protective efficacy on Lecce stone. However, PE % of **C-Glc-OH** is slightly higher than **C-Glc-OAc**, which has no OH groups. **ESF** shows medium high protective efficacy and **DF** contributes to a medium protective efficacy. Both **DSF** and **DF** show medium high PE % values on sandstone. On marble, which has the lowest porosity, **DF** and **DSF** also show medium high PE % values.

Concerning the chromatic effect test, the two partially perfluorinated **C-glycosides**, **ESF**, and **DSTF** show imperceptible chromatic change on Lecce. On sandstone, **DSF**, **DF**, and **ESF** show clear increase of ΔE^* , which is around 10. Only compound **DSTF** shows a ΔE^* around 3,

which is imperceptible to human eyes. On marble, **DF** and **DSF** give a significant chromatic change around 8, while the chromatic change after treatment with the other compounds is imperceptible (**ESF**) or close to imperceptible (**ESTF**, **DSTF**).

ESF can give the largest contact angle to each stone material from 101° (minimum) to 139° (maximum), while **ESTF** failed to contribute to the hydrophobic surface on sandstone and marble.

In the vapor permeability test, all the five partially perfluorinated oligoamides and amine that were tested, can give a good maintenance of the original porosity and pore structures after treatment of Lecce stone. On sandstone, slightly decreased vapor permeability was observed with **DSF** and **DF** treatments (RP % over 80 %). Dramatic decrease of vapor permeability was observed with **DSF** treatment on marble (RP % at 57 %).

Considering all the performance of each compound in all the tests, **ESF** was demonstrated to be a suitable protective agent for Lecce stone with accepted solubility in 2-propanol, good stability under UV, high PE %, high CA and ability to maintaining the original porous structure and chromatic features. **DSF** and **DF** could be potential protective agents of sandstone if the chromatic change can be decreased after coating. **DF** can be also considered as a potential protective agent of marble if the chromatic change can be decreased after coating. Although **C-Glc-OH** showed low protective efficacy, the partial or full protection of the hydroxyls *via* -CO-NH- formation on the C-glycoside could improve its water repellency.

7.2.2 Blanching painting restoration

The new seven partially perfluorinated derivatives together with the reference compound **DC6G900** were tested as restoration compounds for blanching easel paintings.

Concerning the treatment of pure pigments, **C-Glc-OH** could cause darkening in Cu(II) pigments and Carmine. Compounds **C-Glc-OAc** and **ESF** could produce a white deposit on the pigments after solvent evaporation. Therefore, we demonstrated that those three compounds are not suitable for blanching painting restoration.

Concerning the treatment of blanching green earth and raw umber samples, the colorimetric measurements showed that **DSTF**, **C-Glc-OH**, **DSF**, **DC6G900**, **DF**, and **ESTF** could give a less blanching visual effect. In particular, **DSTF**, **C-Glc-OH**, and **DSF** obviously decrease the blanching, with a dramatic decrease of L* value in the treated samples.

The morphological study by FEG-SEM revealed that **DSTF**, **C-Glc-OH**, **DSF**, **DC6G900**, **DF**, and **ESTF** could fill the pores in the blanching mock-ups. The morphological and compound distribution study reveal that **DC6G900** shows a good penetration in the lateral direction, while other compounds show a limited penetration. It is worth to note that **ESTF** showed a better penetration on lateral direction than **DSTF** as demonstrated by the morphological study. The limited penetration could be a result of high concentration, molecular weight, and hydrogen bonding/dipolar interaction by the polar groups in the molecular structures. An optimized concentration could be developed in the future. The partially perfluorinated derivatives with less polar groups could be designed and synthesized in the future.

Concerning the reversibility of the restoration treatments, the compounds in the treated samples could be removed by using TFE or 2-propanol. The L* value could be dramatically increased after removal of the perfluorinated compounds. The highly porous structures

reappear after the compounds were removed. The quantity of Fluorine was decreased effectively after removal of the compounds. Therefore, the reversibility of the restoration treatments by partially perfluorinated derivatives is promising. Optimization of the practical process, to avoid removing extra pigment and the penetration of extra solvent, could be developed in the future.

Based on the results of the tests on pure pigments and blanching mock-up samples, **DSTF**, **DSF**, **DC6G900**, **DF**, and **ESTF** could be considered as promising restoration compounds for blanching painting restoration by acting against blanching effectively. Among those compounds, **DSTF**, **DSF**, and **DC6G900** are recommended as restoration products for blanching paintings, because **DSTF** and **DSF** could dramatically decrease the L* value and **DC6G900** shows a good penetration.

Moreover, based on the structure of those molecules, further modifications could be considered such as controlling the number of polar groups and molecular weight. The optimized concentration for treatment solutions or suspensions could be developed.

Therefore, the results of this study could contribute to improve the restoration efficacy on blanching paintings. In near future, the restoration test of the partially perfluorinated derivatives could be performed on mock-up samples with different supports, such as Canvas.

7.3 Summary

Overall, the partially perfluorinated derivatives **ESF**, **DSF** and **DF** that were synthesized in this PhD research project could be used as potential stone protection agents. **DSTF**, **DSF**, and **DC6G900** could be used for restoration of blanching easel paintings. The partially perfluorinated C-glycoside (**C-Glc-OH**) was demonstrated not to be suitable for stone protection and blanching painting restoration due to its high number of hydroxyl functions. Further optimization of the molecular structure by controlling the number of polar groups and molecular weight, as well as the concentration of solutions/suspensions for practical applications could be studied in the future.

Bibliography

- [1] Ramanujam, E.M. and Brooks, J.S., 2014. Wildlife art and illustration: stone sculpture and painting-some experiments in Auroville, Tamil Nadu, India. *Journal of Threatened Taxa*, 6(10).
- [2] ANTL-WEISER, W.A.L.P.U.R.G.A., 2009. The time of the Willendorf figurines and new results of Palaeolithic research in lower Austria. *Anthropologie (1962-)*, 47(1/2), pp.131-141.
- [3] Calia, A., Tabasso, M.L., Mecchi, A.M. and Quarta, G., 2014. The study of stone for conservation purposes: Lecce stone (southern Italy). *Geological Society, London, Special Publications*, 391(1), pp.139-156.
- [4] <https://www.architecturaldigest.com/story/eternal-city-eternal-marbles-pablo-atcugar-ry>
- [5] Britannica, The Editors of Encyclopaedia. "Easel painting". *Encyclopedia Britannica*, 20 Jul. 1998, <https://www.britannica.com/art/easel-painting>.
- [6] Arrighi, C., Brugioni, M., Castelli, F., Franceschini, S. and Mazzanti, B., 2018. Flood risk assessment in art cities: the exemplary case of Florence (Italy). *Journal of Flood Risk Management*, 11, pp.S616-S631.
- [7] Piacenti, F., 1994. Chemistry for the conservation of the cultural heritage. *Science of the total environment*, 143(1), pp.113-120.
- [8] Genty, A., Baglioni, P., Eveno, M., Bastian, G., Uziel, J., Lubin Germain, N. and Menu, M., 2018. Les chancis des peintures de chevalet: étude des traitements de restauration actuels et proposition d'une alternative innovante. *Technè. La science au service de l'histoire de l'art et de la préservation des biens culturels*, (46), pp.90-95.
- [9] Koller, J. and Burmester, A., 1990. Blanching of unvarnished modern paintings: a case study on a painting by Serge Poliakoff. *Studies in Conservation*, 35(sup1), pp.138-143.
- [10] Britannica, E., 2021. Available online: <https://www.britannica.com/science>. *Geophone* (accessed on 10 March 2021).
- [11] Mibei, G., 2014. Introduction to types and classification of rocks. *Geothermal Development Company*, 1374011.
- [12] Bugani, S., Camaiti, M., Morselli, L., Van de Castele, E. and Janssens, K., 2007. Investigation on porosity changes of Lecce stone due to conservation treatments by means of x-ray nano-and improved micro-computed tomography: preliminary results. *X-Ray Spectrometry: An International Journal*, 36(5), pp.316-320.
- [13] a) Salvatici, T., Calandra, S., Centauro, I., Pecchioni, E., Intrieri, E. and Garzonio, C.A., 2020. Monitoring and evaluation of sandstone decay adopting non-destructive techniques: On-site application on building stones. *Heritage*, 3(4), pp.1287-1301.
b) Antonenko, M., Myshkin, V., Grigoriev, A. and Chubreev, D., 2018, March. Clay-based matrices incorporating radioactive silts: A case study of sediments from spent fuel pool. *In AIP Conference Proceedings* (Vol. 1938, No. 1, p. 020002). AIP Publishing LLC.
- [14] Barnhoorn, A., Bystricky, M., Burlini, L. and Kunze, K., 2004. The role of recrystallisation on the deformation behaviour of calcite rocks: large strain torsion experiments on Carrara marble. *Journal of Structural Geology*, 26(5), pp.885-903.

- [15] Vergès-Belmin, V., 2008. Illustrated glossary on stone deterioration patterns. *Icomos*.
- [16] Labus, M. and Bochen, J., 2012. Sandstone degradation: an experimental study of accelerated weathering. *Environmental Earth Sciences*, 67(7), pp.2027-2042.
- [17] a) Heidari, M., Torabi-Kaveh, M. and Mohseni, H., 2017. Assessment of the effects of freeze–thaw and salt crystallization ageing tests on Anahita Temple Stone, Kangavar, West of Iran. *Geotechnical and Geological Engineering*, 35(1), pp.121-136.
 b) Warscheid, T. and Braams, J., 2000. Biodeterioration of stone: a review. *International Biodeterioration & Biodegradation*, 46(4), pp.343-368.
- [18] Sabbioni, C., 1995. Contribution of atmospheric deposition to the formation of damage layers. *Science of the total environment*, 167(1-3), pp.49-55.
- [19] Ray, S. and Kim, K.H., 2014. The pollution status of sulfur dioxide in major urban areas of Korea between 1989 and 2010. *Atmospheric Research*, 147, pp.101-110.
- [20] Hutchinson, A.J., Johnson, J.B., Thompson, G.E., Wood, G.C., Sage, P.W. and Cooke, M.J., 1993. Stone degradation due to wet deposition of pollutants. *Corrosion science*, 34(11), pp.1881-1898.
- [21] Charola, A.E. and Ware, R., 2002. Acid deposition and the deterioration of stone: a brief review of a broad topic. *Geological society, London, special publications*, 205(1), pp.393-406.
- [22] a) Albaigés, J., 2013. Stanley E. Manahan, Environmental chemistry: Boca Raton, FL, USA, CRC Press, 2010, 783 pp., 96.70 USD (hardback), ISBN 978-1-4200-5920-5.
 b) Massey, S.W., 1999. The effects of ozone and NO_x on the deterioration of calcareous stone. *Science of the total environment*, 227(2-3), pp.109-121.
- [23] Espinosa-Marzal, R.M. and Scherer, G.W., 2010. Advances in understanding damage by salt crystallization. *Accounts of chemical research*, 43(6), pp.897-905.
- [24] Ruedrich, J., Kirchner, D. and Siegesmund, S., 2011. Physical weathering of building stones induced by freeze–thaw action: a laboratory long-term study. *Environmental Earth Sciences*, 63(7), pp.1573-1586.
- [25] Török, Á. and Szemerey-Kiss, B., 2019. Freeze-thaw durability of repair mortars and porous limestone: compatibility issues. *Progress in Earth and Planetary Science*, 6(1), pp.1-12.
- [26] Caneva, G., Nugari, M.P., Nugari, M.P. and Salvadori, O. eds., 2008. Plant biology for cultural heritage: biodeterioration and conservation. *Getty Publications*.
- [27] Guillitte, O., 1995. Bioreceptivity: a new concept for building ecology studies. *Science of the total environment*, 167(1-3), pp.215-220.
- [28] Favaro, M., Mendichi, R., Ossola, F., Russo, U., Simon, S., Tomasin, P. and Vigato, P.A., 2006. Evaluation of polymers for conservation treatments of outdoor exposed stone monuments. Part I: Photo-oxidative weathering. *Polymer Degradation and Stability*, 91(12), pp.3083-3096.
- [29] Cao, Y., Salvini, A. and Camaiti, M., 2020. Current status and future prospects of applying bioinspired superhydrophobic materials for conservation of stone artworks. *Coatings*, 10(4), p.353.
- [30] Lazzarini, L. and LaurenziTabasso, M., 2010. Il restauro della pietra.
- [31] Wheeler, G., 2005. Alkoxysilanes and the Consolidation of Stone. *Getty Publications*.
- [32] a) Tabasso, M.L., 1995. Acrylic polymers for the conservation of stone: Advantages and

- drawbacks. *APT Bulletin: The Journal of Preservation Technology*, 26(4), pp.17-21.
- b) Ciardelli, F., Aglietto, M., Castelvetro, V., Chiantore, O. and Toniolo, L., 2000, March. Fluorinated polymeric materials for the protection of monumental buildings. In *Macromolecular Symposia* (Vol. 152, No. 1, pp. 211-222).
- c) Piacenti, F., Pasetti, A., Matteoli, U. and Strepparola, E., AusimontSpA, 1988. Method for protecting stone materials from atmospheric agents by means of perfluoropolyether derivatives. *U.S. Patent 4,745,009*.
- [33] a) Bracci, S. and Melo, M.J., 2003. Correlating natural ageing and Xenon irradiation of Paraloid® B72 applied on stone. *Polymer Degradation and Stability*, 80(3), pp.533-541.
- b) Sadat-Shojai, M. and Ershad-Langroudi, A., 2009. Polymeric coatings for protection of historic monuments: Opportunities and challenges. *Journal of Applied Polymer Science*, 112(4), pp.2535-2551.
- [34] Mazzola, M., Frediani, P., Bracci, S. and Salvini, A., 2003. New strategies for the synthesis of partially fluorinated acrylic polymers as possible materials for the protection of stone monuments. *European Polymer Journal*, 39(10), pp.1995-2003.
- [35] Price, C.A. and Doehne, E., 2011. Stone conservation: an overview of current research. *Research in Conservation, the Getty Conservation Institute, Getty Publications: Los Angeles, CA, USA*, pp.35-37.
- [36] Snethlage, R. and Wendler, E., 1990. Surfactants and adherent silicon resins-new protective agents for natural stone. *MRS Online Proceedings Library (OPL)*, 185.
- [37] Ni, H., Skaja, A.D. and Soucek, M.D., 2000. Acid-catalyzed moisture-curing polyurea/polysiloxaneceramer coatings. *Progress in Organic Coatings*, 40(1-4), pp.175-184.
- [38] Crick, C.R. and Parkin, I.P., 2010. Preparation and characterisation of super-hydrophobic surfaces. *Chemistry—A European Journal*, 16(12), pp.3568-3588.
- [39] a) Shang, H.M., Wang, Y., Limmer, S.J., Chou, T.P., Takahashi, K. and Cao, G.Z., 2005. Optically transparent superhydrophobic silica-based films. *Thin Solid Films*, 472(1-2), pp.37-43.
- b) Malshe, V.C. and Sangaj, N.S., 2005. Fluorinated acrylic copolymers: Part I: Study of clear coatings. *Progress in Organic Coatings*, 53(3), pp.207-211.
- [40] Frediani, P., Del Fa', C.M., Matteoli, U. and Tiano, P., 1982. Use of perfluoropolyethers as water repellents: study of their behaviour on pietra serena a Florentine building stone. *Studies in Conservation*, 27(1), pp.31-37.
- [41] Piacenti, F. and Camaiti, M., 1994. Synthesis and characterization of fluorinated polyetheric amides. *Journal of fluorine chemistry*, 68(2), pp.227-235.
- [42] Camaiti, M., Brizi, L., Bortolotti, V., Papacchini, A., Salvini, A. and Fantazzini, P., 2017. An environmental friendly fluorinated oligoamide for producing nonwetting coatings with high performance on porous surfaces. *ACS applied materials & interfaces*, 9(42), pp.37279-37288.
- [43] Cao, Y., Salvini, A. and Camaiti, M., 2017. Oligoamide grafted with perfluoropolyether blocks: A potential protective coating for stone materials. *Progress in Organic Coatings*, 111, pp.164-174.
- [44] Cao, Y., Salvini, A. and Camaiti, M., 2020. Superhydrophobic fluorinated oligomers as protective agents for outdoor stone artworks. *Journal of Cultural Heritage*, 44, pp.90-97.

- [45] Mayer, R., 1975. The painter's craft: an introduction to artists' methods and materials. *Viking Press*.
- [46] Stanley Jr, W. and Mayer, J.W., 2006. The science of paintings. *Springer Science & Business Media*.
- [47] Colombini, M.P., Andreotti, A., Bonaduce, I., Modugno, F. and Ribechini, E., 2010. Analytical strategies for characterizing organic paint media using gas chromatography/mass spectrometry. *Accounts of chemical research*, 43(6), pp.715-727.
- [48] Alfeld, M. and Broekaert, J.A., 2013. Mobile depth profiling and sub-surface imaging techniques for historical paintings—A review. *Spectrochimica Acta Part B: Atomic Spectroscopy*, 88, pp.211-230.
- [49] Saunders, D. and Kirby, J., 1994. Light-induced colour changes in red and yellow lake pigments. *National Gallery Technical Bulletin*, 15(1), pp.79-97.
- [50] Secundus, P., Strong, E., Sellers, E. and Urlichs, H.L., 1896. The elder Pliny's chapters on the history of art. *Macmillan*.
- [51] Stoner, J.H. and Rushfield, R.A. eds., 2012. The conservation of easel paintings. *London, UK: Routledge*.
- [52] Borg, B.E., 2010. Painted funerary portraits. *UCLA encyclopedia of Egyptology*, 1(1).
- [53] Welch, E.S., 1997. Art and society in Italy, 1350-1500. *Oxford University Press*.
- [54] Cook, J.G., 1984. Handbook of textile fibres: man-made fibres. *Elsevier*.
- [55] Clark, M. ed., 2011. Handbook of textile and industrial dyeing: principles, processes and types of dyes. *Elsevier*.
- [56] Hackney, S., 2020. On Canvas: Preserving the Structure of Paintings. *Getty Publications*.
- [57] Stols-Witlox, M.J.N., 2014. Historical recipes for preparatory layers for oil paintings in manuals, manuscripts and handbooks in North West Europe, 1550-1900: analysis and reconstructions..
- [58] Emile-Male, G., 1976. The restorer's handbook of easel painting.
- [59] Gettens, R.J. and Mrose, M.E., 1954. Calcium sulphate minerals in the grounds of Italian paintings. *Studies in Conservation*, 1(4), pp.174-189.
- [60] Souza, L.A. and Derrick, M.R., 1995. The use of FT-IR spectrometry for the identification and characterization of gesso-glue grounds in wooden polychromed sculptures and panel paintings. *MRS Online Proceedings Library*, 352(1), pp.573-578.
- [61] King 1653-57: 48, 'Art of painting in oyle by the life' 1664: 94-5, Stalker and Parker 1688:54.
- [62] Furetière 1690, vol. 2: no page nrs, entry 'imprimer', Compendium 1808: 67.
- [63] Matteini, M., Mazzeo, R. and Moles, A., 2016. Chemistry for restoration: painting and restoration materials.
- [64] von Fraunhofer, J.A., 2012. Adhesion and cohesion. *International journal of dentistry*, 2012.
- [65] Emad, S.G.R., Zhou, X., Morsch, S., Lyon, S.B., Liu, Y., Graham, D. and Gibbon, S.R., 2019. How pigment volume concentration (PVC) and particle connectivity affect leaching of corrosion inhibitive species from coatings. *Progress in Organic Coatings*, 134, pp.360-372.
- [66] Masschelein-Kleiner, L., 1985. Ancient binding media, varnishes and adhesives.
- [67] SULTANA, C. "Oleaginous flax in Oils & Fats Manual", *Vol. 1, Intercept Ltd., Andover*.

- 154-168.(1996).
- [68] Js, M. and White, R., 1994. The organic chemistry of museum objects. *Buttersworth: London, UK*.
- [69] Maroger, J., 1948. The secret formulas and techniques of the masters.
- [70] Robert, H.D., 1965. Etienne Gilson, Matières et formes. Poïétiques particulières des arts majeurs. *Revue Philosophique de Louvain*, 63(78), pp.313-316.
- [71] Genty, A., 2017. Les chancis des vernis et des couches picturales des peintures de chevalet à l'huile: Contribution à la caractérisation physico-chimique, à la connaissance des mécanismes de formation et aux traitements de restauration (*Doctoral dissertation, Cergy-Pontoise*).
- [72] Perego, F., 2005. Dictionnaire des matériaux du peintre (Vol. 895). *Paris: Belin*.
- [73] a) Laurie, A.P., 1937. The refractive index of a solid film of linseed oil rise in refractive index with age. *Proceedings of the Royal Society of London. Series A-Mathematical and Physical Sciences*, 159(896), pp.123-133.
 b) O'Hanlon, G., 2013. "Why Some Paints are Transparent and Others Opaque." from <http://www.naturalpigments.com/art-supply-education/transparent-opaque-paints/>
- [74] Gifford, E.M., The aesthetic consequences of painting materials: a study of Dutch tonal landscapes. In *Abstracts of Papers Delivered in Art History Sessions, 71st Annual Meeting, College Art Association of America* (pp. 96-96).
- [75] a) René de la Rie, E. and McGlinchey, C.W., 1990. New synthetic resins for picture varnishes. *Studies in Conservation*, 35(sup1), pp.168-173.
 b) Dietemann, P., Higgitt, C., Kälin, M., Edelmann, M.J., Knochenmuss, R. and Zenobi, R., 2009. Aging and yellowing of triterpenoid resin varnishes—Influence of aging conditions and resin composition. *Journal of cultural heritage*, 10(1), pp.30-40.
 c) Vahur, S., Teearu, A., Haljasorg, T., Burk, P., Leito, I. and Kaljurand, I., 2012. Analysis of dammar resin with MALDI-FT-ICR-MS and APCI-FT-ICR-MS. *Journal of mass spectrometry*, 47(3), pp.392-409.
 d) De la Rie, E.R., 1989. Old master paintings: a study of the varnish problem. *Analytical chemistry*, 61(21), pp.1228A-1240A.
 e) Phenix, A. and Townsend, J., 2020. A brief survey of historical varnishes. In *Conservation of easel paintings* (pp. 262-273). Routledge.
- [76] Groen, K., 1988. Scanning electron microscopy as an aid in the study of blanching. *The first ten years. The examination and conservation of paintings 1977 to 1987. The bulletin of the Hamilton Kerr Institute No. 1*, (1), pp.48-65.
- [77] van Loon, A., 2008. Color changes and chemical reactivity in seventeenth-century oil paintings (pp. 119-204). *Universiteit van Amsterdam [Host]*.
- [78] Koller, J. and Burmester, A., 1990. Blanching of unvarnished modern paintings: a case study on a painting by Serge Poliakoff. *Studies in Conservation*, 35(sup1), pp.138-143..
- [79] Saunders, D. and Kirby, J., 1994. Light-induced colour changes in red and yellow lake pigments. *National Gallery Technical Bulletin*, 15(1), pp.79-97.
- [80] a) Rioux, J. P. "Rapport interne n°1354a, La Manne dans le désert, Giovanni Francesco Romanelli" (1979).
 b) Wyld, M., Mills, J. and Plesters, J., 1980. Some observations on blanching (with special reference to the paintings of Claude). *National Gallery technical bulletin*, 4, pp.49-63.

- c)Nicolaus, K., 1999. Manuel de restauration des tableaux.
- [81] Koch Dandolo, C.L., Detalle, V., Bodiguel, J.B., Lopez, M., Bai, X., Martos-Leviv, D., Genty, A., Pasquali, C. and Menu, M., 2020. Insights into the Blanching of Water-Damaged Varnish by Means of Spectral-Domain Optical Coherence Tomography. *Studies in Conservation*, pp.1-10.
- [82] Lank, H., 1972. The use of dimethyl formamide vapour in reforming blanched oil paintings. *Studies in Conservation*, 17(sup1), pp.809-813.
- [83] Spring, M. and Keith, L., 2009. Aelbert Cuyp's Large Dort: colour change and conservation. *National Gallery technical bulletin*, 30, pp.71-85.
- [84] Genty, A., Eveno, M., Nowik, W., Bastian, G., Ravaud, E., Cabillic, I., Uziel, J., Lubin-Germain, N. and Menu, M., 2015. Blanching of paint and varnish layers in easel paintings: contribution to the understanding of the alteration. *Applied Physics A*, 121(3), pp.779-788.
- [85] Tanhuanpää, A., 2000. Blanching on a large scale: changes in a monumental painting entitled H_2SO_4 by Unto Pusa. In *Conservation without limits: IIC Nordic Group XV congress, August 23-26, 2000, Helsinki, Finland* (pp. 171-184).
- [86] Genty, A., Van Song, T.P., Andraud, C. and Menu, M., 2017. Four-flux model of the light scattering in porous varnish and paint layers: towards understanding the visual appearance of altered blanched easel oil paintings. *Applied Physics A*, 123(7), pp.1-9.
- [87] Del Grosso, C.A., Mosleh, Y., Beerkens, L., Poulis, J.A. and de la Rie, E.R., 2021. The photostability and peel strength of ethylene butyl acrylate copolymer blends for use in conservation of cultural heritage. *Journal of Adhesion Science and Technology*, pp.1-23.
- [88] Baglioni, M., Raudino, M., Berti, D., Keiderling, U., Bordes, R., Holmberg, K. and Baglioni, P., 2014. Nanostructured fluids from degradable nonionic surfactants for the cleaning of works of art from polymer contaminants. *Soft Matter*, 10(35), pp.6798-6809.
- [89] Epley, "Jan Both's Italian landscape," 131.
- [90] Serrano-Ruiz, J.C. and Dumesic, J.A., 2011. Catalytic routes for the conversion of biomass into liquid hydrocarbon transportation fuels. *Energy & Environmental Science*, 4(1), pp.83-99.
- [91] Monrad, R.N. and Madsen, R., 2011. Modern methods for shortening and extending the carbon chain in carbohydrates at the anomeric center. *Tetrahedron*, 67(46), p.8825.
- [92] Coté, G.L., Flitsch, S., Ito, Y., Kondo, H., Nishimura, S.I. and Yu, B., 2008. Glycoscience: chemistry and chemical biology. *Springer Science & Business Media*.
- [93] Lalitha, K., Muthusamy, K., Prasad, Y.S., Vemula, P.K. and Nagarajan, S., 2015. Recent developments in β -C-glycosides: Synthesis and applications. *Carbohydrate research*, 402, pp.158-171.
- [94] Cavezza, A., Boulle, C., Guéguinat, A., Pichaud, P., Trouille, S., Ricard, L. and Dalko-Csiba, M., 2009. Synthesis of Pro-Xylane™: A new biologically active C-glycoside in aqueous media. *Bioorganic & medicinal chemistry letters*, 19(3), pp.845-849.
- [95] Rodrigues, F., Canac, Y. and Lubineau, A., 2000. A convenient, one-step, synthesis of β -C-glycosidic ketones in aqueous media. *Chemical Communications*, (20), pp.2049-2050.
- [96] Witte, S.N., Voigt, B. and Mahrwald, R., 2015. Amine-catalyzed cascade reactions of unprotected and unactivated carbohydrates: direct access to C-glycosides. *Synthesis*,

- 47(15), pp.2249-2255.
- [97] Yang, Y., Zhang, X. and Yu, B., 2015. *O*-Glycosylation methods in the total synthesis of complex natural glycosides. *Natural product reports*, 32(9), pp.1331-1355.
- [98] Postema, M.H., 2020. *C*-Glycoside synthesis. *CRC press*.
- [99] Levy, D.E. and Tang, C. eds., 1995. The Chemistry of *C*-glycosides. *Elsevier*.
- [100] Araki, Y., Kobayashi, N., Watanabe, K. and Ishido, Y., 1985. Synthesis of Glycosyl Cyanides and *C*-Allyl Glycosides by the use of Glycosyl Fluoride Derivatives. *Journal of Carbohydrate Chemistry*, 4(4), pp.565-585.
- [101] Somsák, L., 2001. Carbanionic reactivity of the anomeric center in carbohydrates. *Chemical reviews*, 101(1), pp.81-136.
- [102] Gong, H., Sinisi, R. and Gagné, M.R., 2007. A room temperature Negishi cross-coupling approach to *C*-alkyl glycosides. *Journal of the American Chemical Society*, 129(7), pp.1908-1909.
- [103] Dawe, R.D. and Fraser-Reid, B., 1981. α -*C*-Glycopyranosides from Lewis acid catalysed condensations of acetylated glycals and enol silanes. *Journal of the Chemical Society, Chemical Communications*, (22), pp.1180-1181.
- [104] Ansari, A.A., Lahiri, R. and Vankar, Y.D., 2013. The carbon-Ferrier rearrangement: an approach towards the synthesis of *C*-glycosides. *ARKIVOC: Online Journal of Organic Chemistry*.
- [105] Ferrier, R.J., Overend, W.G. and Ryan, A.E., 1962. 712. The reaction between 3, 4, 6-tri-*O*-acetyl-*D*-glucal and *p*-nitrophenol. *Journal of the Chemical Society (Resumed)*, pp.3667-3670.
- [106] Gómez, A.M., Lobo, F., Uriel, C. and López, J.C., 2013. Recent developments in the Ferrier rearrangement. *European Journal of Organic Chemistry*, 2013(32), pp.7221-7262.
- [107] Yadav, J.S. and Reddy, B.V.S., 2002. InBr_3 -catalyzed Ferrier rearrangement: an efficient synthesis of *C*-pseudoglycals. *Synthesis*, 2002(04), pp.0511-0514.
- [108] Yadav, J.S., Reddy, B.V.S., Reddy, K.S., Chandraiah, L. and Sunitha, V., 2004. $\text{Bi}(\text{OTf})_3$ as novel and efficient catalyst for the stereoselective synthesis of *C*-pseudoglycals. *Synthesis*, 2004(15), pp.2523-2526.
- [109] Swamy, N.R., Srinivasulu, M., Reddy, T.S., Goud, T.V. and Venkateswarlu, Y., 2004. Zirconium (IV) chloride catalyzed synthesis of 2, 3-unsaturated *C*, *N*, *O*, *S*, and heteroaromatic glycosylation in the ferrier rearrangement. *Journal of carbohydrate chemistry*, 23(6-7), pp.435-441.
- [110] Tiwari, P., Agnihotri, G. and Misra, A.K., 2005. Synthesis of 2, 3-unsaturated *C*-glycosides by $\text{HClO}_4\text{-SiO}_2$ catalyzed Ferrier rearrangement of glycals. *Carbohydrate research*, 340(4), pp.749-752.
- [111] Bai, Y., Kim, L.M.H., Liao, H. and Liu, X.W., 2013. Oxidative Heck reaction of glycals and aryl hydrazines: a palladium-catalyzed *C*-glycosylation. *The Journal of organic chemistry*, 78(17), pp.8821-8825.
- [112] Boucard, V., Larrieu, K., Lubin-Germain, N., Uziel, J. and Augé, J., 2003. *C*-glycosylated phenylalanine synthesis by palladium-catalyzed cross-coupling reactions. *Synlett*, 2003(12), pp.1834-1837.
- [113] Ousmer, M., Boucard, V., Lubin-Germain, N., Uziel, J. and Augé, J., 2006. Gram-scale

- preparation of a p-(C-glucopyranosyl)-L-phenylalanine derivative by a Negishicross-coupling reaction. *European journal of organic chemistry*, 5, p.1216.
- [114] Bordessa, A., Ferry, A. and Lubin-Germain, N., 2016. Access to Complex C2-Branched Glycoconjugates via Palladium-Catalyzed Aminocarbonylation Reaction of 2-Iodoglycals. *The Journal of organic chemistry*, 81(24), pp.12459-12465.
- [115] Subramanian, P. and Kaliappan, K.P., 2013. A One-Pot, Copper-Catalyzed Cascade Route to 2-Indolyl-C-glycosides. *European Journal of Organic Chemistry*, 2013(3), pp.595-604.
- [116] Kumar, R.S., Karthikeyan, K., Kumar, B.P., Muralidharan, D. and Perumal, P.T., 2010. Synthesis of densely functionalized C-glycosides by a tandem oxy Michael addition–Wittig olefination pathway. *Carbohydrate research*, 345(4), pp.457-461.
- [117] Deshpande, P.P., Ellsworth, B.A., Buono, F.G., Pullockaran, A., Singh, J., Kissick, T.P., Huang, M.H., Lobinger, H., Denzel, T. and Mueller, R.H., 2007. Remarkable β -selectivity in the synthesis of β -1-C-arylglucosides: stereoselective reduction of acetyl-protected methyl 1-C-arylglucosides without acetoxy-group participation. *The Journal of organic chemistry*, 72(25), pp.9746-9749.
- [118] Terauchi, M., Abe, H., Matsuda, A. and Shuto, S., 2004. An efficient synthesis of β -C-glycosides based on the conformational restriction strategy: Lewis acid promoted silane reduction of the anomeric position with complete stereoselectivity. *Organic letters*, 6(21), pp.3751-3754.
- [119] Guo, C., Hu, M., DeOrazio, R.J., Usyatinsky, A., Fitzpatrick, K., Zhang, Z., Maeng, J.H., Kitchen, D.B., Tom, S., Luche, M. and Khmel'nitsky, Y., 2014. The design and synthesis of novel SGLT2 inhibitors: C-glycosides with benzyltriazolopyridinone and phenylhydantoin as the aglycone moieties. *Bioorganic & medicinal chemistry*, 22(13), pp.3414-3422.
- [120] Lee, D.Y., Zhang, W.Y. and Karnati, V.V.R., 2003. Total synthesis of puerarin, an isoflavone C-glycoside. *Tetrahedron letters*, 44(36), pp.6857-6859.
- [121] Deshpande, P.P., Ellsworth, B.A., Buono, F.G., Pullockaran, A., Singh, J., Kissick, T.P., Huang, M.H., Lobinger, H., Denzel, T. and Mueller, R.H., 2007. Remarkable β -selectivity in the synthesis of β -1-C-arylglucosides: stereoselective reduction of acetyl-protected methyl 1-C-arylglucosides without acetoxy-group participation. *The Journal of organic chemistry*, 72(25), pp.9746-9749.
- [122] Ohba, K. and Nakata, M., 2015. Total synthesis of Paecilomycin B. *Organic letters*, 17(12), pp.2890-2893.
- [123] Yang, Y. and Yu, B., 2017. Recent advances in the chemical synthesis of C-glycosides. *Chemical reviews*, 117(19), pp.12281-12356.
- [124] Johnson, S. and Tanaka, F., 2016. Direct synthesis of C-glycosides from unprotected 2-N-acyl-aldohexoses via aldol condensation–oxa-Michael reactions with unactivated ketones. *Organic & biomolecular chemistry*, 14(1), pp.259-264.
- [125] Johnson, S., Bagdi, A.K. and Tanaka, F., 2018. C-Glycosidation of Unprotected Di- and Trisaccharide Aldopyranoses with Ketones Using Pyrrolidine-Boric Acid Catalysis. *The Journal of organic chemistry*, 83(8), pp.4581-4597.
- [126] Young, I.S. and Baran, P.S., 2009. Protecting-group-free synthesis as an opportunity for invention. *Nature chemistry*, 1(3), pp.193-205.
- [127] Trost, B.M., 1991. The atom economy--a search for synthetic efficiency. *Science*, 254(5037), pp.1471-1477.

- [128] Gonzalez, M.A., Requejo, J.L.J., Albarran, J.C.P. and Perez, J.A.G., 1986. Facile preparation of C-glycosylbarbiturates and C-glycosylbarbituric acids. *Carbohydrate research*, 158, pp.53-66.
- [129] a) Misra, A.K. and Agnihotri, G., 2004. Preparation of polyhydroxyalkyl-and C-glycosylfuran derivatives from free sugars catalyzed by cerium (III) chloride in aqueous solution: an improvement of the Garcia Gonzalez reaction. *Carbohydrate research*, 339(7), pp.1381-1387.
 b) Bartoli, G., Fernandez-Bolanos, J.G., Di Antonio, G., Foglia, G., Giuli, S., Gunnella, R., Mancinelli, M., Marcantoni, E. and Paoletti, M., 2007. SiO₂-Supported CeCl₃·7H₂O– NaI Lewis Acid Promoter: Investigation into the Garcia Gonzalez Reaction in Solvent-Free Conditions. *The Journal of organic chemistry*, 72(16), pp.6029-6036.
- [130] a) Yadav, J.S., Reddy, B.V.S., Sreenivas, M. and Satheesh, G., 2007. Indium (III) chloride/water: A versatile catalytic system for the synthesis of C-furyl glycosides and trihydroxyalkyl furan derivatives. *Synthesis*, 2007(11), pp.1712-1716.
 b) Nagarapu, L., Chary, M.V., Satyender, A., Supriya, B. and Bantu, R., 2009. Iron (III) chloride in ethanol-water: highly efficient catalytic system for the synthesis of Garcia Gonzalez polyhydroxyalkyl-and C-glycosylfurans. *Synthesis*, 2009(13), pp.2278-2282.
- [131] Calvo-Flores, F.G., 2009. Sustainable chemistry metrics. *ChemSusChem: Chemistry & Sustainability Energy & Materials*, 2(10), pp.905-919.
- [132] Anastas, P. and Eghbali, N., 2010. Green chemistry: principles and practice. *Chemical Society Reviews*, 39(1), pp.301-312.
- [133] Augé, J., 2008. A new rationale of reaction metrics for green chemistry. Mathematical expression of the environmental impact factor of chemical processes. *Green Chemistry*, 10(2), pp.225-231.
- [134] Augé, J. and Scherrmann, M.C., 2012. Determination of the global material economy (GME) of synthesis sequences—A green chemistry metric to evaluate the greenness of products. *New Journal of Chemistry*, 36(4), pp.1091-1098.
- [135] Philippe, M., Cavezza, A., Pichaud, P., Trouille, S. and Dalco-Csiba, M., 2014. C-glycosylation invented by PrLubineau's team: a key-reaction for innovation in cosmetics. *Carbohydrate Chemistry*, 40, pp. 1-10
- [136] Wurtz, A., 1872. Sur un aldéhyde-alcool. *Bull. Soc. Chim. Fr*, 17, pp.426-442.
- [137] Kane, R., 1838. Ueber den Essiggeist und einigedavonAbgeleiteteVerbindungen. *Journal für PraktischeChemie*, 15(1), pp.129-155.
- [138] Nagarajan, S., Shanmugam, M.J. and Das, T.M., 2011. Studies on the synthesis of ether-, substituted alkyl-, or aryl-linked C-disaccharide derivatives. *Carbohydrate research*, 346(6), pp.722-727.
- [139] Price, N.P., Bowman, M.J., Le Gall, S., Berhow, M.A., Kendra, D.F. and Lerouge, P., 2010. Functionalized C-glycoside ketohydrazones: carbohydrate derivatives that retain the ring integrity of the terminal reducing sugar. *Analytical chemistry*, 82(7), pp.2893-2899.
- [140] Larsen, K., Thygesen, M.B., Guillaumie, F., Willats, W.G. and Jensen, K.J., 2006. Solid-phase chemical tools for glycobiology. *Carbohydrate research*, 341(10), pp.1209-1234.
- [141] Grün, C.H., van Vliet, S.J., Schiphorst, W.E., Bank, C.M., Meyer, S., van Die, I. and van Kooyk, Y., 2006. One-step biotinylation procedure for carbohydrates to study

- carbohydrate–protein interactions. *Analytical biochemistry*, 354(1), pp.54-63.
- [142] Hemamalini, A., Nagarajan, S., Ravinder, P., Subramanian, V. and Das, T.M., 2011. An easy access to novel sugar-based spirooxindole-pyrrolidines or-pyrrolizidines through [3+ 2] cycloaddition of azomethine ylides. *Synthesis*, 2011(15), pp.2495-2504.
- [143] Nagarajan, S., Das, T.M., Arjun, P. and Raaman, N., 2009. Design, synthesis and gelation studies of 4, 6-O-butylidene- α , β -unsaturated- β -C-glycosidic ketones: application to plant tissue culture. *Journal of Materials Chemistry*, 19(26), pp.4587-4596.
- [144] Howard, S. and Withers, S.G., 1998. Bromoketone C-glycosides, a new class of β -glucanase inactivators. *Journal of the American Chemical Society*, 120(40), pp.10326-10331.
- [145] Kolypadi, M., Fontanella, M., Venturi, C., André, S., Gabius, H.J., Jiménez - Barbero, J. and Vogel, P., 2009. Synthesis and conformational analysis of (α -d-galactosyl) phenylmethane and α -, β -difluoromethane analogues: Interactions with the plant lectin viscumin. *Chemistry—A European Journal*, 15(12), pp.2861-2873.
- [146] Price, N.P., Bowman, M.J., Le Gall, S., Berhow, M.A., Kendra, D.F. and Lerouge, P., 2010. Functionalized C-glycoside ketohydrazone: carbohydrate derivatives that retain the ring integrity of the terminal reducing sugar. *Analytical chemistry*, 82(7), pp.2893-2899.
- [147] Emerson, W.S., 2004. The preparation of amines by reductive alkylation. *Organic Reactions*, 4, pp.174-255.
- [148] Schellenberg, K.A., 1963. The synthesis of secondary and tertiary amines by borohydride reduction. *The Journal of Organic Chemistry*, 28(11), pp.3259-3261.
- [149] Tadanier, J., Hallas, R., Martin, J.R. and Stanaszek, R.S., 1981. Observations relevant to the mechanism of the reductive aminations of ketones with sodium cyanoborohydride and ammonium acetate. *Tetrahedron*, 37(7), pp.1309-1316.
- [150] Abdel-Magid, A.F. and Mehrman, S.J., 2006. A review on the use of sodium triacetoxyborohydride in the reductive amination of ketones and aldehydes. *Organic Process Research & Development*, 10(5), pp.971-1031.
- [151] Sato, S., Sakamoto, T., Miyazawa, E. and Kikugawa, Y., 2004. One-pot reductive amination of aldehydes and ketones with α -picoline-borane in methanol, in water, and in neat conditions. *Tetrahedron*, 60(36), pp.7899-7906.
- [152] Emerson, W.S. and Uraneck, C.A., 1941. Secondary and tertiary amines from nitro compounds. *Journal of the American Chemical Society*, 63(3), pp.749-751.
- [153] Klyuev, M.V.E., 1980. Catalytic amination of alcohols, aldehydes, and ketones. *Russian Chemical Reviews*, 49(1), p.14.
- [154] Skita, A. and Keil, F., 1928. Basenbildung aus Carbonylverbindungen. *Berichte der deutschen chemischen Gesellschaft (A and B Series)*, 61(7), pp.1452-1459.
- [155] Roe, A. and Montgomery, J.A., 1953. Kinetics of the Catalytic Hydrogenation of Certain Schiff Bases. *Journal of the American Chemical Society*, 75(4), pp.910-912.
- [156] Rylander, P., 2012. Catalytic hydrogenation over platinum metals. *Elsevier*.
- [157] Billman, J.H. and McDOWELL, J.W., 1961. Reduction of Schiff bases. III. Reduction with dimethylamine borane. *The Journal of Organic Chemistry*, 26(5), pp.1437-1440.
- [158] Schellenberg, K.A., 1963. The synthesis of secondary and tertiary amines by borohydride reduction. *The Journal of Organic Chemistry*, 28(11), pp.3259-3261.
- [159] Borch, R.F., Bernstein, M.D. and Durst, H.D., 1971. Cyanohydrinborate anion as a

- selective reducing agent. *Journal of the American Chemical Society*, 93(12), pp.2897-2904.
- [160] Moormann, A.E., 1993. Reductive amination of piperidines with aldehydes using borane-pyridine. *Synthetic communications*, 23(6), pp.789-795.
- [161] Lenga, R.E., 1988. The Sigma-Aldrich library of chemical safety data. *Sigma-Aldrich Corp.*
- [162] Abdel-Magid, A.F., Maryanoff, C.A. and Carson, K.G., 1990. Reductive amination of aldehydes and ketones by using sodium triacetoxyborohydride. *Tetrahedron letters*, 31(39), pp.5595-5598.
- [163] Abdel-Magid, A.F., Carson, K.G., Harris, B.D., Maryanoff, C.A. and Shah, R.D., 1996. Reductive amination of aldehydes and ketones with sodium triacetoxyborohydride. studies on direct and indirect reductive amination procedures. *The Journal of organic chemistry*, 61(11), pp.3849-3862.
- [164] Derives de monosaccharides et leur utilisation pour regular l'homeostasie cutanee, *L'oreal patent*
- [165] McGonagle, F.I., MacMillan, D.S., Murray, J., Sneddon, H.F., Jamieson, C. and Watson, A.J., 2013. Development of a solvent selection guide for aldehyde-based direct reductive amination processes. *Green chemistry*, 15(5), pp.1159-1165.
- [166] Riess, Jean G. "Highly fluorinated systems for oxygen transport, diagnosis and drug delivery." *Colloids and Surfaces A: Physicochemical and Engineering Aspects* 84.1 (1994): 33-48.
- [167] Zur, C., Miller, A.O. and Miethchen, R., 1998. Organofluorine compounds and fluorinating agents part 21: perfluoroalkylidene sugars by non-classical acetalation of pyranoses. *Journal of fluorine chemistry*, 90(1), pp.67-76.
- [168] Riess, J.G. and Greiner, J., 2000. Carbohydrate- and related polyol-derived fluorosurfactants: an update. *Carbohydrate research*, 327(1-2), pp.147-168.
- [169] Clary, L., Greiner, J., Santaella, C. and Vierling, P., 1995. Synthesis of single- and double-chain fluorocarbon and hydrocarbon β -linked galactose amphiphiles derived from serine. *Tetrahedron letters*, 36(4), pp.539-542.
- [170] Razgulín, A.V. and Mecozzi, S., 2015. Synthesis, emulsification and self-assembly properties of sugar-containing semifluorinated amphiphiles. *Carbohydrate research*, 406, pp.10-18.
- [171] Peters, D., Zur, C. and Miethchen, R., 1998. Organofluorine compounds and fluorinating agents; 20: The nucleophilic perfluoroalkylation of sugar aldehydes using a sonochemical Barbier-type reaction. *Synthesis*, 1998(07), pp.1033-1038.
- [172] Leclerc, E., Pannecoucke, X., Ethève-Quelquejeu, M. and Sollogoub, M., 2013. Fluoro-C-glycosides and fluoro-carbasugars, hydrolytically stable and synthetically challenging glycomimetics. *Chemical Society Reviews*, 42(10), pp.4270-4283.
- [173] Kałdoński, T.J., Gryglewicz, Ł., Stańczyk, M. and Kałdoński, T., 2011. Investigations on lubricity and surface properties of selected perfluoropolyether oils. *Journal of KONES*, 18, pp.199-212.
- [174] Bagnier, N. and Scherrmann, M.C., 2005. One-step synthesis of β -C-glycosidic ketones in aqueous media: the case of 2-acetamido sugars. *Synthesis*, 2005(05), pp.814-818.
- [175] Chiavarini, M., Gaggini, F., Guidetti, V. and Massa, M., 1993, June. Stone protection:

- from perfluoropolyethers to polyfluorourethanes. In Conservation of stone and other materials. Vol. One: causes of disorders and diagnosis. Vol. Two: prevention and treatments. *Proceedings of the international RILEM/UNESCO congress in Paris*, pp. 725-732.
- [176] Guidetti, V., Chiavarini, M. and Parrini, P., 1992. Polyfluorourethanes as stone protectives. In *Proceedings of the 7th International Congress on Deterioration and Conservation of Stone, Lisbon*, pp. 1279-1288.
- [177] Sardon, H., Pascual, A., Mecerreyes, D., Taton, D., Cramail, H. and Hedrick, J.L., 2015. Synthesis of polyurethanes using organocatalysis: a perspective. *Macromolecules*, 48(10), pp.3153-3165.
- [178] Duspara, P.A., Islam, M.S., Lough, A.J. and Batey, R.A., 2012. Synthesis and reactivity of N-alkyl carbamoylimidazoles: development of N-methyl carbamoylimidazole as a methyl isocyanate equivalent. *The Journal of organic chemistry*, 77(22), pp.10362-10368.
- [179] Riemann, I., Fessner, W.D., Papadopoulos, M.A. and Knorst, M., 2002. C-Glycosides by aqueous condensation of β -dicarbonyl compounds with unprotected sugars. *Australian journal of chemistry*, 55(2), pp.147-154.
- [180] Norsikian, S., Zeitouni, J., Rat, S., Gérard, S. and Lubineau, A., 2007. New and general synthesis of β -C-glycosylformaldehydes from easily available β -C-glycosylpropanones. *Carbohydrate research*, 342(18), pp.2716-2728.
- [181] Carraher Jr, C.E., 2017. Introduction to polymer chemistry. *CRC press*.
- [182] Gohlke, U., 1985. Polymer chemistry. The basic concepts. Von PC Hiemenz. ISBN 0-8247-7082-X. New York/Basel: Marcel Dekker, Inc. 1984. XI, 738 S. geb. *Acta Polymerica*, 36(9), pp.520-520.
- [183] Horie, C.V., 2013. Materials for conservation. *Routledge*.
- [184] Asensio, R.C., Moya, M.S.A., de la Roja, J.M. and Gómez, M., 2009. Analytical characterization of polymers used in conservation and restoration by ATR-FTIR spectroscopy. *Analytical and bioanalytical chemistry*, 395(7), pp.2081-2096.
- [185] Marchildon, K., 2011. Polyamides—still strong after seventy years. *Macromolecular reaction engineering*, 5(1), pp.22-54.
- [186] Reglero Ruiz, J.A., Trigo-López, M., García, F.C. and García, J.M., 2017. Functional aromatic polyamides. *Polymers*, 9(9), p.414.
- [187] Sease, C., 1981. The case against using soluble nylon in conservation work. *Studies in Conservation*, 26(3), pp.102-110.
- [188] Carothers, W.H., 1937. Linear Condensation Superpolymers Suitable for Production of Pliable, Strong, Elastic Fibers. In *Chem. Abstr*, 1938.
- [189] Schlack, P., 1941. Preparation of Polyamides. *US 2241321*.
- [190] Beija, M., Charreyre, M.T. and Martinho, J.M., 2011. Dye-labelled polymer chains at specific sites: Synthesis by living/controlled polymerization. *Progress in polymer science*, 36(4), pp.568-602.
- [191] Hsiao, S.H., Wang, H.M., Chang, P.C., Kung, Y.R. and Lee, T.M., 2013. Novel organosoluble aromatic polyetheramides bearing triphenylamine moieties: synthesis, electrochemistry, and electrochromism. *Journal of Polymer Research*, 20(7), pp.1-10.
- [192] Bou, J.J. and Mun, S., 1995. Synthesis and characterization of a polytartaramide based

- on l-lysine. *Polymer*, 36(1), pp.181-186.
- [193] Okada, M., 2002. Chemical syntheses of biodegradable polymers. *Progress in polymer science*, 27(1), pp.87-133.
- [194] Kiely, D.E. and Lin, T.H., Research Corp Technologies Inc, 1989. Polyhydroxypolyamides and process for making same. *U.S. Patent 4,833,230*.
- [195] Kelland, M.A., 2011. A review of kinetic hydrate inhibitors: Tailormade water-soluble polymers for oil and gas industry applications. *Advances in materials science research*, 8, pp.171-210.
- [196] Oliva, R., Albanese, F., Cipriani, G., Ridi, F., Giomi, D., Malavolti, M., Bernini, L. and Salvini, A., 2014. Water soluble trehalose-derived oligoamides. *Journal of Polymer Research*, 21(7), pp.1-12.
- [197] Cipriani, G., Salvini, A., Fioravanti, M., Di Giulio, G. and Malavolti, M., 2013. Synthesis of hydroxylated oligoamides for their use in wood conservation. *Journal of applied polymer science*, 127(1), pp.420-431.
- [198] Wolfrom, M.L., Toy, M.S. and Chaney, A., 1958. Condensation polymers from tetra-o-acetylgalactaroyl dichloride and diamines^{1, 2}. *Journal of the American Chemical Society*, 80(23), pp.6328-6330.
- [199] Ogata, N. and Hosoda, Y., 1974. Synthesis of hydrophilic polyamide by active polycondensation. *Journal of Polymer Science: Polymer Letters Edition*, 12(6), pp.355-358.
- [200] Minoura, Y., Urayama, S. and Noda, Y., 1967. Syntheses of optically active polymers by condensation polymerization of d-tartaric acid with some diamines. *Journal of Polymer Science Part A-1: Polymer Chemistry*, 5(9), pp.2441-2451.
- [201] Cipriani, G., Salvini, A., Fioravanti, M., Di Giulio, G. and Malavolti, M., 2013. Synthesis of hydroxylated oligoamides for their use in wood conservation. *Journal of applied polymer science*, 127(1), pp.420-431.
- [202] Oliva, R., Albanese, F., Cipriani, G., Ridi, F., Giomi, D., Malavolti, M., Bernini, L. and Salvini, A., 2014. Water soluble trehalose-derived oligoamides. *Journal of Polymer Research*, 21(7), pp.1-12.
- [203] Nishino, T., Meguro, M., Nakamae, K., Matsushita, M. and Ueda, Y., 1999. The lowest surface free energy based on- CF₃ alignment. *Langmuir*, 15(13), pp.4321-4323.
- [204] Moggi, G., Guidetti, V., Passetti, A. and Vicini, S., 2004. Sistemi innovativi a base di polimeri fluorurati per la conservazione di materiali lapidei artificiali. In *Architettura e materiali del Novecento: conservazione, restauro, manutenzione. Atti del convegno di studi, Bressanone*, pp. 1249-1259.
- [205] Sianesi, D., Marchionni, G. and De Pasquale, R.J., 1994. Perfluoropolyethers (PFPEs) from perfluoroolefin photooxidation. In *Organofluorine chemistry, Springer, Boston, MA*.
- [206] Ukaji, Y. and Soeta, T., 2012. 3.6 Acetogenin (Polypropionate) Derived Auxiliaries: Tartaric Acid, pp. 176-201.
- [207] Merrylin, J., Kannah, R.Y., Banu, J.R. and Yeom, I.T., 2020. Production of organic acids and enzymes/biocatalysts from food waste. In *Food Waste to Valuable Resources. Academic Press*.
- [208] Kiely, D.E., Chen, L. and Lin, T.H., 1994. Hydroxylated nylons based on unprotected

- esterified D-glucaric acid by simple condensation reactions. *Journal of the American Chemical Society*, 116(2), pp.571-578.
- [209] Muñoz-Viñas, S., 2012. Contemporary theory of conservation. *Routledge*.
- [210] Amoroso, G.G. and Camaiti, M., 1997. Scienzadeimateriali e restauro. *Firenze, Alinea editrice*.
- [211] Alessandrini, G., Toniolo, L. and Colombo, C., 2000. Partially fluorinated acrylic copolymers as coatings for calcareous stone materials. *Studies in Conservation*, 45(sup1), pp.1-6.
- [212] EN16581, U.N.I., 2016. Conservation of Cultural Heritage–Surface Protection for Porous Inorganic Materials–Laboratory Test Methods for the Evaluation of the Performance of Water Repellent Products. *Enteitaliano di Normazione, Milano*.
- [213] UNI, E., 2009. 15801: 2010, Conservation of cultural property-test methods-determination of water absorption by capillarity. *Official Italian version of EN, 15801*.
- [214] Cao, Y., 2018. Stone artifacts conservation: synthesis and study of new partially fluorinated compounds (*Doctoral dissertation, Ph.D. Thesis, University of Florence, Florence, Italy, 31 October*).
- [215] UNI, E., 2009. 15801: 2010, Conservation of cultural property-test methods-measurement of the color of the surface. *Official Italian version of EN, 15801*.
- [216] Commission Internationale de l’Eclairage. 1986. Colorimetry, 2nd edn. *CIE publication 15.2, Vienna*.
- [217] Grossi, C.M., Brimblecombe, P., Esbert, R.M. and Alonso, F.J., 2007. Color changes in architectural limestones from pollution and cleaning. *Color Research & Application: Endorsed by Inter-Society Color Council, The Colour Group (Great Britain), Canadian Society for Color, Color Science Association of Japan, Dutch Society for the Study of Color, The Swedish Colour Centre Foundation, Colour Society of Australia, Centre Français de la Couleur*, 32(4), pp.320-331.
- [218] UNI, E., 2009. 15801: 2010, Conservation of cultural property–test methods–determination of the permeability of water vapor. *Official Italian version of EN, 15801*.
- [219] Hansen, C.M., 2007. Hansen solubility parameters: a user's handbook. *CRC press*.
- [220] Chiantore, O. and Lazzari, M., 2001. Photo-oxidative stability of paraloid acrylic protective polymers. *Polymer*, 42(1), pp.17-27.
- [221] Wypych, G., 2018. Handbook of material weathering. *Elsevier*.
- [222] Davis, A., Sims, D. and Sims, D., 1983. Weathering of polymers. *Springer Science & Business Media*.
- [223] Yousif, E. and Haddad, R., 2013. Photodegradation and photostabilization of polymers, especially polystyrene. *SpringerPlus*, 2(1), pp.1-32.
- [224] Fratini, F., Pecchioni, E., Cantisani, E., Rescic, S. and Vettori, S., 2015. Pietra Serena: the stone of the Renaissance. *Geological Society, London, Special Publications*, 407(1), pp.173-186.
- [225] Sun, T., Feng, L., Gao, X. and Jiang, L., 2005. Bioinspired surfaces with special wettability. *Accounts of chemical research*, 38(8), pp.644-652.
- [226] Li, X.M., Reinhoudt, D. and Crego-Calama, M., 2007. What do we need for a superhydrophobic surface? A review on the recent progress in the preparation of

- superhydrophobic surfaces. *Chemical Society Reviews*, 36(8), pp.1350-1368.
- [227] Young, T., 1805. III. An essay on the cohesion of fluids. *Philosophical transactions of the royal society of London*, (95), pp.65-87.
- [228] Reick, F.G., Michael, E., 1976. Substrate coated with super-hydrophobic layers. *U.S. Patent 3,931,428*.
- [229] Kota, A.K., Kwon, G. and Tuteja, A., 2014. The design and applications of superomniphobic surfaces. *NPG Asia Materials*, 6(7), pp. 109-109.
- [230] Alter, M., Binet, L., Touati, N., Lubin-Germain, N., Le Hô, A.S., Mirambet, F. and Gourier, D., 2019. Photochemical Origin of the Darkening of Copper Acetate and Resinate Pigments in Historical Paintings. *Inorganic chemistry*, 58(19), pp.13115-13128.
- [231] Coccato, A., Moens, L. and Vandenaabeele, P., 2017. On the stability of mediaeval inorganic pigments: a literature review of the effect of climate, material selection, biological activity, analysis and conservation treatments. *Heritage Science*, 5(1), pp.1-25.
- [232] Dapson, R.W., 2007. The history, chemistry and modes of action of carmine and related dyes. *Biotechnic & Histochemistry*, 82(4-5), pp.173-187.
- [233] Gabrielli, L., Origgi, D., Zampella, G., Bertini, L., Bonetti, S., Vaccaro, G., Meinardi, F., Simonutti, R. and Cipolla, L., 2018. Towards hydrophobic carminic acid derivatives and their incorporation in polyacrylates. *Royal Society open science*, 5(7), pp.172399.
- [234] Schmitt, P., Günther, H., Hägele, G. and Stilke, R., 1984. A ^1H and ^{13}C NMR study of carminic acid. *Organic magnetic resonance*, 22(7), pp.446-449.
- [235] Gervais, C., Boon, J.J., Marone, F. and Ferreira, E.S., 2013. Characterization of porosity in a 19th century painting ground by synchrotron radiation X-ray tomography. *Applied Physics A*, 111(1), pp.31-38.
- [236] Baij, L., Hermans, J., Ormsby, B., Noble, P., Iedema, P. and Keune, K., 2020. A review of solvent action on oil paint. *Heritage Science*, 8(1), pp.1-23.
- [237] Sletten, E.M. and Swager, T.M., 2014. Fluorofluorophores: fluorescent fluororous chemical tools spanning the visible spectrum. *Journal of the American Chemical Society*, 136(39), pp.13574-13577.

Abstract

Stone artworks and easel paintings are challenged by diverse degradations. In particular, this thesis focuses on two restoration issues mainly induced by liquid water or moisture, which are stone degradation and blanching of easel paintings. From previous research, partially perfluorinated derivatives have been proved to provide promising restoration performance on those two restoration issues, by showing good water repellency as stone protective products and decreasing blanching in easel paintings. Inspired by those results, two families of partially perfluorinated derivatives with hydroxyl groups are proposed and designed as stone protection and blanching painting restoration products in this thesis. Those hydroxyl groups could give good adhesion on polar stone substrates by hydrogen bonding. Meanwhile, hydrophobicity of the compounds can be realized by the perfluorinated chains.

The first compounds proposed and synthesized are partially perfluorinated C-glycosides. C-glycosides are carbon-linked analogues of naturally occurring sugars, which have high hydrophilic properties due to the polar hydroxyl groups. In addition to the hydrophilicity and water repellency, C-glycosides themselves possess an improved stability towards hydrolysis. Starting from the unprotected carbohydrate, the natural, renewable and cheap D-glucose, *via* Lubineau reaction and followed by the convenient one-pot reductive amination reaction, the target compound (partially perfluorinated C-glycoside) was successfully obtained. Moreover, partially perfluorinated C-glycoside with acetyl groups as protecting groups has been successfully synthesized as a control compound, in order to investigate if hydroxyl groups in C-glycoside can improve the restoration efficacy as expected. Then, those new partially perfluorinated C-glycosides have been tested on stone materials as protective products, and on blanching mock-up painting samples. The results indicated that different properties of those C-glycosides caused by the hydroxyls, like physical states, solubility, color and interaction with stone and painting substrates, have been influenced their behaviors as the restoration products.

The other series of compounds proposed is partially perfluorinated hydroxylated oligoamides. In order to further improve the interaction between partially perfluorinated oligomers and polar substrates, new partially perfluorinated hydroxylated oligoamides derived from different monomers (dimethyl L-tartrate, diethyl succinate, diethylenetriamine or ethylenediamine) have been successfully synthesized. Those compounds have different structures and properties, *i.e.* solubility, hydrophilicity, chain length, molecular weight, and *etc.* Moreover, in order to understand the roles of hydroxyl group and amine in the applicative performance, new partially perfluorinated oligoamides with no hydroxyl groups, but with the unchanged amine and succinate sources were successfully synthesized. Then, those new partially perfluorinated derivatives were tested on stone and mock-up blanching painting samples. The results showed that their efficacy for restoration was highly influenced by the structures and properties of the molecules.

At the end, 4 promising new partially perfluorinated derivatives for stone protection and blanching painting restoration have been selected. Further optimization of the structures of molecules and their practical process for the application on stone artefacts and easel paintings worth being developed in the future to go deeper on this main cultural heritage approach.

Key words: cultural heritage, stone protection, blanching on/of easel painting, natural and artificial ageing, restoration, partially perfluorinated C-glycosides, partially perfluorinated hydroxylated oligoamides, water repellency, contact angle, spectro-colorimetry measurement, binocular observations, SEM-EDS, FEG-SEM, FT-IR

Résumé

Les œuvres d'art en pierre et les peintures de chevalet subissent diverses dégradations, conduisant à des peintures chancées et à des pierres altérées. D'après des recherches antérieures, il a été prouvé que les dérivés partiellement perfluorés offrent des propriétés prometteuses pour la restauration de ces deux matériaux. En effet, ces composés ont montré une bonne imperméabilité en tant que produits de protection de la pierre et diminuent le blanchiment des peintures de chevalet. Inspirés par ces résultats, nous proposons deux familles de dérivés partiellement perfluorés et possédant des groupes hydroxyle polaires, conçus pour la protection de la pierre et le blanchiment de la peinture dans cette thèse. Ces groupes hydroxyle pourraient donner une bonne adhérence sur des substrats de pierre polaire par liaison hydrogène. Au contraire, les chaînes perfluorées apporteront un caractère hydrophobe et hydrofuge, nécessaire pour la préservation des matériaux.

La première série de composés synthétisés est celle des C-glycosides partiellement perfluorés. Les C-glycosides sont des analogues carbonés de structures naturelles. Ces derniers possèdent des propriétés hydrophiles élevées grâce aux groupes hydroxyle polaires. En plus de leur caractère hydrophile, les C-glycosides eux-mêmes possèdent une stabilité améliorée vis-à-vis de l'hydrolyse grâce à la liaison carbone-carbone en position anomère. Les composés cibles ont été obtenus la réaction de Lubineau puis par amination réductrice. Ces nouveaux glycosides partiellement perfluorés ont été testés sur différentes pierres comme agents de protection et sur des échantillons de peinture ayant subi un blanchiment artificiel pour leur restauration. Les résultats ont indiqué que différentes propriétés liées à la présence des hydroxyles ont influencé leurs propriétés protectrices.

L'autre série de composés proposée est celle des oligoamides hydroxylés partiellement perfluorés. Afin d'améliorer encore l'interaction entre les oligomères partiellement perfluorés et les substrats polaires, de nouveaux oligoamides dérivés de différents monomères (diméthyl L-tartrate, diéthyl succinate, diéthylènetriamine ou éthylènediamine) ont été synthétisés avec succès. Ces nouveaux dérivés ont été testés sur des échantillons de peinture blanchies et de pierre. Les résultats ont montré que leur efficacité pour la restauration était fortement influencée par les structures et les propriétés des molécules

Au final, 4 nouveaux dérivés sont prometteurs. Une optimisation plus poussée des structures des molécules et de leur processus d'application sur des objets des pierres et des peintures de chevalet mérite d'être développée à l'avenir pour approfondir cette approche importante du patrimoine culturel.

Mots clés : patrimoine culturel, protection de la pierre, blanchiment sur/de peinture de chevalet, vieillissement naturel et artificiel, restauration, C-glycosides partiellement perfluorés, oligoamides hydroxylés partiellement perfluorés, hydrofuge, angle de contact, mesure spectro-colorimétrique, observations binoculaires, MEB- EDS, FEG-SEM, FT-IR